NUREG/CR-0457

DEVELOPMENT OF A LASER DOPPLER ANEMOMETER TECHNIQUE FOR THE MEASUREMENT OF TWO PHASE DISPERSED FLOW

J. Srinivasan

State University of New York at Stony Brook

Prepared for
U.S. Nuclear Regulatory Commission

Available from
National Technical Information Service
Springfield, Virginia 22161
Price: Printed Copy $9.25 ; Microfiche $3.00

The price of this document for requesters outside of the North American Continent can be obtained from the National Technical Information Service.

NUREG/CR-0457

DEVELOPMENT OF A LASER DOPPLER ANEMOMETER TECHNIQUE FOR THE MEASUREMENT OF TWO PHASE DISPERSED FLOW

J. Srinivasan

Manuscript Completed: May 1978
Date Published: November 1978

Department of Mechanical Engineering
State University of New York at Stony Brook
Stony Brook, NY 11794

Prepared for the
Division of Reactor Safety Research
Office of Nuclear Regulatory Research
U.S. Nuclear Regulatory Commission
Under Contract No. FIN B6211

STATE UNIVERSITY OF NEW YORK

AT STONY BROOK

THE GRADUATE SCHOOL

Jagannathan Srinivasan

We, the thesis committee for the above candidate for the Ph.D. degree, hereby recommend acceptance of the dissertation.

R. Chevray, Committee Chairman

Richard S. C. Lee

R. S. L. Lee, Advisor

W. S. Bradfield

Y. M. Chen, Dept. of Applied Math and Statistics

The dissertation is accepted by the Graduate School.

Herbert Weisinger, Dean
Graduate School

May 1978

Abstract of the Dissertation

DEVELOPMENT OF A LASER DOPPLER ANEMOMETER

TECHNIQUE FOR THE MEASUREMENT

OF TWO-PHASE DISPERSED FLOW

by

Jagannathan Srinivasan

Doctor of Philosophy

in

Mechanical Engineering

State University of New York at Stony Brook

May, 1978

A new optical technique using Laser-Doppler Anemometry is presented for the measurement of the local number densities and two-dimensional velocity probability densities of a turbulent dilute two-phase dispersion which has a distribution of particle size and a predominant direction of flow. This technique establishes that by a suitable scheme of discrimination on the signal amplitude, residence time and frequency of the Doppler signals caused by the scattered light from individual particles in the probing volume, the size distribution of moderately large particles in a dilute dispersed flow can be determined.

The newly developed Laser-Doppler Anemometer (LDA) technique was applied to a solid particle-water two-phase flow and a water

droplet-air two-phase flow. Particular emphasis was placed on turbulent two-phase water droplet-air flow inside a vertical rectangular channel. At each of nine different measuring locations along the transverse axis (starting at 250μ from the channel wall), over 20,000 Doppler signals were individually examined.

The particle size and number denisty distributions, and the axial and lateral velocity distributions of both phases are reported. The analysis reveals some interesting features of two-phase dispersed flow. A film of water on the channel wall was formed due to the deposition of droplets from the flow. The water droplet entrainment from the wall film and the subsequent breakup of some of these into the flow are discussed. A discussion of the relationship between the particle distributions and turbulent flow characteristics is presented.

This work is dedicated to

my parents

TABLE OF CONTENTS

LIST OF SYMBOLS

A	Doppler signal amplitude (volts).
A_v	Base amplitude level (volts).
A^*	Normalized Doppler signal amplitude (A/A_{max}).
B	Projected cross-sectional area of the measuring volume (μ^2).
$\overline{B}_o$	Projected cross-sectional area of the central core of the measuring volume (μ^2).
d	Diameter of particle (μ).
d^*	Normalized particle size (d/d_{max}).
k	Correction factor (ratio of actual number count to corrected number count).
ℓ	Particle path length in the measuring volume (μ).
$\overline{\ell}_v$	Limiting path length (μ).
ℓ_m	Maximum path length (μ).
n	Particle number count over a period of time, t.
$\dot{n}$	Probability density (number per unit time unit cross-sectional flow area, per unit velocity range and unit size range).
$[n]$	Accumulative signal number count over a period, t.
N	Particle number density (number per unit volume).
$[N]$	Accumulative number density (number per unit volume).
T_o	Tape recording time (sec).
u_k	Lateral velocity (m/sec).
v_j	Particle velocity in measuring direction (m/sec).
α	Deviation of flow direction from measuring direction (radians).
τ	Time duration of the signal (μsec).

LIST OF FIGURES

Figure | Page

LIST OF TABLES

ACKNOWLEDGEMENTS

The undertaking of this project has been a very large one, requiring a variety of skills as well as many hours of work. However, these experiments would not have been successful without the contributions of others. Especially, I am very grateful to Dr. R. S. L. Lee who worked untiringly, always assisting and guiding. His dedication, knowledge, professionalism and expertise are major attributes which contributed to the completion of the experiments which formed the basis of this thesis.

I would like to acknowledge and thank the following:

Dr. Raashid Malik for his abilities displayed in the development of the electronics; Messrs. Charles Hill for his development of the computer program; Richard Hitzigrath for his contributions to the development of the flow systems and editing the thesis; Philip Pritchard for his contribution in the developing stages of the experiments and Mrs. Robin Spencer for typing the manuscript.

I also thank my beloved wife, Lalitha, for her patience and sacrifices during the course of the work. She was always there to give me comfort, warmth and encouragement when needed.

This work was supported in its initial stages by Brookhaven National Laboratory under Subcontract No. 360584-S—for the United States Nuclear Regulatory Commission under Contract No. A3014(03534)—and in the final stages by the United States Nuclear Regulatory Commission under Contract No. NRC-04-78-194. I express my deep appreciation to these agencies for making the funds available.

I. INTRODUCTION

Recently there has been a great deal of interest in the study of two-phase flows involving solid particles or droplets. Although there are a number of conventional techniques available for single-phase flow measurements, most of them are inadequate for measurement of two-phase flows. They fail to distinguish the motion and size of individual particles or droplets and introduce a local disturbance to the flow. Some photographic techniques have been used to obtain the size of the droplets or particles. The majority of these methods are seriously handicapped by the discontinuous nature of accumulation of data. Also, the large number of samples and the size of particles involved makes anything but an electronic counting method very tedious. In addition to size measurement a simultaneous particle velocity measurement is of equal interest. Most of these methods cannot make such a measurement.

The laser-Doppler Anemometer (LDA) with its unique properties has developed into a powerful research tool for the study of single phase flows. Its success has encouraged some researchers to extend the laser-Doppler technique for measurement of two-phase dispersed flows. The two-phase flow properties of primary interest to be measured are the particle size, number density and the velocity distribution of both phases. These properties can only be obtained by statistical analysis of the characteristics of many individual particles. The LDA is still met with considerable problems which

hinder its effectiveness for such measurement. Only under particular circumstances, some of these problems can be handled relatively easily.

One problem which creates an ambiguity in the Doppler signal has been due to the possible presence in the measuring volume of more than one scattering particle at the same time. However, if the LDA measuring volume is extremely small and if the dispersed flow is reasonably dilute, this ambiguity can be removed. Consequently most measurements of two-phase dispersed flows have been restricted to some rather over-simplified conditions [1-6].

Another problem causing signal ambiguity stems from the oscillatory behavior of signal amplitude as a combined function of scattering angle and particle size in accordance with the Mie scattering theory. Strictly speaking, the Mie scattering theory is applicable for observing the scattering from a fixed angle. Any variation in the angle of observation will shift the scattering pattern. In a LDA, since the incident beams are focused, the scattering from a single particle will result in a range of observation angles. Also, because of the combined effect of the finiteness of the size of the particle and the finiteness of its displacement through the measuring volume the observation angle will be continuously varying. These are some of the most pronounced contributions to an uncertainty in the scattering angle.

A numerical analysis of the amplitude function from Mie scat-

tering theory reveals certain characteristics of the oscillations [21] For particles of moderately large sizes, the frequency of these oscillations is found to increase with increase in size, displaying a damped behavior about the mean. The mean of the amplitude function also increases monotonically with size in a confined manner. Hence for particles of moderately large sizes, the average amplitude can be described as a function of particle size.

However, for a large class of problems of practical interest, such as the interpretations of the zodiacal light and of the light scattered from Venus'and Mars'atmospheres, the interest is concerned with ranges of particle size rather than certain precise sizes. This amounts to an integration. over these size ranges, of the scattering light intensity from a cloud of particles with a given distribution of sizes. The numerous maxima and minima shift in position with the size so that, to a large extent the effects of these particular maxima and minima are washed out with the integration [7]. For the present study, where only one particle at a time is considered in the measuring volume, a treatment similar to the above can be made. Here the same washing out effect can be assumed to occur because of the angular variations previously discussed.

In addition, deviation of the actual conditions from those assumed to fit the theory would further enhance this effect. Moreover, though the theoretical computations predict these oscillations, there does not seem to be any experimental verifications, particular-

ly for particles above 6μ in diameter. Therefore, in dilute dispersed flows, if the selected width of the size window is narrow enough the mean amplitude of the signals can be expected to vary monotonically with the mean size of particles.

One additional serious problem causing signal ambiguity stems from the inherent non-uniformity of illumination in the optical measuring volume [8]. Two examples of efforts which have been made to by-pass this difficulty are: a) the use of two optical systems—one for measuring the velocity and the other for particle sizing—which are focused at the same probing point [9] and b) by using two laser beams, each directed toward one photo transistor [10]. Also, considerable effort has been made using large enough particles to render useful the techniques of geometrical optics [6] and by making use of an additional property of the signal [8,11]. It still remains desirable to devise a scheme by which a central core region of the measuring,volume where the illumination is nearly uniform, can be isolated to serve as controlled measuring volume in the flow.

In order to isolate the central core an entirely new methodology [12] and experimental hardware have been developed. This dissertation describes the new methodology, the accompanying calibration scheme and the experimental hardware. Finally, the results of some more extensive experiments with two-phase dilute dispersed flows are presented.

II. THEORY OF THE PROPOSED SCHEME

LASER DOPPLER ANEMOMETER

Historically LDA grew out of work by Cummins et al. on light beating spectroscopy in the early ninteen sixties [13,14] and the principle [15,16,17] has now been well established. In the following paragraphs the fundamental concepts of LDA and some pertinent definitions which relate to this investigation in particular are outlined.

Laser-Doppler anemometry is a technique which utilizes scattered light from tracer particulates in a fluid to measure the velocity of that fluid. In prinicple the laser anemometer is linear, needs no calibration, and measures velocity independent of fluid properties. A relatively small measuring volume and inherently fast response give it the ability to follow rapidly changing velocities in the fluid. Only light needs to enter the fluid at the measuring point (causing no disturbance to the flow). Generally the two basic modes of operation used are dual beam mode and reference beam mode.

Dual beam mode is the crossing of two laser beams of equal intensity at a point in the fluid to be measured. Where these beams cross, they interface with each other to form 'fringes'. A particle moving through the crossing point in the plane of the two beams then goes through a region of very low light intensity (light cancelling) to a region of high intensity and back again. A photo detector is used to pick up the scattered light from the particle.

The frequency of the signal, so obtained, is proportional to the velocity with which the particle is moving across fringes.

Reference beam operation is generally described in terms of Doppler frequency shift of the scattered light and it requires only one light beam at the measuring point. The scattered light from a particle is mixed with a reference beam, to detect the shift in frequency. The photo-detector responds to the difference in frequency which is proportional to the velocity of the particle. In this investigation the reference beam mode of operation has been used.

In both operations the shape of the measuring volume is approximately ellipsoidal as shown in Figure 1. The light intensity has a Caussian distribution with maximum occuring at the center of the measuring volume. The three measurable characteristic parameters of a Doppler signal (Figure 2) are the Doppler signal amplitude, Doppler frequency and path time. The particle velocity is directly proportional to the Doppler signal frequency.

Another important concept in LDA-measurements is that of optical frequency preshift. Frequency shift by means of Bragg cells was used early on in the study of diffusion broadened optical spectra [1]. Since then a number of practical methods have been developed and the use of frequency shift has become a concept of great significance [18]. An optical frequency shift not only allows the direction of the flow velocity to be determined, but also improves the performance of electronic signal processors for measurement of

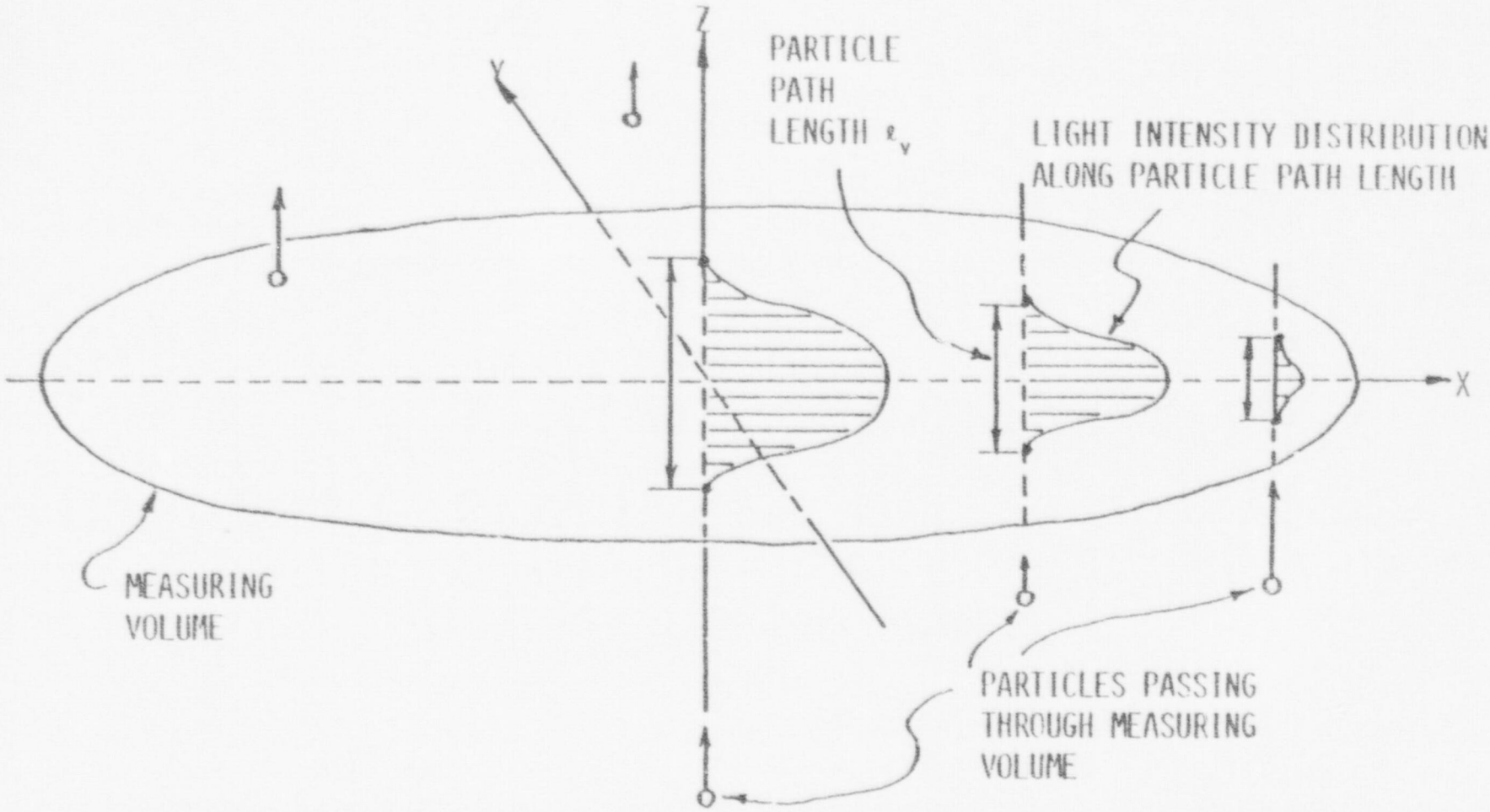

FIGURE 1. SKETCH OF OPTICAL MEASURING VOLUME

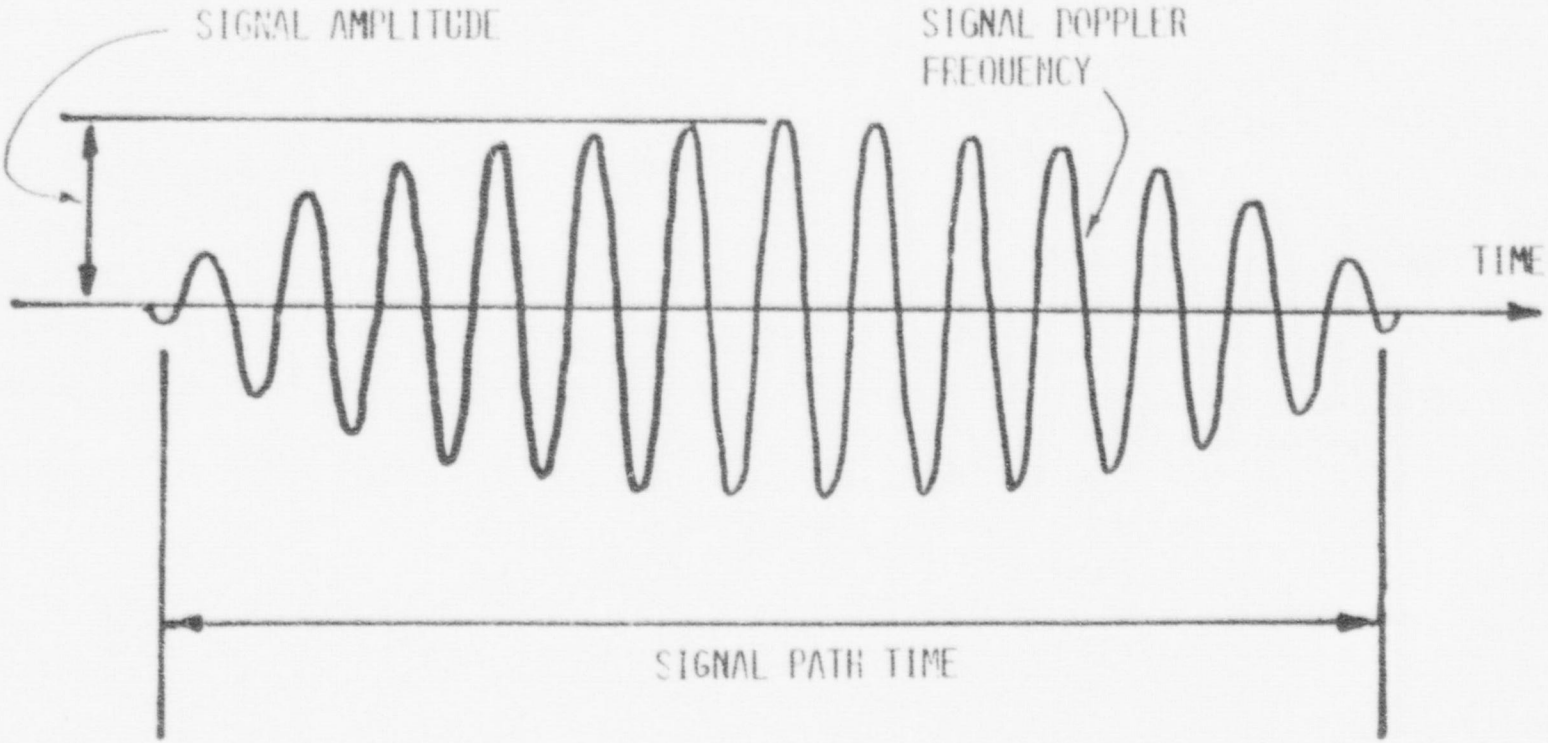

FIGURE 2. SKETCH OF PARTICLE DOPPLER SIGNAL

highly fluctuating flow velocity [19].

THE METHODOLOGY

For a given optical arrangement, for the relatively simple case of spherical scattering of a particular material the Doppler, signal amplitude is mainly a function of the scattering particle size, the number of scattering particles and their instantaneous location in the measuring volume. The Gaussian intensity distribution of the laser beams causes the signal amplitude variation for a single scattering particle as shown in Figure 1.

Using a reasonably dilute dispersed flow (i.e. with a low number density) it can be assumed that there is only one particle in the measuring volume at a time. However, because the measuring volume of the laser-Doppler arrangement is so small the number density allowable actually can be quite large. The maximum number density (particles per cubic centimeter) allowable is merely the number of measuring volumes which would fit in one cubic centimeter. In general, this can be as high as 10^5/cc. Thus, in a statistical analysis, if the number density is less than 10^5/cc, most probably there will not be more than one droplet (of size less than measuring volume) in the measuring volume at one time. The other determining factor, the volumetric concentration, will vary with the size of particles in the disperse phase. This concentration can be calculated by computing the ratio of one particle volume to the measuring volume. However, the maximum diameter of the particle

is again restricted by the size of the measuring volume. For the present set up the maximum particle diameter is less than 120μ and a number density of up to 10^5/cc can be measured. Thus, the problem of ambiguity in the signal amplitude due to presence in the measuring volume of more than one scattering particle at the same time can be reduced by using sufficiently dilute dispersed flows. With such a flow the Doppler signal amplitude is mainly a function of the scattering particle size and the path length of the particle in the measuring volume.

A second necessary assumption is that the predominant direction of flow coincides with one of the measuring directions of the LDA-System. If the flow direction should deviate from the measuring direction by an angle, α, it can be shown that the associated errors in the results are on the order of α^4 (where α is in radians). This is an extremely small quantity. (Appendix-1)

From Figure 1 it is seen that the path length of a particle passing through the measuring volume and the incident light intensity distribution along this path are essentially functions of the location of the path in the measuring volume. The particle path length, ℓ_v, can be obtained from the product of time duration of the signal, τ, and velocity of the particle v_j, which is determined by the Doppler frequency of the signal itself, $\ell_v = \tau v_j$. In order to suppress the ambiguity of the particle size determination from a Doppler signal it is neccessary to consider only the central core of the measuring volume. Here the peak incident light inten-

sity along any particle path length falls within an arbitrarily small, preselected range. In this new probing volume the signal amplitude will be a function of particle size only. The effective measuring volume, i.e., the central core, is electronically isolated by the following discrimination scheme.

SIGNAL AMPLITUDE DISCRIMINATION AND ISOLATED CENTRAL CORE OF MEASURING VOLUME.

Figure 3 gives a sketch of the dependence on path length ℓ_v of the peak amplitude of signals from particles of a certain size d_i, as shown by curve (i), with the maximum peak amplitude A_i located along the maximum path length, ℓ_m, passing through the center of the measuring volmme. A narrow amplitude discrimination window can be selected to operate on the signal peak amplitude, $\Delta A_i = (1-\delta)A_i$, such that $(1-\delta)<<1$, where δ is a constant close to unity. If all the particles are of exactly the same size d_i, the allowable signals are those from particles passing through the central core of the measuring volume, $\bar{\ell}_v<\ell_v<\ell_m$, where $\bar{\ell}_v$ is the limiting path length of the central core. However, when the flow contains particles having a distribution in size the situation needs some clarification. In this case the observed signals in the central core region are determined by the signals from particles of size d_i and by the signals from two adjacent particle size ranges, $d_{i'}\leqslant d\leqslant d_i$ and $d_i\leqslant d\leqslant d_{i''}$, $d_{i'}$ and $d_{i''}$ being represented by curves (i') and (i'') respectively (Figure 3). The relationship between observed signals and the contributions from d_i, $d_{i'}$ and $d_{i''}$ actually varies randomly. How-

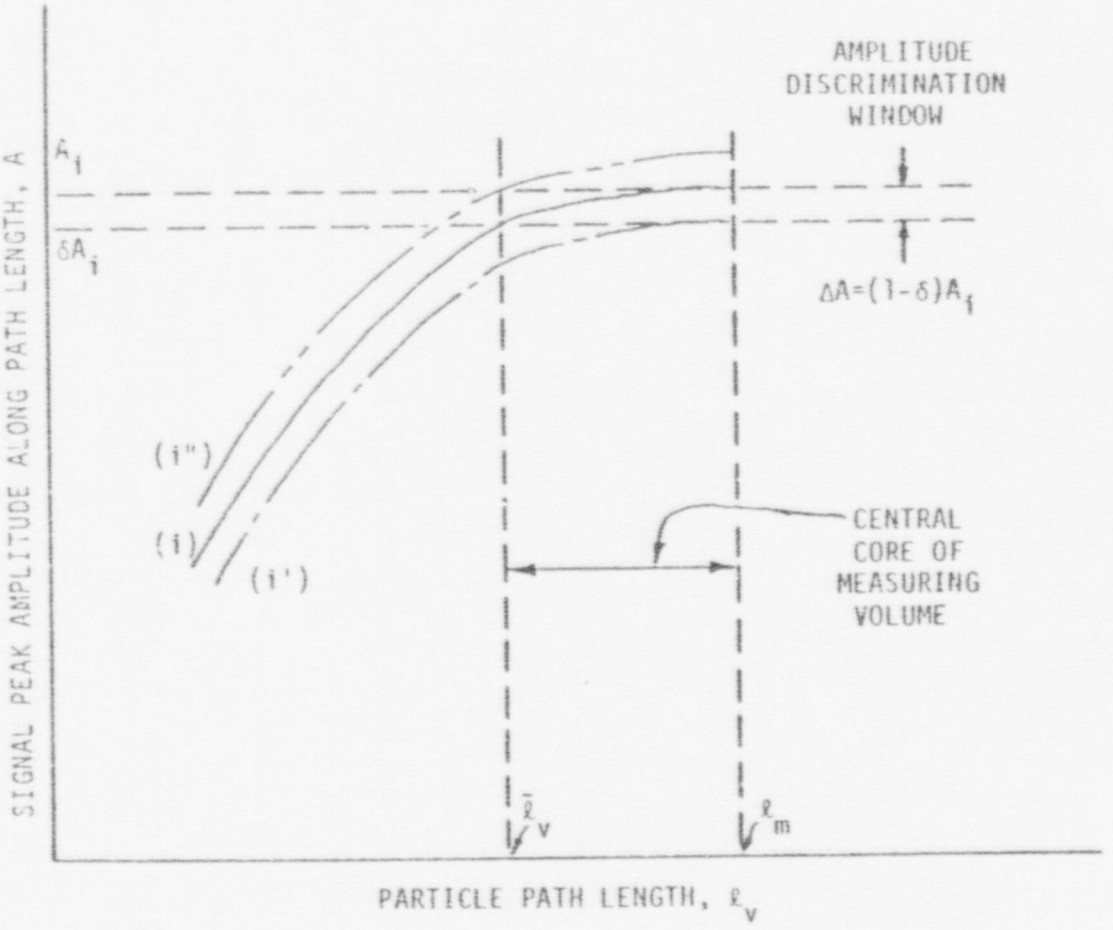

FIGURE 3 SKETCH OF SIGNAL AMPLITUDE DISCRIMINATION SCHEME

ever, for an extremely narrow amplitude window, say, for instance, $\Delta A_i = 0{,}05A_i$, the number density of particles within the affected size range can be considered statistically stable. Then the signals, so discriminated, should accurately represent those with a peak amplitude within the amplitude window ΔA_i around the mean peak amplitude A_i.

The path length of a scattering particle through the measuring volume, ℓ_v, is as shown in Figure 4. By ignoring all signals whose corresponding path length is smaller than a chosen lower limiting value $\bar{\ell}_v$, the dependency of signal ampltiude on the particle position in the measuring volume can essentially be eliminated. This is because the intensity of the incident light in the measuring volume is distributed approximately in a Gaussian manner, so that if only those particles passing through the central core region of the measuring volume ($\bar{\ell}_v \leq \ell_v \leq \ell_m$) are considered, the maximum amplitude of the Doppler signal envelope will then be dependent only on the particle size. The maximum path length, ℓ_m (the one going through the geometrical center of the measuring volume) is obtained empirically by determining the path lengths of many particles through calibration. The lower limiting value of the path length for the central core, $\bar{\ell}_v$, is determined by the choice of a window size for the amplitude discrimination. The window size is properly determined from the amplitude range of untreated Doppler signals from the particular flow under consideration.

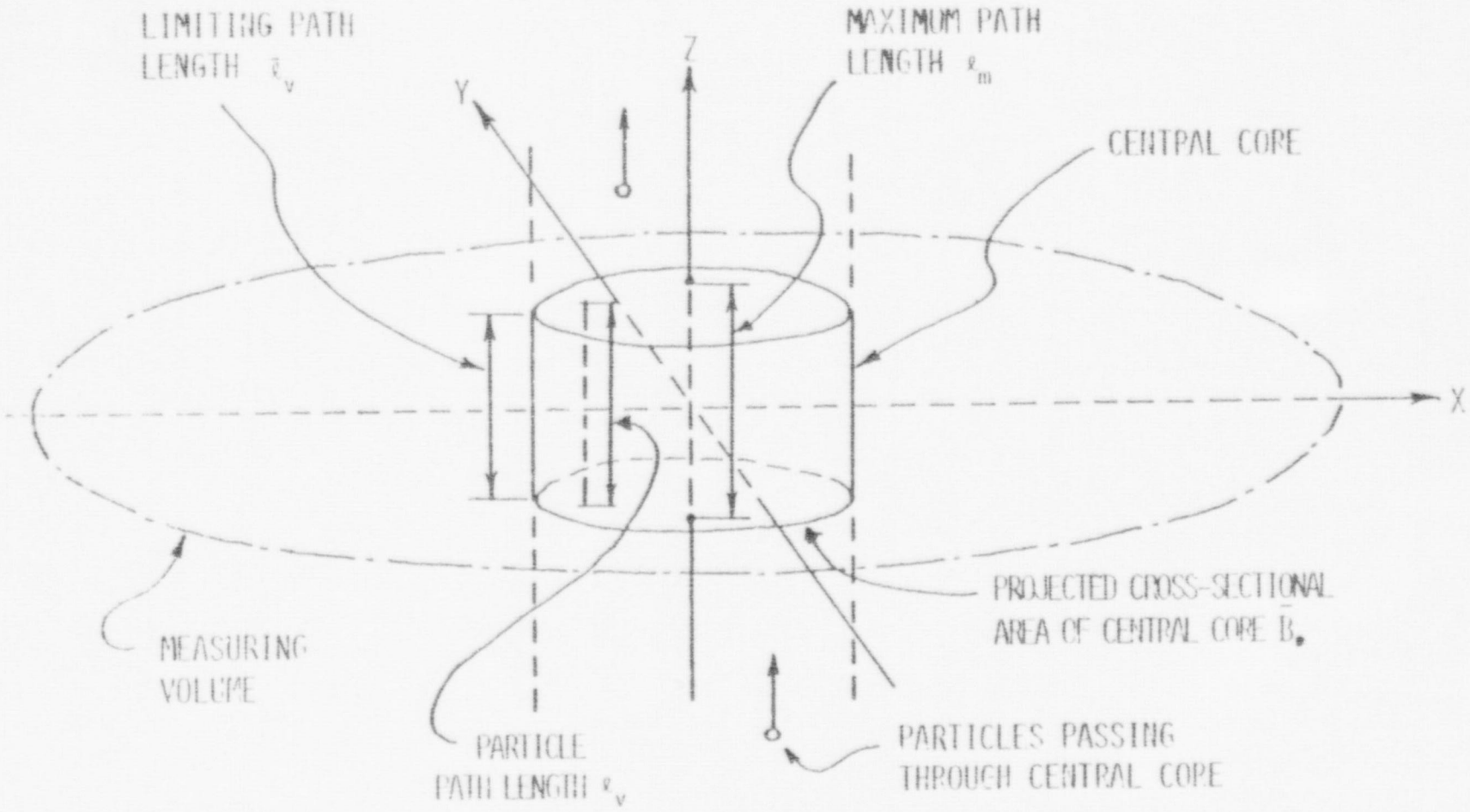

FIGURE 4. SKETCH OF ELECTRONICALLY ISOLATED CENTRAL CORE OF MEASURING VOLUME

PATH LENGTH AND VELOCITY DISCRIMINATIONS

After signal amplitude discrimination, a discrimination against the path length ℓ_v, is made using the limiting path length $\bar{\ell}_v$, of the measuring volume as the lower bound. Only signals within the selected amplitude window, discriminated from particles passing through the central core (Figure 4) will be allowed to go through. Then an additional discrimination of velocity will produce the desired statistics of particle size and velocity distributions in the dispersed flow. Unfortunately it is the particle path time and velocity, rather than the particle path length, which are readily obtainable from signals. However, the product of the particle path time and velocity can be used for the path length discrimination scheme.

Since the amplitude of the envelope of a Doppler signal varies approximately in a Gaussian fashion along a particle path through the measuring volume, the path length determination depends entirely on the base amplitude level, say A_v, at which the measurement is made. It would first seem reasonable to set this base level at zero amplitude. However, in dispersed flow containing particles of sizes which are not negligible compared to the size of the measuring volume, ambiguities on the Doppler signals associated with the particles entering and leaving the measuring volume can no longer be ignored. Because of this point and the inherent noise level of the measuring system the base amplitude level for path length or the equivalent path time determination is to be set at a level which is high enough to be safe yet still low enough for the mod-

erately low amplitude signals to be analyzed. However, the measured path length can be converted to equivalent path length at zero amplitude (Appendix-2). As a matter of fact the very low amplitude signals can be used as tracer signals for the fluid phase in the dispersed flow.

PARTICLE SIZE, NUMBER DENSITY DISTRIBUTIONS AND VELOCITY DISTRIBUTIONS

Based upon the above methodology, the central core of the measuring volume can be isolated and used as a new probing volume. In this central core the signal amplitude will be a function of particle size. This function can be exp imentally determined by using particles of known diameter and velocity. Then by knowing the size and the axial and lateral velocities associated with each particle, the number count, $n_{i,j,k}$, over a period of time, t, can be obtained with an associated size and velocity range. The number density, N_i (number per unit volume and unit size range, with d_i being the average size) can then be determined if the value of the projected cross-sectional area, $\overline{B}_o$, of the central core is known. This value of $\overline{B}_o$ can again be obtained by using single sized particles as explained in the following section.

It should be noted that each of the quantities d_i, v_j and u_k, strictly speaking should refer to a unit range of distribution. For simplicity they will be used to refer to the mean values of their respective unit ranges of distribution. Then for different particle size ranges, d_i, the number densities can be obtained.

The axial and lateral velocity distributions associated with

each size range can readily be obtained using the axial and lateral velocity ranges associated with each size range.

CALIBRATION

The calibration of the Doppler signal amplitude against particle size has to be obtained experimentally using a precisely uniform stream of particles, all having the same size. The particles are sent one after another through the center of the measuring volume. The largest amplitude signals for different sizes can be obtained and the size can be expressed as a function of the signal amplitude.

The projected cross-sectional area, $\overline{B}_o$, of the central core can also be determined by sending the single size particles in a single stream and traversing the measuring volume in two dimensions so that the limiting path length determines the boundary of the central core cross-sectional area. Once these calibrations are performed the distribution of the particle size, number density, axial and lateral velocities can be obtained using the proposed scheme.

HOMOGENEOUS PHASE VELOCITY

As discussed earlier the very low amplitude signals from very small particles serving as tracers can be used to determine the homogeneous phase velocity. Since only the very low amplitude signals are important here the base amplitude level can be set very low. The high amplitude signal envelopes are used to elimin-

ate the analog velocity outputs due to large droplets. Thus only the velocity outputs due to very small droplets will be obtained and are sampled for the determination of homogeneous phase velocity distributions.

III. MEASUREMENTS USING THE DEVELOPED METHODOLOGY: TWO-PHASE DISPERSED FLOW, (Solid particles-water)

The developed methodology was first tested using a relatively simple dispersed flow of neutrally buoyant hollow glass spheres, with a distributed size range, suspended in water in a closed-loop water channel. Only the predominant velocity component was measured. Since the product of particle path time and velocity was not readily obtained, a special scheme of combined time and velocity discriminations was developed, instead of a path length discrimination, to isolate the central core of the measuring volume. According to the calibration scheme only particles of one single precise size can be allowed in the flow. This is not easily attainable because of the difficulty of obtaining such particles. However, a substitute way had been found in experimenting with dilute dispersed flow. The combined time and velocity discrimination scheme and the alternate way of calibration are elaborated in the following discussions.

COMBINED TIME AND VELOCITY DISCRIMINATIONS

By setting a lower limit on the time duration τ, say $\overline{\tau}$, using a time discrimination scheme, and a related lower limit on the velocity v_j, $\overline{\ell}_v/\overline{\tau}$, using velocity discrimination one can retain signals within the velocity range $\overline{\ell}_v/\overline{\tau} < v_j < \ell_v/\overline{\tau}$ which can be produced by particles going through the central core region of the measuring volume, $\overline{\ell}_v < \ell_v < \ell_m$, as shown by the sketch in Figure 5. However, this is not to say that these signals represent the signals

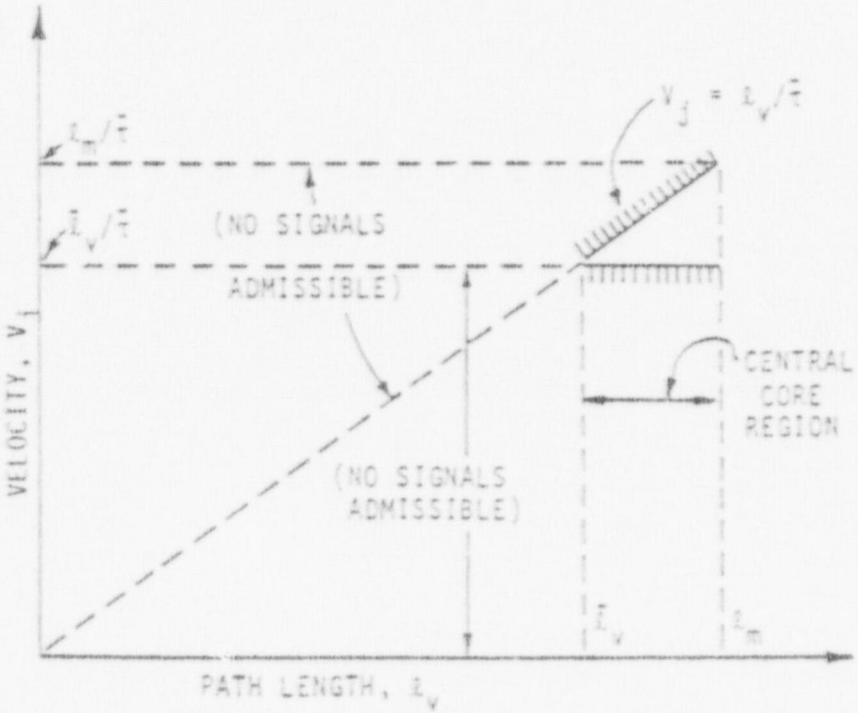

FIGURE 5. SKETCH OF CRITERION OF SIGNAL ADMISSIBILITY DUE TO DURATION TIME DISCRIMINATION

produced by all the particles of the specified size d_i (corresponding to signals of amplitude A_i) which pass through the central core region, because the signals from those particles which have a velocity above the upper limit of the local admissable velocity range, $\frac{\ell_v}{\overline{\tau}}$, that pass through the central core region, will not be registered. In order to obtain the correct number count appropriate for the determination of the velocity probability density distributions and particle size number densities from the measured number count so obtained, the following correction scheme is used.

The number count per unit time per unit cross-sectional area of flow, per unit velocity range, and unit size range, $n_{i,j}$, for the small velocity range considered ($\frac{\overline{\ell}_v}{\overline{\tau}} < v_j < \frac{\ell_m}{\overline{\tau}}$) in the central core region can be considered approximately constant for a statistically steady flow. Conceptually, the number count for each elementary annular region within the central core region and for the permissible local velocity range and size range, can be first determined from the product of the number count $\dot{n}_{i,j}$, the cross-sectional flow area of the elementary annulus, dB_o, and the size of the local admissible velocity range, $(\ell_v/\overline{\tau} - \overline{\ell}_v/\overline{\tau})$ where $\overline{\ell}_v < \ell_v < \ell_m$, and size range, Δd_i, in which d_i is the mean particle size, $\dot{n}_{i,j}$ $dB_o(\frac{\ell_v}{\overline{\tau}} - \frac{\overline{\ell}_v}{\overline{\tau}})\Delta d_i$. By summing these number counts over all elementary annular regions within the central core region,

$$\int_o^{\overline{B}_o} n_{i,j} \Delta d_i \left(\frac{\ell}{\overline{\tau}} - \frac{\overline{\ell}_v}{\overline{\tau}}\right) dB_o,$$

where $\overline{B}_o$ is the projected cross-sectional area of central core and $\ell_v = \ell_v(B_o)$, a total number count for the entire central core region including the effect of the local permissible velocity range can be obtained. On the other hand, however, the appropriate correct number count for this case would be obtained by considering the maximum velocity range $(\frac{\ell_v}{\overline{\tau}} < v_j < \frac{\ell_m}{\overline{\tau}})$ to be operational over the entire central core region instead of the local permissible velocity range, $\dot{n}_{i,j} \cdot \Delta d_i \cdot \overline{B}_o (\frac{\ell_m}{\overline{\tau}} - \frac{\ell_v}{\overline{\tau}})$. The ratio of the former to the latter computed total number counts provides the needed correction factor K to adjust each measured total number count to the corresponding appropriate total number count:

$$K = \frac{\text{Actual number count}}{\text{Correct number count}} = \int_0^{\overline{B}_o} \frac{(\ell_v - \overline{\ell}_v)}{(\ell_m - \overline{\ell}_v)} \frac{dB_o}{\overline{B}_o} .$$

Once the correction factor K is determined, the actual number count divided by K will give the corrected number count. This corrected number count is then divided by the velocity range considered $(\ell_m/\overline{\tau} - \overline{\ell}_v/\overline{\tau})$ and the size range Δd_i and the cross-sectional area of the central core region $(\overline{B}_o)$, to give the probability density $\dot{n}_{i,j}$, which is the number count per unit time, per unit cross-sectional flow area, per unit velocity range and unit size range, for particles of size d_i and velocity v_j where v_j is now the mean velocity in the small velocity range considered (i.e. $v_j = (\ell_m/\overline{\tau} + \overline{\ell}_v/\overline{\tau})/2$).

Let $N_{i,j}$ = No. of particles of size d_i per unit volume, per unit velocity range and unit size range with the center velocity v_j.

Then

$$\dot{n}_{i,j} = N_{i,j}\, v_j \tag{1}$$

and

$$N_i = \sum_j N_{i,j} = \sum_j \frac{\dot{n}_{i,j}}{v_j} \tag{2}$$

where N_i = number density of particles of size d_i.

Thus, the number density N_i of each particle size can be obtained if the probability density $\dot{n}_{i,j}$ of each particle size and velocity is known. Before the probability density $\dot{n}_{i,j}$ can be determined the value of the cross-sectional area $\overline{B}_o$ is required as described above. This value of $\overline{B}_o$ is determined from calibration with a flow of known number density $(N_i)_o$ and a uniform particle size d_i with the same velocity $(v_j)_o$ as shown in Figure 6. The value of $(\dot{n}_{i,j})_o$, the probablility density for this case, can be computed from the known number density $(N_i)_o$ and the measured velocity $(v_j)_o$, $(\dot{n}_{i,j})_o = (N_i)_o \cdot (v_j)_o$. It should be noted that for this over-simplified case, $(\dot{n}_{i,j})_o$ simply stands for the number count of particles of size d_i having velocity $(v_j)_o$ per unit cross-sectional area of flow. By comparing this to the total number count for the whole central core region, obtained by a scheme of gradually raising the lower limit on the duration time discrimination, $\overline{\tau}$, the value of $\overline{B}_o$ can be obtained since $\overline{B}_o$ is simply the ratio of this total number count to the number count per unit cross-sectional area

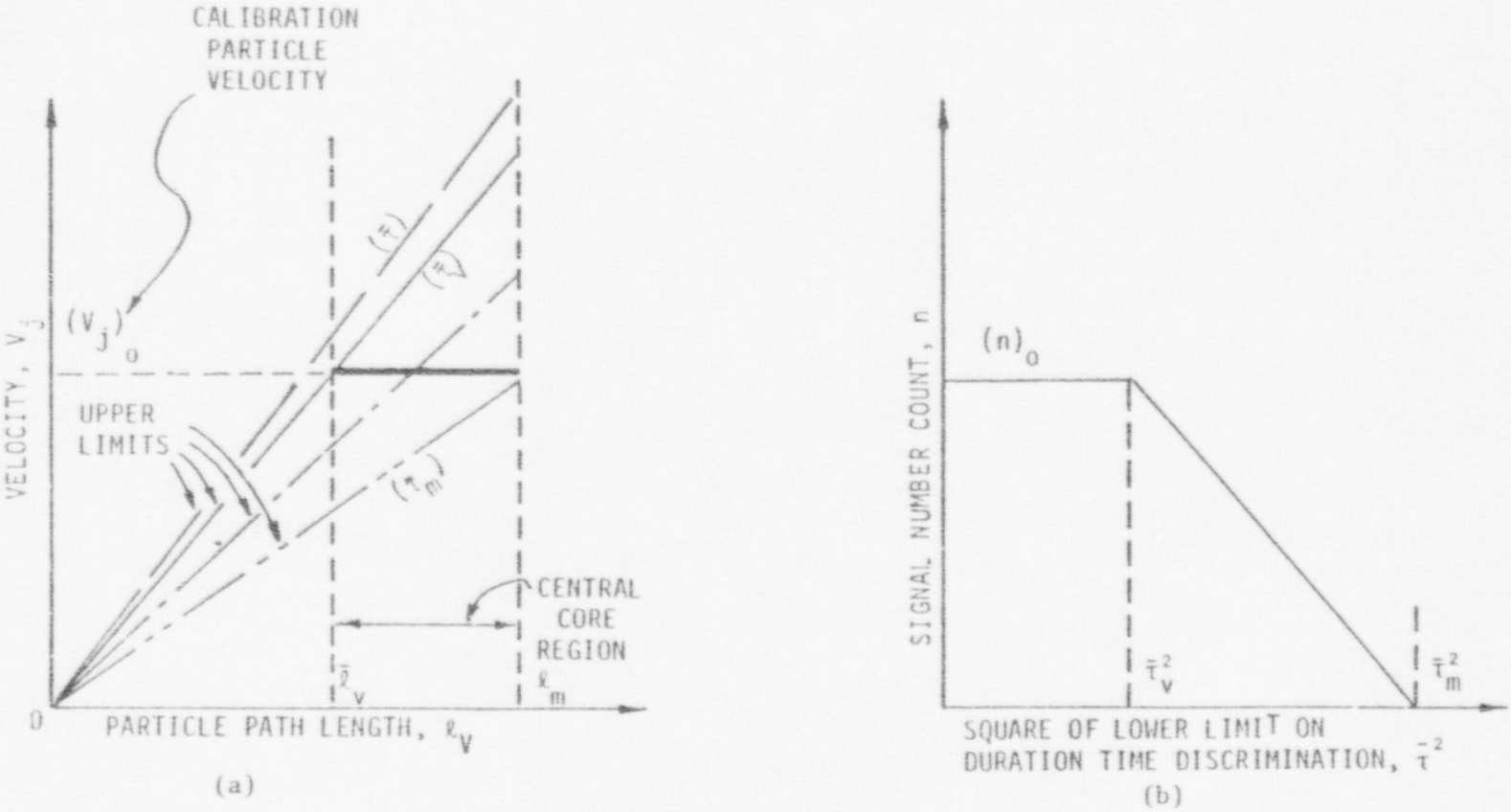

FIGURE 6. SKETCH OF CALIBRATION SCHEME

of the central core, $(\dot{n}_{i,j})_o$. Here $\bar{\tau}$ is gradually raised to such a critical value, say $\bar{\tau}_v$, that the number count n starts to decrease from the previously stable value $(n)_c$. This situation corresponds to the condition $\bar{\ell}_v/\bar{\tau}_v = (v_j)_o$ by which signals from all particles passing through the central core region ($\ell_v < \ell_v < \ell_m$) are registered, and the bounding path length for the central core, $\bar{\ell}_v$, is simply $\bar{\tau}_v(v_j)_o$ evaluated with the measured $(v_j)_o$ and the value of $\bar{\tau}_v$ so obtained. As $\bar{\tau}$ is finally raised to another critical value, say $\bar{\tau}_m$, the number count of signals becomes zero. This situation corresponds to the condition $\ell_m/\bar{\tau}_m = (v_j)_o$, and the maximum path length ℓ_m (the one passing through the center of the measuring volume) is simply $\bar{\tau}_m(v_j)_o$ evaluated with the measured velocity $(v_j)_o$ and the value of $\bar{\tau}_m$ so obtained. To facilitate the determination of $\bar{\tau}_v$ and $\bar{\tau}_m$, the number count n is plotted against $(\bar{\tau})^2$ as suggested by an analysis of the path length through an ellipsoid. For a measuring volume approximately elliptical in shape the plot should be made up of two approximately straight segments as shown in Figure 6. (Appendix-3).

It is of interest to note that since the number count n and the path length ℓ_v for this oversimplified case are proportional respectively to B_o and $\bar{\tau}$, the correction factor K, needed for converting the actual number count to corrected number count, can be readily obtained from (Appendix-3).

$$K = \frac{1}{3} \frac{(2\bar{\tau}_m^2 - \bar{\tau}_m\bar{\tau}_v - \bar{\tau}_v^2)}{(\bar{\tau}_m^2 - \bar{\tau}_v^2)} \qquad (3)$$

INSTRUMENTATION AND EXPERIMENTAL APPARATUS

The operational arrangement of the reference-mode Laser-Doppler Anemometer is shown in the sketch of Figure 7. The oncoming laser beam from a 15mw He-Ne laser was split into two beams: the scatter beam which formed an angle of 7.5° with the transverse axis in a horizontal plane, and the reference beam. The measuring volume was approximately ellipsoidal, 250μ in diameter and 800μ in length. However, a variable aperture used in the receiving optics further reduced the effective measuring volume length. The receiving lenses were symmetrical with the sending lenses and the scattering angle was fixed at 15 degrees. The scattered light received from a moving scattering body passing through the scattering volume was mixed with an unshifted reference beam to generate a heterodyne on the photomultiplier tube surface, producing the Doppler frequency shift signal.

The flow apparatus consisted of a precision close-loop water channel which has a length of 6.10 m and inside dimensions of 457 mm wide and 305 mm deep. The walls were made of optical grade plate glass. The entire optical system was mounted on top of a heavy traversing base which was aligned with the water channel. The device was capable of positioning the optical measuring volume inside the water channel accurately to within 25μ in all three directions. The water channel received its water supply from a micronite filter with a maximum pore size of 3μ. Precision neutrally buoyant hollow

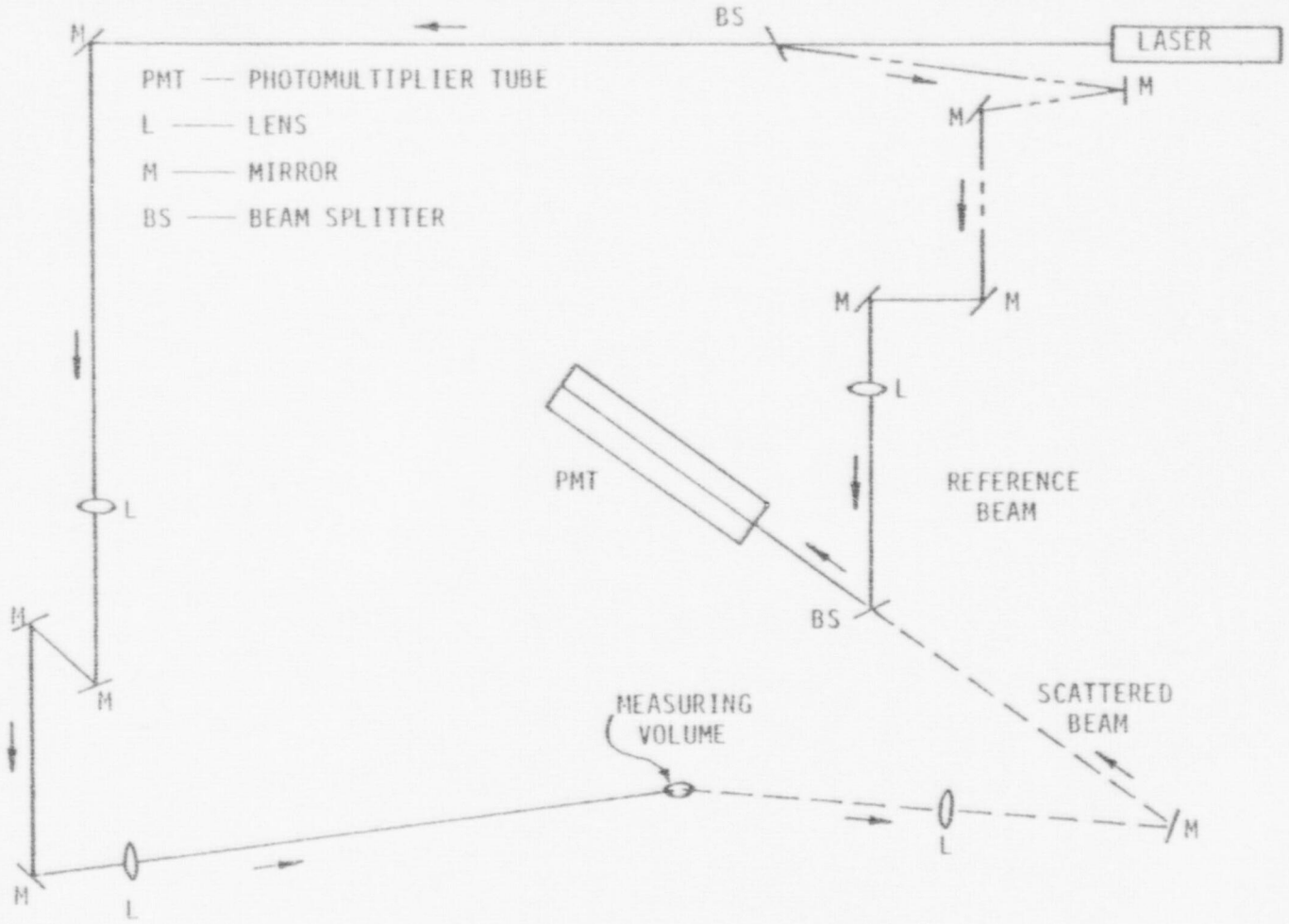

FIGURE 7. OPTICAL ARRANGEMENT

glass spheres of sizes having a distributed size range of up to 35μ were added to the channel flow loop to serve as the disperse phase. The Doppler signals from the optical anemometry system were first recorded on a magnetic tape and later played back at a slower speed for data processing in the instrumentation system.

Instead of measuring the amplitude (A_i), time duration (τ) and velocity (v_j) of each signal, the output of the LDA was filtered as shown in Figure 8. With the amplitude discrimination set on signal amplitude A_i and the time discrimination set on the lower limit of the signal path duration time $\overline{\tau}$, only the signals having an amplitude within the pre-selected narrow amplitude window in the neighborhood of A_i and a duration time $\tau > \overline{\tau}$ could reach the tracker. The tracker then converted the Doppler frequency of the signals into voltage signals proportional to the particle velocities. The output of the tracker was passed to a velocity discriminator circuit which passed only those signals with a voltage (corresponding to the particle velocities) above a certain value (equal to $\frac{\overline{\ell}_v}{\overline{\tau}}$). This resulted in signals for which the product $v_j \cdot \tau = \ell_v$ was a value greater than $\overline{\ell}_v$, and hence only for those particles passing through the central core region. The number count of such signals was executed on an electronic counter to give the measured number count of particles of a particular size and a particular velocity as previously described. By changing the time discriminator lower limit $\overline{\tau}$ and the corresponding velocity discriminator lower limit $\frac{\overline{\ell}_v}{\overline{\tau}}$, the

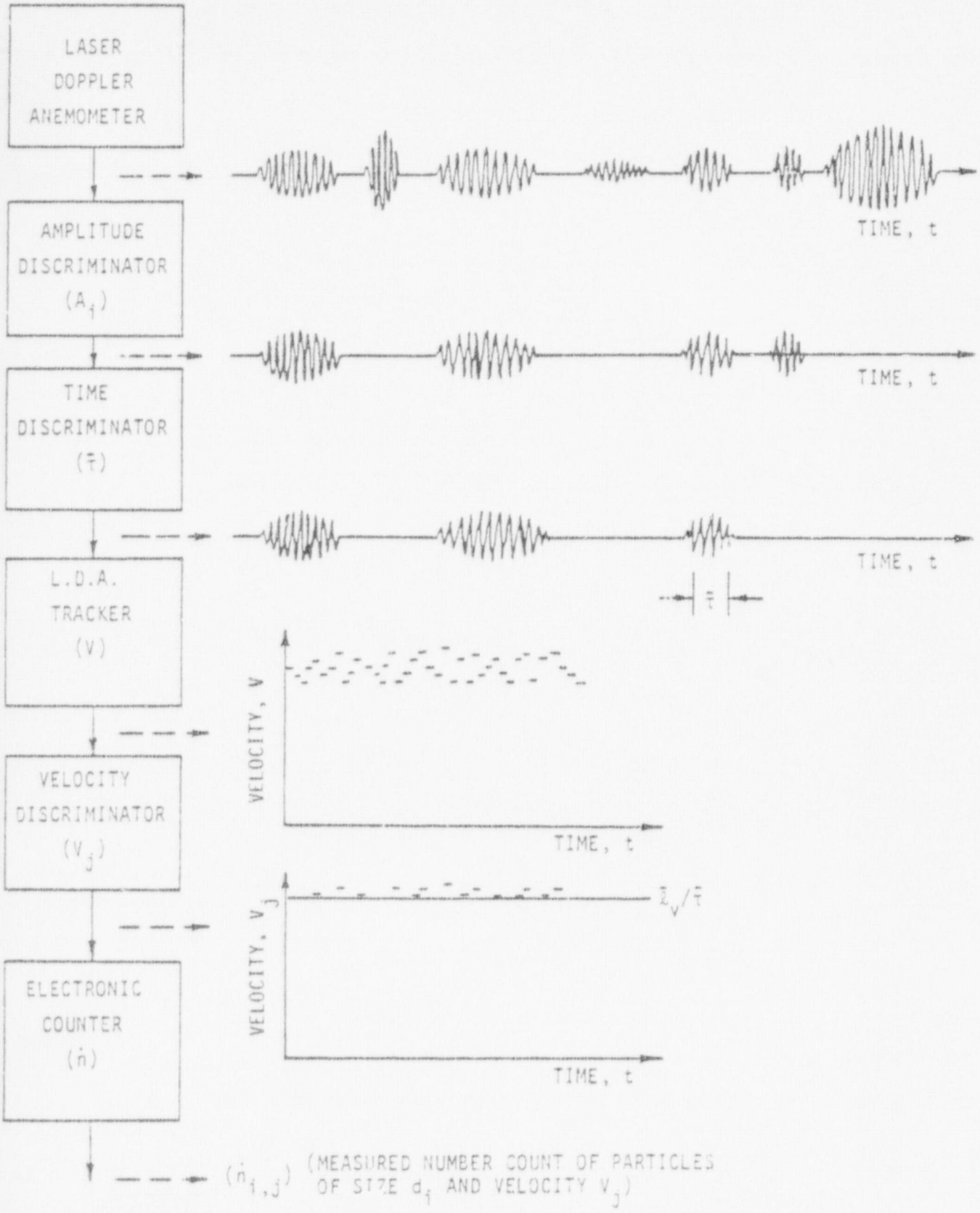

FIGURE 8. OPERATIONAL BLOCK DIAGRAM FOR SIGNAL DISCRIMINATION SCHEME

number counts at different velocities could be obtained for particles in the same size range. Then, by systematically changing the setting of the amplitude discriminator and repeating the aforementioned time and velocity discrimination schemes, the statistics of the complete particle size range could be determined. Furthermore, by analyzing signals from particles of small enough size the velocity probability distribution for the fluid phase could also be obtained, using these small particles as tracers. An instrumentation block diagram is shown in Figure 9.

CALIBRATION

As was mentioned concerning the calibration scheme as shown in Figure 6, a substitute way was found by experimenting with very dilute suspension of particles of distributed sizes [21].

The optical measuring volume was placed in that portion of the water channel where a laminar uniform free stream flow, $(v_j)_o$ = 6.43 cm/sec, was established as shown in Figure 10. In a preliminary trial run the amplitude discrimination window was deliberately made very narrow to scan over the whole amplitude range and to obtain a rough picture of the signal amplitude distribution pattern. Due to the dilution of particles and the very narrow amplitude window size used the signal amplitude displayed a discrete size distribution at a very few isolated amplitudes. Any of these amplitudes could be tested for suitability as a substitute for the single sized particles needed for calibration. One of them, A_i = 770~810 mV

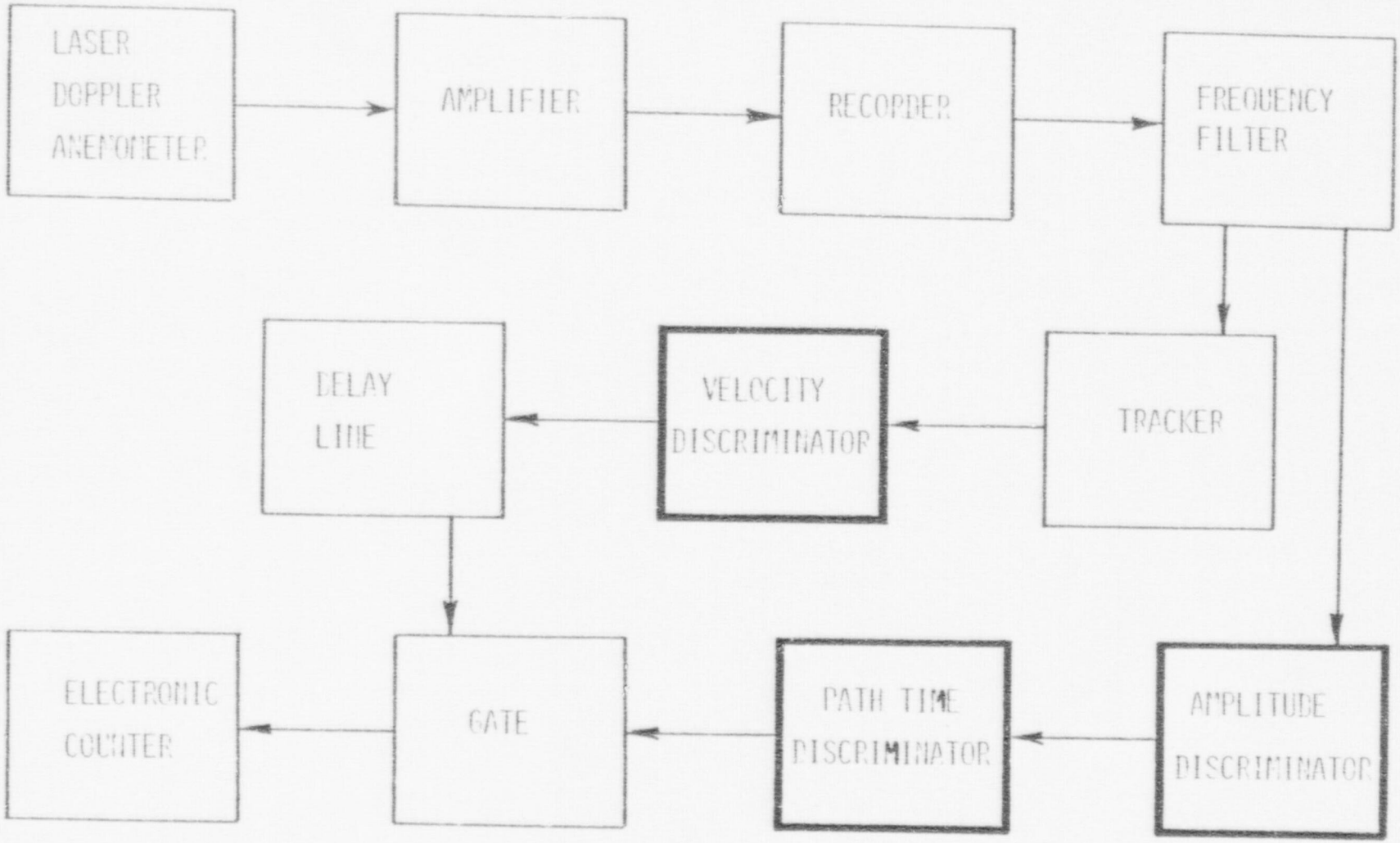

FIG. 9. INSTRUMENTATION BLOCK DIAGRAM

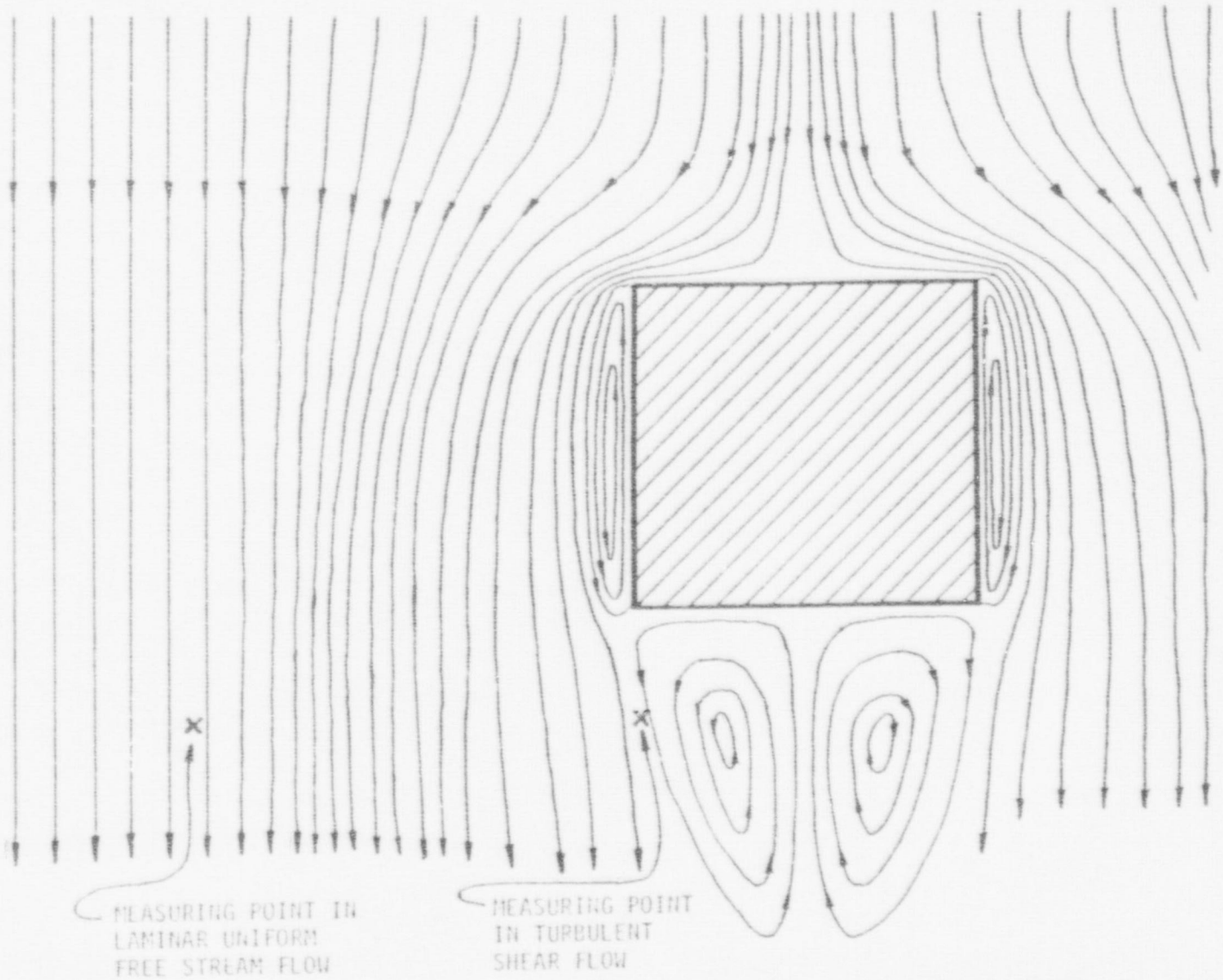

FIGURE 10. FLOW OF A TWO-PHASE SUSPENSION AROUND A TRANSVERSE RECTANGULAR BODY

was finally adopted and its suitability for this task was demonstrated in the well behaved calibration curve $\bar{\tau}^2$, shown in Figure 11. The duration time $\tilde{\tau}$, based on a tape speed of 15 inches/sec., was twice as large as $\bar{\tau}$, based on the recording speed of 30 inches/sec., and the operational amplitude window size $\Delta A_i = 0.05A_i$. The total tape length was 605 ft. The two important quantities characterizing the central core of the measuring volume for this case were found to be:

$$\bar{\ell}_v = 228\mu$$

$$\ell_m = 267\mu.$$

And the correction factor needed to convert the actual number count to the corrected number count, according to Eqn. (3), has the value:

$$K = 0.536.$$

The next step was to establish a calibration between the signal amplitude and particle size from the signal number count and particle number density by an independent measurement of the water sample. The accumulative actual signal number count, [n], for signals in the amplitude range A_i to A_{max}, the maximum amplitude for the various signal amplitudes is plotted in Figure 12. The curve gives the limiting value:

$$[n] = 1, \text{ at } A_{max} = 1.08v.$$

Water samples taken immediately downstream of the measuring volume with an isokinetic probe were analyzed with a Coulter (Model B) counter. The resulting accumulative particle number density

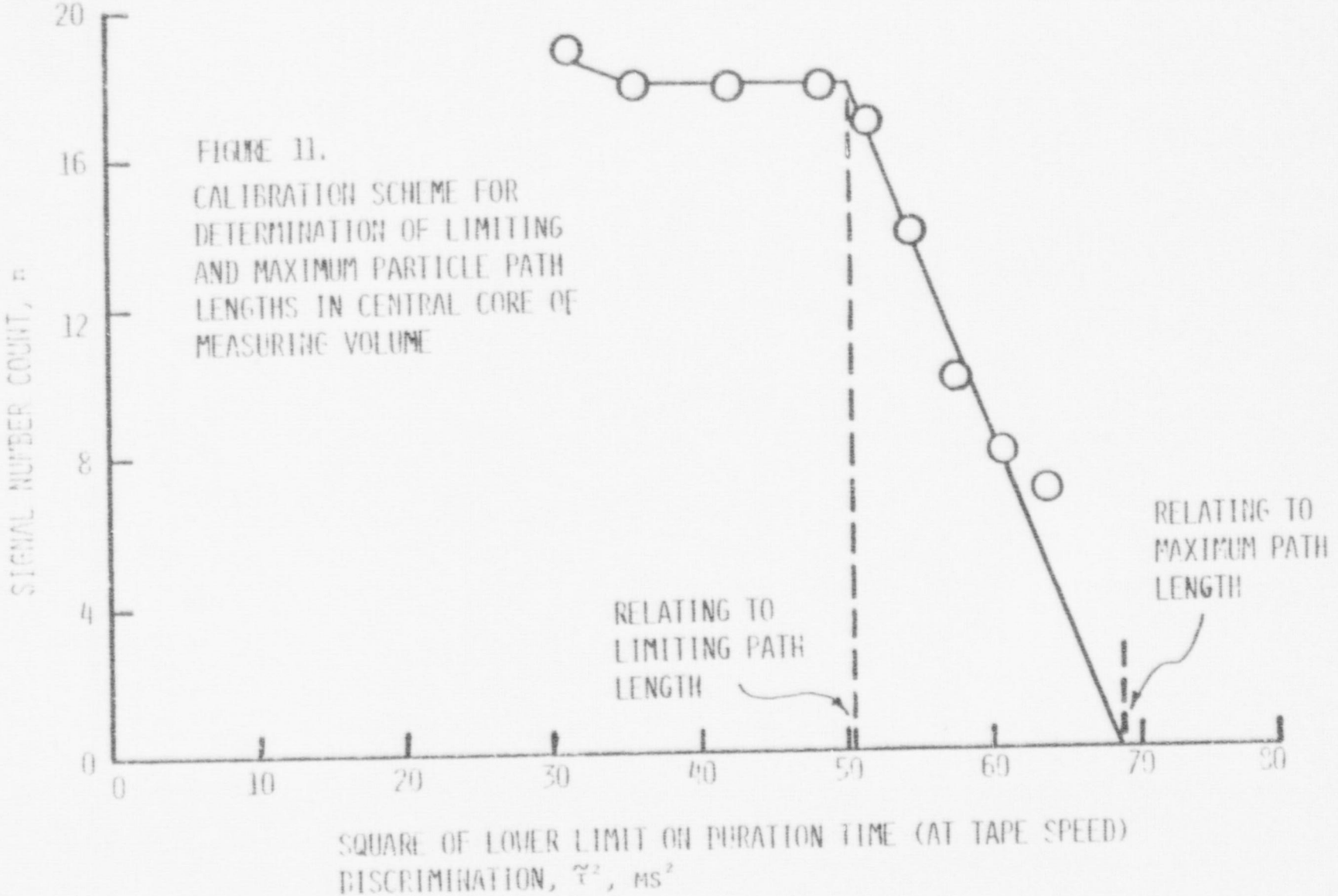

FIGURE 11.
CALIBRATION SCHEME FOR DETERMINATION OF LIMITING AND MAXIMUM PARTICLE PATH LENGTHS IN CENTRAL CORE OF MEASURING VOLUME

FIG. 12. SIGNAL AMPLITUDE AND NUMBER COUNT DISTRIBUTION

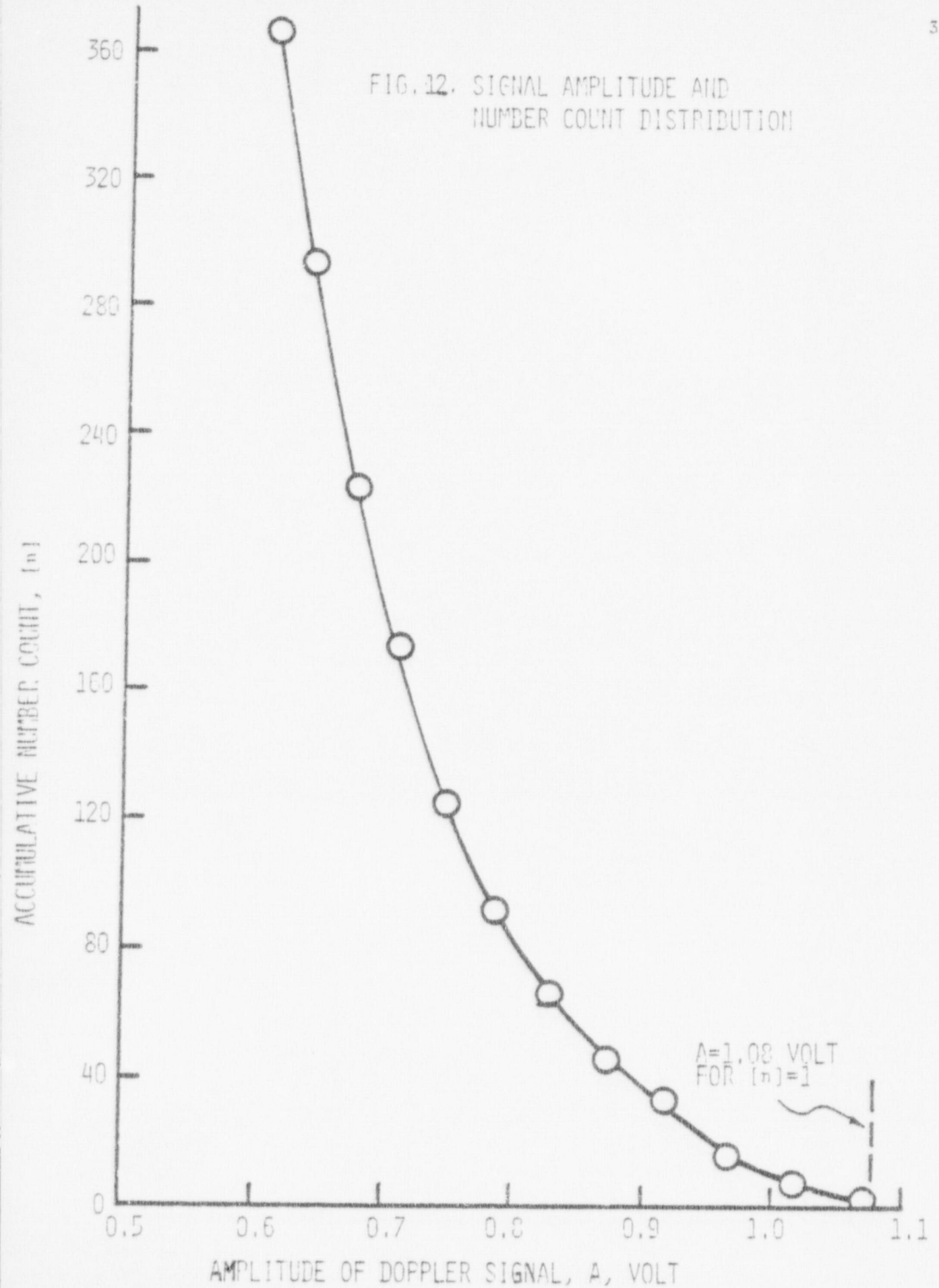

count, [N], for particles in the size range d_i to d_{max}, the maximum size for the various particle sizes is plotted in Figure 13. The curve gives the limiting value:

$$[N] = 1, \text{ at } d_{max} = 33.4\mu$$

By definition, for the uniform flow,

$$n_i = K\, N_i (v_j)_o\, \bar{B}_o\, T_o = k\, N_i$$

where n_i = actual signal number count of signals of amplitude A_i

K = correction factor for signal number count

N_i = number density of particles of size d_i

$(v_j)_o$ = uniform mixture velocity

$\bar{B}_o$ = base cross-sectional area of central core of measuring volume,

T_o = tape recording time

k = $K(v_j)_o\, \bar{B}_o\, T_o$, a constant

Therefore we have the relationship

$$[n] = k[N]$$

between the two accumulative quantities. Furthermore, if we let

$$A^* = A_i/A_{max} \text{ and } d^* = d_i/d_{max}$$

the following relations can be established:

$$\frac{d\{\ell n[N]\}}{d(d^*)} = \frac{d\{\ell n[N]\}}{d(A^*)} \cdot \frac{d(A^*)}{d(d^*)}$$

$$\frac{d\{\ell n[N]\}}{d(A^*)} = \frac{1}{[N]} \frac{d[N]}{d(A^*)} = \frac{k}{[n]} \frac{1}{k} \frac{d[n]}{d(A^*)} = \frac{d\{\ell n[n]\}}{d(A^*)}$$

Therefore,

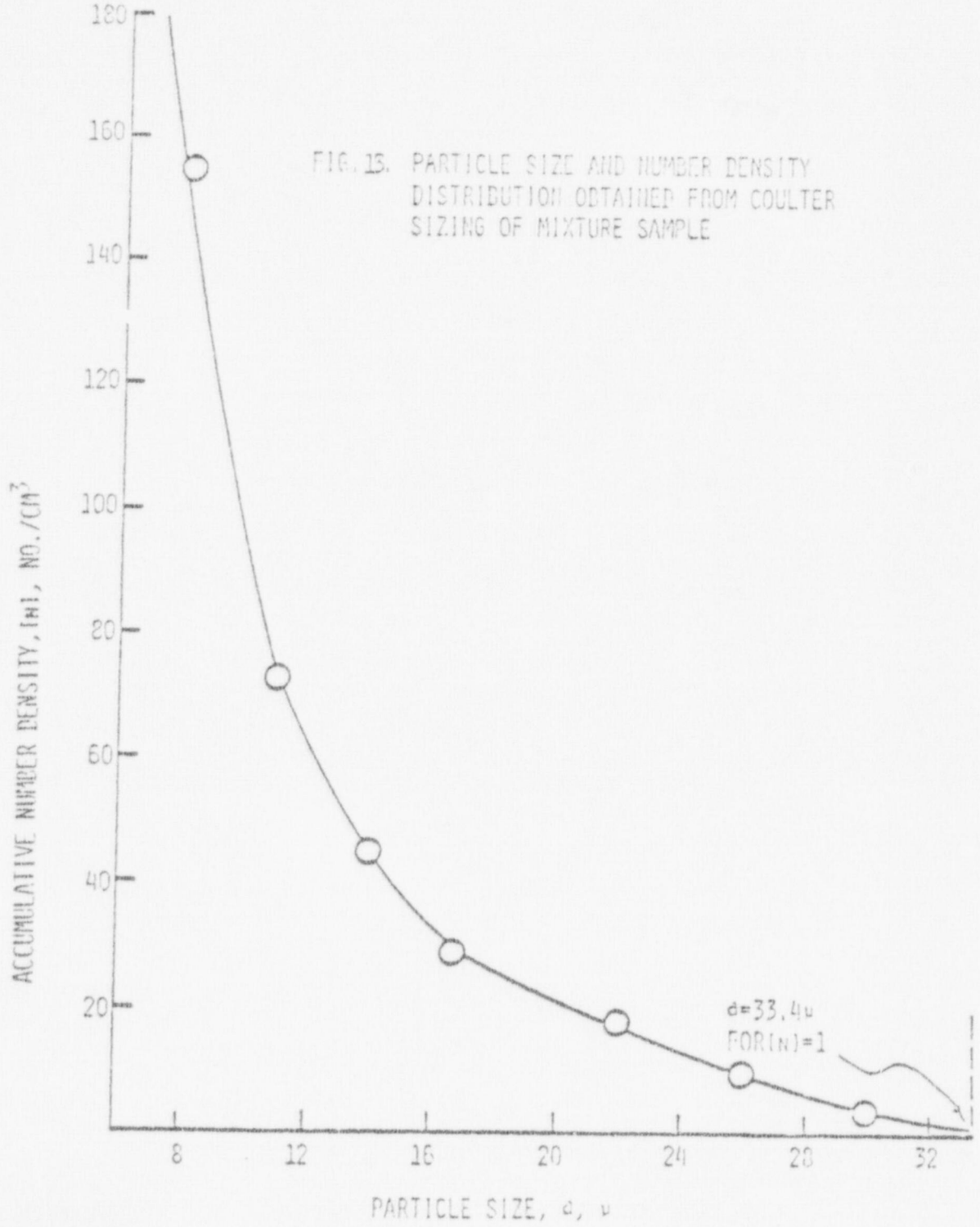

FIG. 13. PARTICLE SIZE AND NUMBER DENSITY DISTRIBUTION OBTAINED FROM COULTER SIZING OF MIXTURE SAMPLE

$$\frac{d\{\ell n[N]\}}{d(d^*)} = \frac{d\{\ell n[n]\}}{d(A^*)} \cdot \frac{d(A^*)}{d(d^*)}$$

which, after integration, becomes

$$\{\ell n[N]\} \Big|_{d^*}^{d^*=1} = \{\ell n[n]\} \Big|_{A^*}^{A^*=1}$$

Since, at $d^*=1$: $N=1$ and $\ell n[N]=0$

and at $A^*=1$: $n=1$ and $\ell n[n]=0$

the relationship reduces to:

$$\ell n[N] \Big|_{\text{at } d^*} = \ell n[n] \Big|_{\text{at } A^*}$$

which establishes a unique correlation relationship between d* and A* as shown by computational scheme of Figure 14. The resultant calibration curve between the normalized particle size d* and signal amplitude is shown in Figure 15. Results from direct amplitude measurement using particles of five precise size ranges are also plotted for comparison. The dimensional calibration curve between particle size and signal amplitude is plotted in Figure 16. Using this calibration, the resultant particle size and number density distribution in this laminar uniform free stream flow is plotted in Figure 17.

Further, in the previous calibration run for the determination of $\overline{\ell}_v$, ℓ_m and K as shown in Figure 11, we have

$$(n)_o = (N_i)_o \, (v_j)_o \, \overline{E}_o \, T_o$$

where $(n)_o = 18$, the stabilized number count

$(N_i)_o = 26/\text{cm}^3$, the number density of particles with sizes

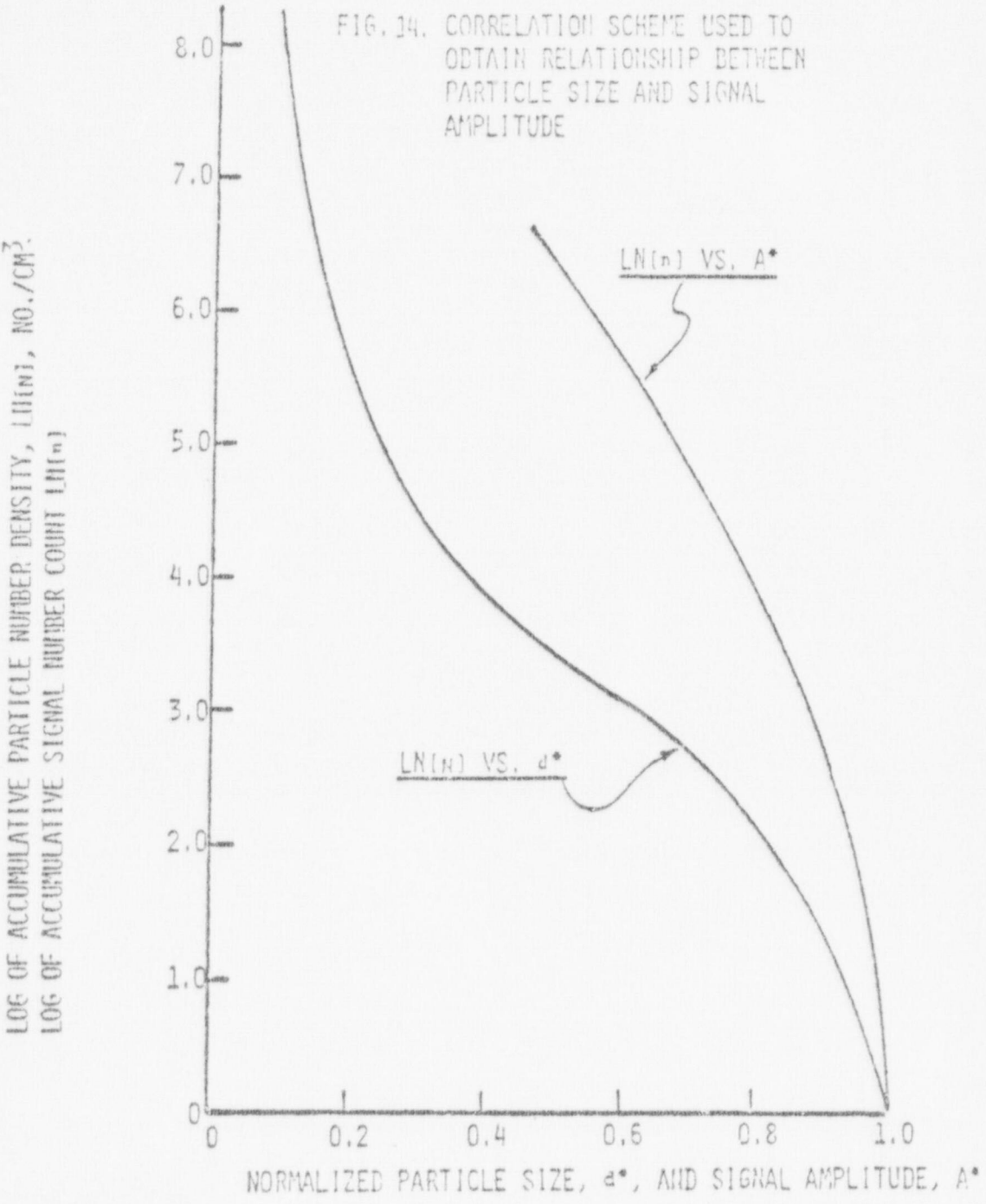
FIG. 14. CORRELATION SCHEME USED TO OBTAIN RELATIONSHIP BETWEEN PARTICLE SIZE AND SIGNAL AMPLITUDE
LN(n) VS. A*
LN(n) VS. d*
LOG OF ACCUMULATIVE PARTICLE NUMBER DENSITY, LN(n), NO./CM³.
LOG OF ACCUMULATIVE SIGNAL NUMBER COUNT LN(n)
8.0
7.0
6.0
5.0
4.0
3.0
2.0
1.0
0
0
0.2
0.4
0.6
0.8
1.0
NORMALIZED PARTICLE SIZE, d*, AND SIGNAL AMPLITUDE, A*

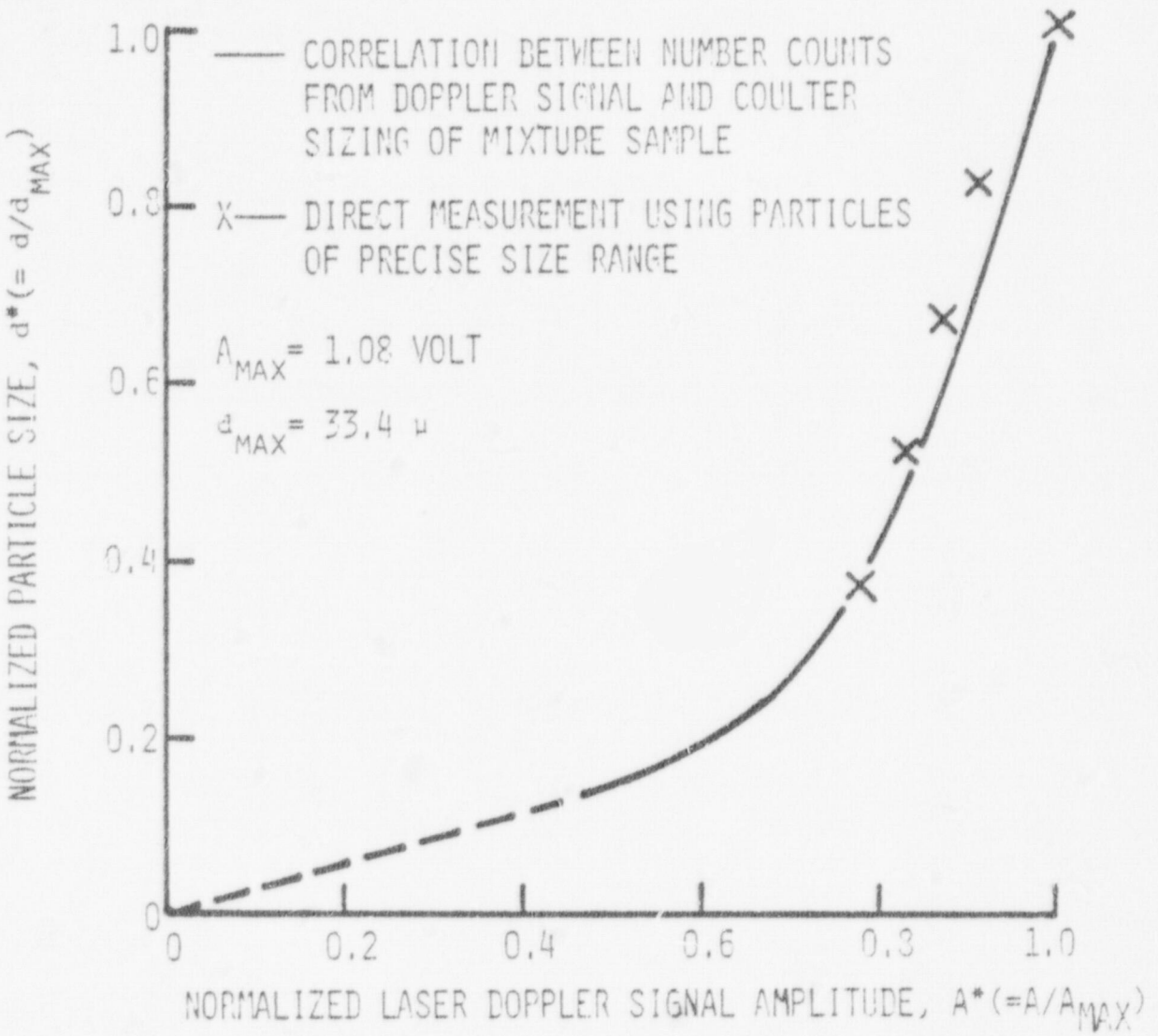

FIG. 15. COMPARISON OF SIGNAL AMPLITUDE CALIBRATION RESULTS FROM NUMBER COUNT CORRELATION AND DIRECT MEASUREMENT USING PARTICLES OF PRECISE SIZE RANGE

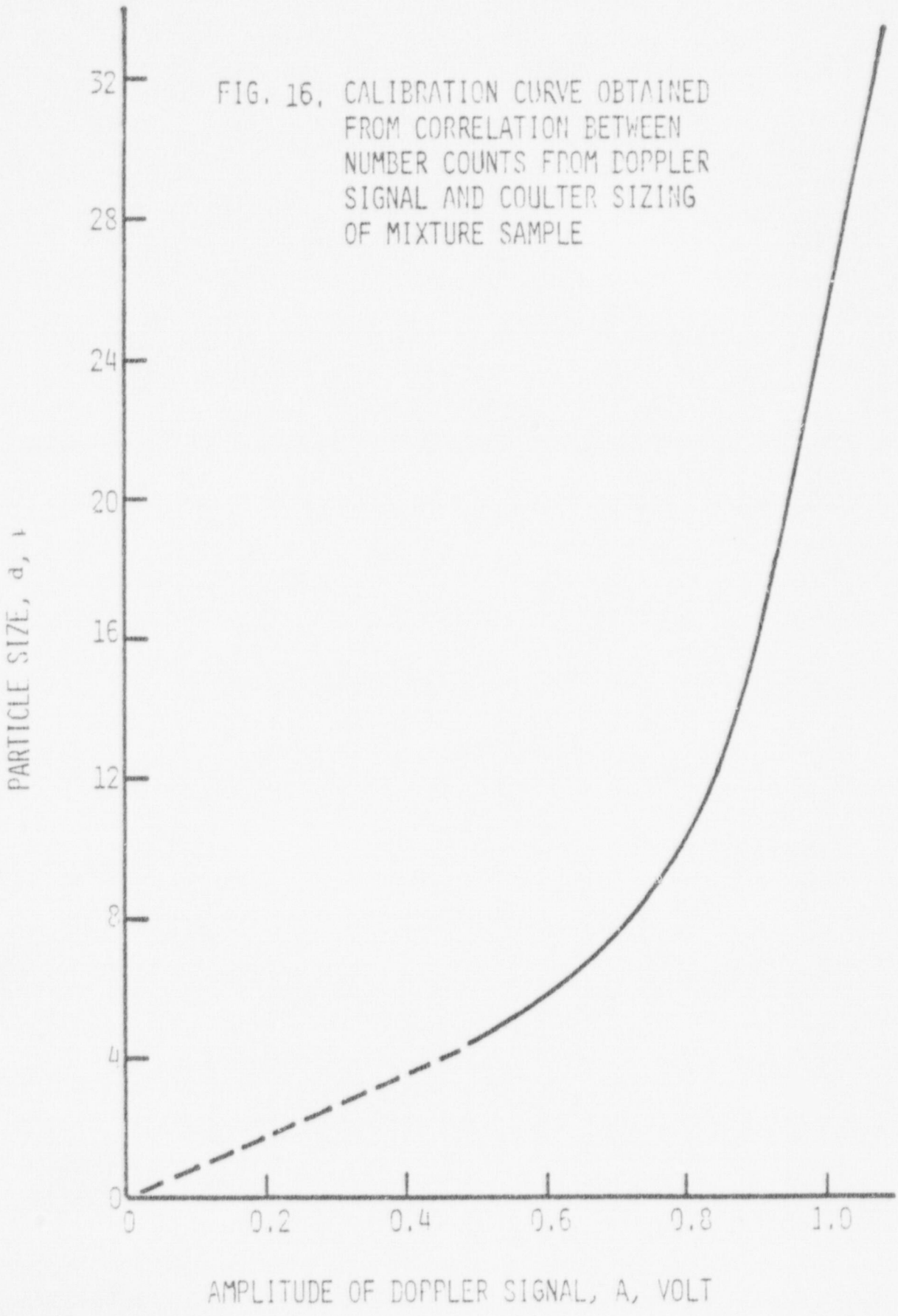

FIG. 16. CALIBRATION CURVE OBTAINED FROM CORRELATION BETWEEN NUMBER COUNTS FROM DOPPLER SIGNAL AND COULTER SIZING OF MIXTURE SAMPLE

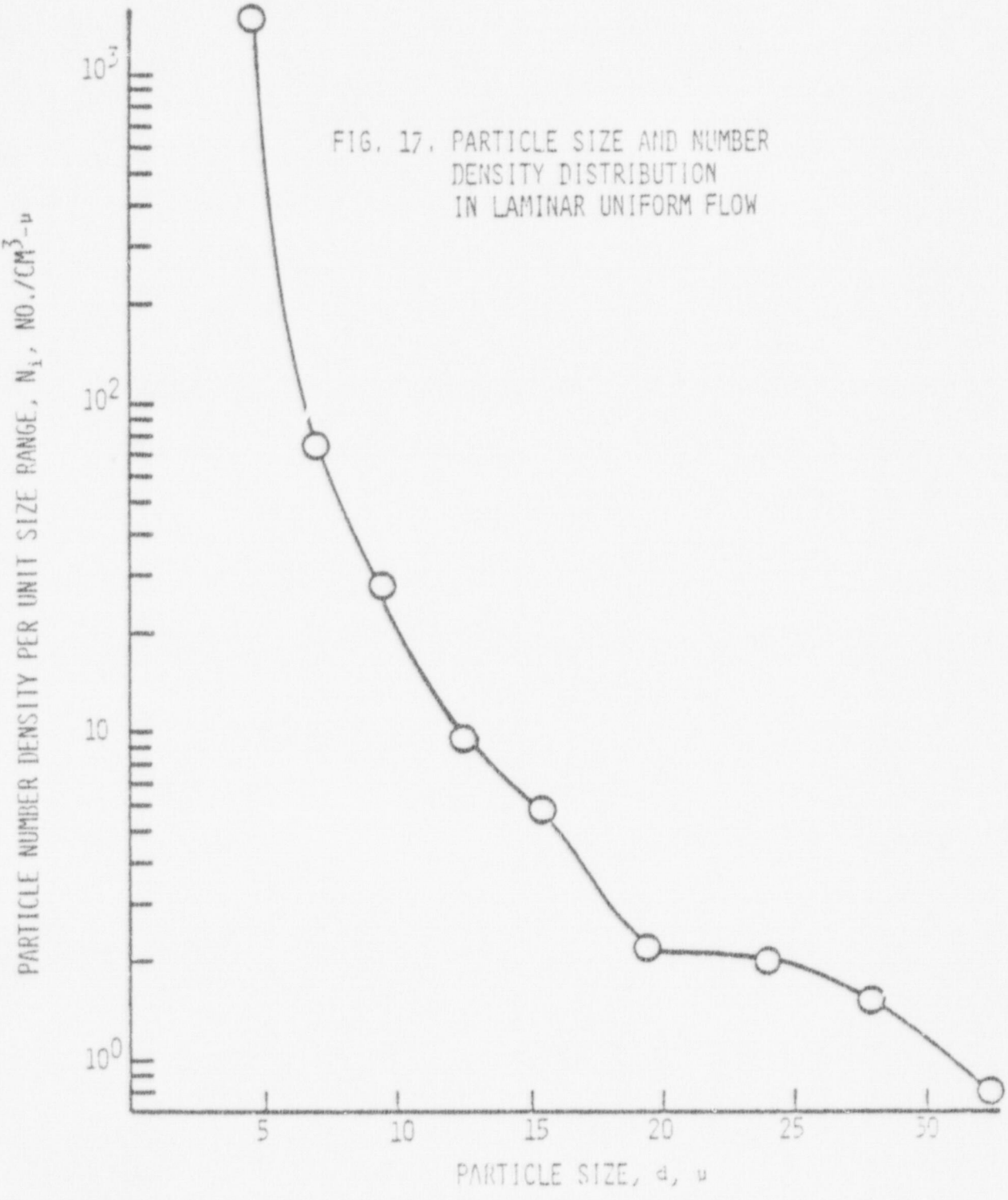

FIG. 17. PARTICLE SIZE AND NUMBER DENSITY DISTRIBUTION IN LAMINAR UNIFORM FLOW

between 10.5μ and 12.5μ. This corresponds to signal amplitudes of 770 mv and 810 mv respectively, through calibration curves shown in Figures 16 and 17.

$(v_j)_o$ = 6.43 cm/sec, the uniform free stream velocity

T_0 = 484 sec., the tape recording time,

and therefore the base cross-sectional area of the measuring volume central core

$$B_o = 4.44 \times 10^4 \mu^2$$

MEASUREMENT IN TURBULENT SHEAR FLOW

A measuring point was selected in a turbulent shear flow on the edge of the wake behind a transverse rectangular body, as shown in Figure 10, where significant particulate accumulations and sizable velocity fluctuations are expected. The particle number counting rate per unit cross-sectional area per unit velocity range and unit size range was obtained using a 325 feet length of tape recorded at 30 inches/sec. for a total of 16 selected mean particle sizes ranging from 4.45μ to 32.5μ. A three-dimensional plot of these results is shown in Figure 18 exposing many interesting fine structural details.

After summing up the number density computed from each of the velocity ranges for the same mean particle size, the particle number densities per unit size range for each of the 16 mean particle sizes were obtained and are as shown by the plot of Figure 19. For comparison purposes the ratio of the particle number densities for a

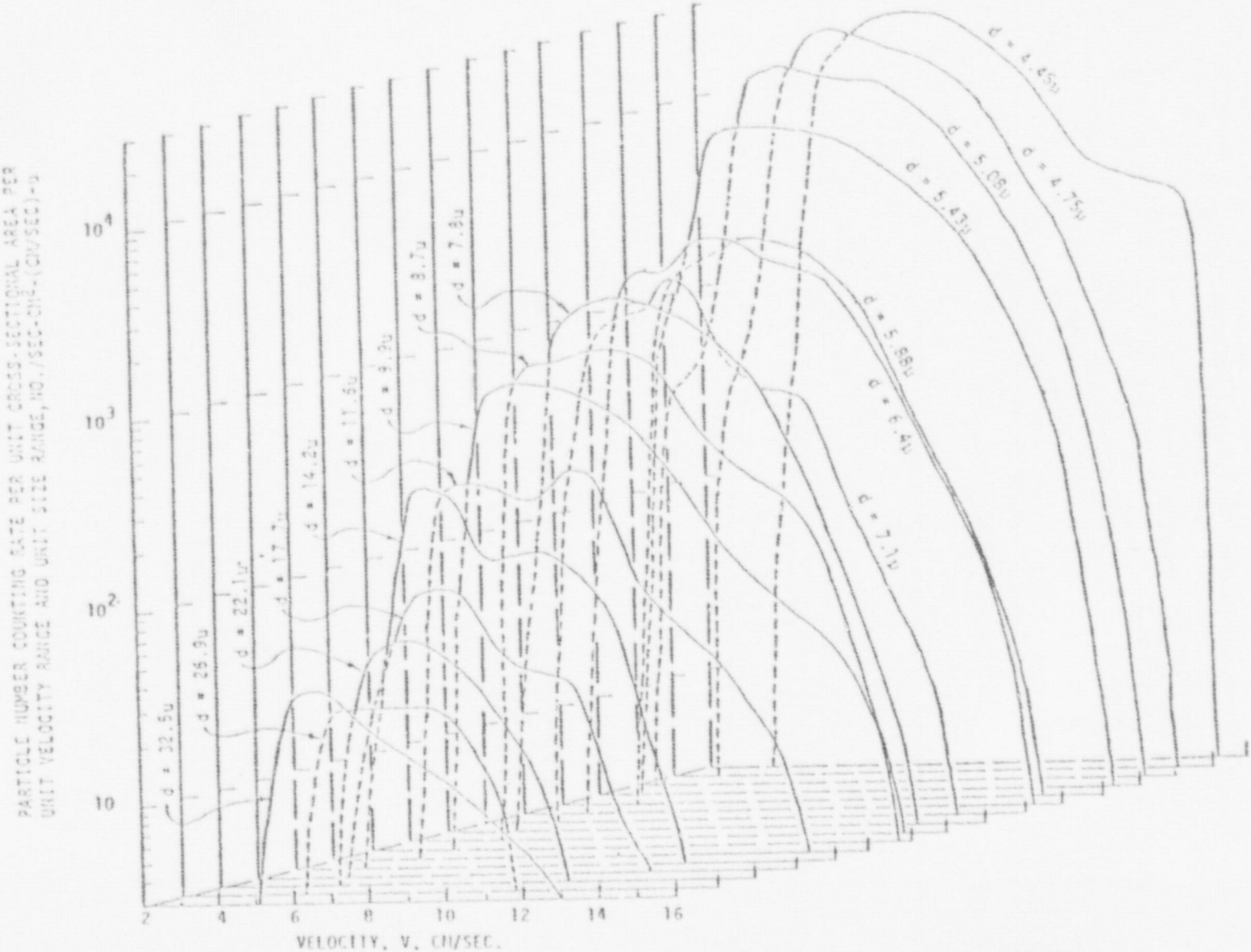

FIGURE 18. SAMPLE PARTICLE SIZE AND VELOCITY DISTRIBUTION IN A TURBULENT SHEAR FLOW OF A SUSPENSION

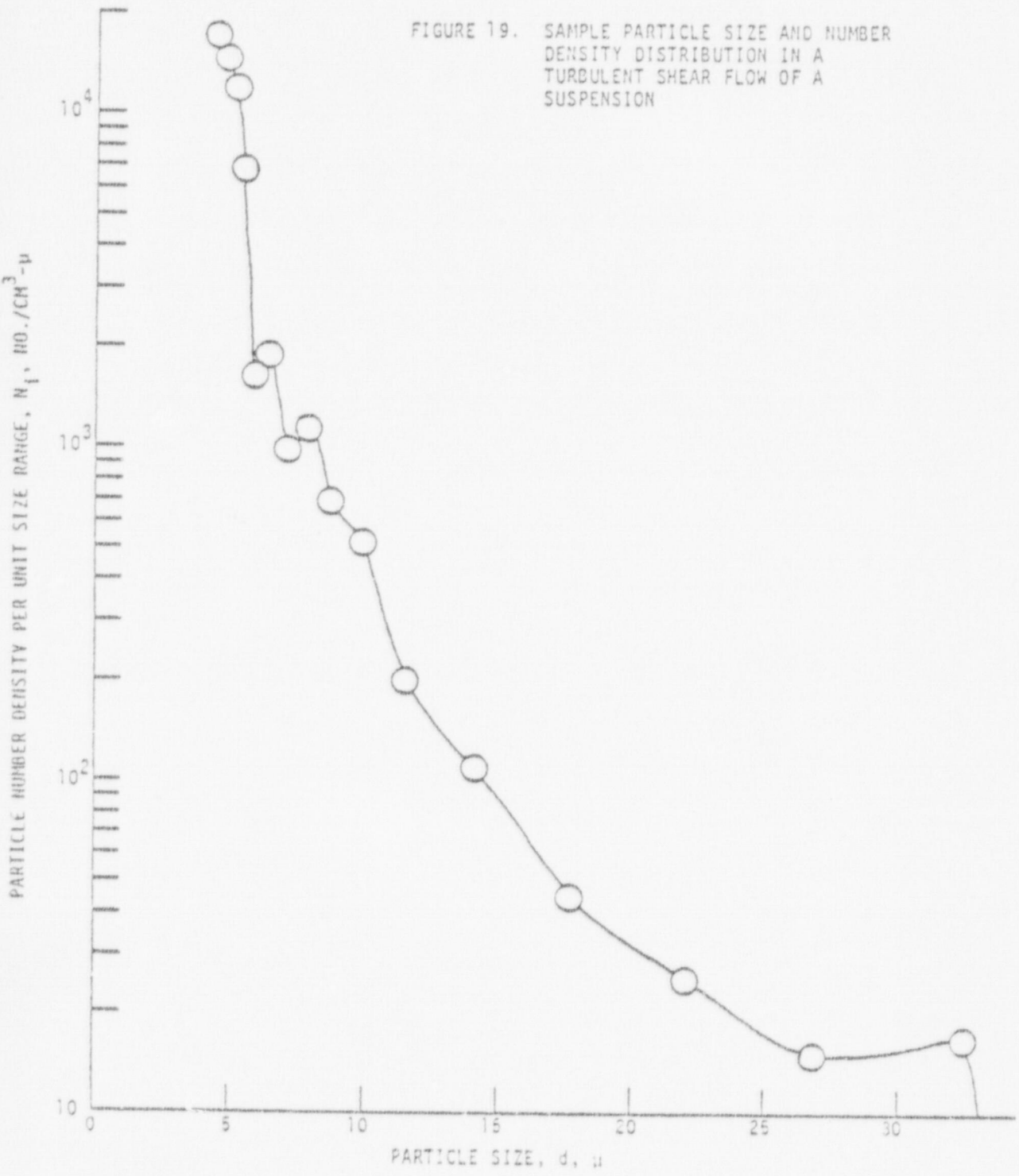

FIGURE 19. SAMPLE PARTICLE SIZE AND NUMBER DENSITY DISTRIBUTION IN A TURBULENT SHEAR FLOW OF A SUSPENSION

measuring point in a turbulent shear flow to the particle number density for a measuring point in the uniform laminar free stream flow for each of the 16 selected nominal particle sizes is plotted in Figure 20. First, it is interesting to note that there is an order of magnitude increase in particulate content for all particle sizes in this turbulent shear flow over the ambient free stream flow apparently due to the enormous accumulation of particulates in the stagnation point flow in the upstream side of the rectangular transverse body, which is dumped into the neighboring regions downstream. Secondly, the fine structure of this distribution curve seems to indicate dynamic interactions experienced by particles in a complex flow such as this one. Thirdly, at the smaller size end this distribution curve drops off rapidly toward a value of unity at a particle size slightly less than 4u. This point is quite significant in that the number density for the turbulent shear flow remains the same as that of the free stream flow for particles less than 4u. The implication is then that such particles will closely follow the fluid motion and consequently can be used as tracers for fluid phase velocity measurement.

A segment of tape 15 feet long was analyzed in this light, using an amplitude discrimination scheme which blocked out signals with amplitudes larger than a selected small value. Results of the fluid phase velocity probability distribtuion in a turbulent shear flow are plotted using particles below 4.0u and 3.7u respectively

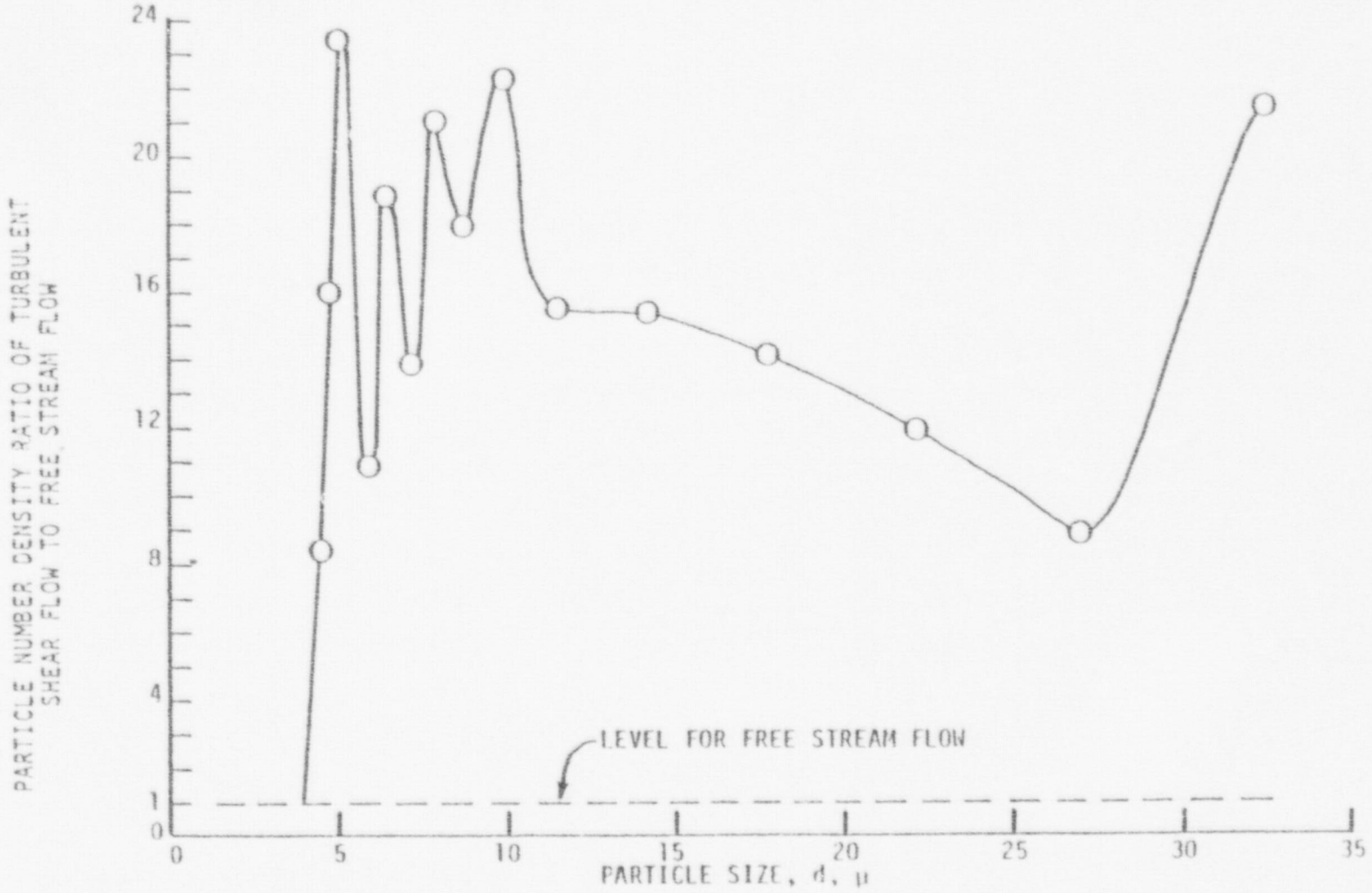

FIGURE 20. DISTRIBUTION OF PARTICLE NUMBER DENSITY RATIO OF TURBULENT SHEAR FLOW TO FREE STREAM FLOW

as tracers for fluid as shown in Figure 21.

A plot of the mean particle velocity as a function of mean particle size in this turbulent two-phase dispersed flow is shown in Figure 22.

This experiment with solid particles-in-water two-phase dispersed flow was performed to develop and verify the methodology. The alternate way of finding particle size and number density of sampling and using a Coulter counter provided a check on the results. With this done the scheme can be applied to another, less manageable (complicated) two-phase flow.

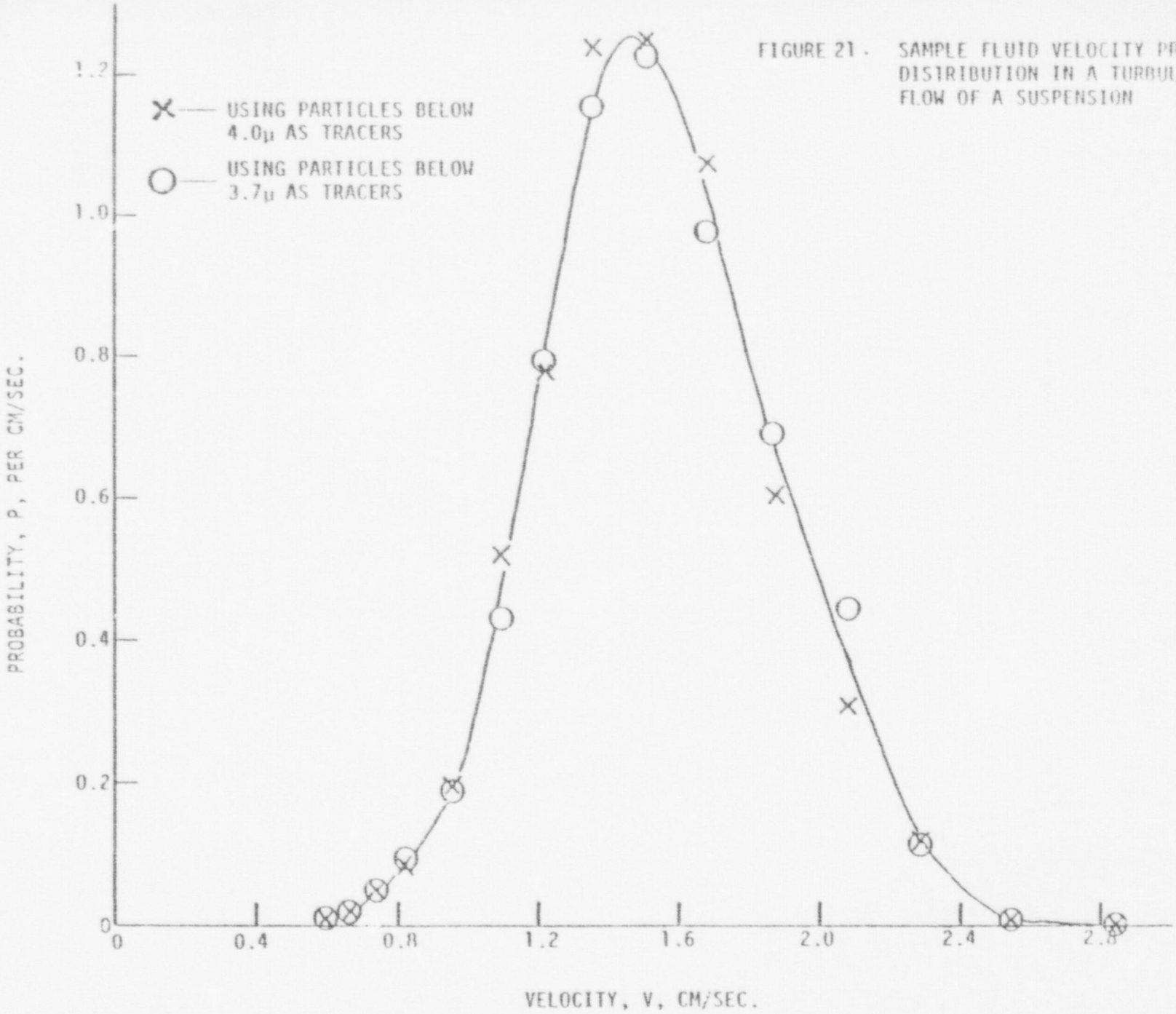

FIGURE 21 - SAMPLE FLUID VELOCITY PROBABILITY DISTRIBUTION IN A TURBULENT SHEAR FLOW OF A SUSPENSION

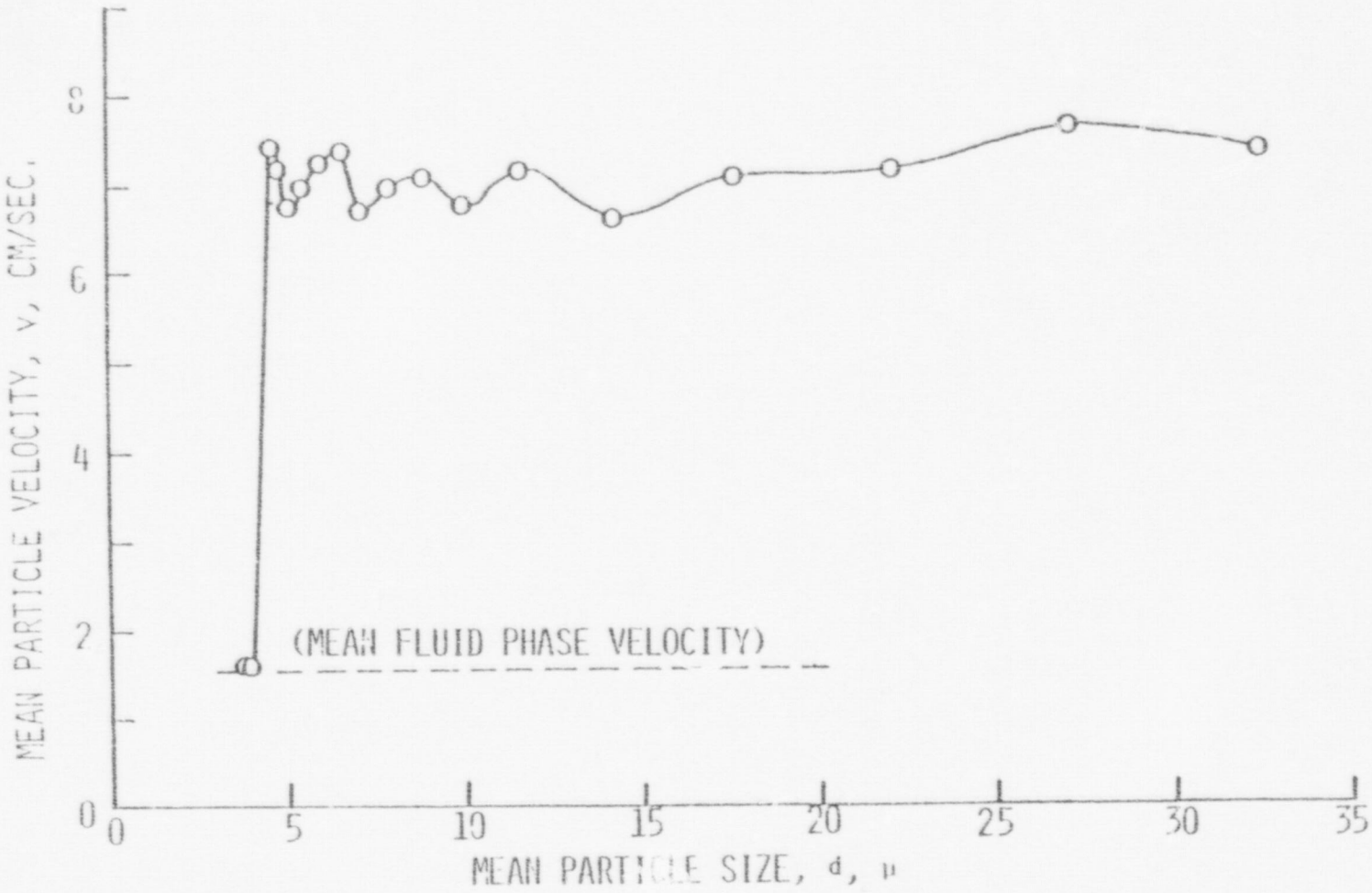

FIGURE 22. DISTRIBUTION OF MEAN PARTICLE VELOCITY IN A TURBULENT SHEAR FLOW OF A SUSPENSION

IV. APPLICATION OF THE TECHNIQUE TO DILUTE TWO-PHASE FLOW, (water droplets-air)

The deposition of a dispersion from a gas flowing turbulently over a surface or through a channel is a very complex phenomenon. It is important when dealing with technical problems such as the calculation of the heat transfer rate in a falling film evaporator or the prediction of a critical heat flux and burnout during the reflood process of a hypothetical loss of coolant accident in a pressurized water nuclear power reactor. There have been very few experiments which are meaningful enough to provide an insight into this complex phenomenon. Consequently, corresponding theoretical efforts have been rather slow in coming. To gain a better understnding of deposition from turbulent flow some information about the local properties of the dispersion is required. It is apparent that a probeless measuring device such as the developed optical technique will best lend itself to this kind of sensitive measurement. It is important to note here that the lateral velocity of the particles in a predominantly axial flow is also required. Hence experiments were planned to obtain the local flow properties in a turbulent flow of a dilute water droplet-in-air, two-phase dispersion upwards through a vertical rectangular channel.

OPTICAL ARRANGEMENT

The operational arrangement of the laser-Doppler anemometer

used in this part of the investigation was a modified, improved T.S.I. laser optical system capable of measuring two velocity components simultaneously at a single location in the flow field. The incoming laser beam from a 15 mv He-Ne laser was split into thr e beams, one reference beam and two scattering beams as shown in Figure 23. These beams were polarized so that the two scattering beams becom orthogonally polarized to each other and polarized to form a 45° angle with respect to the polarity of the reference beam. The axial velocity was obtained from the reference beam heterodyning with the scattered light of the axial scattering beam. Similarly, the lateral velocity was obtained from the reference beam and the lateral scattering beam. By separating the collected light by polarity the two components of collected light are separated into two beams which were focused onto two separate photo-detectors. The result is the simultaneous measurement of two velocity components at a single measuring point in the flow. This system had been tested and improved to produce high quality signals. The polarization rotators had been tested and improved by using linear polarizers, giving the correct polarity of the three beams. The reference beam was also optically shifted using a Bragg cell (T.S.I.). However two separate downmix electronics systems were used to independently shift either of the axial or lateral Doppler signals. Only one crystal controled oscillator was used for both of the downmixing systems, ensuring the required synchronization. The entire optical system was mounted

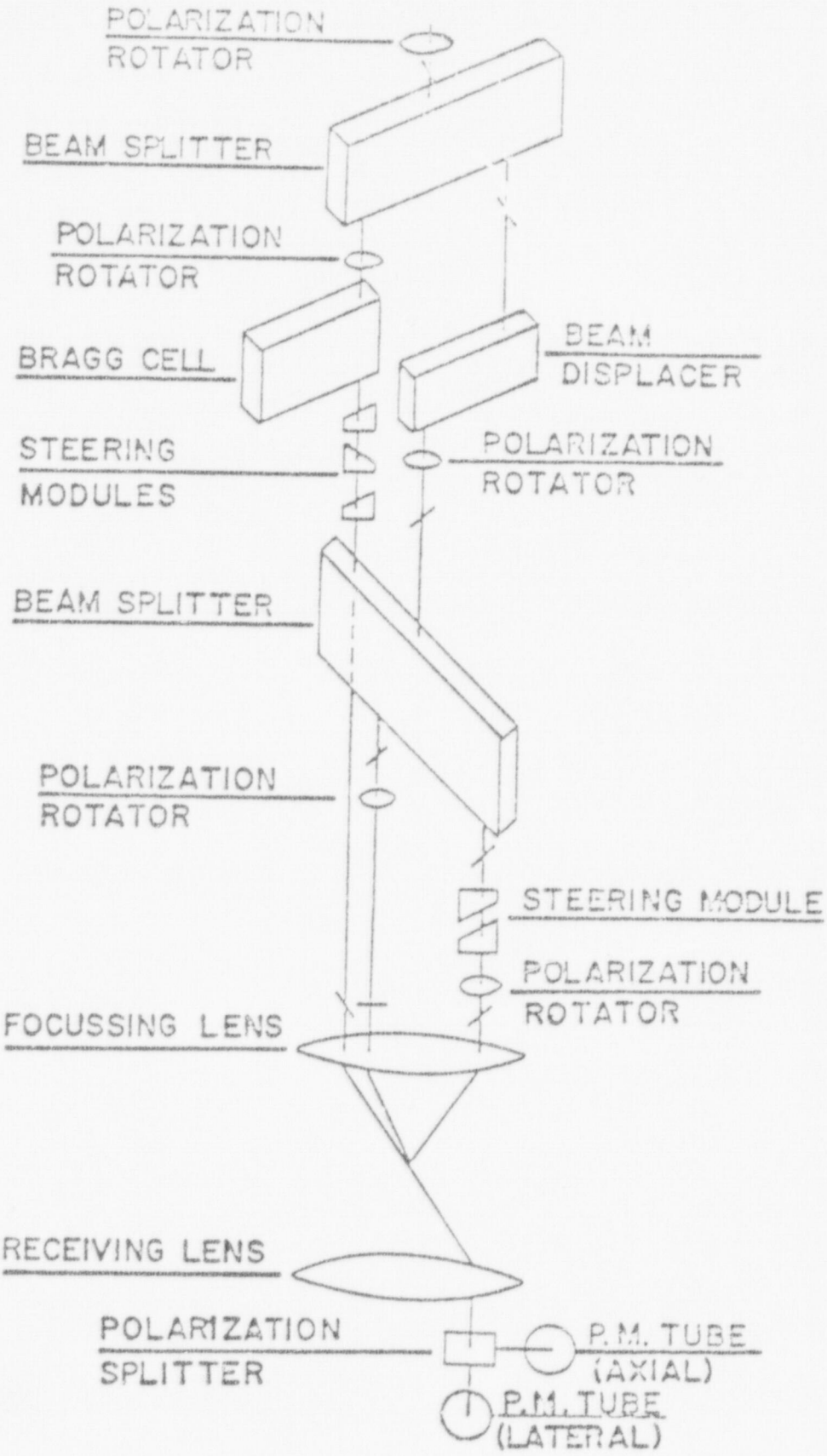

FIGURE 23. OPTICAL ARRANGEMENT

on top of a milling machine base equiped with dial indicators, offering positional accuracy in three dimensions to within a few microns.

ELECTRONIC CIRCUITS

The electronic package for this portion of the work was redesigned to obtain the signal amplitude, time duration of the signal and both axial and lateral velocities for each individual Doppler signal. This was achieved by first obtaining analog voltages proportional to these four parameters and then digitalizing them using an Analog-to-Digital (A/D) convertor in the PDP-15 digital computer. The instrumentation block diagram is shown in Figure 24. The signal processing electronics was specially designed to handle a wide variation in the signal frequency (from a few K.Hz to 3.0 M.Hz) which occurred at random intervals.

The Doppler signals with axial velocity information were split into two signals of equal strength using a power splitter. One of these signals was sent to a tracker (T.S.I.) for determination of axial velocity. The envelope of the other signal was obtained using a demodulator and used for determination of particle size. The demodulator consisted of a linear half-wave rectifier and a low-pass filter. A great deal of effort was necessary to obtain a one-to-one amplitude ratio between signal and the rectified signal, because of the non-linear characteristic of the diode. This was achieved by using a high frequency response amplifier and fast switching diodes, and thus a linear rectifier which could handle

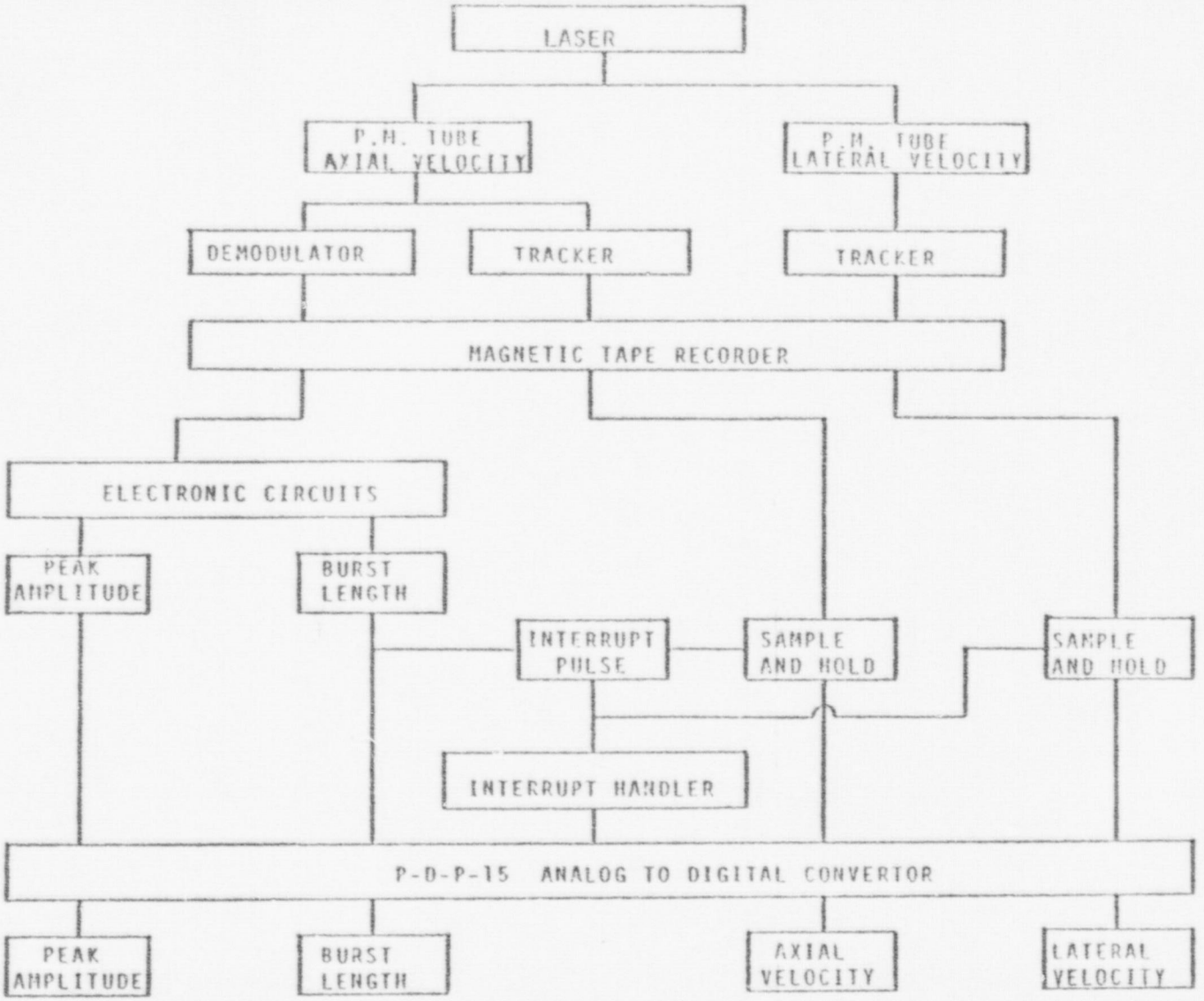

FIGURE 24. INSTRUMENTATION BLOCK DIAGRAM

frequencies of up to 2.5 M.Hz was built.

The Doppler signals with lateral velocity information were processed through a second tracker (T.S.I.) for obtaining analog voltages proportional to frequencies. Thus, there were three analog signals; one for the axial velocity, one for the lateral velocity and a third—the envelope of the axial velocity Doppler signals—for the determination of size. These three signals were recorded simultaneously on three separate channels of an analog tape recorder (Honey-well, Model 101) at a tape speed of 120 inches per second. These signals were later played back at a tape speed of 15 inches per second into the custom built computer interface electronic circuits. The Analog-to-Digital (A/D) convertor in the PDP-15 computer needed at least 200 micro-seconds to digitalize four analog signals and hence the recorded signals were played back at a slower speed, avoiding loss of any valid signals. The functional diagram of the electronic circuits is as shown in Figure 25. The operational diagram for electronic circuits is as shown in Figure 26.

The signal envelope was passed through a peak detector module which gave an output proportional to maximum input voltage. This maximum voltage was held constant by setting the peak detector in the "hold" mode. The burst envelope was also sent into a voltage comparator. The output of the comparator was a rectangular pulse and its duration was measured using the pulse to gate open a digital counter. The number (count) in the counter at the end of the

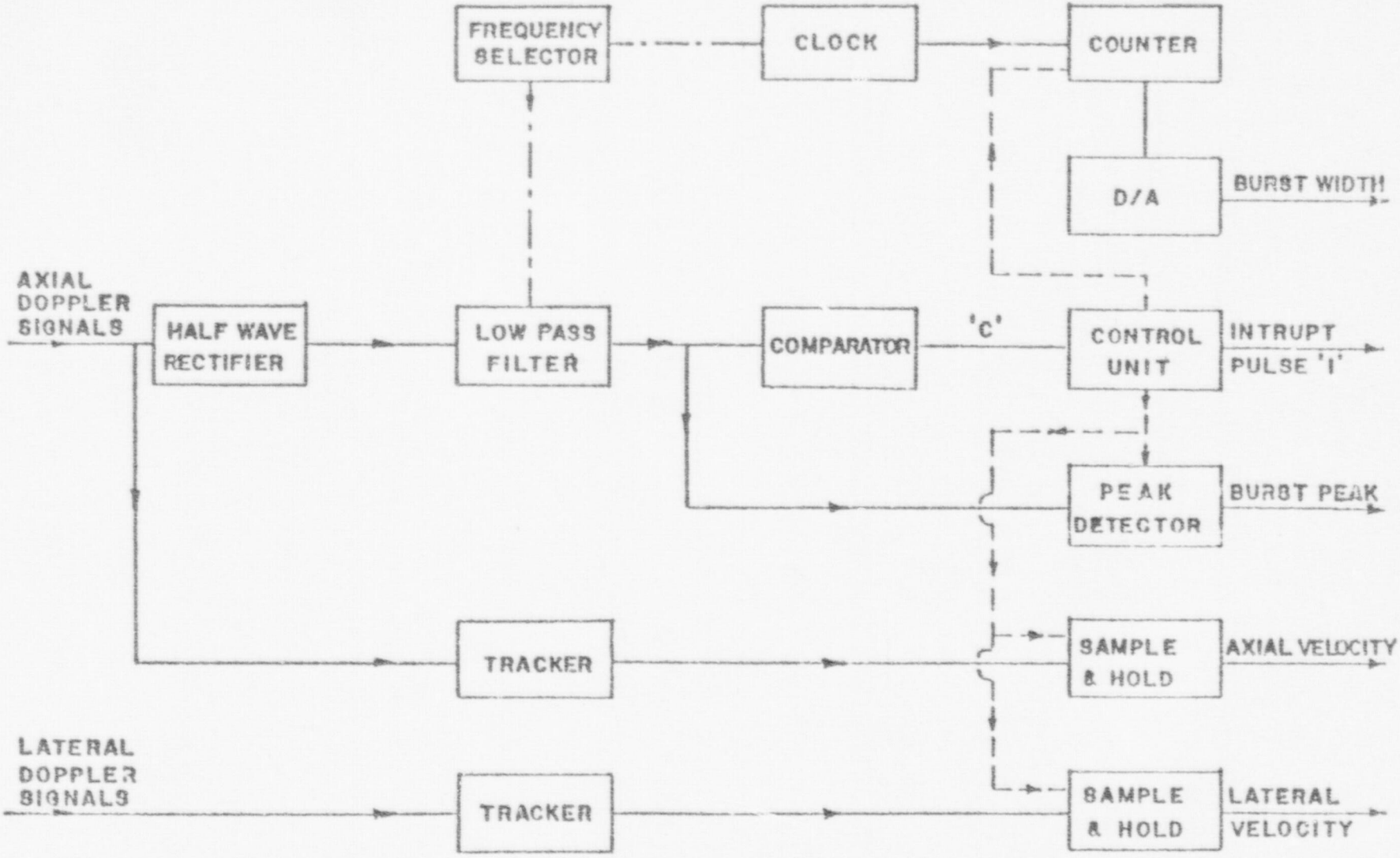

FIGURE 25. FUNCTIONAL BLOCK DIAGRAM OF THE ELECTRONIC CIRCUITS

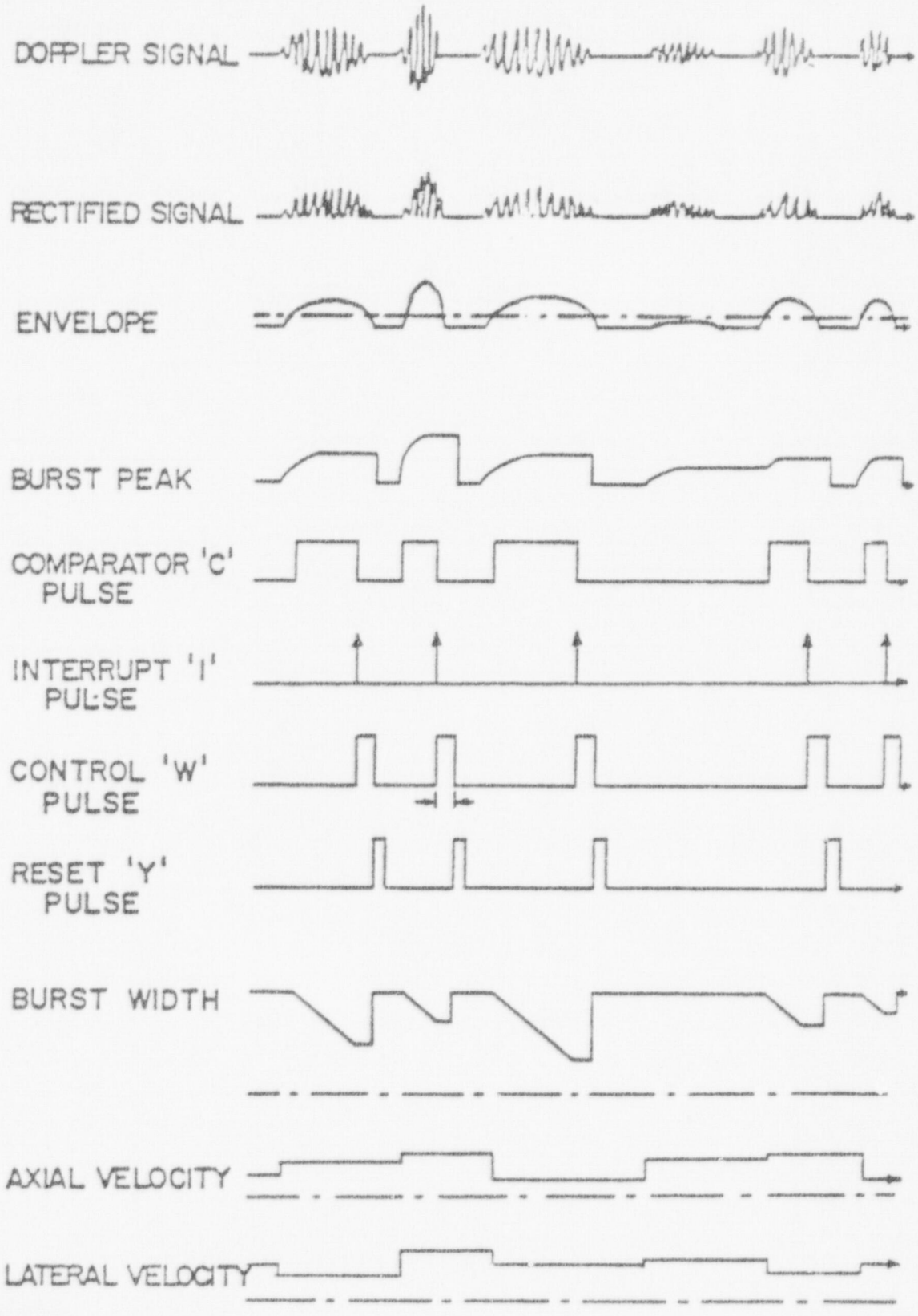

FIGURE 26. OPERATIONAL DIAGRAM FOR ELECTRONIC CIRCUITS

pulse duration was proportional to burst width at the base level set for the voltage comparator. Hysteresis was introduced using a feed back circuit in the voltage comparator to avoid any instabilities at the switching edges which may occur with slow rising signal envelope due to the presence of noise.

A control unit was designed using Transistor Transistor Logic (TTL) integrated circuits (I.C.) to generate the necessary signal pulses for the other components of the unit and the interrupt pulse to the A/D convertor. This interrupt pulse was generated in the control unit at the end of burst width.

The control unit also sent control signals to two sample-and-hold modules connected to axial and lateral velocity analog voltage signals. This was done to assure that these voltages correspond to the same burst in question. This holding action occurred just as the comparator level 'c' went low. The control unit generated the control pulse 'w' with a duration equal to the time required by the A/D convertor to sample the four parameters. A control pulse 'y' was also generated to reset the various modules (peak detector, sample and holds and counter).

INTERRUPT HANDLER

The A/D convertor was a part of PDP-15 computer. The four parameters were digitalized one after another when an interrupt pulse triggered the convertor. The requirements of this pulse were; it should have a rise time of 100 n.s. or less, its pulse duration

should be a minimum of 200 n.s, and it should go from + 3v to 0v to trigger the conversion. These requirements were met by H.P. function generator Model 3312A and it was triggered by the control pulse generated from the control unit.

DATA ANALYSIS

The PDP-15 computer sorted the raw digitalized data on a magnetic disc. A computer program (Appendix-4) discriminated the signals which have path lengths smaller than the limiting path length. The data was then processed to determine maximum peak amplitude, maximum axial velocity, maximum lateral velocity, minimum axial and lateral velocities by scanning through the discriminated data. The diameter range was determined by chosing 95% of the maximum amplitude ranges. In each range the lower limit was 95% of the upper limit. The range between the maximum and minimum velocity was divided into ten equal subranges. Then the entire data was sorted to obtain the number of droplets within a particular diameter range and axial and lateral velocity range. The mean axial and lateral velocities and the standard deviation on these quantities were also computed for all the diameter ranges considered.

AIR VELOCITY

The air velocity was determined from signals produced by very small droplets as described earlier. The discriminated analog voltages were digitalized at equal time intervals and the computer was

programmed to compute the mean axial and lateral air velocities and the standard deviations.

CALIBRATION

The relationship between Doppler signal amplitude and the droplet size was determined using a commercially available Berglund-Liu monodisperse aerosol generator which generated uniform size aerosols [20]. Since any instabilities in the flow would change the diameter of droplets generated,the pumping system must supply liquid to the generator uniformly. The syringe pump which came with the package was a positive displacement gear pump. However, this was abandoned and a steadier pneumatic system was fabricated to force water through the orifice at a constant rate. The test area was isolated from ambient air movements to insure that the droplets had the same trajectory. By varying the water flow rate, the frequency at which water droplets were generated and the orifice size,different uniform-size droplets were generated. These droplets were sent in a single stream, one after another through the center of the measuring volume, giving the maximum signal amplitude for each droplet size. The resultant calibration curve between the droplet diameter and Doppler signal amplitude is shown in Figure 27. The calibration curve obtained in the earlier experimental investigation using a solid particle-water system is also shown by the dotted lines for comparison.

The base area, $\overline{B}_o$, of the central core of the measuring volume

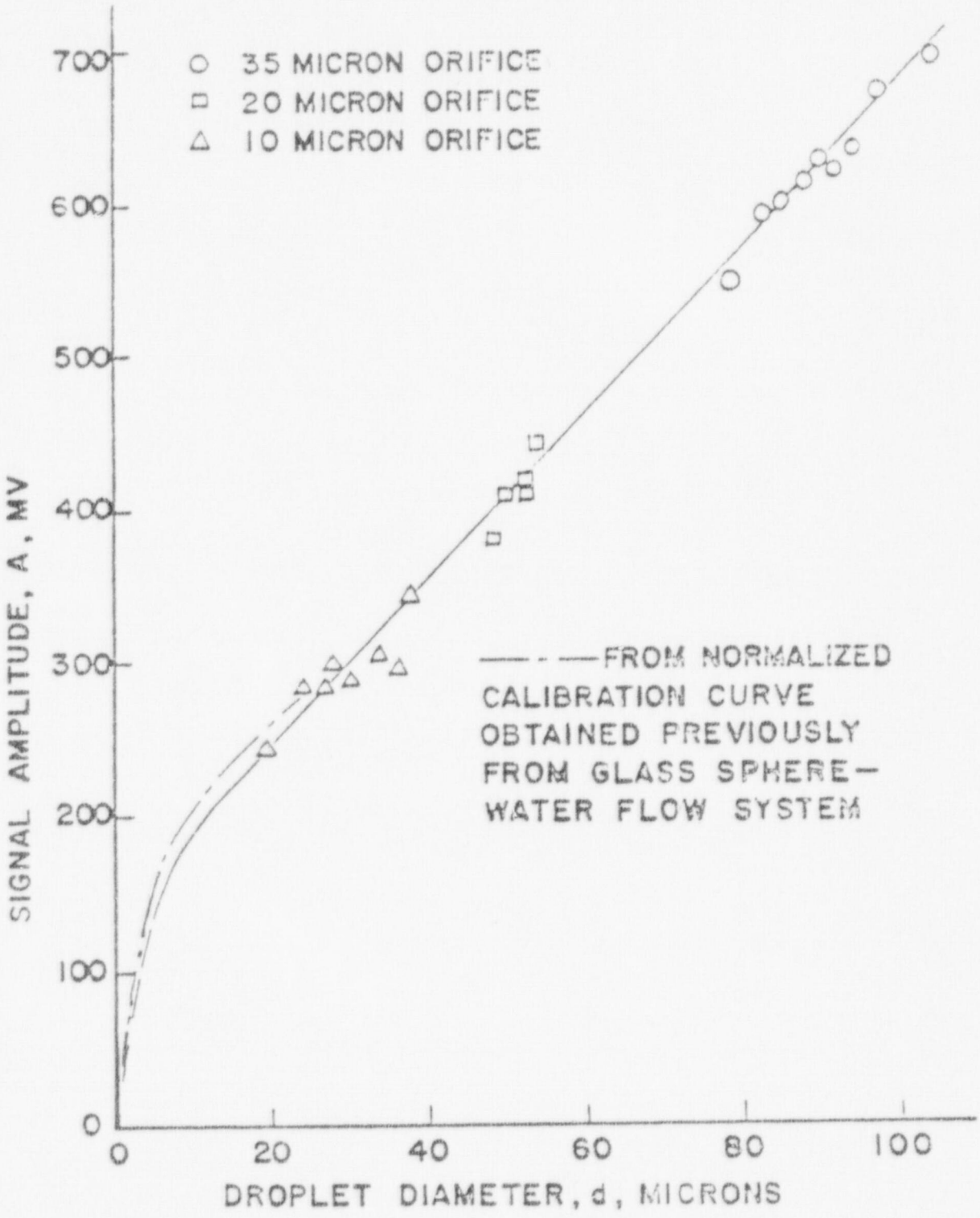

FIGURE 27. CALIBRATION CURVE OBTAINED FROM DIRECT MEASUREMENT USING UNIFORM SIZE DROPLETS BETWEEN DROPLET SIZE AND DOPPLER SIGNAL AMPLITUDE

and the limiting path length, $\bar{\ell}_v$, were also obtained using the precise size water droplet generator. The measuring volume was placed systematically at different locations in two dimensions with respect to the uniform stream of droplets and the Doppler signal amplitude was obtained for each location. The limiting path length was determined by noting the signal path length when the signal amplitude was 95% of the maximum. The boundary of the base area, $\bar{B}_o$, was similarly obtained by joining the locus of points having this limiting path length.

The limiting path length and maximum path length were obtained using the above procedure and they were found to be 190μ and 215μ at the base level selected. The base area, $\bar{B}_o$, was computed to be equal to $1.837 \times 10^4 \mu^2$ for this particular optical arrangement.

MEASUREMENTS IN TURBULENT FREE STREAM AIR FLOW AND ADJACENT TO A SOLID SURFACE

Experiments were planned using a simple air flow system to gain confidence in the data analysis and instrumentation. The flow system consisted of an atomizer generating water droplets varying from sub-microns to about 90μ in diameter. The water droplets were carried through a vertical plexiglass pipe 25 mm. in diameter and 1000 mm. in length. A flatplate of dimensions 35 mm. x 600 mm. with a sharp leading edge was set parallel to the axis of the pipe with its leading edge placed 25 mm. above the exit of the pipe. This plate was so aligned with the laser beams that measurements adjacent to the wall

could be made.

The measuring volume was placed 80 mm. from the leading edge and 30 mm. away from the solid surface. The Doppler signals were recorded on over 600 feet of magnetic tape at a taping speed of 60 inches per second. Measurement was also taken at 0.25 mm. from the solid surface at the same elevation. The air and droplet velocities were restricted by the frequency response of the tape recorder. The axial velocity Doppler signal was downshifted to match the frequency response to the electronics and the lateral velocity Doppler frequency was upshifted to eliminate the directional ambiguity.

The signals were analyzed using the custom built electronic circuits and the raw data was stored in PDP-15 computer. The data analysis was performed as described earlier and the droplet counting rate per unit cross-sectional area, per unit axial velocity range, per unit lateral velocity range, and the unit size range was obtained. A total of twenty-two mean droplet diameters ranging grom 10.62μ to 87.7μ was selected. All of the data recorded was analyzed to obtain the statistics for the size-number density distributions and axial and lateral velocity distributions.

The droplet size and number density distribution for the free stream turbulent air flow and adjacent to the plate are shown in Figure 28. Sample axial velocity distributions for a selected droplet size with lateral velocity are shown in Figure 29 and Figure

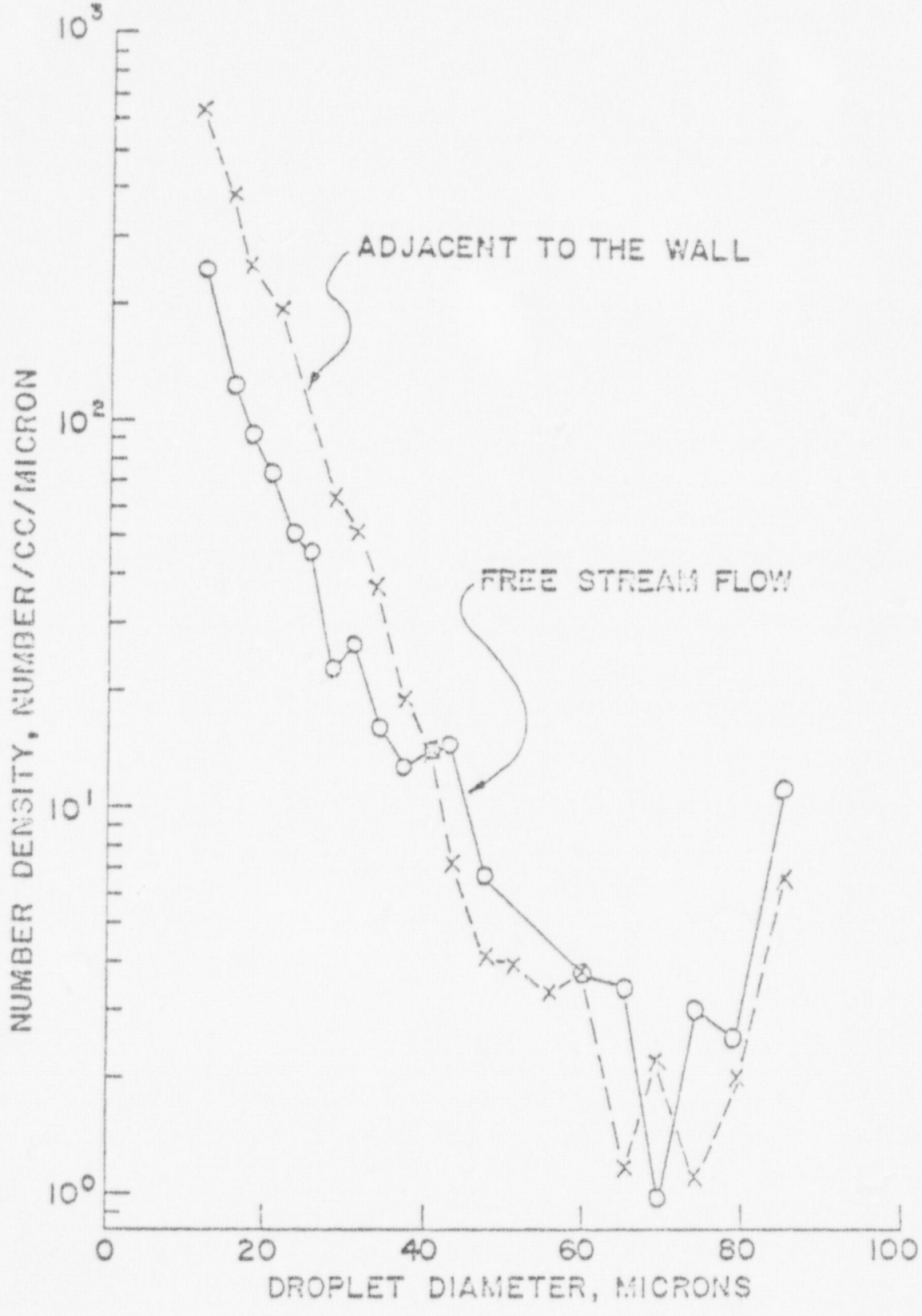

FIGURE 28. DROPLET SIZE AND NUMBER DENSITY DISTRIBUTION

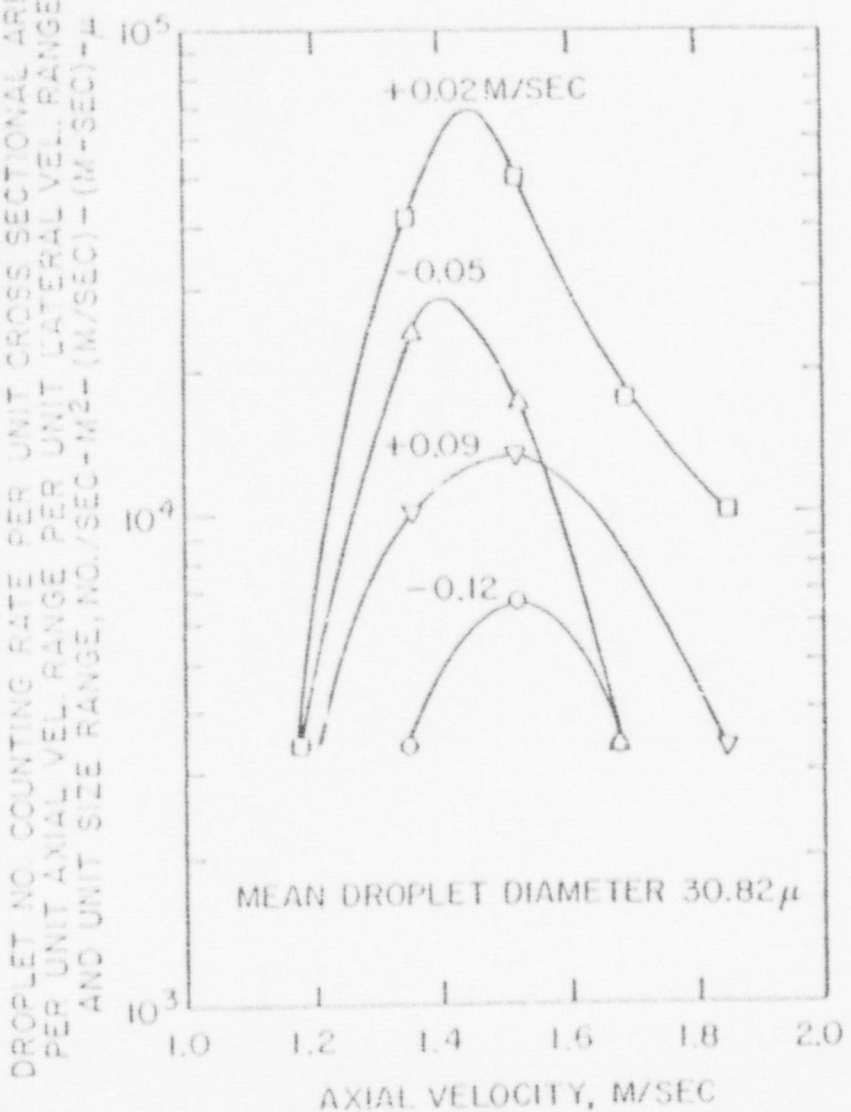

FIGURE 29. SAMPLE AXIAL VELOCITY DISTRIBUTION FOR DIFFERENT LATERAL VELOCITIES IN THE FREE STREAM TURBULENT AIR FLOW

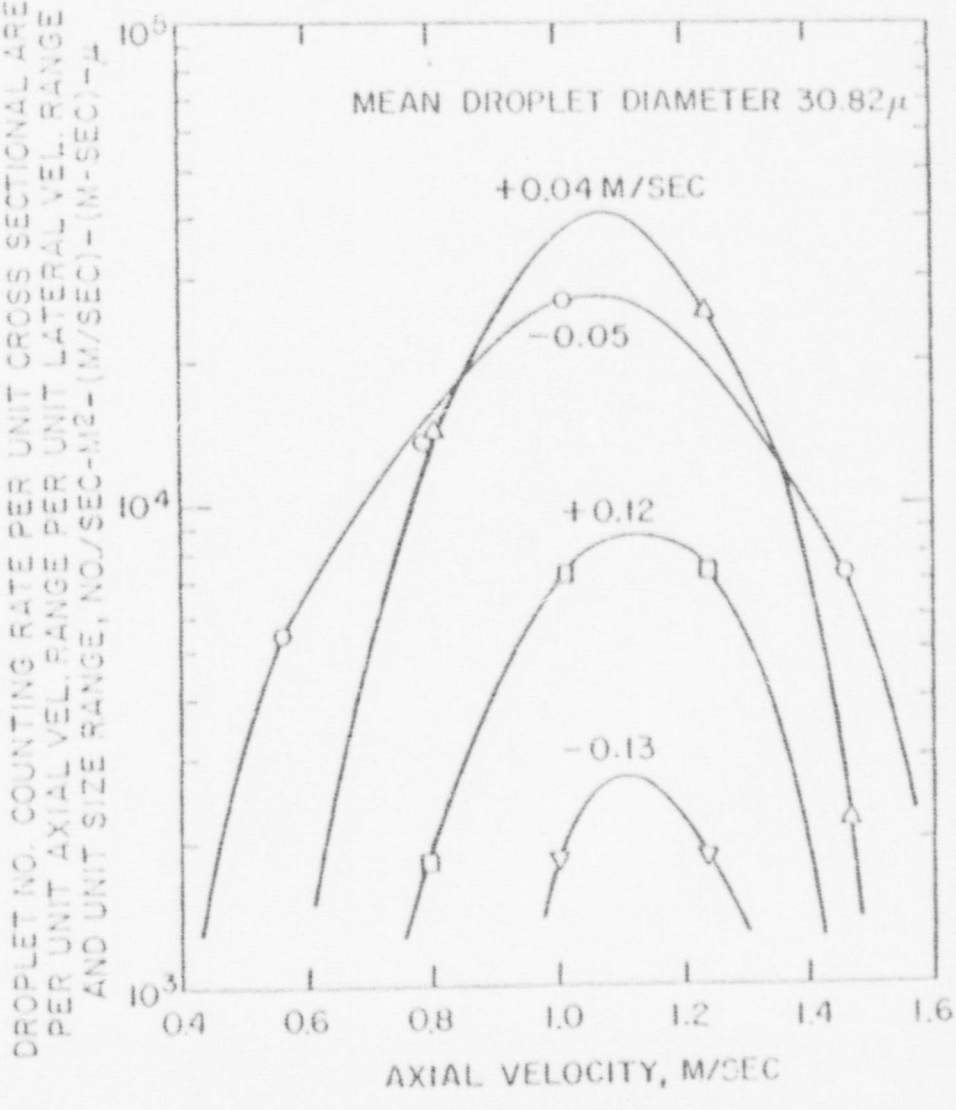

FIGURE 30. SAMPLE AXIAL VELOCITY DISTRIBUTION FOR DIFFERENT LATERAL VELOCITIES IN TURBULENT AIR FLOW ADJACENT TO THE WALL

30. The entire results of the data analysis are given in Appendix-5. The air velocity probability distributions of the turbulent air flow are shown in Figure 31 and 32. It is clear from Figure 28 that the presence of the plate changes the turbulent flow field; in particular the number of smaller droplets increased near the wall. As expected the axial velocity near the wall was less then the axial velocity at the free stream measuring point for all droplet sizes.

With the experience derived from this experiment with a turbulent free jet of a dispersion, a more complicated measurement of flow through a vertical rectangular channel was undertaken.

MEASUREMENTS IN A DILUTE TWO-PHASE DISPERSED FLOW IN A RECTANGULAR CHANNEL (water droplets-air system)

The flow system was designed to generate a two-phase turbulent flow of water droplets (ranging from submicrons to 100μ in diameter) in air through a vertical rectangular channel of dimensions 10 mm. x 25 mm. with measurements to be taken at points along the lateral axis across its smaller dimension.

The system consisted of a nozzle supplying water to be atomized by a high velocity annular air jet encircling the nozzle. The droplet generation and turbulent air supply were thus coupled in a device which resembled an ejector pump. The atomizer was aimed at the entrance end of the channel and the whole assembly—the atomizer and the end of the channel—was enclosed in a plexiglass box to collect excess water. To better control droplet size the air supplied

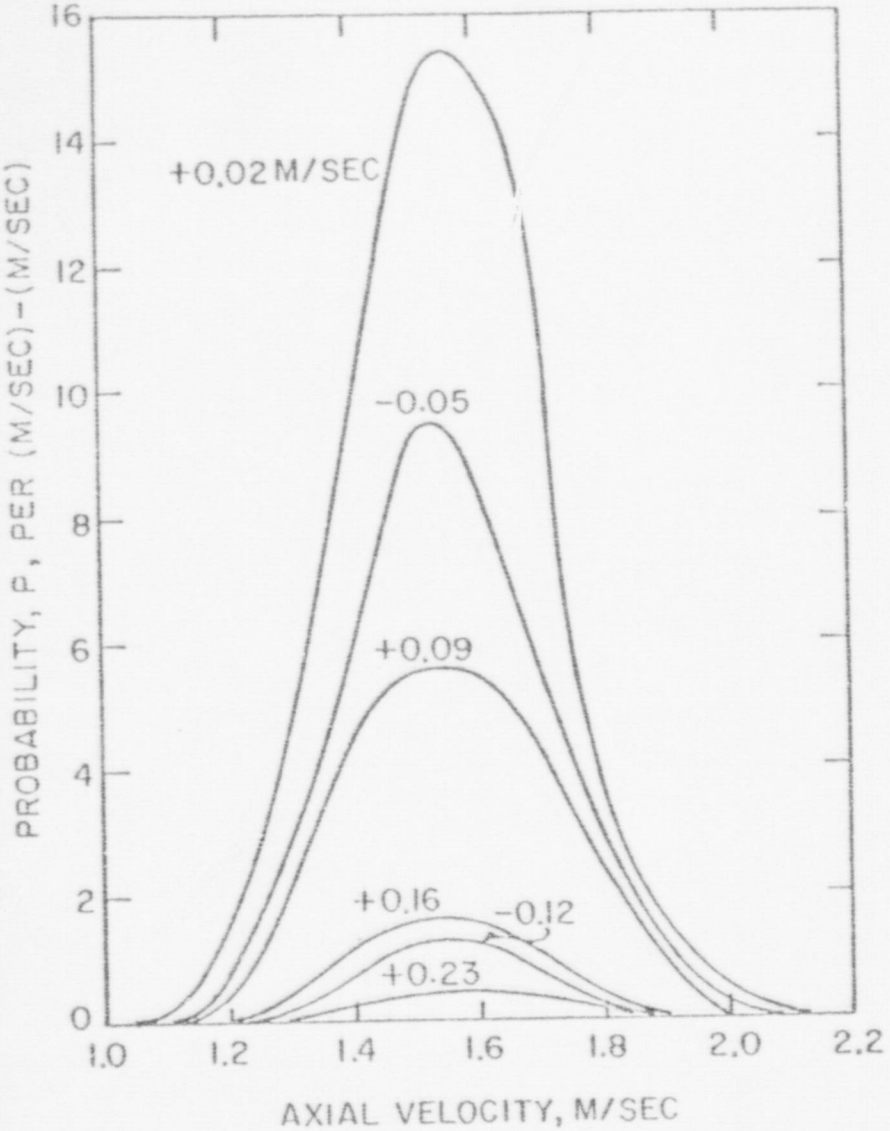

FIGURE 31. SAMPLE AIR VELOCITY PROBABILITY DISTRIBUTION IN A FREE STREAM TURBULENT AIR FLOW FOR DIFFERENT LATERAL VELOCITIES

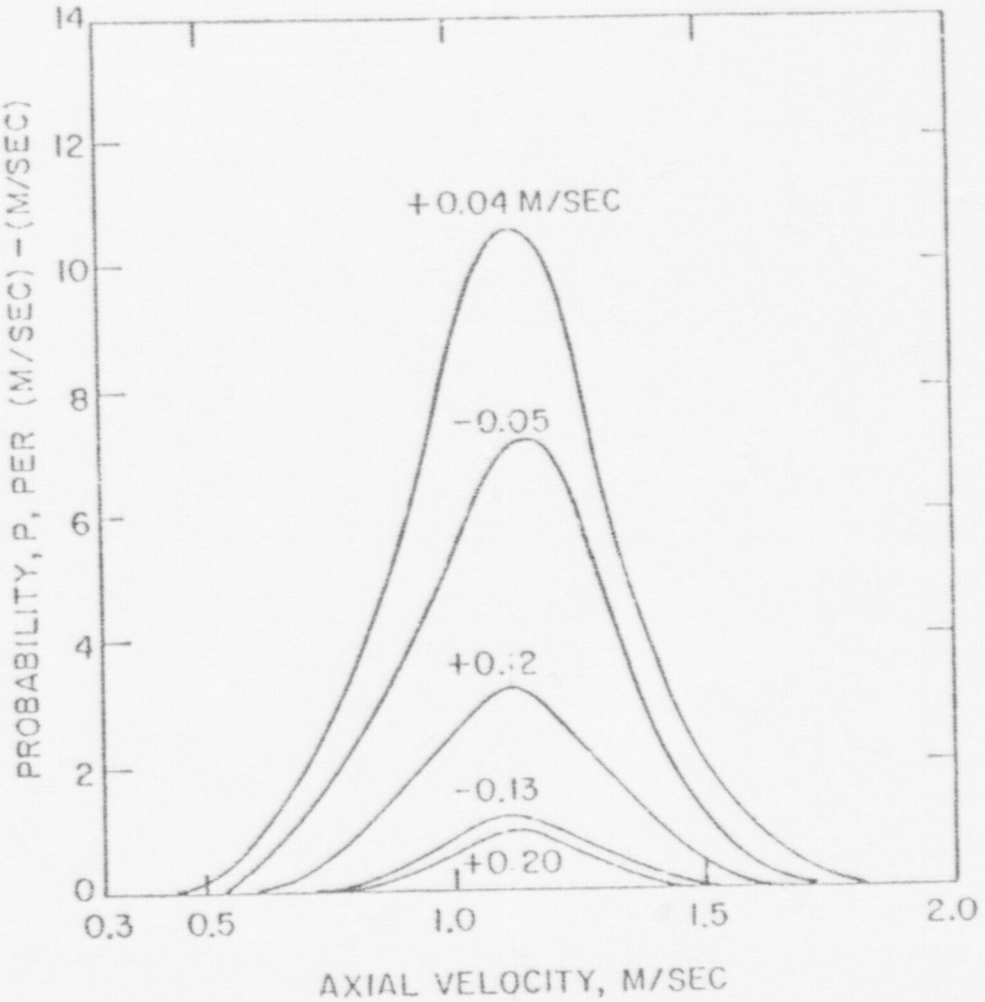

FIGURE 32. SAMPLE AIR VELOCITY PROBABILITY DISTRIBUTION ADJACENT TO A WALL IN A TURBULENT AIR FLOW FOR DIFFERENT LATERAL VELOCITIES

to the atomizer was pre-saturated with water to suppress any possible evaporation of the droplets. Also, to control the number of droplets and to limit the size range entering the test section, a thin perforated plate was placed between the atomizing device and the entrance to the channel. A plate with 18-1.5 mm. diameter holes was selected as it provided the necessary control. Finally, to prevent the droplets from falling back into the channel, a jet of air was aimed at the exiting flow so that it blew the droplets away, and yet did not disturb the flow inside the channel. The test section was equiped with two-100 mm. long plate glass observation windows mounted on opposite sides of the rectangular channel near the exit end. An adjustable mounting brace was used so that the test section could be aligned. The glass plates were aligned to be parallel to each other and the entire test section was aligned so that measurements could be made at locations near the wall. The flow arrangement is shown in Figure 33.

The center point of the optical measuring volume was placed at a level of 582 mm. from the channel entrance and measurements were taken successively at nine different lateral positions across the channel. The three analog signals were recorded at each measuring location on over 4000 feet of magnetic tape at a taping speed of 120 inches per second. The tape recorder had a higher frequency response and hence measurements could be made at higher velocities.

The recorded signals were played back at 15 inches per second

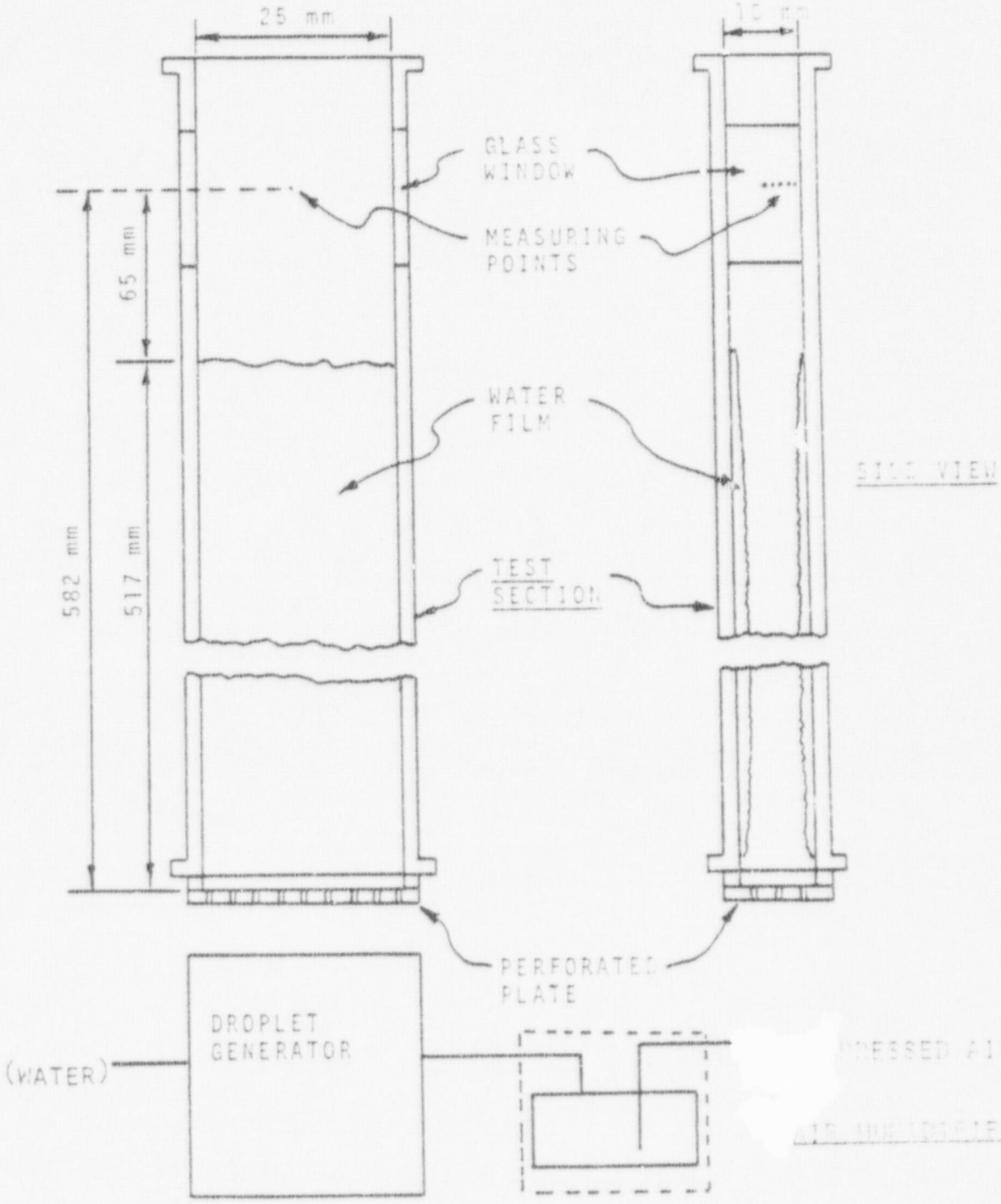

FIGURE 33. FLOW ARRANGEMENT WITH LIQUID FILM ON WALL

through the electronic circuits into PDP-15 digital computer for data analysis. Typical data output samples are shown in Tables 1 and 2 and the entire summary of the data analysis is presented in Appendix-6. The measured number densities of the different size droplets at various distances from the wall are shown in Figures 34 to 40. The mean axial and lateral velocity distributions and the standard deviations for droplets at different distances are shown in Figures 41 to 47. Axial and lateral velocities of the air were determined using submicron size droplets. Their distribution is shown in Figure 48.

It was noted in this particular flow that the droplets formed a continuous water film on the wall upstream of the observation section. An analysis of the experimental data revealed that very near the wall (0.25 mm.) there were large droplets (80μ to 95μ). At 0.5 mm. the number of large droplets was less and at 1 mm. the number of smaller droplets increased by at least one order of magnitude. When this was analyzed, taking lateral velocity data into consideration, the following observations were made: There was active generation of large droplets from the wall film. These droplets [illegible] into a large number of smaller droplets due to the [illegible] flow of air. These small droplets were found to move [illegible] higher lateral velocities in the away-from-the-wall direction, and coalesce, forming large droplets at 2 mm. from the wall, and then breakup again into medium-size droplets at 3 mm. from the wall.

TABLE 1. SAMPLE DATA SHEET

DROPLET SIZE - VELOCITY DISTRIBUTION

DIAMETER RANGE	AXIAL VEL. RANGE	LATERAL VEL. RANGE	NUMBER COUNT	DROPLET RATE
29.33:26.56	8.55: 9.21	0.57: 0.75	2	0.9[illegible]
29.33:26.56	9.21: 9.87	-0.49:-0.31	2	0.9[illegible]
29.33:26.56	9.21: 9.87	-0.31:-0.13	3	0.13[illegible]
29.33:26.56	9.21: 9.87	-0.13: 0.04	8	0.37[illegible]
29.33:26.56	9.21: 9.87	0.04: 0.22	1	0.4[illegible]
29.33:26.56	9.21: 9.87	0.22: 0.40	1	0.46[illegible]
29.33:26.56	9.87:10.54	-0.31:-0.13	1	0.46[illegible]
29.33:26.56	9.87:10.54	-0.13: 0.04	1	0.46[illegible]
29.33:26.56	9.87:10.54	0.04: 0.22	1	0.46[illegible]
26.56:23.92	7.22: 7.88	-0.13: 0.04	2	0.9[illegible]
26.56:23.92	7.22: 7.88	0.22: 0.40	1	0.43[illegible]
26.56:23.92	7.22: 7.88	0.40: 0.57	1	0.43[illegible]
26.56:23.92	7.88: 8.55	-0.13: 0.04	1	0.43[illegible]
26.56:23.92	7.88: 8.55	0.04: 0.22	2	0.9[illegible]
26.56:23.92	7.88: 8.55	0.22: 0.40	1	0.[illegible]
26.56:23.92	8.55: 9.21	-0.49:-0.31	1	0.43[illegible]
26.56:23.92	8.55: 9.21	-0.31:-0.13	4	0.17[illegible]
26.56:23.92	8.55: 9.21	-0.13: 0.04	6	0.29[illegible]
26.56:23.92	8.55: 9.21	0.04: 0.22	1	0.43[illegible]
26.56:23.92	8.55: 9.21	0.22: 0.40	1	0.43[illegible]
26.56:23.92	9.21: 9.87	-0.31:-0.13	6	0.23[illegible]
26.56:23.92	9.21: 9.87	-0.13: 0.04	9	0.41[illegible]
26.56:23.92	9.21: 9.87	0.04: 0.22	2	0.9[illegible]
26.56:23.92	9.21: 9.87	0.22: 0.40	2	0.9[illegible]
26.56:23.92	9.87:10.54	-0.13: 0.04	1	0.43[illegible]
26.56:23.92	9.87:10.54	0.04: 0.22	1	0.43[illegible]
26.56:23.92	10.54:11.20	0.22: 0.40	1	0.43[illegible]
23.92:21.41	5.22: 5.89	0.57: 0.75	2	0.19[illegible]
23.92:21.41	5.89: 6.55	0.22: 0.40	1	0.51[illegible]
23.92:21.41	6.55: 7.22	-0.31:-0.13	1	0.51[illegible]
23.92:21.41	7.22: 7.88	-0.13: 0.04	1	0.51[illegible]
23.92:21.41	7.22: 7.88	0.22: 0.40	1	0.51[illegible]
23.92:21.41	7.88: 8.55	-0.31:-0.13	3	0.15[illegible]
23.92:21.41	7.88: 8.55	-0.13: 0.04	1	0.51[illegible]
23.92:21.41	7.88: 8.55	0.40: 0.57	1	0.51[illegible]
23.92:21.41	8.55: 9.21	-0.49:-0.31	1	0.51[illegible]
23.92:21.41	8.55: 9.21	-0.31:-0.13	7	0.35[illegible]
23.92:21.41	8.55: 9.21	-0.13: 0.04	8	0.41[illegible]
23.92:21.41	8.55: 9.21	0.04: 0.22	1	0.51[illegible]
23.92:21.41	8.55: 9.21	0.22: 0.40	2	0.10[illegible]
23.92:21.41	8.55: 9.21	0.40: 0.57	2	0.10[illegible]
23.92:21.41	8.55: 9.21	0.75: 0.92	1	0.51[illegible]
23.92:21.41	9.21: 9.87	-0.31:-0.13	1	0.51[illegible]
23.92:21.41	9.21: 9.87	-0.13: 0.04	15	0.77[illegible]

TABLE 2. SAMPLE DATA SUMMARY

DROPLET SIZE DISTRIBUTION

MEASURING LOCATION: 3.00mm FROM WALL

MEAN DIAMETER (MICRONS)	NUMBER DENSITY (#/CC/MICRON)	MEAN AXIAL VEL (M/SEC)	STD DEV AXIAL VEL (M/SEC)	MEAN LATERAL VEL (M/SEC)	STD DEV LATERAL VEL (M/SEC)
96.76	0.171E-01	5.59	0.84	0.03	0.32
73.96	0.372E-02	7.92	0.00	0.07	0.00
64.21	0.655E-02	4.99	0.00	-0.13	0.00
59.69	0.899E-02	7.65	1.44	-0.01	0.10
55.40	0.129E-01	8.39	0.35	0.13	0.38
51.32	0.309E-01	7.38	1.47	0.09	0.17
43.77	0.432E-01	8.81	0.30	-0.11	0.18
40.28	0.245E-01	9.08	0.36	0.16	0.41
36.96	0.118E+00	9.08	0.43	0.04	0.21
33.80	0.184E+00	9.06	0.48	0.01	0.31
30.79	0.202E+00	9.20	0.43	-0.02	0.27
27.95	0.397E+00	8.77	1.52	0.08	0.34
25.24	0.340E+00	9.10	0.69	0.01	0.22
22.66	0.480E+00	9.03	1.12	0.08	0.29
20.22	0.586E+00	9.30	0.64	0.04	0.27
17.89	0.569E+00	9.27	0.52	-0.01	0.20
15.68	0.758E+00	9.53	0.61	0.01	0.25
13.59	0.900E+00	9.44	0.51	0.08	0.26
11.60	0.915E+00	9.45	0.64	0.06	0.26
10.09	0.124E+01	9.50	0.93	0.09	0.31
9.03	0.916E+00	3.41	0.87	0.18	0.33
8.02	0.744E+00	9.50	0.84	0.25	0.39
7.06	0.681E+00	9.20	0.80	0.40	0.40
6.14	0.168E+01	9.23	1.19	0.22	0.35

MEAN AXIAL AIR VELOCITY = 9.75
STANDARD DEVIATION OF AXIAL AIR VELOCITY = 0.53
MEAN LATERAL AIR VELOCITY = 0.25
STANDARD DEVIATION OF LATERAL AIR VELOCITY = 0.31

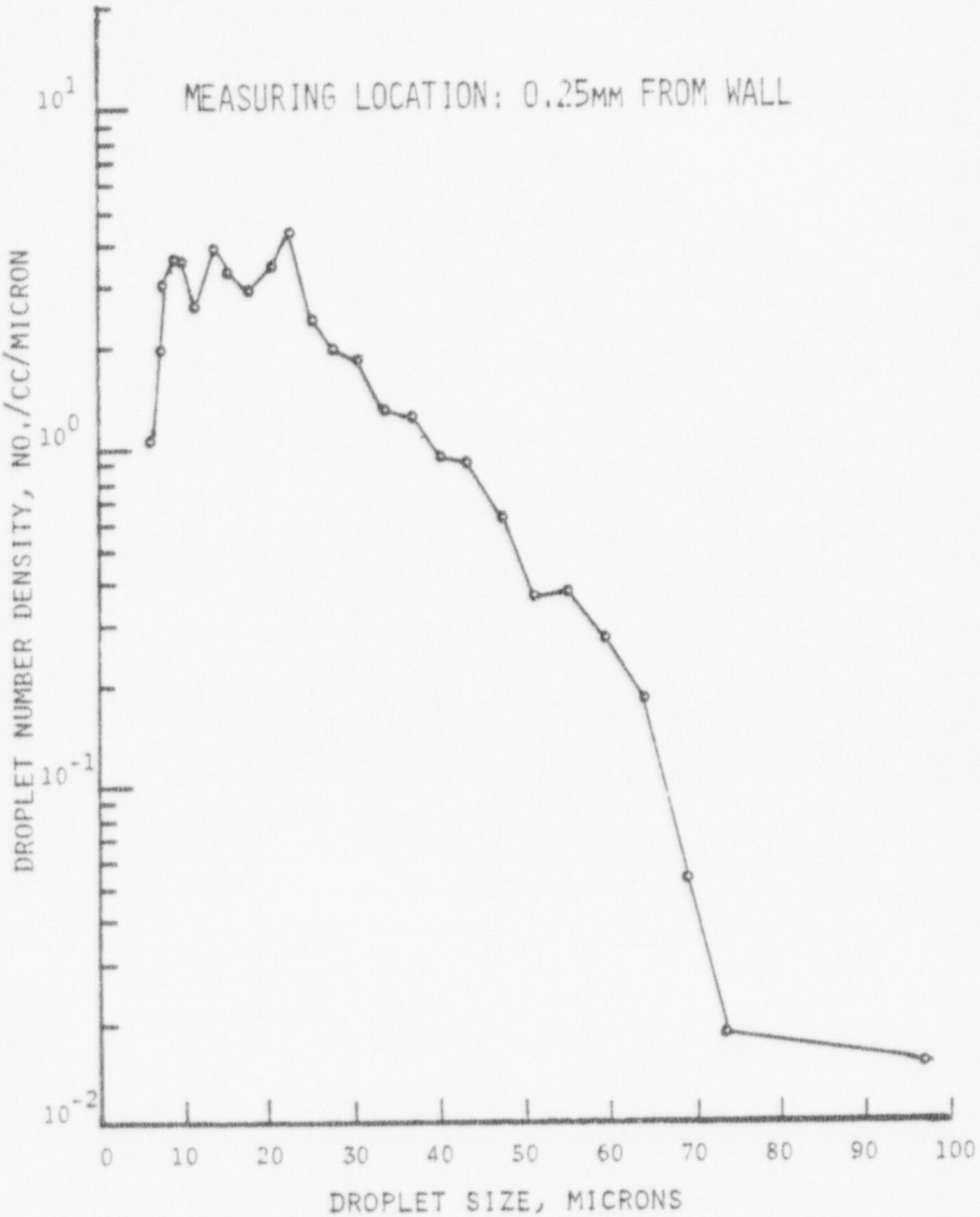

FIGURE 34. DROPLET SIZE AND NUMBER DENSITY DISTRIBUTIONS WITH LIQUID FILM ON WALL

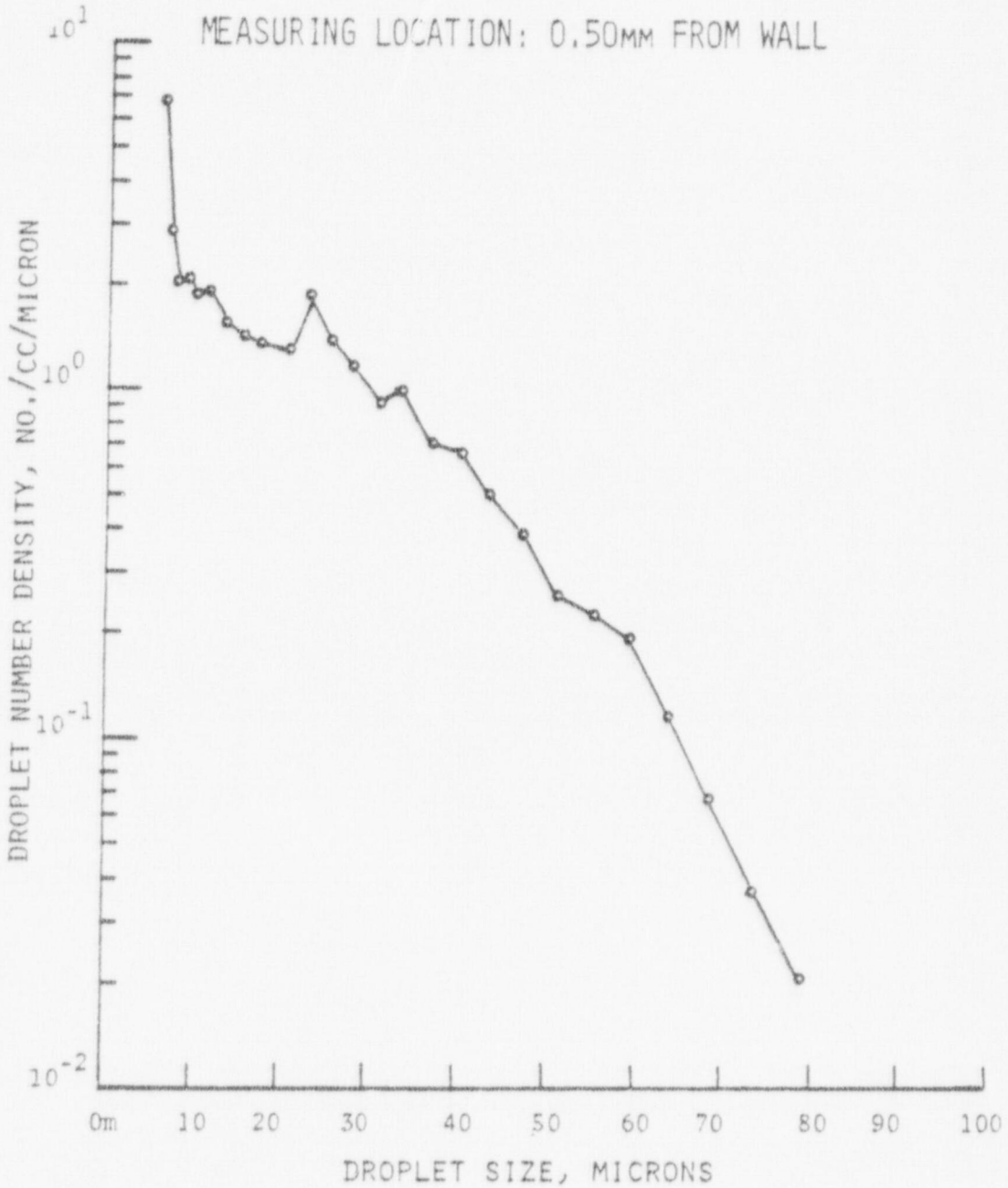

FIGURE 35. DROPLET SIZE AND NUMBER DENSITY DISTRIBUTIONS WITH LIQUID FILM ON WALL

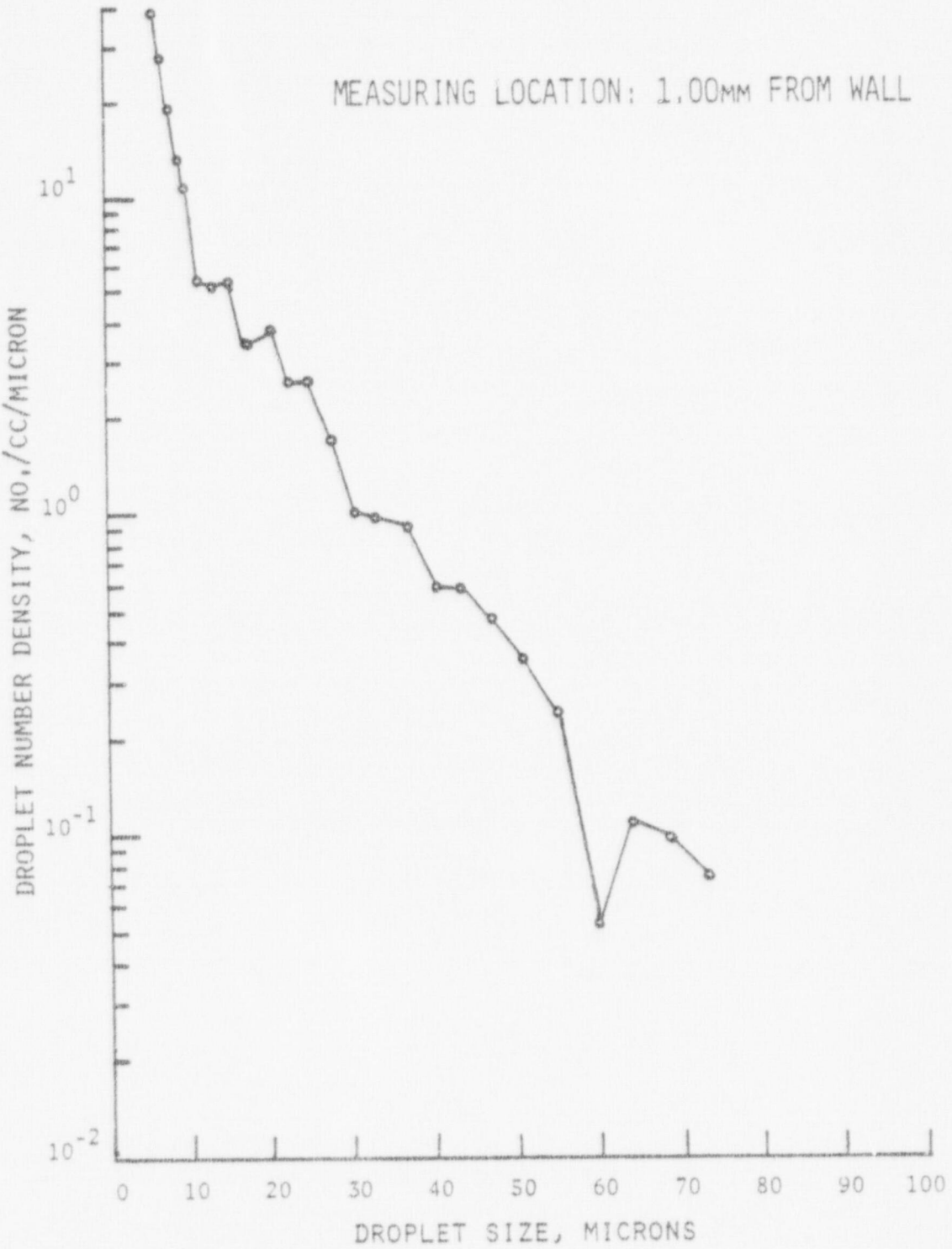

FIGURE 36. DROPLET SIZE AND NUMBER DENSITY DISTRIBUTIONS WITH LIQUID FILM ON WALL

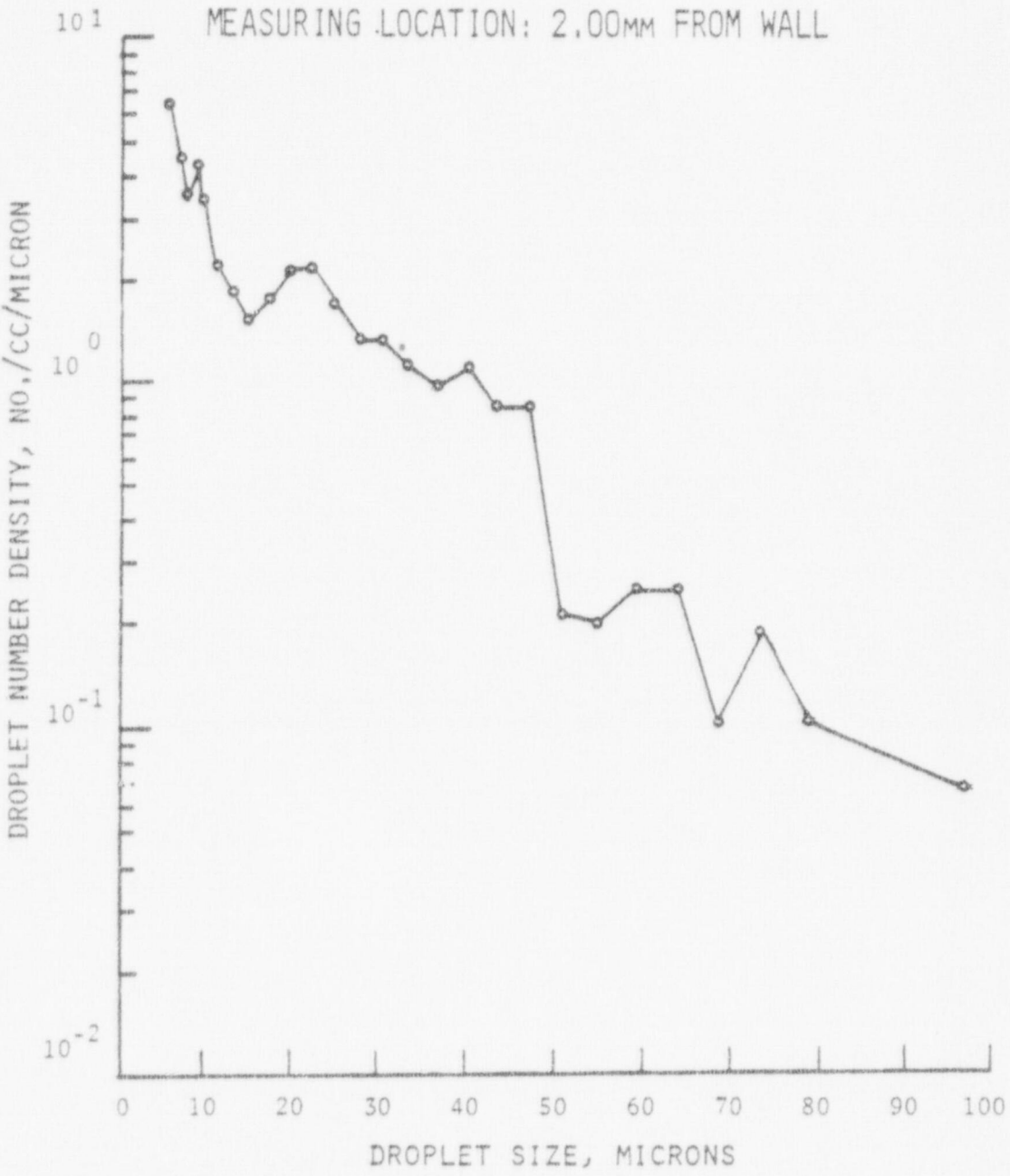

FIGURE 37. DROPLET SIZE AND NUMBER DENSITY DISTRIBUTIONS WITH LIQUID FILM ON WALL

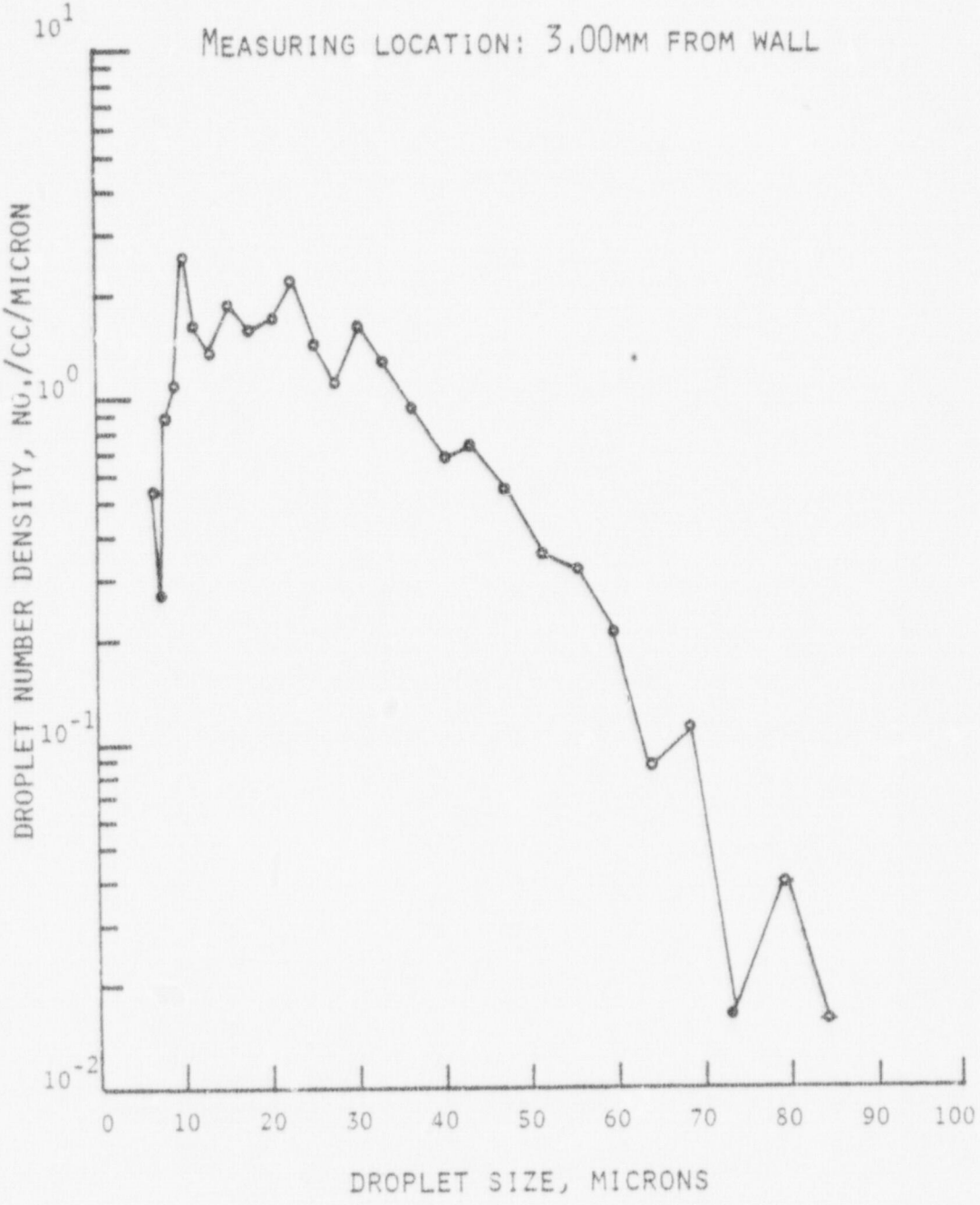

FIGURE 38. DROPLET SIZE AND NUMBER DENSITY DISTRIBUTIONS WITH LIQUID FILM ON WALL

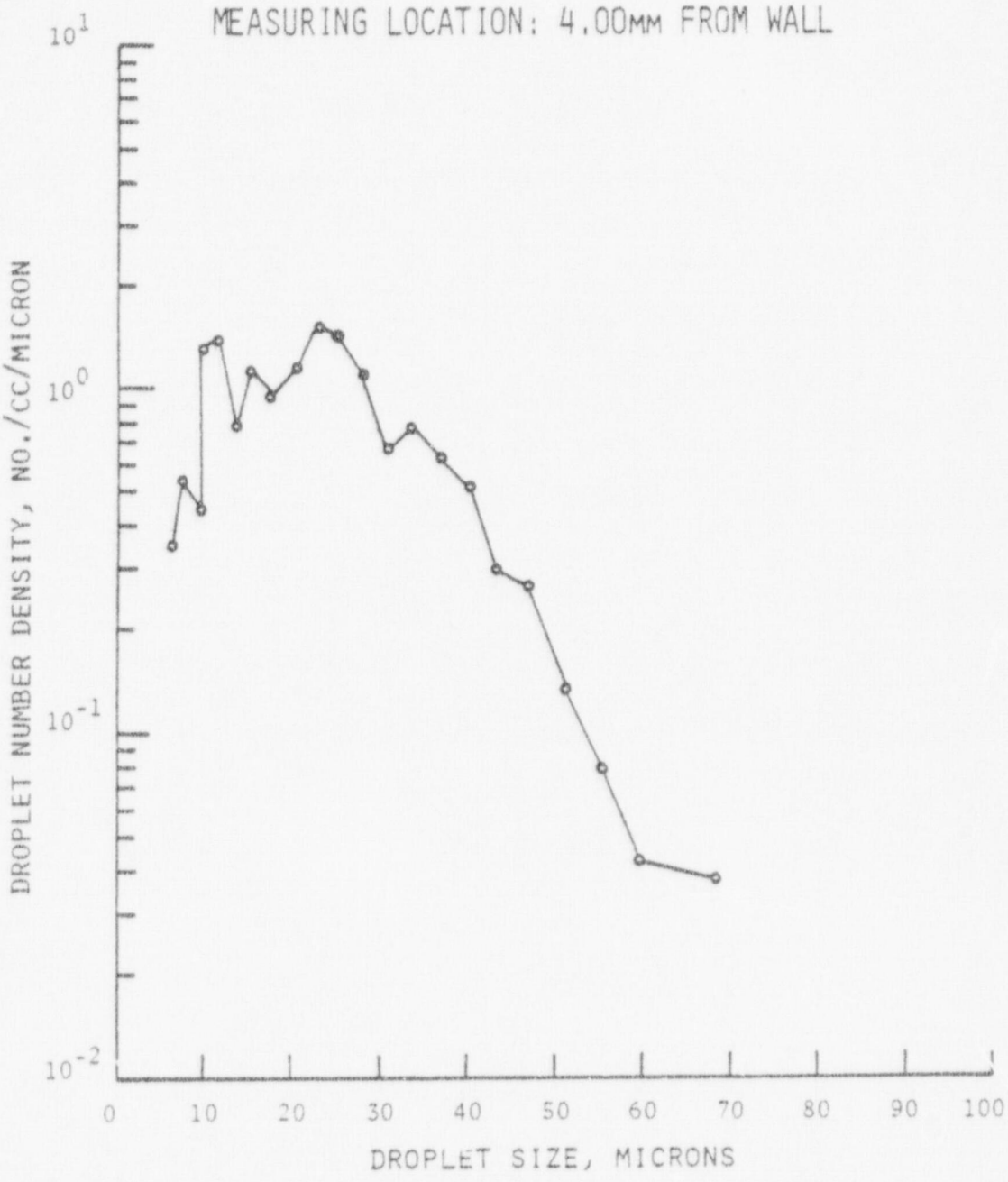

FIGURE 39. DROPLET SIZE AND NUMBER DENSITY DISTRIBUTIONS WITH LIQUID FILM ON WALL

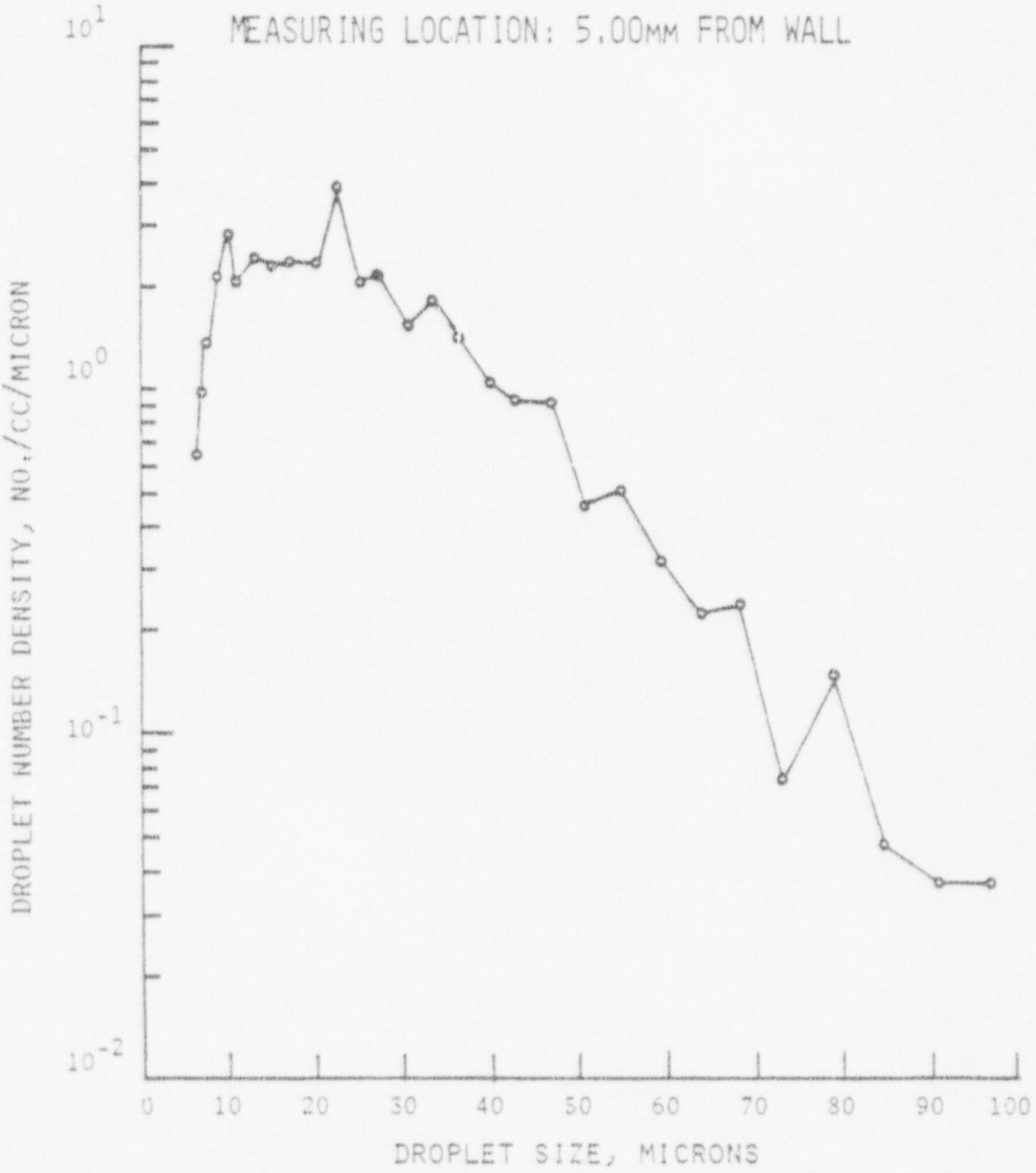

FIGURE 40. DROPLET SIZE AND NUMBER DENSITY DISTRIBUTIONS WITH LIQUID FILM ON WALL

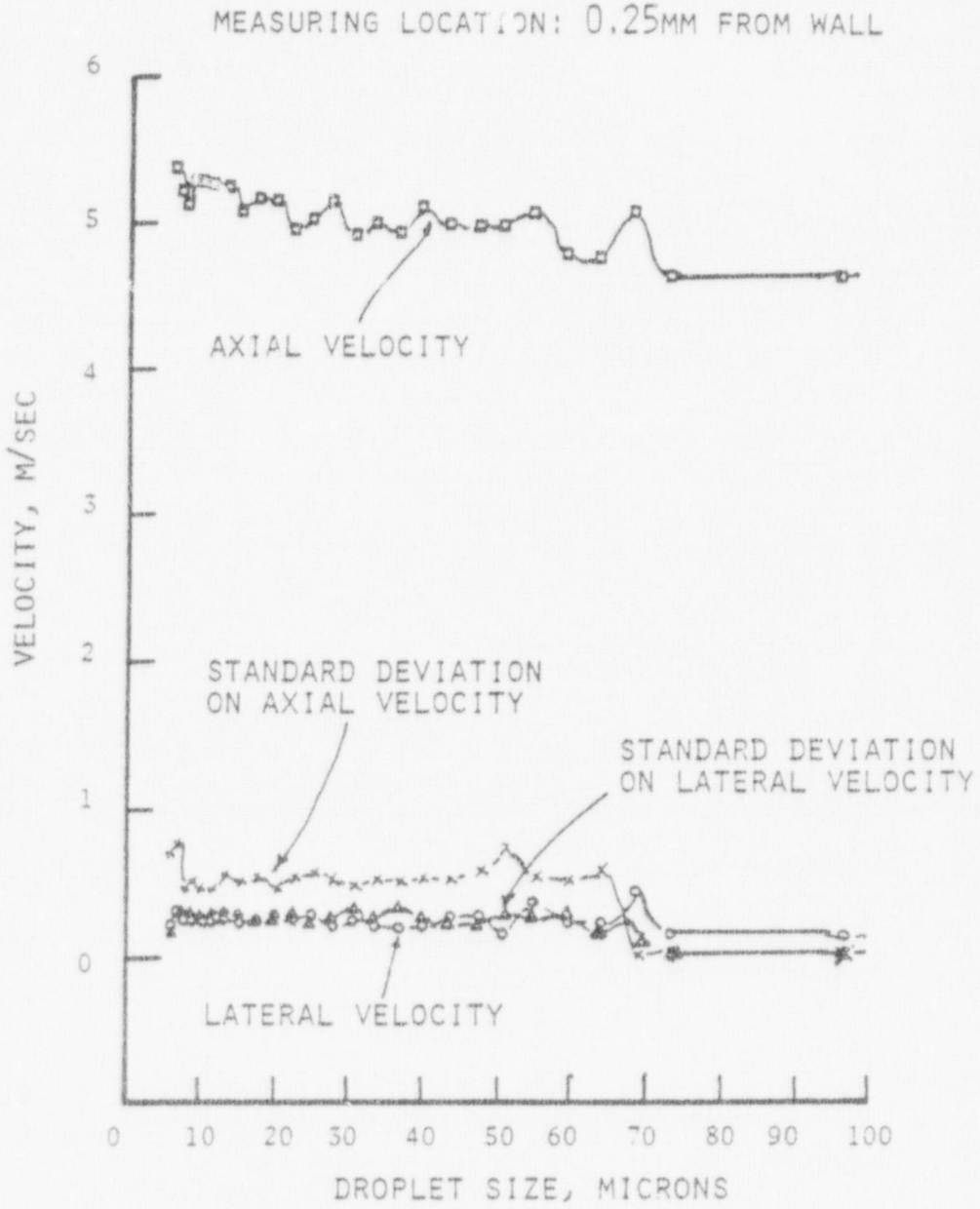

FIGURE 41. DROPLET VELOCITY DISTRIBUTIONS WITH LIQUID FILM ON WALL

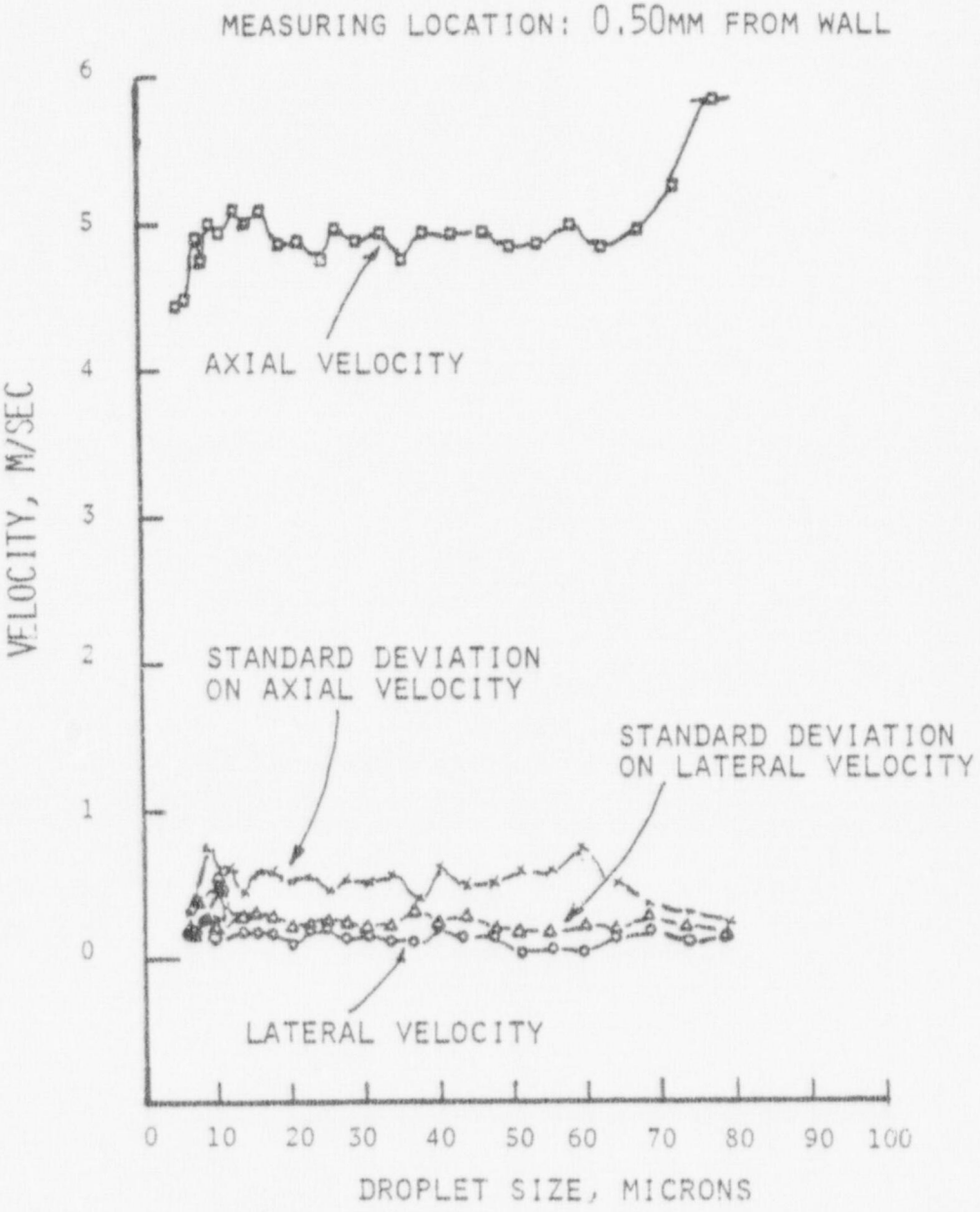

FIGURE 42. DROPLET VELOCITY DISTRIBUTIONS WITH LIQUID FILM ON WALL

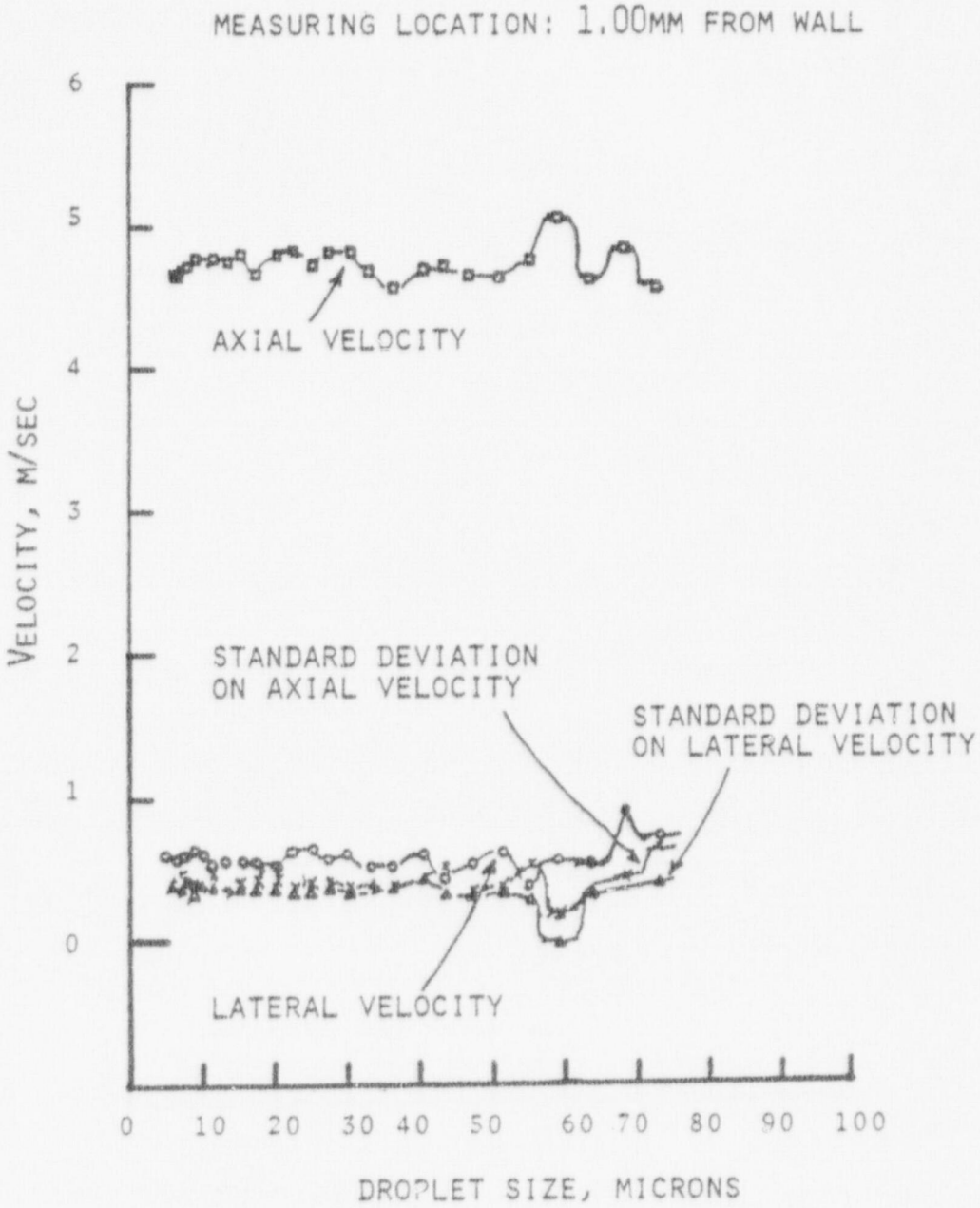

FIGURE 43. DROPLET VELOCITY DISTRIBUTIONS WITH LIQUID FILM ON WALL

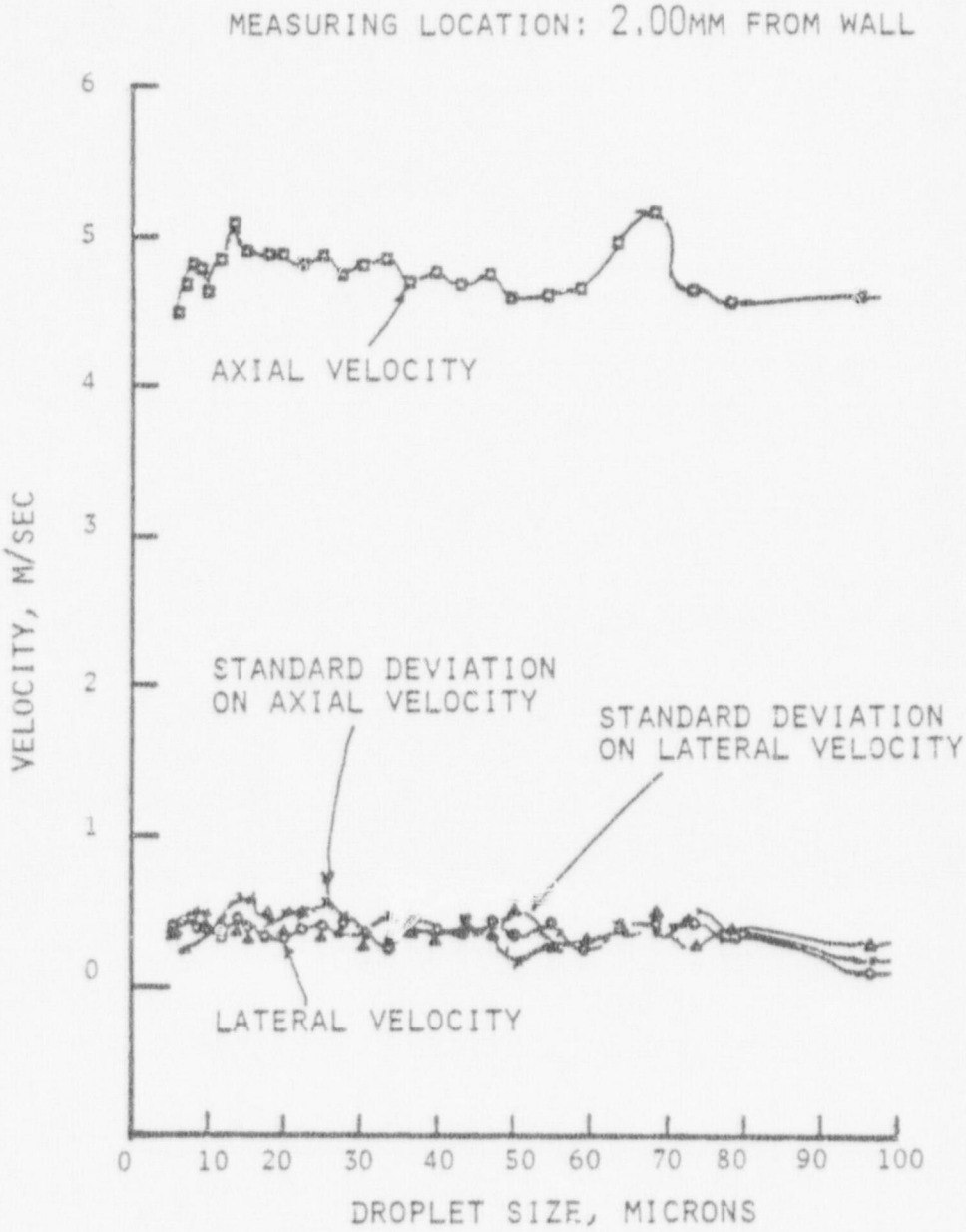

FIGURE 44. DROPLET VELOCITY DISTRIBUTIONS WITH LIQUID FILM ON WALL

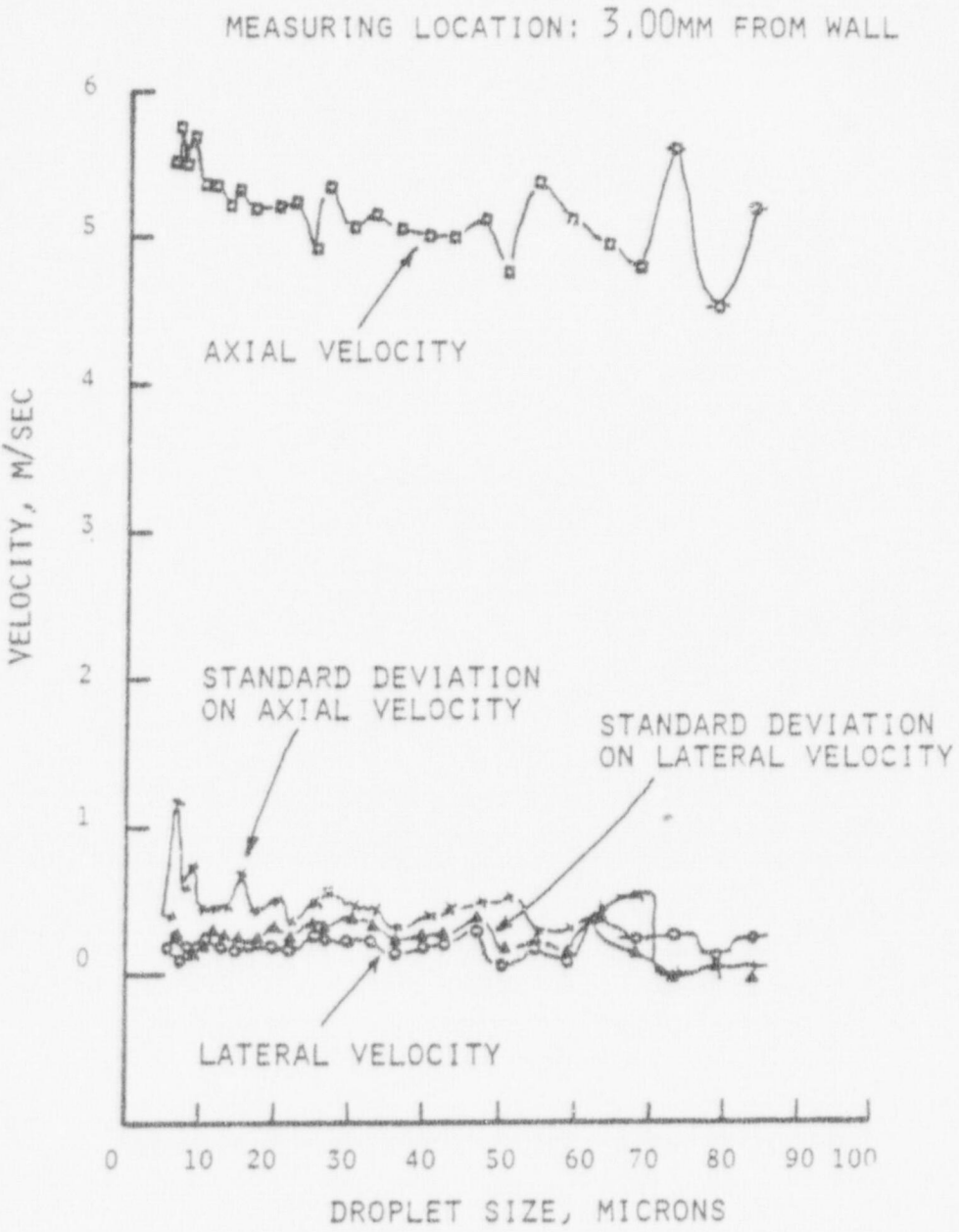

FIGURE 45. DROPLET VELOCITY DISTRIBUTIONS WITH LIQUID FILM ON WALL

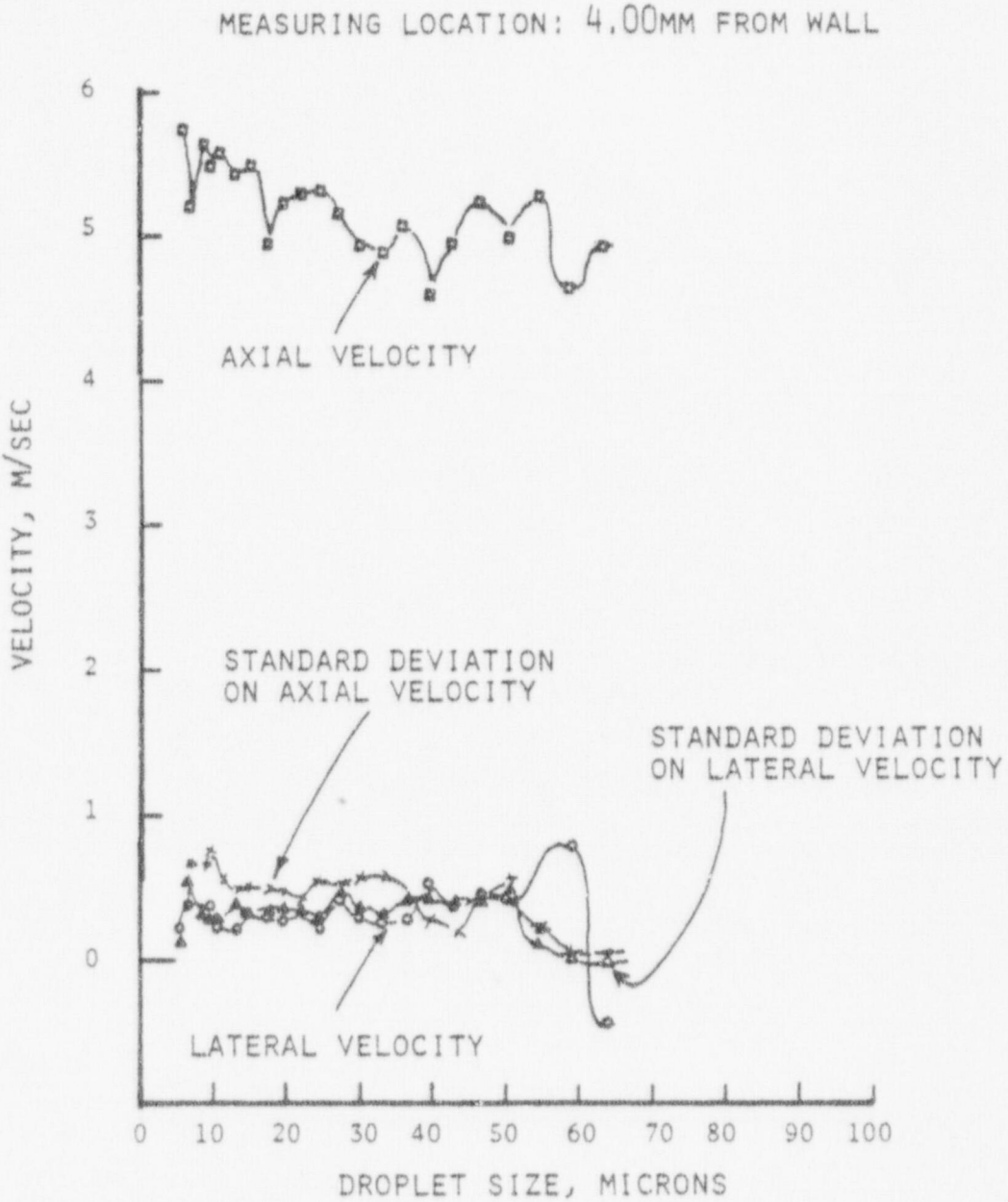

FIGURE 46. DROPLET VELOCITY DISTRIBUTIONS WITH LIQUID FILM ON WALL

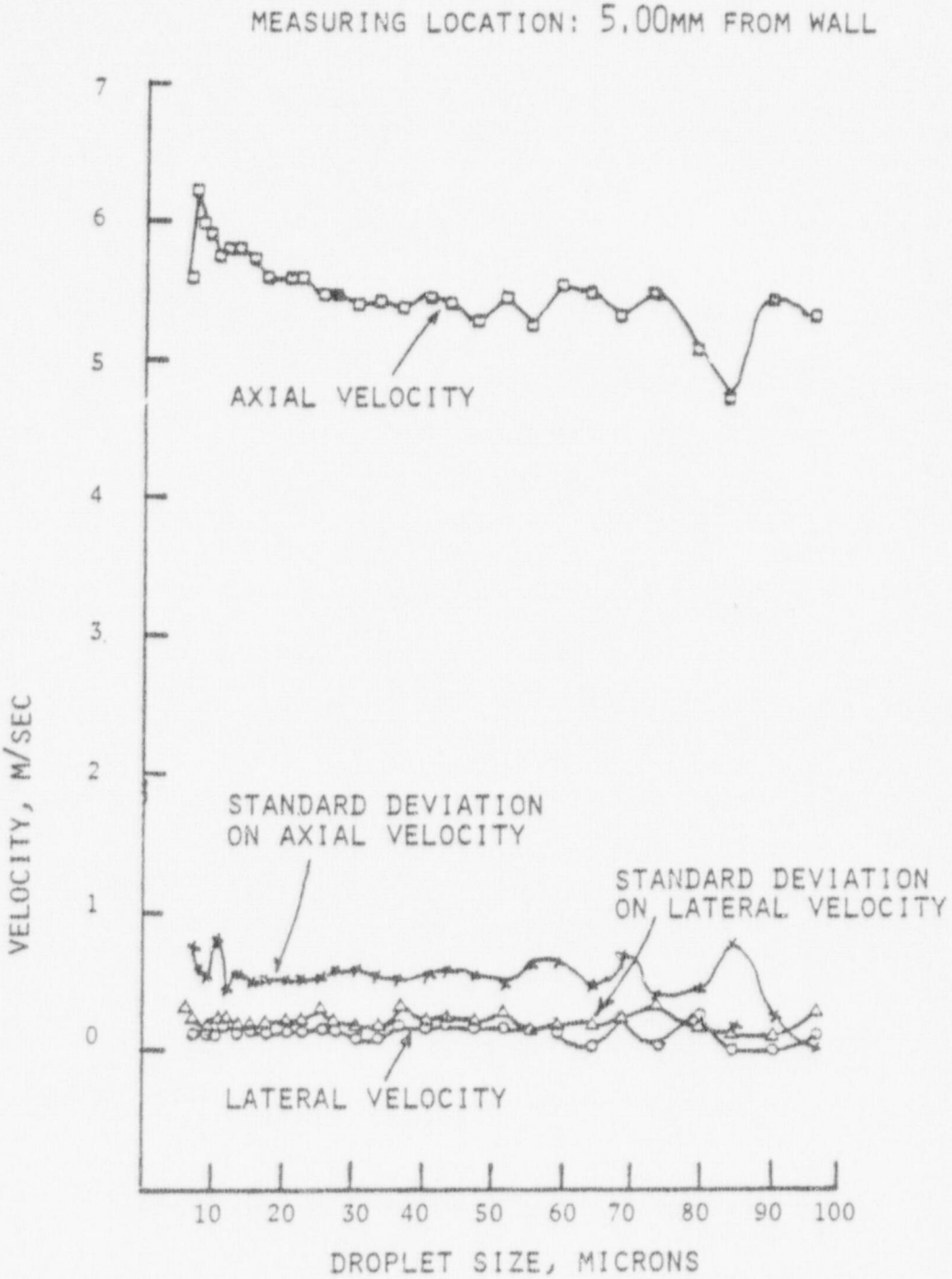

FIGURE 47. DROPLET VELOCITY DISTRIBUTIONS WITH LIQUID FILM ON WALL

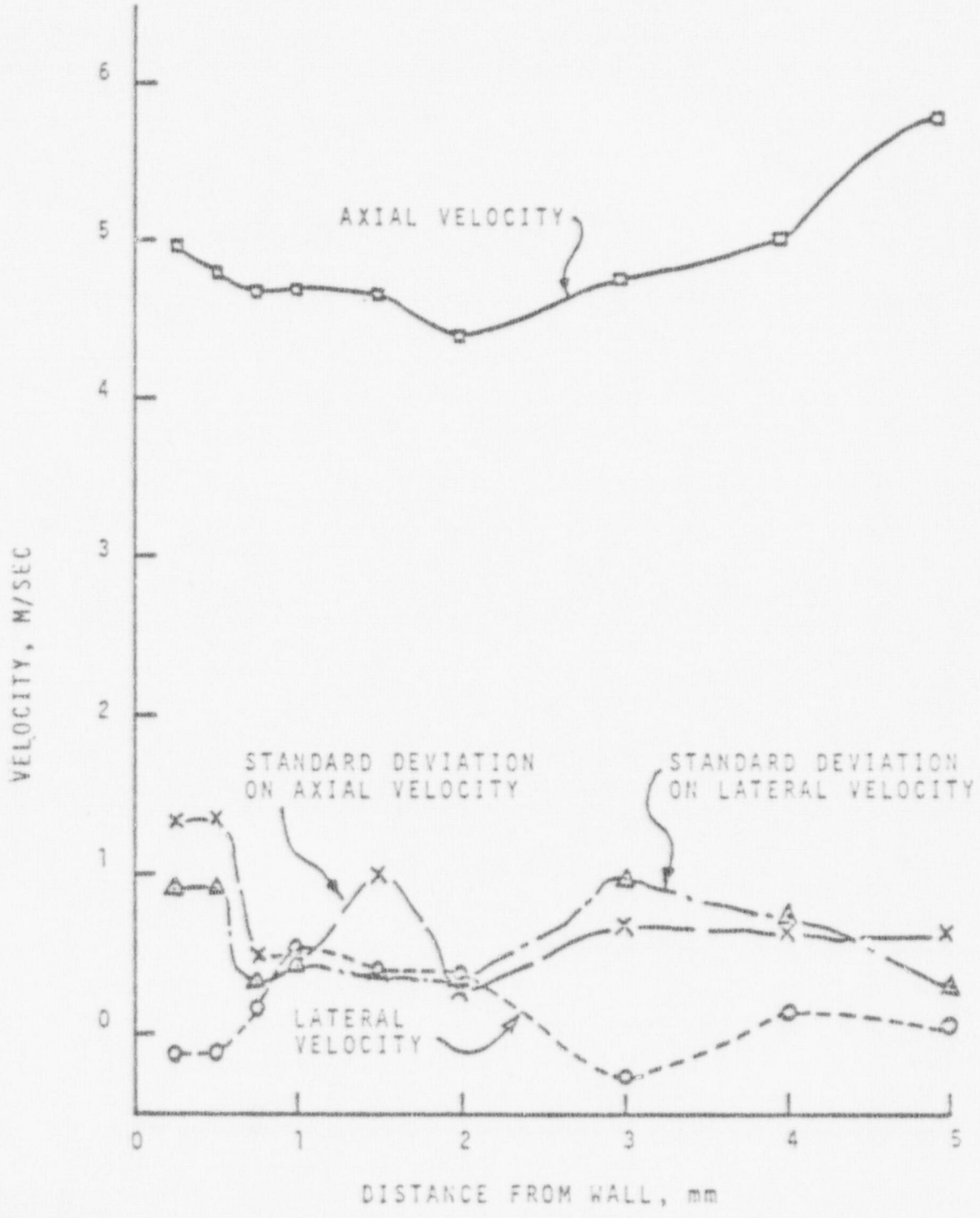

FIGURE 48. AIR VELOCITY DISTRIBUTIONS WITH LIQUID FILM ON WALL

This is shown in Figure 49.

It was observed that the flow in the channel was unsteady due to the droplet entrainment from the wall film. Hence attempts were made to study the droplet distribution without any wall film.

MEASUREMENTS IN A DILUTE DISPERSED FLOW THROUGH A VERTICAL RECTANGULAR CHANNEL WITHOUT LIQUID FILM ON THE WALL

The flow system was modified to generate a two-phase turbulent flow of water droplets without any visible water film present on the wall. In order to achieve this the following changes were made: The water flow was reduced and the air flow going into the atomizing device was increased. The perforated plate was replaced by a small rectangular orifice. This flow arrangement is shown in Figure 50. The flow conditions for both experiments are listed for comparision in Table 3.

The measuring volume was placed at a level of 541 mm. from the channel entrance and, as before, it was moved along the lateral axis through nine successive measuring locations. The data accumulation and analysis were done using the same procedure outlined for the previous experiment.

The measured number densities of various size droplets at different distances from the wall are shown in Figures 51-59; the droplet velocity distribution and the corresponding standard deviations are shown in Figures 60 to 68; and the air velocity distributions at different distances from the wall are shown in Figure 69.

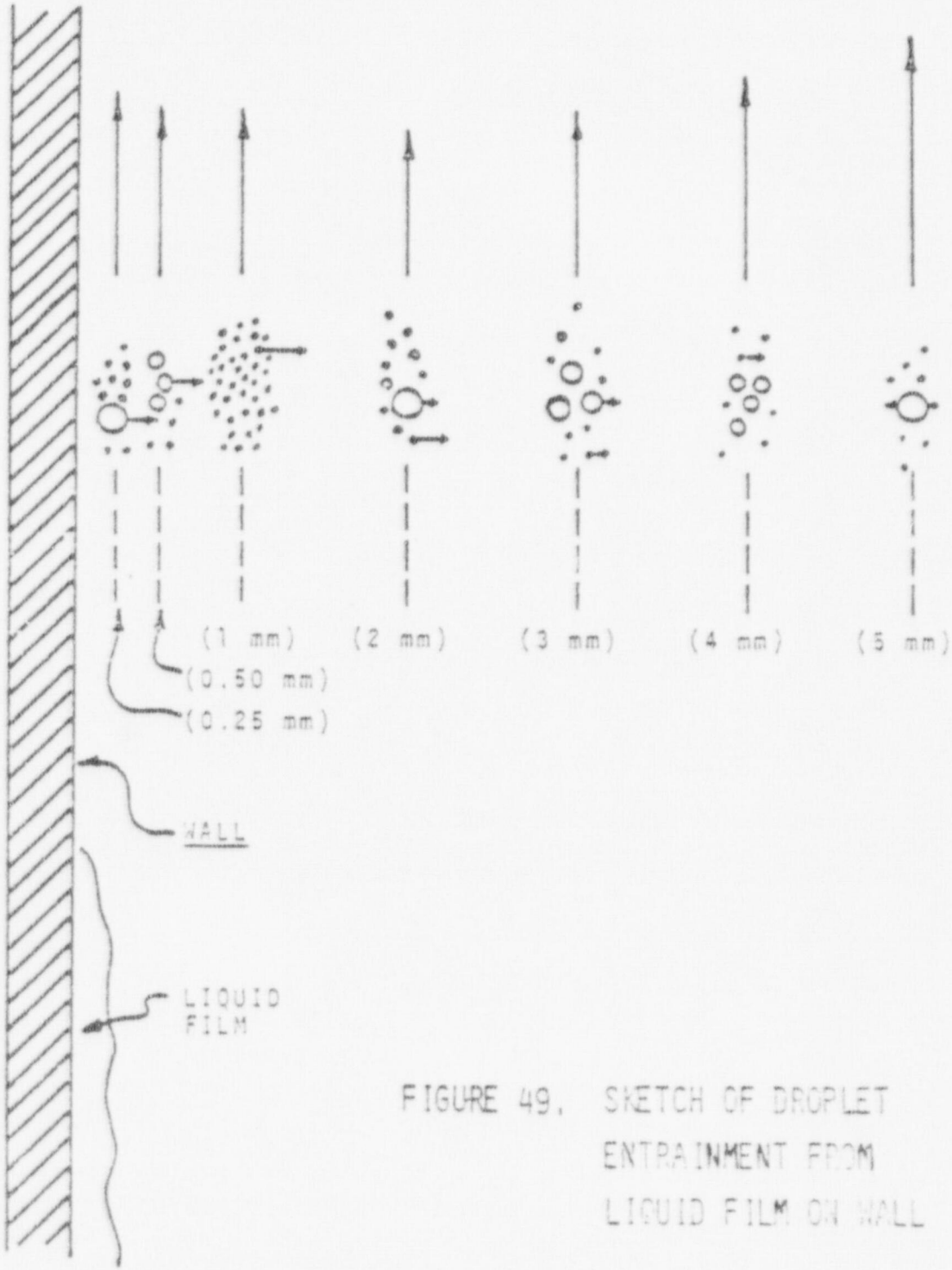

FIGURE 49. SKETCH OF DROPLET ENTRAINMENT FROM LIQUID FILM ON WALL

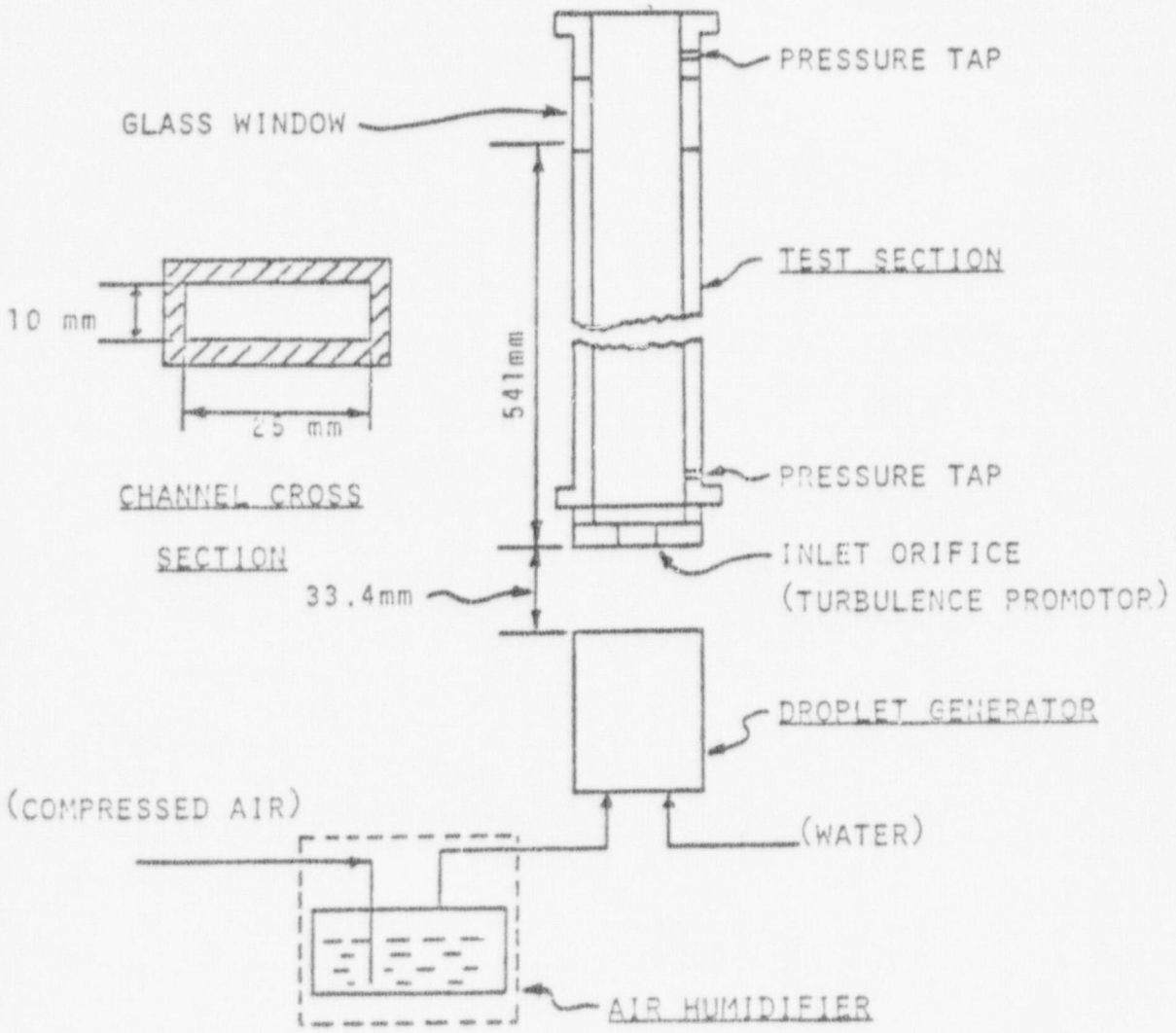

FIGURE 50. FLOW ARRANGEMENT

TABLE. 3.

FLOW CONDITIONS

- WITH LIQUID FILM ON THE CHANNEL WALL

  AVERAGE AIR VELOCITY = 5.21 M/SEC

  FLOW REYNOLDS NO. = 3,600

  AXIAL PRESSURE GRADIENT = 1.32 MM GF H_2O/M

  TEMPERATURE = 20^oC

  DROPLET SIZE RANGE : UP TO 100 μ

  DISTANCE FROM THE ENTRANCE TO THE

  MEASURING LEVEL : 582MM

- WITHOUT LIQUID FILM ON THE CHANNEL WALL

  AVERAGE AIR VELOCITY = 9.52 M/SEC

  FLOW REYNOLDS NO. = 6,600

  AXIAL PRESSURE GRADIENT = 1.54 MM OF H_2O/M

  TEMPERATURE = 20^oC

  DROPLET SIZE RANGE : UP TO 100 μ

  DISTANCE FROM THE ENTRANCE TO THE

  MEASURING LEVEL : 541MM

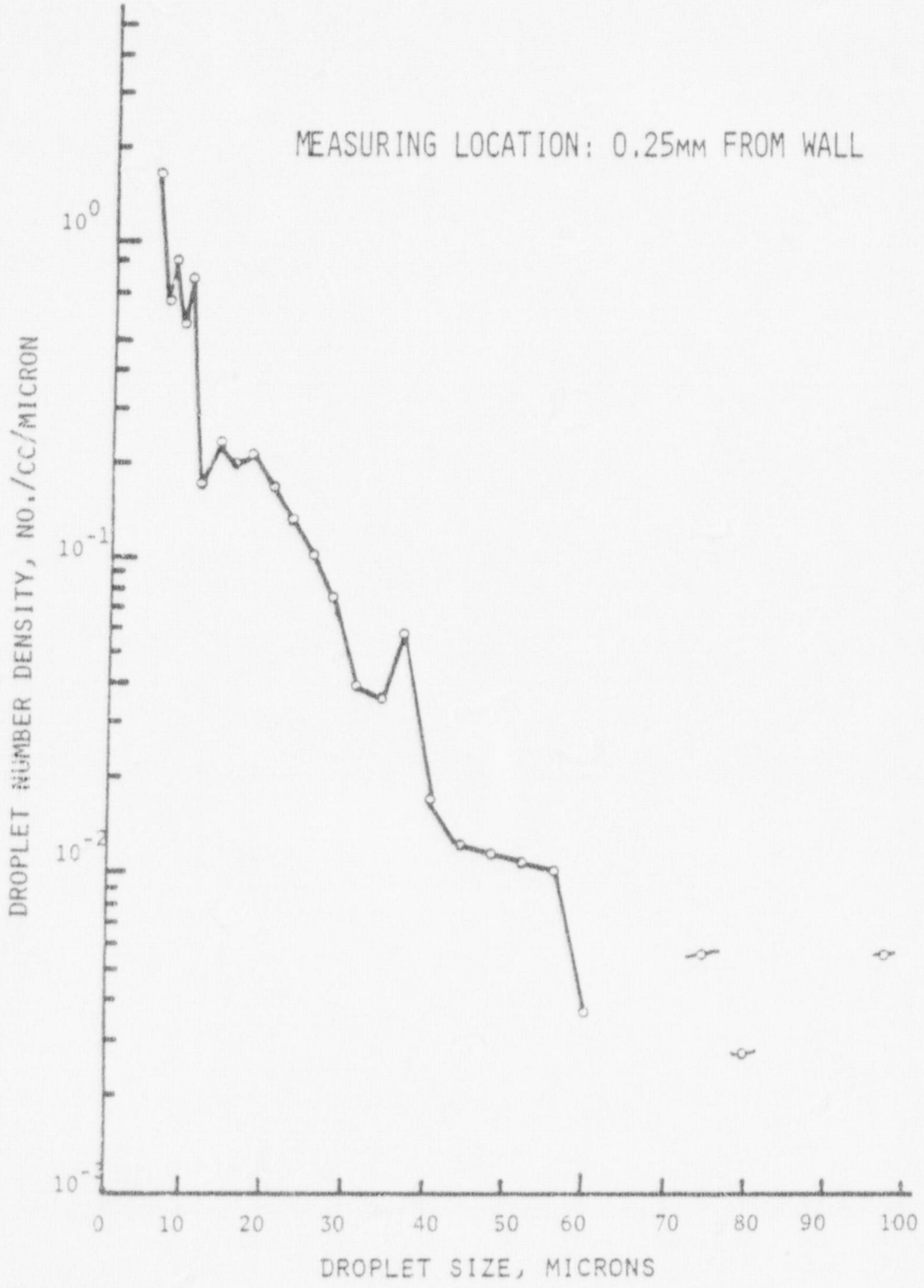

FIGURE 51. DROPLET SIZE AND NUMBER DENSITY DISTRIBUTIONS WITHOUT LIQUID FILM ON WALL

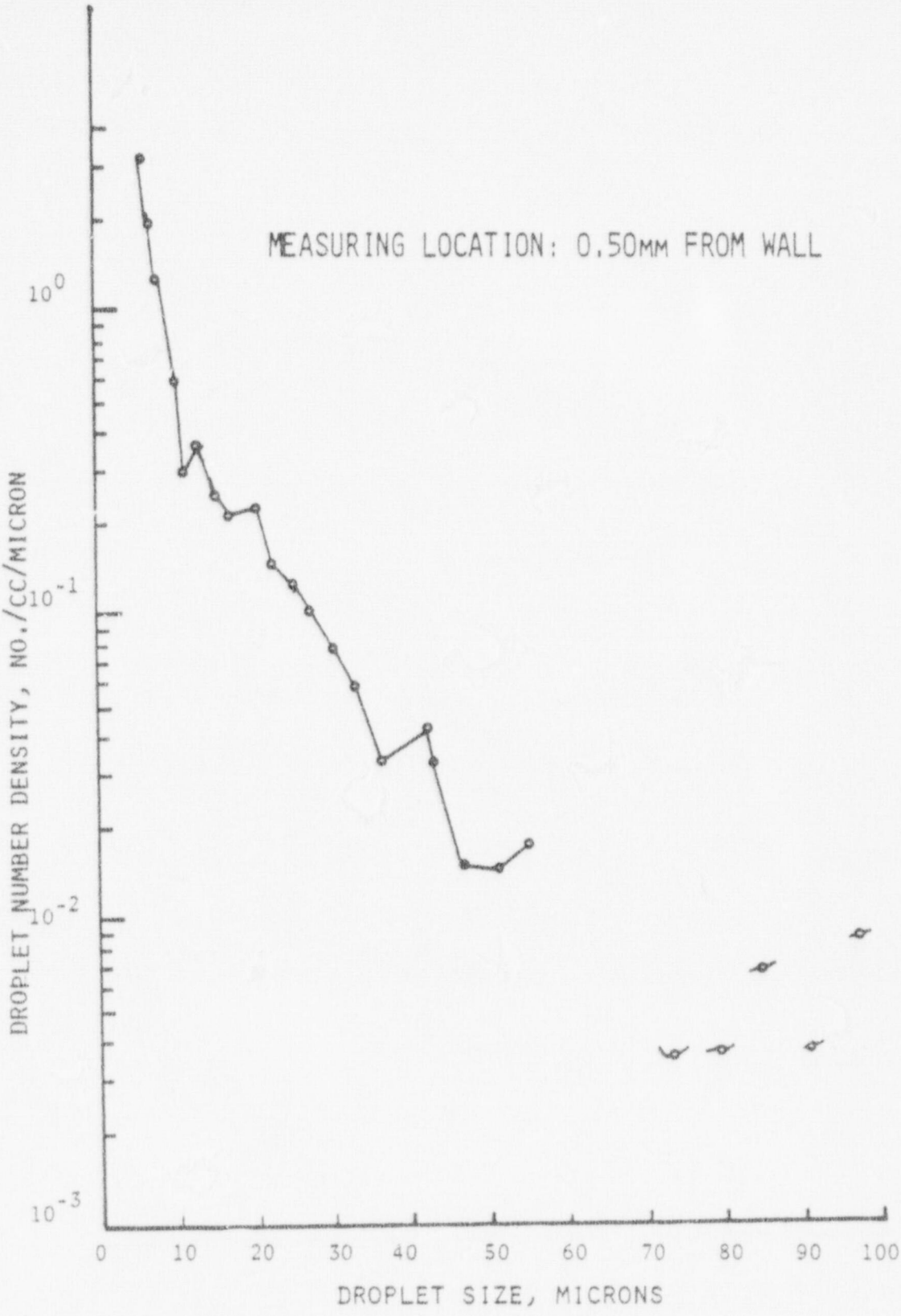

FIGURE 52. DROPLET SIZE AND NUMBER DENSITY DISTRIBUTIONS WITHOUT LIQUID FILM ON WALL

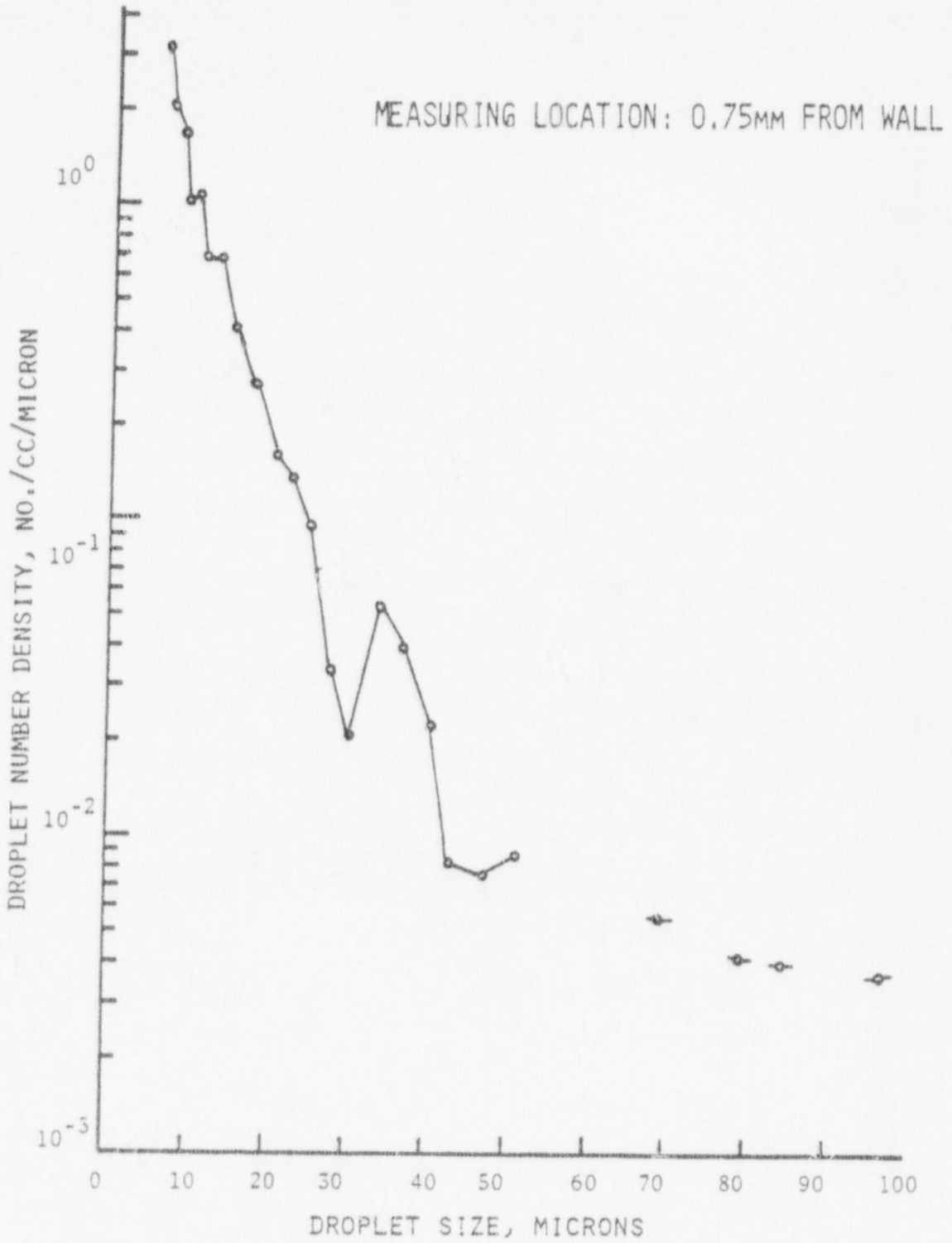

FIGURE 53. DROPLET SIZE AND NUMBER DENSITY DISTRIBUTIONS WITHOUT LIQUID FILM ON WALL

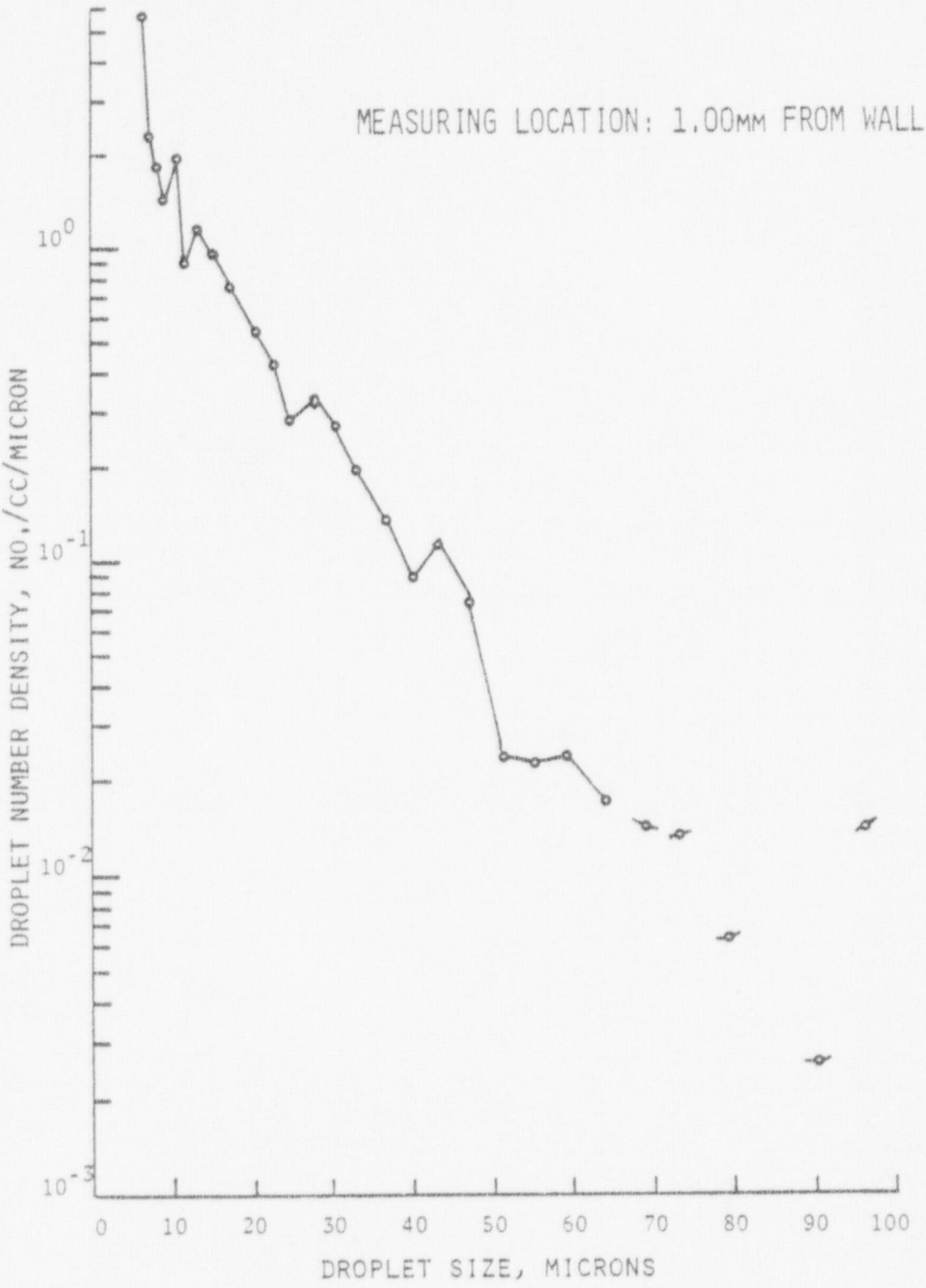

FIGURE 54. DROPLET SIZE AND NUMBER DENSITY DISTRIBUTIONS WITHOUT LIQUID FILM ON WALL

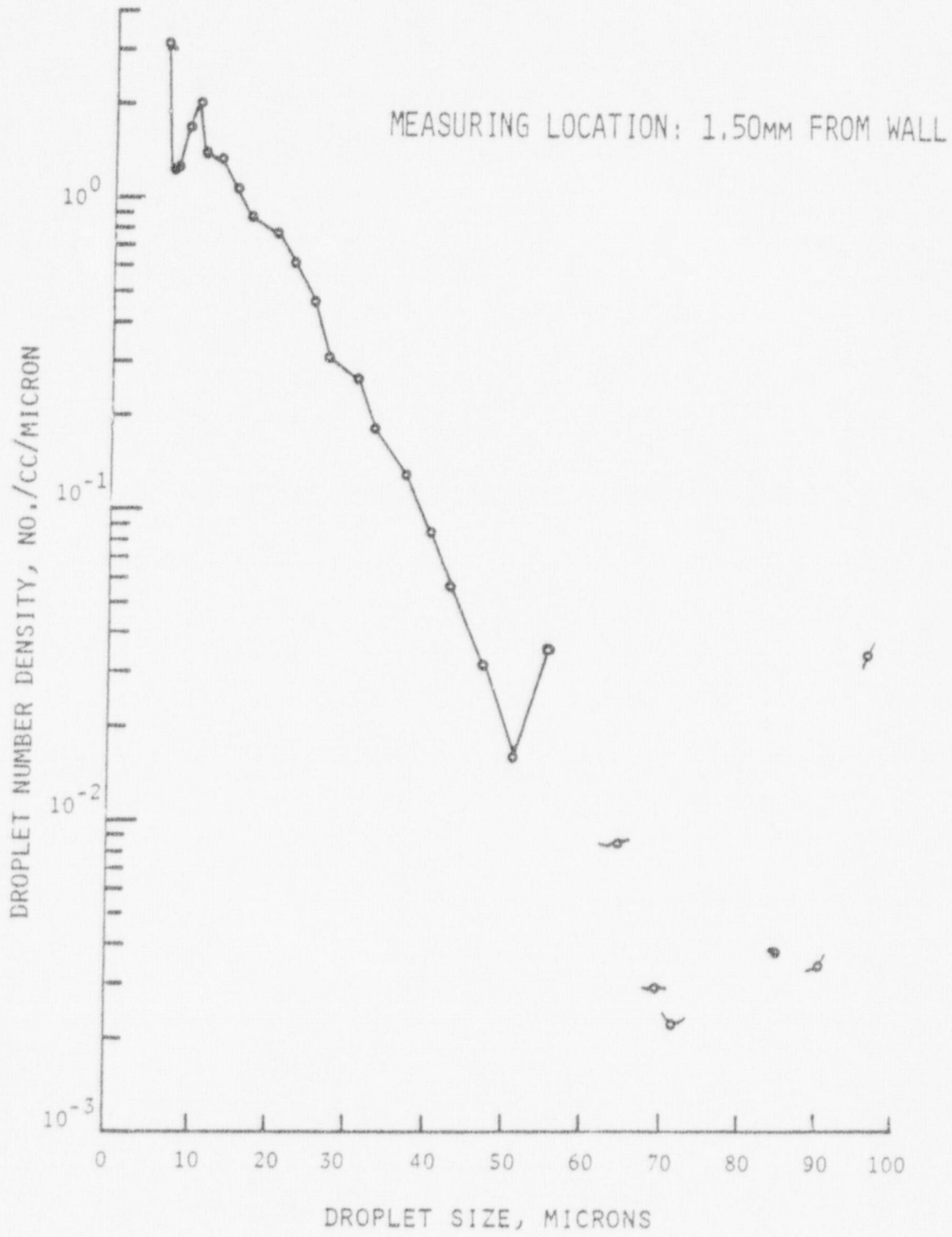

FIGURE 55. DROPLET SIZE AND NUMBER DENSITY DISTRIBUTIONS WITHOUT LIQUID FILM ON WALL

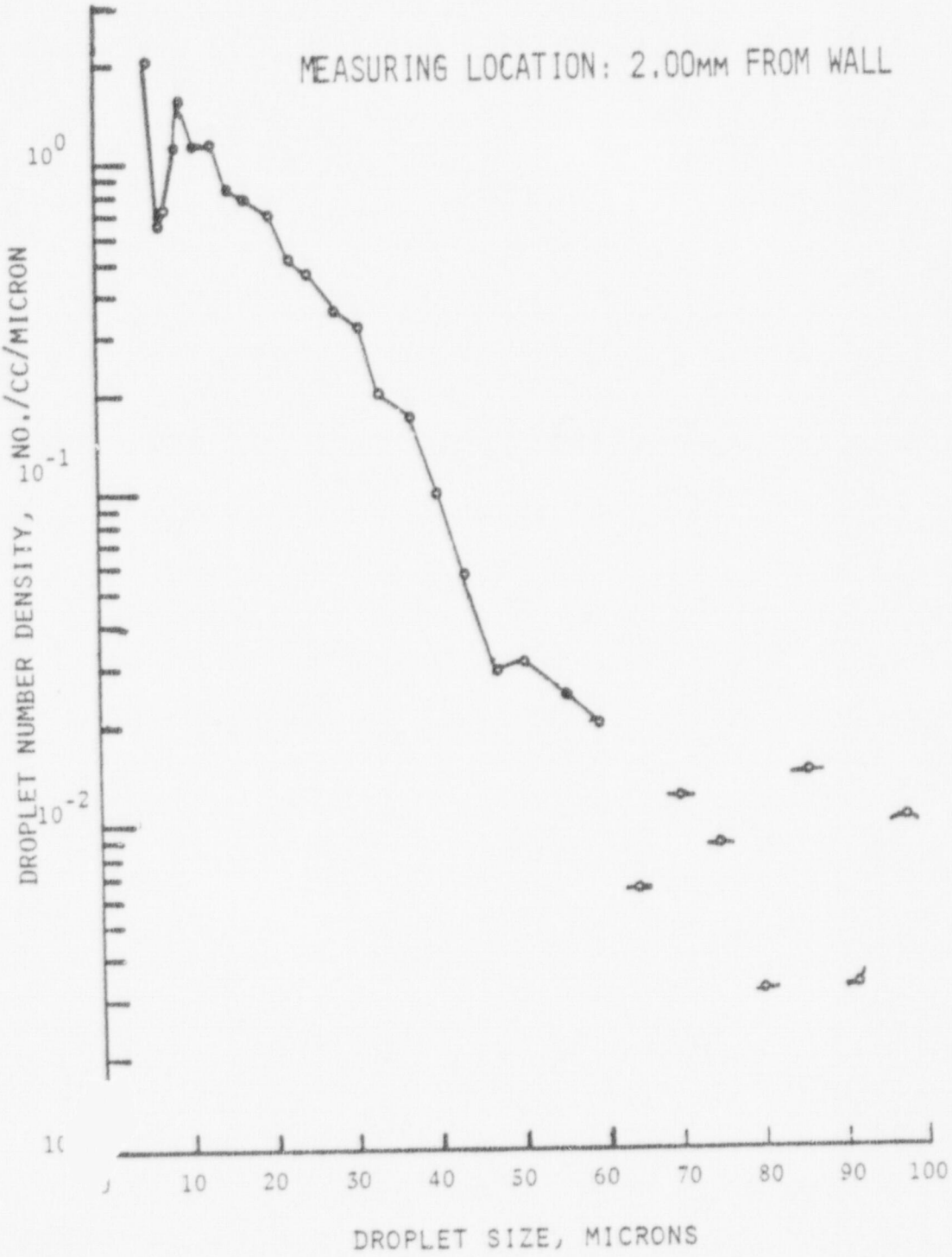

FIGURE 56. DROPLET SIZE AND NUMBER DENSITY DISTRIBUTIONS WITHOUT LIQUID FILM ON WALL

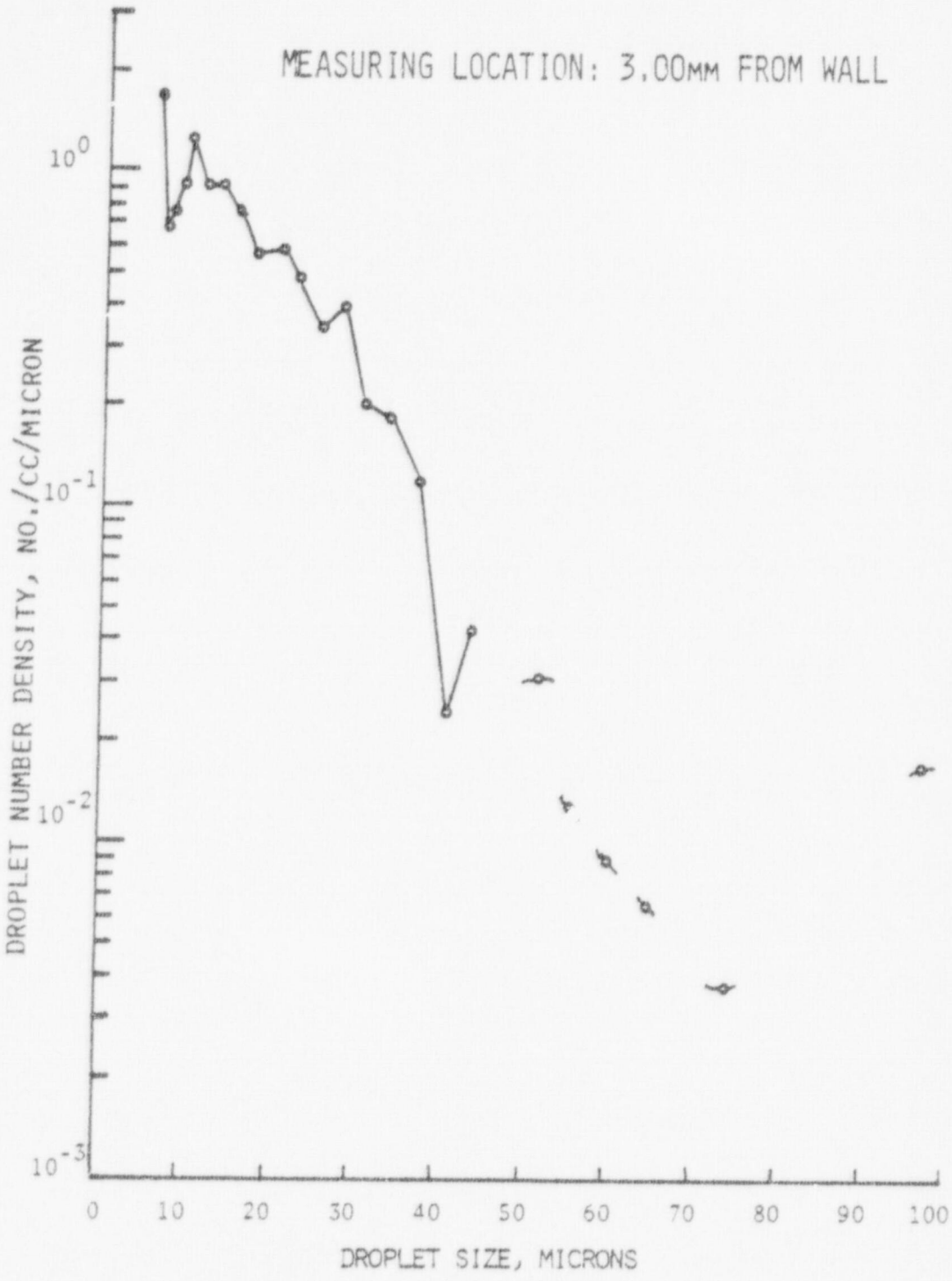

FIGURE 57. DROPLET SIZE AND NUMBER DENSITY DISTRIBUTIONS WITHOUT LIQUID FILM ON WALL

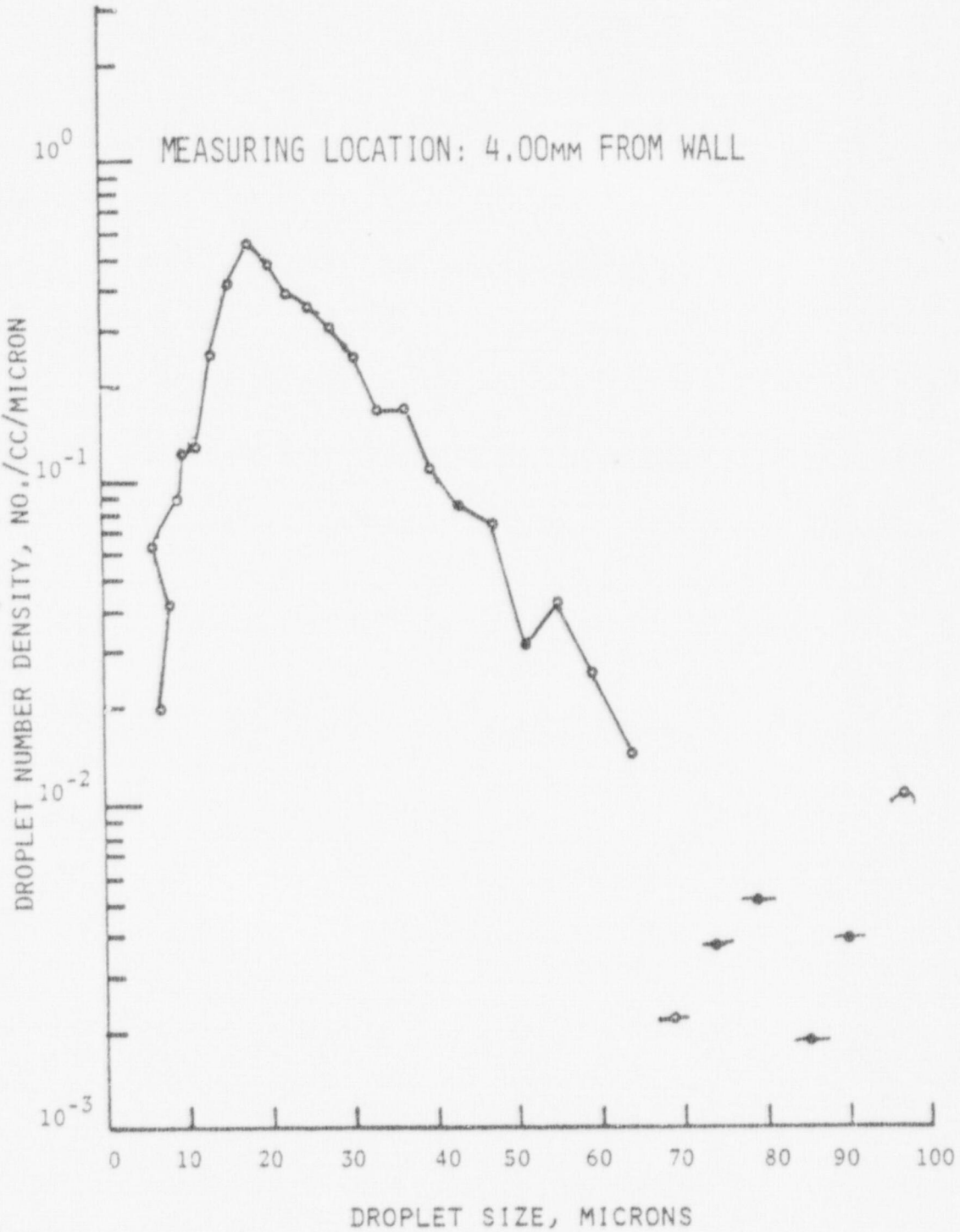

FIGURE 58. DROPLET SIZE AND NUMBER DENSITY DISTRIBUTIONS WITHOUT LIQUID FILM ON WALL

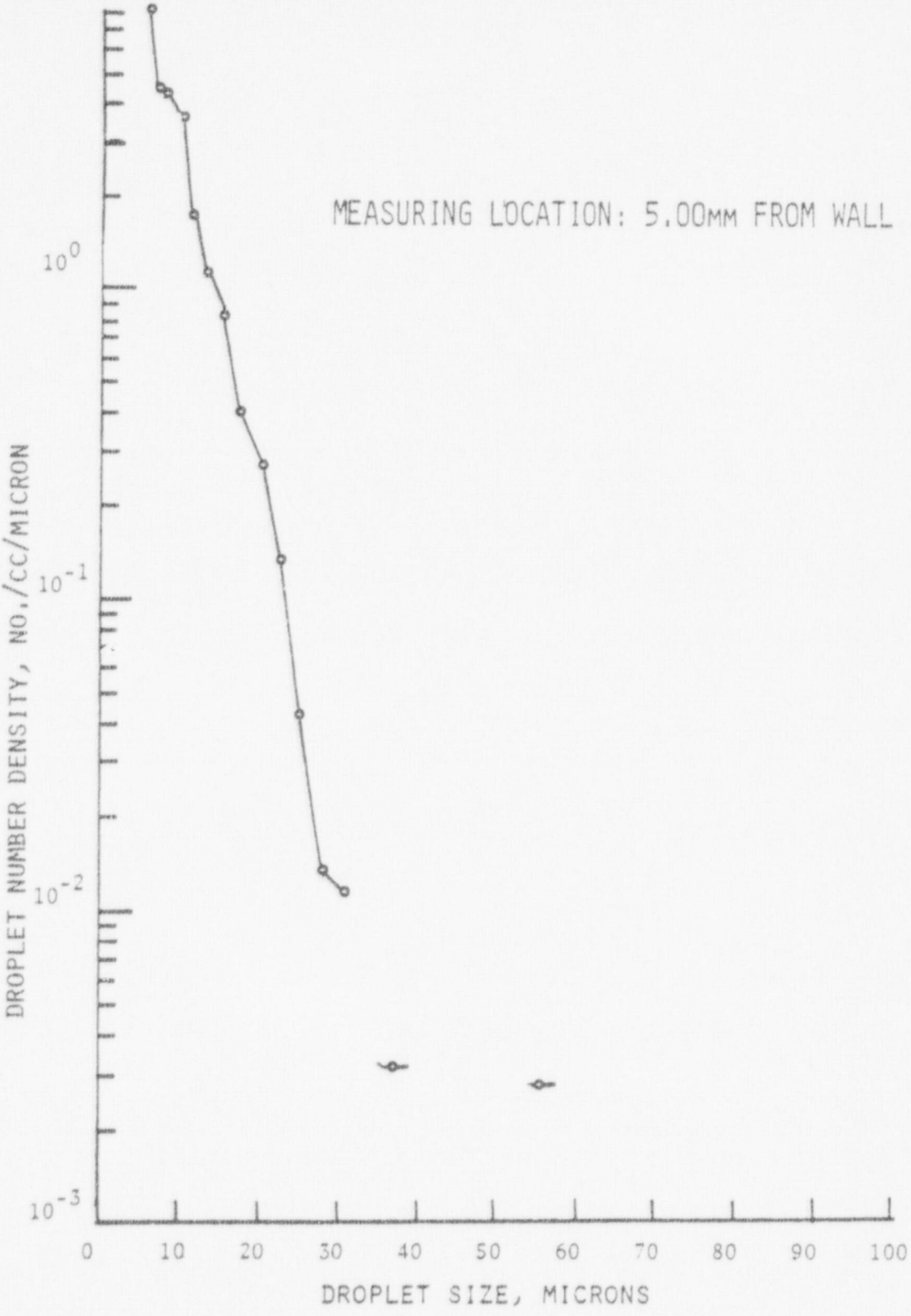

FIGURE 59. DROPLET SIZE AND NUMBER DENSITY DISTRIBUTIONS WITHOUT LIQUID FILM ON WALL

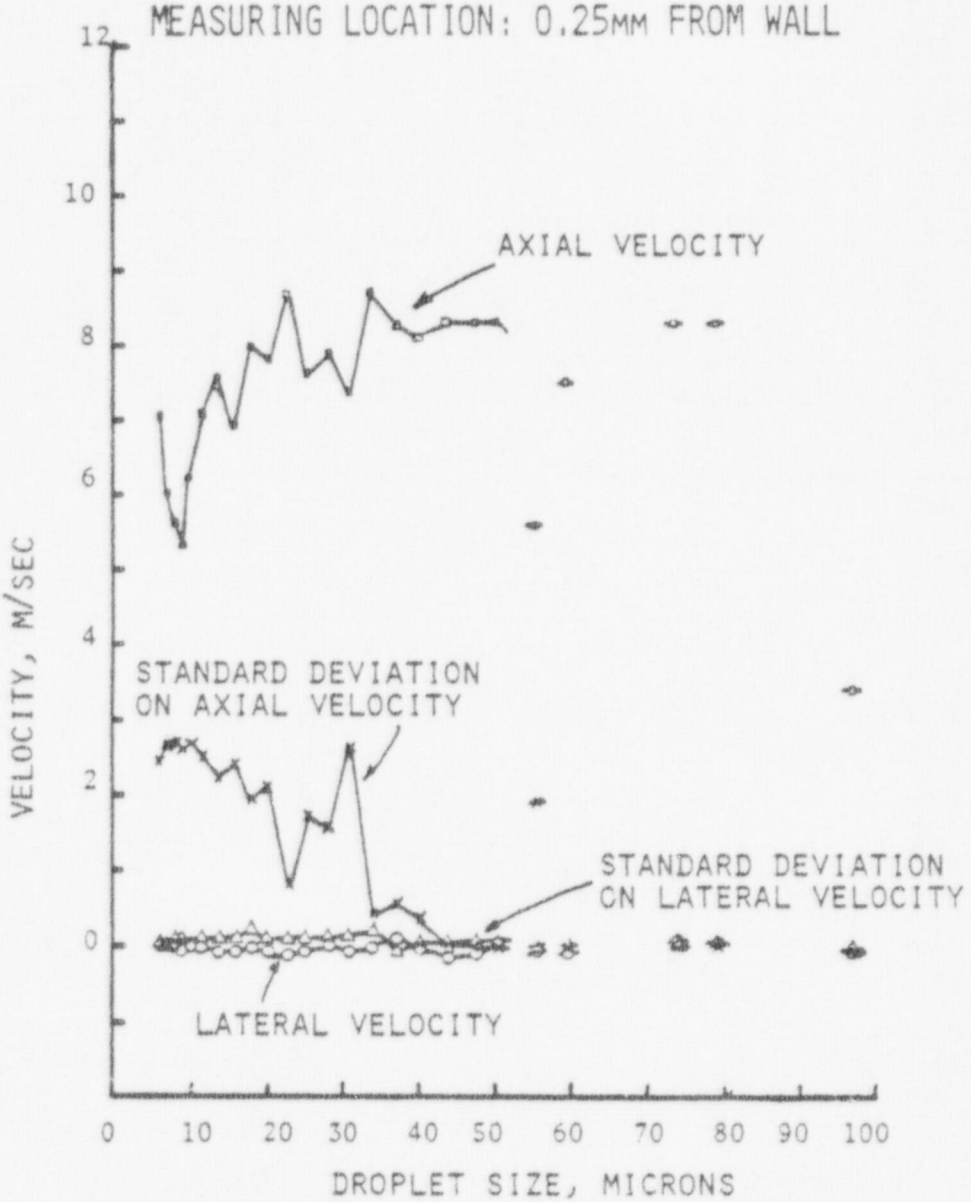

FIGURE 60. DROPLET VELOCITY DISTRIBUTIONS WITHOUT LIQUID FILM ON WALL

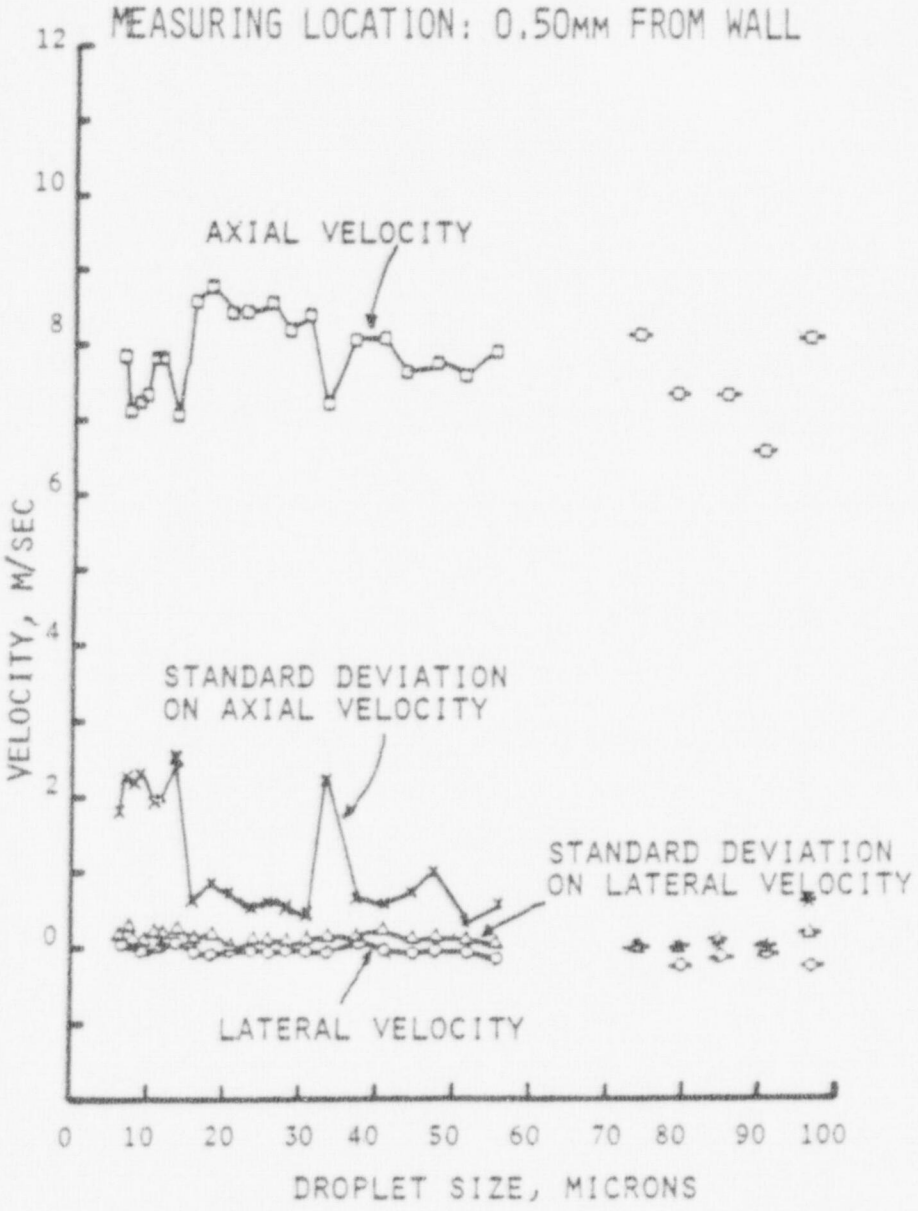

FIGURE 61. DROPLET VELOCITY DISTRIBUTIONS WITHOUT LIQUID FILM ON WALL

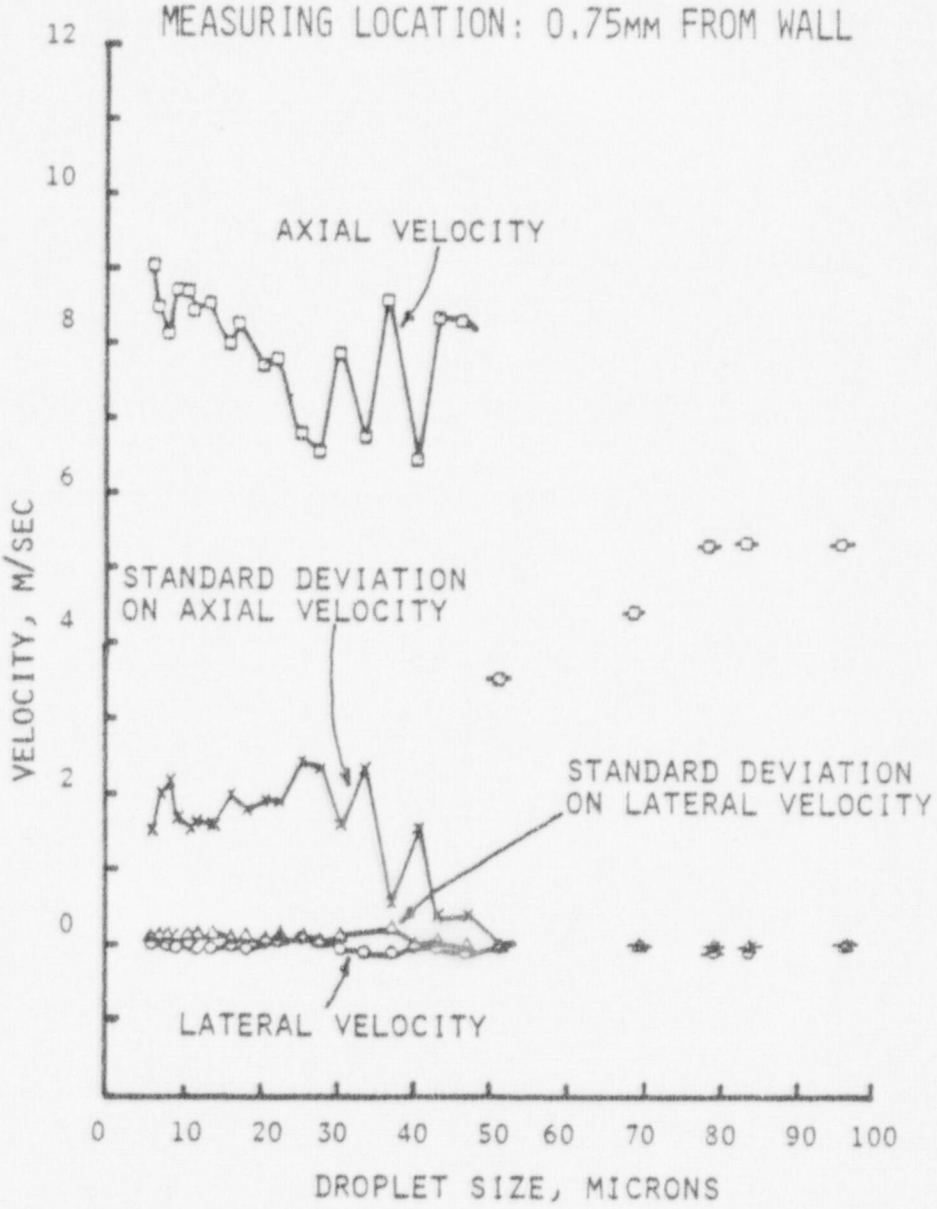

FIGURE 62. DROPLET VELOCITY DISTRIBUTIONS WITHOUT LIQUID FILM ON WALL

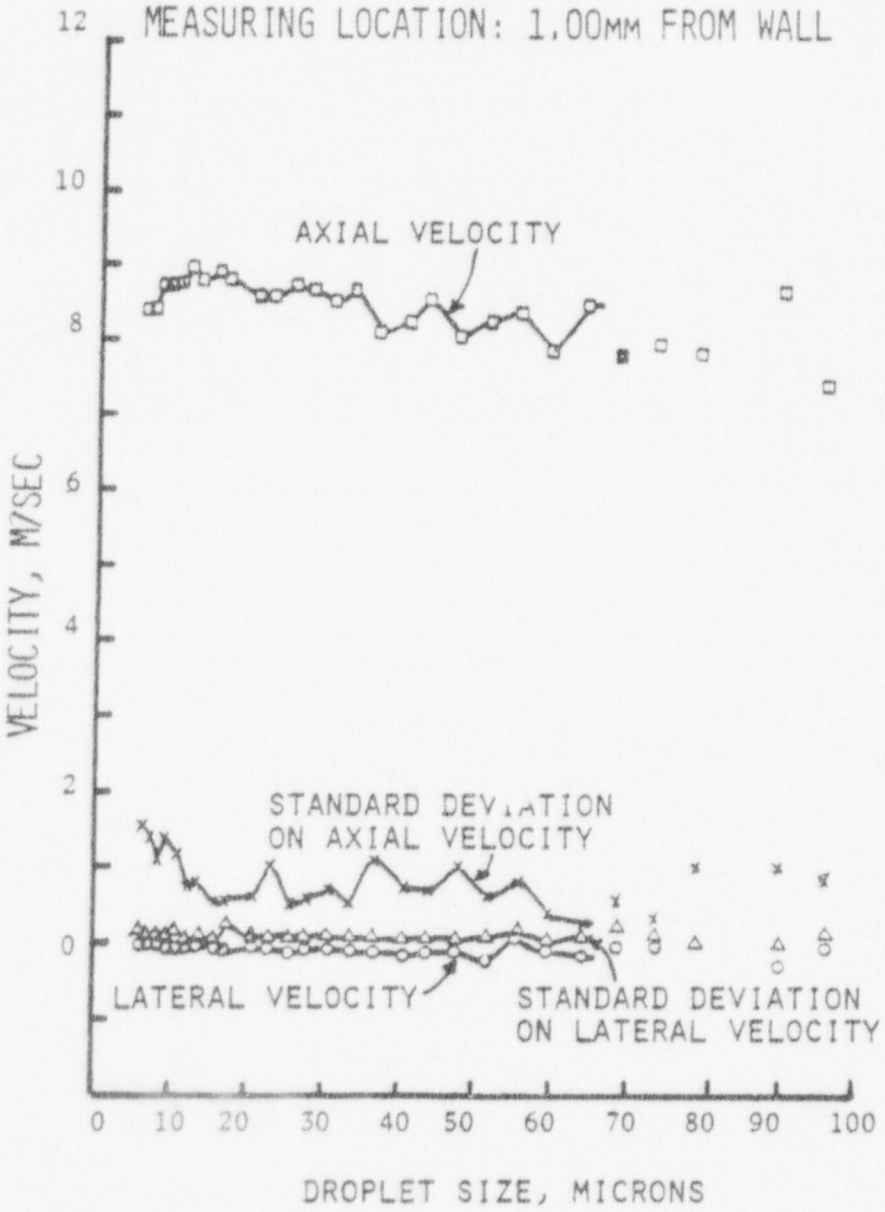

FIGURE 63. DROPLET VELOCITY DISTRIBUTIONS WITHOUT LIQUID FILM ON WALL

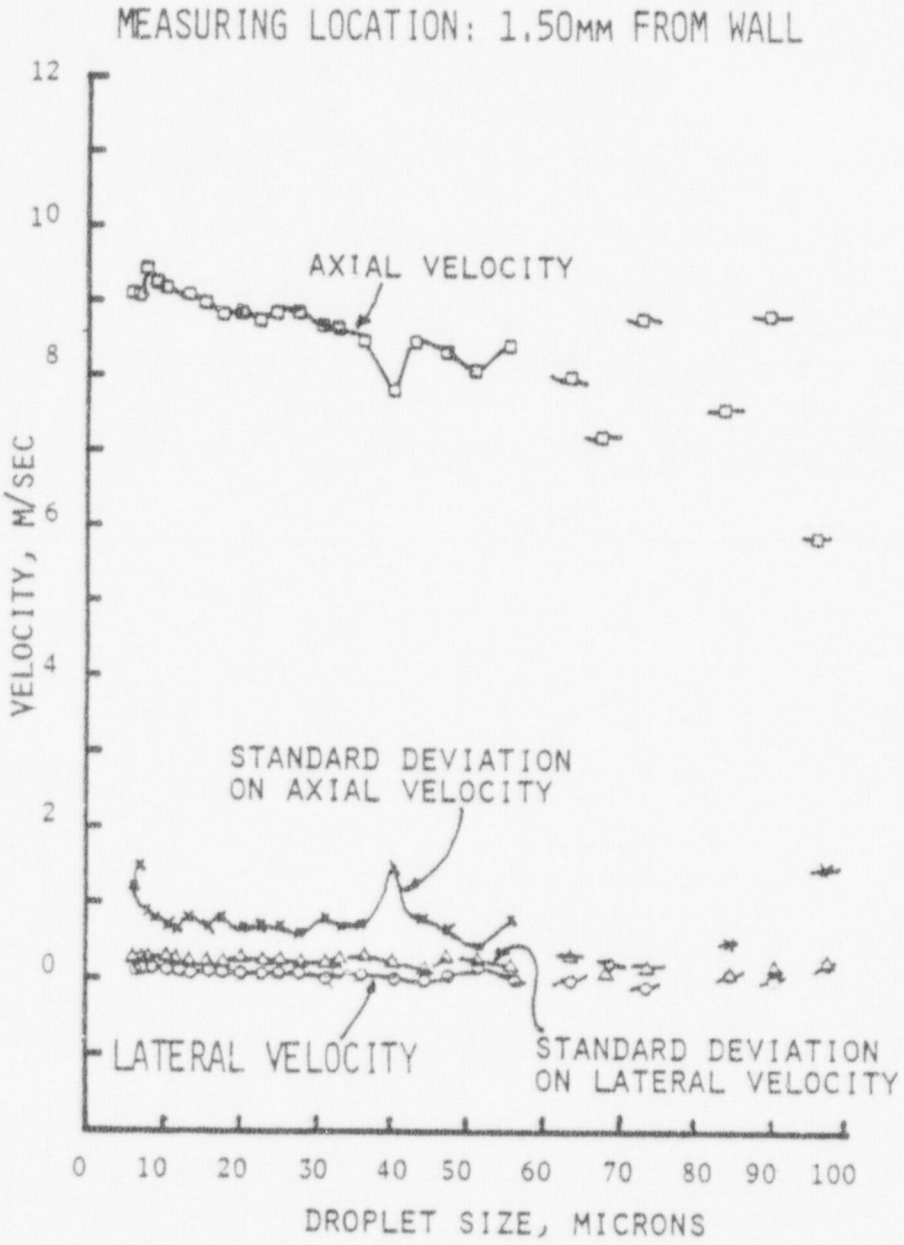

FIGURE 64. DROPLET VELOCITY DISTRIBUTION WITHOUT LIQUID FILM ON WALL

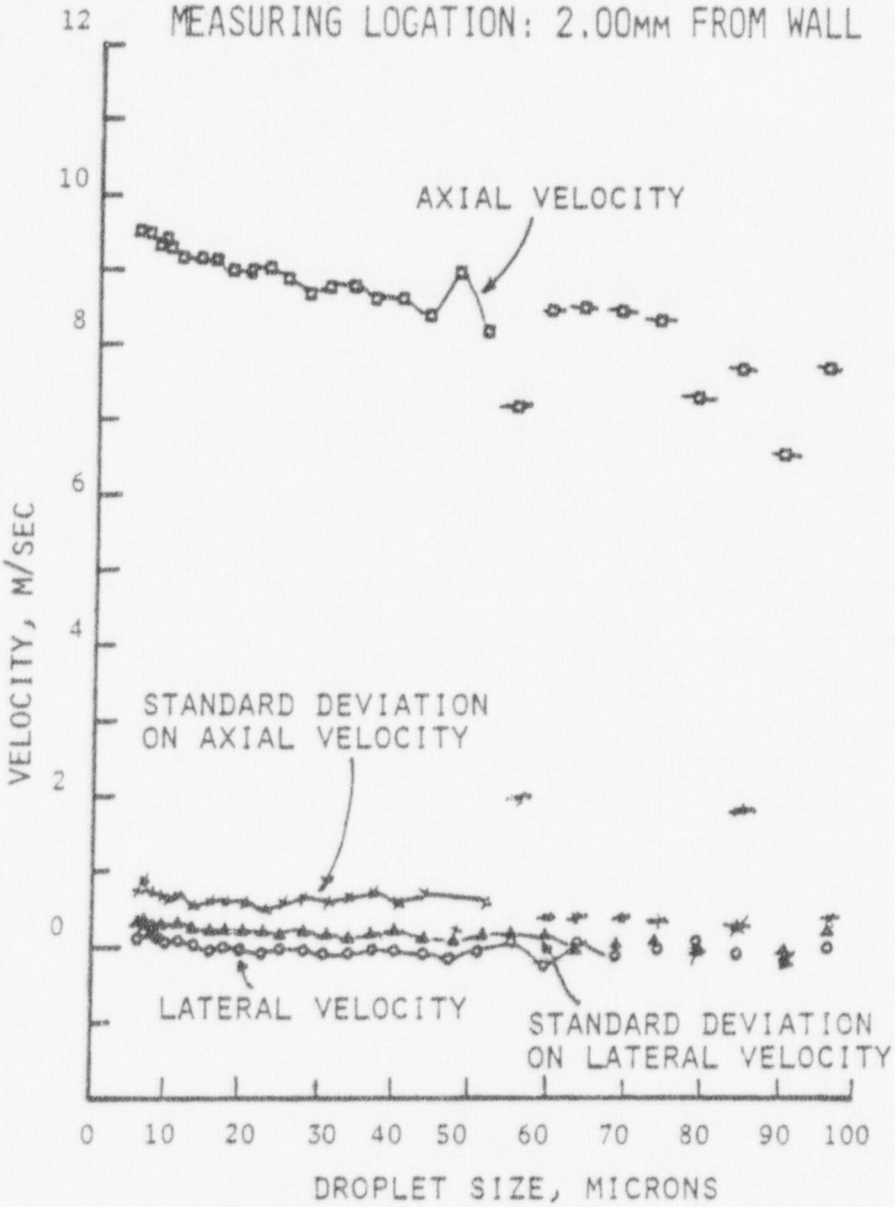

FIGURE 65. DROPLET VELOCITY DISTRIBUTIONS WITHOUT LIQUID FILM ON WALL

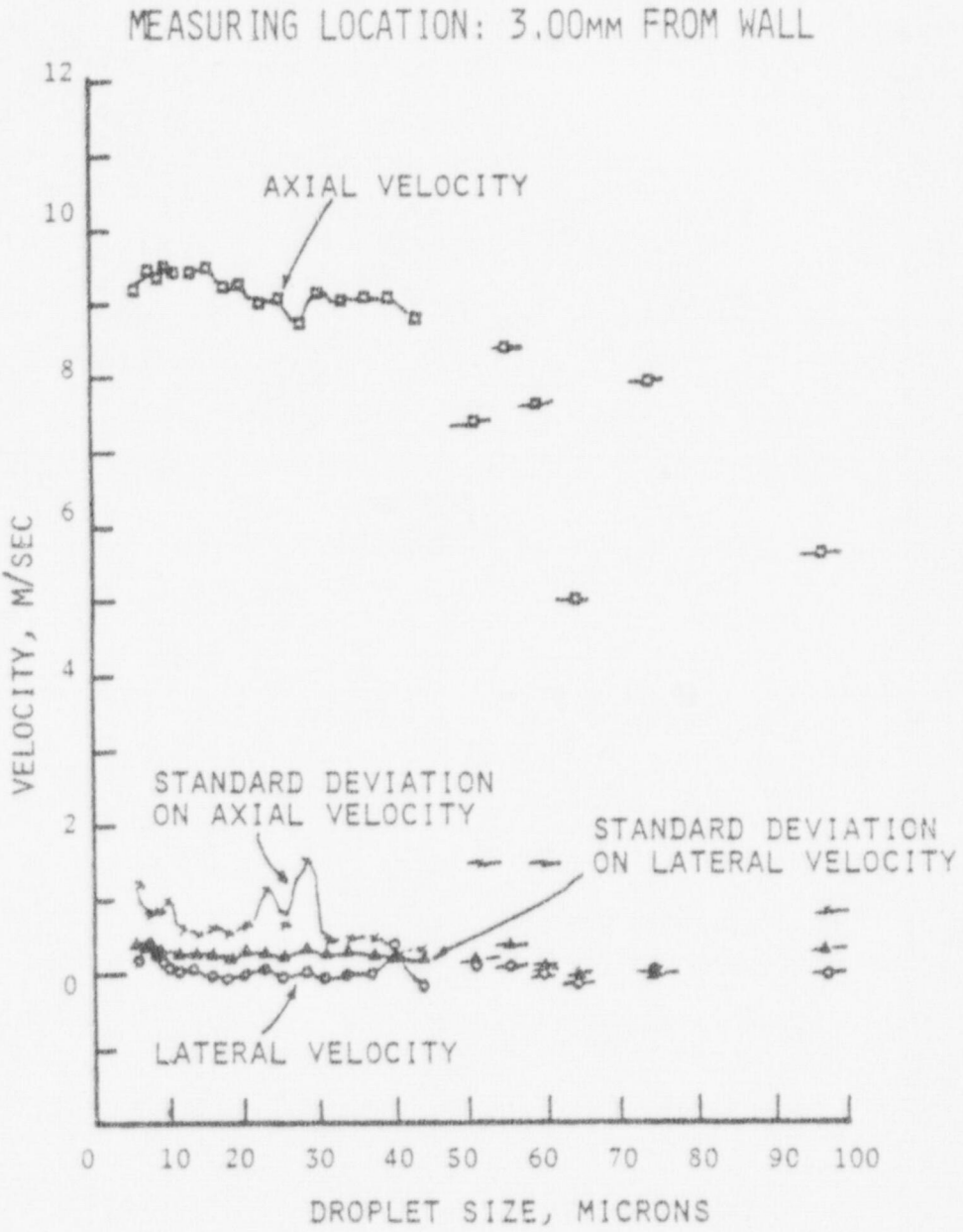

FIGURE 66. DROPLET VELOCITY DISTRIBUTIONS WITHOUT LIQUID FILM ON WALL

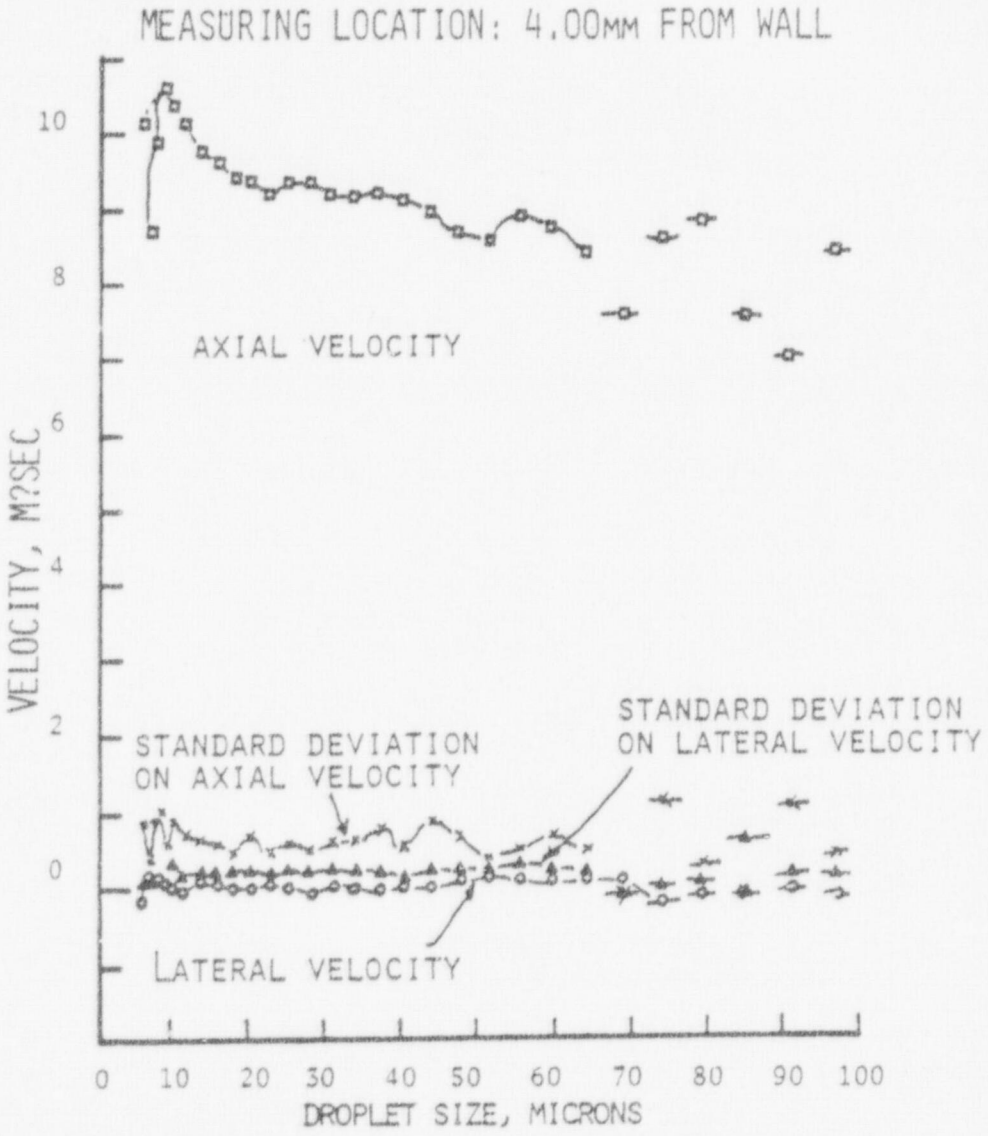

FIGURE 67. DROPLET VELOCITY DISTRIBUTIONS WITHOUT LIQUID FILM ON WALL

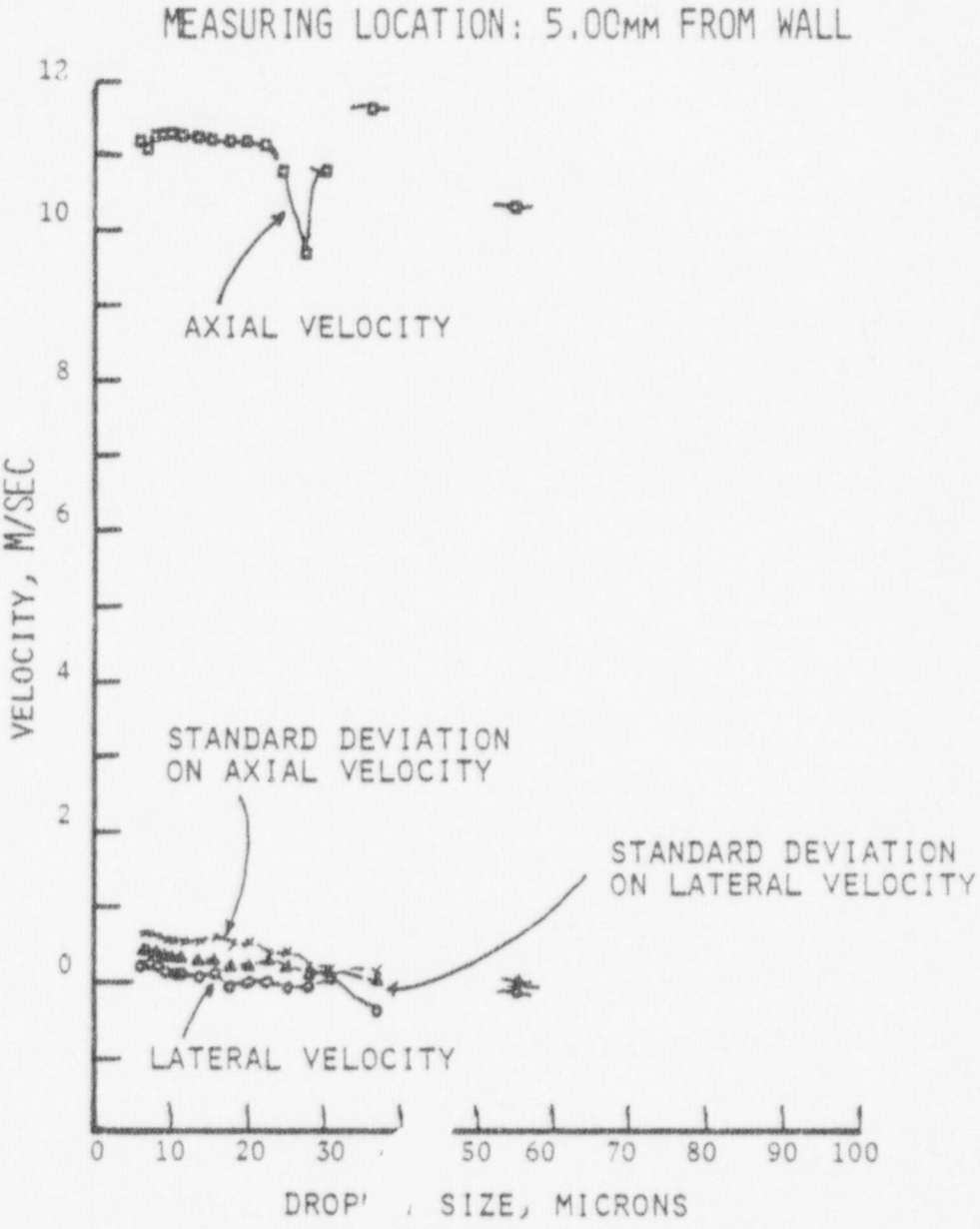

FIGURE 68. DROPLET VELOCITY DISTRIBUTIONS WITHOUT LIQUID FILM ON WALL

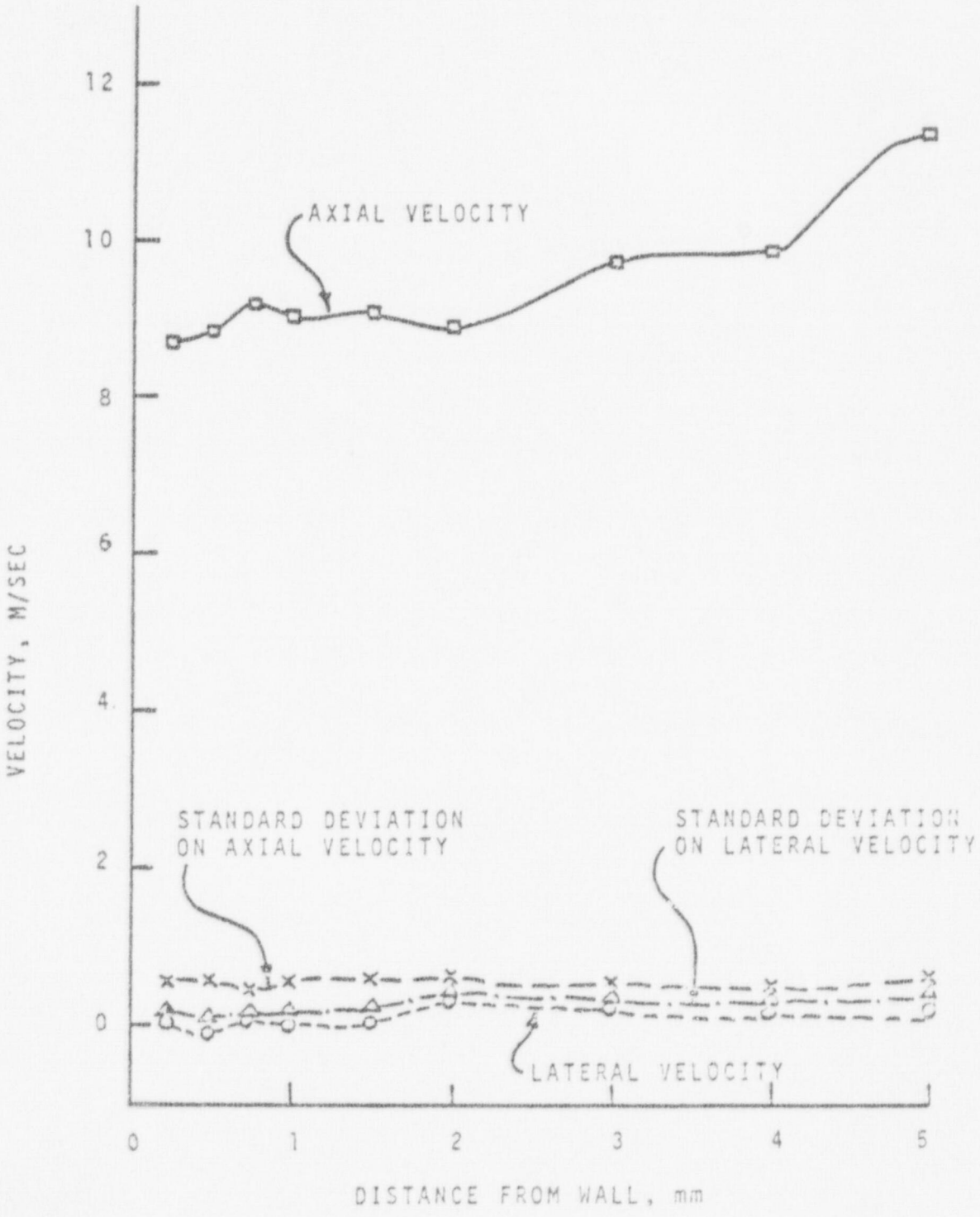

FIGURE 69. AIR VELOCITY DISTRIBUTIONS WITHOUT LIQUID FILM ON WALL

The data summary for these nine locations is presented in Appendix-7. An analysis of the experimental data revealed some interesting features of the two-phase dispersed flow. The droplets were generally found to lag behind the air flow in the axial direction. The amount of this lagging was found to increase with droplet size. However, in the lateral direction the medium and small sized droplets near the wall were generally found to migrate towards the wall. The response of various size droplets for the same turbulent field was different and hence the number densities of the various size droplets had different distributions and they had a peak at different distances from the wall as shown in Figure 70. Furthermore, the large size droplets above 55μ were not present at the center of the channel.

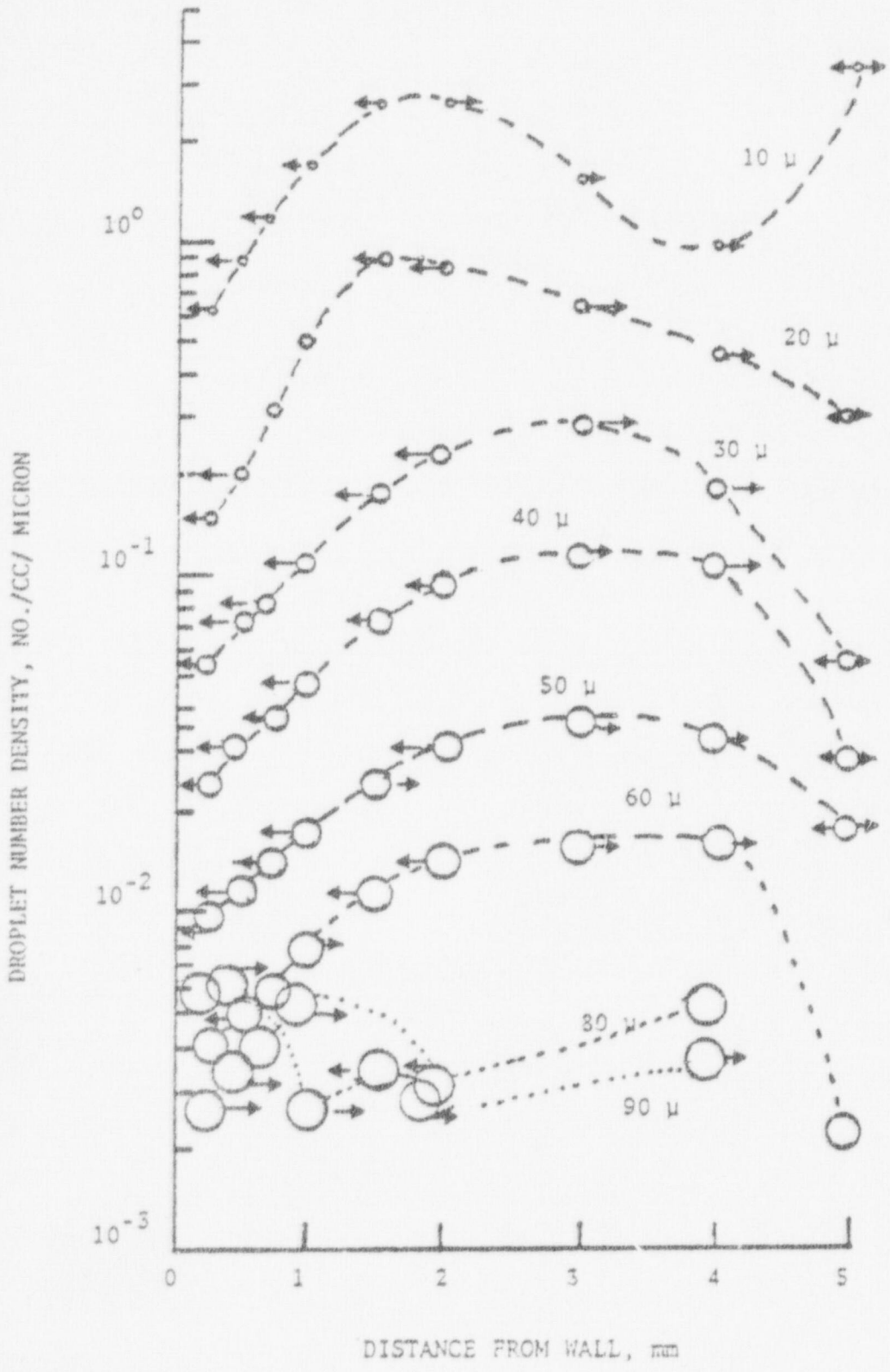

FIGURE 70. DROPLET DISTRIBUTIONS WITHOUT LIQUID FILM ON WALL

V. CONCLUSION

A new LDA technique has been developed to study two-phase dilute dispersed flow. This has been successfully applied to two different types of two-phase dispersed flows (solid particles-water, water droplets-air). It is shown that for a reasonably dilute dispersed flow (having a maximum particle number density of 10^5/cc) and particle sizes less than one third of the measuring volume diameter, the size of the particles can be uniquely determined by analysis of the Doppler signal. With this development the size-number density for the dispersed phase can be obtained. Both dispersed phase and homogeneous phase velocity distributions have been obtained. The results of particle size-number density distributions obtained using LDA-measurement technique has been verified by making another independent measurement.

The analysis of experimental data on the flows studied reveals some interesting features of two-phase dispersed flow. It is apparent that this technique can be used to generate experimental data for the development of a model for predicting the deposition of dispersion during turbulent flow of gas through channels or pipes. Such a model is currently being developed [21] and, indeed, some agreement with the results has been observed.

This technique can also be used to provide more information about local flow properties, giving some new insight in the study of turbulent flow of dispersions. Simple two-phase turbulent flow

problems where the flow conditions can be simulated and controlled more systematically should be studied to gain a better understanding of the turbulence, migration of the particles, and the particle size responses to the turbulent eddies.

REFERENCES

1. Lee, S. L. and Einav, S., "Migration in a Laminar Suspension Boundary Layer Measured by the Use of a Two-Dimensional Laser-Doppler Anemometer", Progress in Heat and Mass Transfer, Vol. 6, pp. 385-403, Pergamon Press, 1972.

2. Ben-Yosef, N., Ginio, O., Mahlab, D. and Weitz, A., "Bubble Size Distribution Measurement by Doppler Velocimeter", Journal of Applied Physics, Vol. 46, No. 2, pp. 738-740, February, 1975.

3. Mason, J. S. and Birchenaugh, A., "The Application of Laser Measurement Techniques to the Pneumatic Transport of Fine Alumina Particles", Conference and Exhibition on the Engineering Uses of Coherent Optics, Univ. of Strathclyde, Scotland, April 8-11, 1975.

4. Golovin, V. A., et al., "Study of the Model of a Two-Phase Flow Using an Optical Quantum Generator (Laser)." UDC 541.12.012, 1971.

5. Matthes, W., et al., "Measurement of the Velocity of Gas Bubbles in Water by a Correlation Method", Rev. of Sci. Inst., Vol. 41, June, 1970.

6. Durst, F. and Zaré, M., "Laser Doppler Measurements in Two-Phase Flows", The Accuracy of Flow Measurements by Laser Doppler Methods, Proceedings of the LDA-Symposium, Copenhagan, 1975, pp. 403-429.

7. Van deHulst, H. C., "Light Scattering by Small Particles", John Wiley and Sons, Inc., New York, 1957.

8. Farmer, W. M., "Dynamic Particle Size and Number Analysis Using a Laser Doppler Velocity Meter", Applied Optics 11, 2603, 1972.

9. Durst, F. and Umhauer, H., "Local Measurements of Particle Velocities, Size Distribution and Concentration with a Combined Laser-Doppler Particle Sizing System", The Accuracy of Flow Measurements by Laser Doppler Methods, Proceedings of the LDA-Symposium, Copenhagan, 1975, pp. 430-456.

10. Jin Wu, "Fast-Moving Suspended Particles: Measurement of Their Size and Velocity", Applied Optics, Vol. 16, No. 3, March, 1977.

11. Durst, F. and Eliasson, B., "Properties of Laser Doppler Signals and Their Exploitation for Particle Size Measurements", The Accuracy of Flow Measurements by Laser Doppler Methods, Proceedings of the LDA-Symposium, Copenhagan, 1975, pp. 457-477.

12. Lee, S. L. and Srinivasan, J., "Measurement of Local Size and Velocity Probability Density Distributions in Two-Phase Suspension Flows by Laser-Doppler Technique", International Journal of Multi-Phase Flows, in press, 1978.

13. Cummins, H. Z., Knable, N. and Yeh, Y., "Observation of Diffusion Broadening of Rayleigh Scattered Light", Phys. Rev. Lett., Vol. 12, No. 6, pp. 150-153, 1964.

14. Yeh, Y. and Cummins, H. Z., "Localized Fluid Measurements with He-Ne Laser Spectrometer", Appl. Phys. Lett., Vol. 4, pp. 176-178.

15. Durst, F., Melling, A. and Whitelaw, J. G., Principle and Practice of Laser-Doppler Anemometry, Academic Press, 1976.

16. "The Accuracy of Flow Measurements by Laser Doppler Methods", Proceedings of the LDA-Symposium , Copenhagan, 1975.

17. "The Use of Laser Doppler Velocimeter for Flow Measurements", Proceedings of a Workshop Co-Sponsored by the U.S. Army Missle Command held at Purdue University on March 9-10, 1972.

18. Durst, F. and Zaré, M., "Removal of Pedestals and Directional Ambiguity of Optical Anemometer Signals", Appl. Optics, Vol. 13, pp. 2562-2579, November, 1974.

19. Buchhave, P., "Laser Doppler Velocimeter with Variable Optical Frequency Shift", Optics and Laser Techn., Vol. 7, pp. 11-16, 1975.

20. Berglund, R. N., and Liu, B. Y. A., "Generation of Monodisperse Aerosol Standards", Environmental Science and Technology, Vol. 7, No. 2, pp. 147-153, 1973.

21. Lee, R. S. L., Private Communications.

Appendix-1

ERROR ANALYSIS FOR THE DEVIATION OF THE FLOW DIRECTION FROM THE MEASURING DIRECTION [21].

The following is an analysis of the error introduced if the flow direction deviates from the measuring direction by a small angle α, where α is in radians.

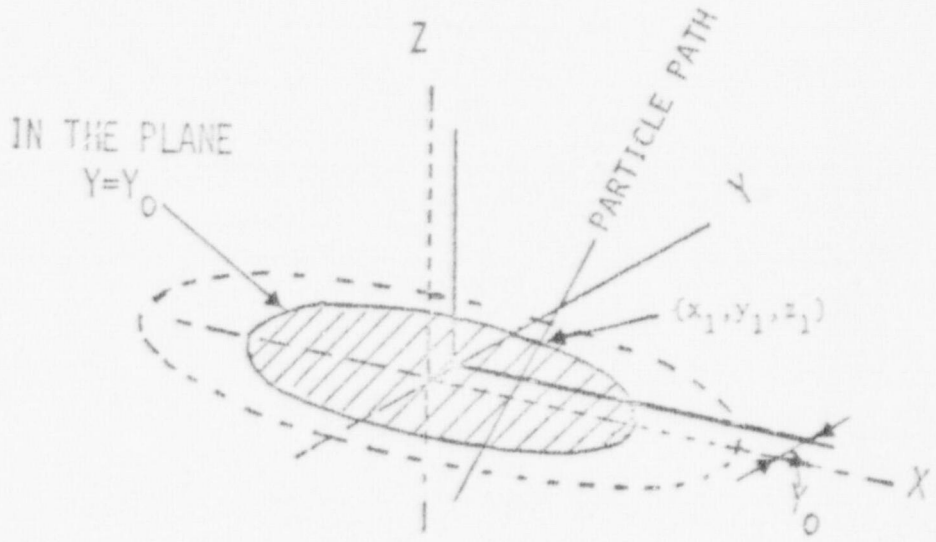

FIGURE 71. SKETCH OF THE MEASURING VOLUME WITH THE CO-ORDINATE AXES.

The measuring volume is considered to be ellipsoidal. Let the co-ordinate axis be defined as shown in the sketch (Figure 71). The equation of the ellipscid is

$$\frac{x^2}{a^2} + \frac{y^2}{b^2} + \frac{z^2}{b^2} = 1 \qquad (1)$$

The z-axis is along the measuring direction. The co-ordinates of the geometric center of the measuring volume are (0,0,0). Let the particle path be inclined to the z axis by an angle α and contained in the plane $y=y_o$. x_1, y_1, z_1 are the co-ordinates of the point where the particle exits from the measuring volume. (x_o,y_o) are the co-ordinates of the point of intersection of the particle trajectory and the plane of $z = 0$. (Figure 72).

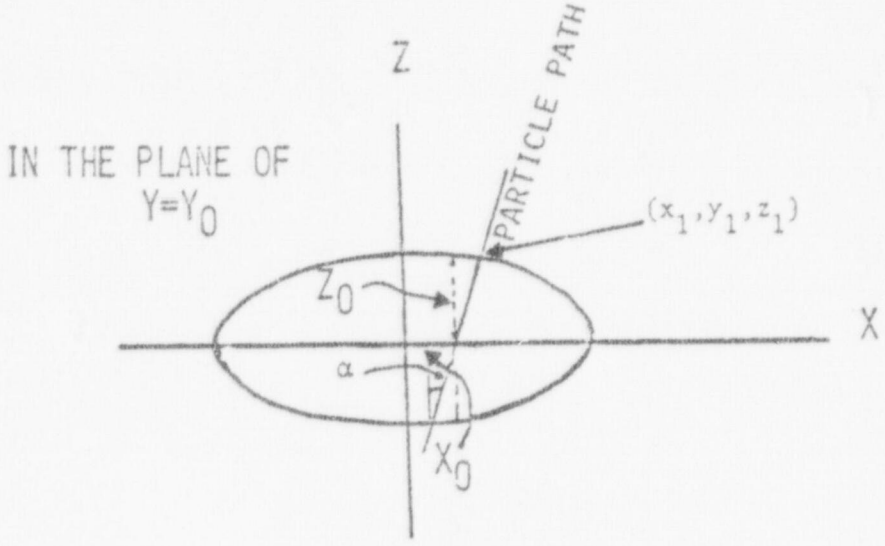

FIGURE 72. CROSS-SECTION IN THE PLANE OF $Y=Y_o$.

$$x_1 = (x_o + z_1 \tan \alpha) = x_o + \alpha z_1 \quad \text{(for small } \alpha) \qquad (2)$$

$$y_1 = y_o \qquad (3)$$

substituting equations (2) and (3) in equation (1):

$$\frac{(x_o + 2x_o \alpha z_1 + \alpha^2 z_1^2)}{a^2} + \frac{y_o^2}{b^2} + \frac{z_1^2}{b^2} = 1$$

$$\left(\frac{1}{b^2}+\frac{\alpha^2}{a^2}\right) z_1^2 + \left(\frac{2x_o\alpha}{a^2}\right) z_1 + \left(\frac{x_o^2}{a^2}+\frac{y_o^2}{b^2}-1\right) = 0$$

This reduces to

$$\left(\frac{1}{b^2}+\frac{\alpha^2}{a^2}\right) z_1^2 + \left(\frac{2x_o\alpha}{a^2}\right) z_1 - \frac{z_o^2}{b^2} = 0$$

Hence

$$z_1 = \frac{-\left(\frac{2x_o\alpha}{a^2}\right) \pm \left\{\left(\frac{2x_o\alpha}{a^2}\right)^2 + 4\left(\frac{1}{b^2}+\frac{\alpha^2}{a^2}\right)\frac{z_o^2}{b^2}\right\}^{1/2}}{2\left(\frac{1}{b^2}+\frac{\alpha^2}{a^2}\right)} \qquad (4)$$

Let 'ℓ' be the actual path length of the particle. The particle velocity measured is actually the component of particle velocity component (v') in z - direction and the path time measured corresponds to the total time (t) taken by the particle to pass through the measuring volume. Hence $tv' = \ell \cos\alpha$ (Figure 72). If the particle path was in the measuring direction the path length would be $2z_o$. Hence the error introduced is $(\ell \cos\alpha - 2z_o)$.

From equation (4),

$$\ell \cos\alpha = \frac{\left\{\left(\frac{2x_o\alpha}{a^2}\right)^2 + 4\left(\frac{1}{b^2}+\frac{\alpha^2}{a^2}\right)\left(\frac{z_o^2}{b^2}\right)\right\}^{1/2}}{\left(\frac{1}{b^2}+\frac{\alpha^2}{a^2}\right)}$$

$$= \frac{2\left(\frac{z_o}{b}\right)}{\left(\frac{1}{b^2}+\frac{\alpha^2}{a^2}\right)^{1/2}} \left\{\frac{\left(\frac{x_o^2\alpha^2}{a^4}\right)}{\left(\frac{1}{b^2}+\frac{\alpha^2}{a^2}\right)}\left(\frac{b^2}{z_o^2}\right) + 1\right\}^{1/2} \qquad (5)$$

$$\text{Let } c^2 = \frac{\left(\frac{x_o^2}{a^4}\right)\left(\frac{b^2}{z_o^2}\right)}{\left(\frac{1}{b^2} + \frac{\alpha^2}{a^2}\right)} \quad \text{and } d = \frac{b}{a}$$

Equation (5) reduces to

$$\ell \cos \alpha = \frac{2z_o \left(1 + \alpha^2 c^2\right)^{1/2}}{\left(1 + \alpha^2 d^2\right)^{1/2}}$$

$$\simeq \frac{2z_o \left(1 + \alpha^2 c^2/2\right)}{\left(1 + \alpha^2 d^2/2\right)}$$

$$\simeq 2z_o \left(1 + \frac{x_o^2 \alpha^2 d^4}{z_o^2}\right)$$

$$\simeq 2z_o \left\{1 + \alpha^2 d^4 \left(\frac{x_o}{z_o}\right)^2\right\} \qquad (6)$$

Hence the error introduced is of the order of $\alpha^2 d^4 \left(\frac{x_o}{z_o}\right)^2$.

Since only the central core of the measuring volume is considered, (x_o/z_o) will be a very small quantity, of the same order as α. So the error introduced is of the order α^4.

In another extreme case when the particle path is inclined to the z-axis but contained in the plane $x=x_o$, equation (6) is reduced to

$$\ell \cos \alpha = 2z_o \left\{1 + \alpha^2 \left(\frac{y_o}{z_o}\right)^2\right\}$$

since $d = \frac{b}{a} = 1$,

Still the error introduced will be of the order α^4. Any other deviation in particle path direction will result in an error value between these two limits.

Appendix-2

SIGNAL BURST WIDTH CORRECTION [21]

The amplitude of the envelope of a Doppler Signal varies in a near Caussian fashion along a particle path length. The measurements were made at a base amplitude A_v as discussed in Chapter II for the reasons discussed earlier. The path length or the equivalent path time can be corrected using the relationship between path length measured and the path length at zero amplitude level.

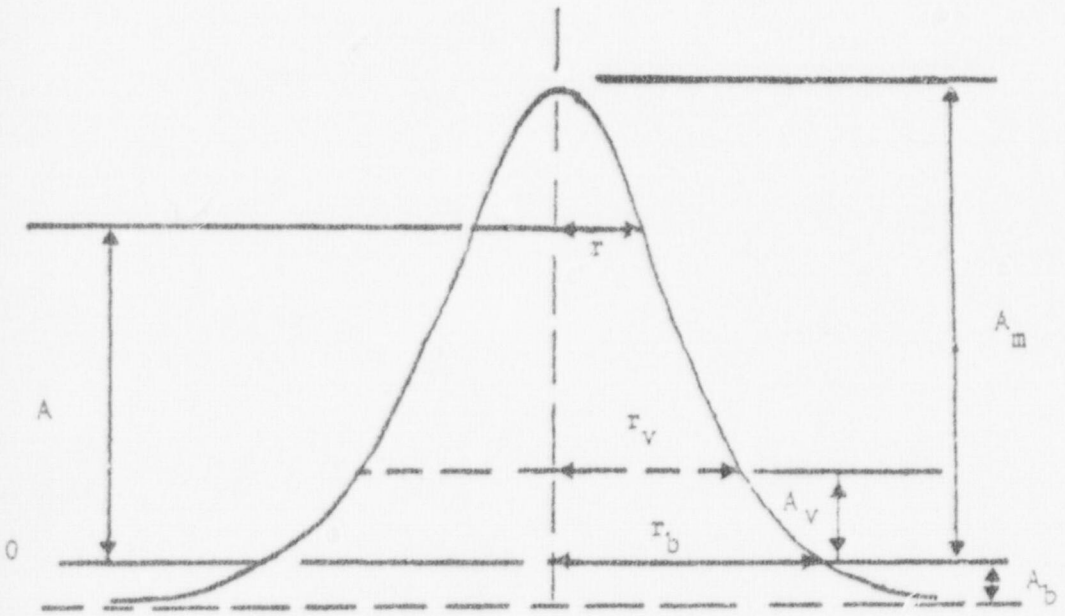

FIGURE 73. SIGNAL AMPLITUDE-ENVELOPE

The signal amplitude will asymtotically approach the zero amplitude line if a truly Gaussian distribution is present. But with fixed receiving optics the signal amplitude reaches zero amplitude in a finite time. Hence a Gaussian distribution can be assumed to be true at an artifical amplitude level, say $-A_B$ (as shown in Figure 73). The signal amplitude envelope can be expressed as

$$(A + A_b) = (A_m + A_b) \exp\left(-\frac{r^2}{\varepsilon^2 r_b^2}\right)$$

where ε, the forcing variable is less than 1.

The boundary conditions are

$$r \to r_b \ , \quad A = 0 \tag{1}$$

$$r \to r_v \ , \quad A = A_v \tag{2}$$

therefore

$$A_b = \frac{1}{e^{1/\varepsilon^2}} (A_m + A_b) \text{ from (1)}$$

$$A_b = A_m/(e^{1/\varepsilon^2} - 1) \tag{3}$$

Also from boundary condition (2)

$$(A_v + A_b) = (A_m + A_b) \exp\left(-\frac{r_v^2}{\varepsilon^2 r_b^2}\right)$$

Thus:

$$\left(\frac{-r_v^2}{\varepsilon^2 r_b^2}\right) = \ln\left(\frac{A_v + A_b}{A_m + A_b}\right) = \ln\left[\frac{\frac{A_v}{A_m} + \frac{1}{e^{1/\varepsilon^2} - 1}}{1 + \frac{1}{e^{1/\varepsilon^2} - 1}}\right]$$

But $r_v = \tau_v \times v$

$r_b = \tau_b \times v$

Therefore

$$\left(\frac{\tau_v^2}{\varepsilon^2 \tau_b^2}\right) = \ln \left[\frac{\dfrac{e^{1/\varepsilon^2}}{e^{1/\varepsilon^2} - 1}}{\left(\dfrac{A_v}{A_m}\right) + \dfrac{1}{(e^{1/\varepsilon^2} - 1)}} \right]$$

Hence if ε is determined from experimental values, the time measured at the base amplitude level can be corrected to get the time at zero amplitude.

In general

$$\frac{\tau^2}{(\varepsilon \tau_b)^2} = \ln \left[\frac{1 + \dfrac{1}{(e^{1/\varepsilon^2} - 1)}}{\left(\dfrac{A}{A_m}\right) + \dfrac{1}{(e^{1/\varepsilon^2} - 1)}} \right]$$

Let $\alpha = (\varepsilon \tau_b)^2$

$$\beta = \frac{1}{(e^{1/\varepsilon^2} - 1)}$$

therefore

$$\frac{\tau^2}{\alpha} = \ln \left[\frac{1 + \beta}{\left(\dfrac{A}{A_m}\right) + \beta} \right]$$

$$\frac{\tau^2}{\alpha} = \ln \left[\frac{(1 + \beta)}{\left\{\left(\dfrac{A}{A_m}\right) - 1\right\} + (1 + \beta)} \right]$$

$$= \ln\left[\frac{1}{\frac{(A/A_m) - 1}{(\frac{}{1 + \beta}) + 1}}\right]$$

$$\frac{\tau^2}{\alpha} = -\ln\left[\frac{(A/A_m) - 1}{(1 + \beta)} + 1\right]$$

Let $P = \tau^2$

$$Q = \left(\frac{A}{A_m} - 1\right)$$

therefore $\frac{P}{\alpha} = -\ln\left\{\frac{Q}{(1 + \beta)} + 1\right\}$

Differentiating w. r. t. P

$$\frac{1}{\alpha} = \frac{-\,dQ/dP}{\left\{\left(\frac{Q}{1 + \beta}\right) + 1\right\}} \times \frac{1}{1 + \beta}$$

i.e. $$-\alpha \frac{dQ}{dP} = Q + (1 + \beta)$$

$$Q = -\alpha \frac{dQ}{dP} - (1 + \beta)$$

There is a linear relationship between Q and (dQ/dP). The Q-intercept will be equal to $(1 + \beta)$, where $\beta = \frac{1}{e^{1/\varepsilon^2} - 1}$.

By observing the time at different amplitude levels data can be collected and the value of ε can be determined statistically.

This linear relationship was tested (Figure 74) for different amplitude signals and the value of ε was found to be 0.573. Therefore

$$\frac{\tau_v^2}{(0.573)^2 \tau_b^2} = \ln\left[\frac{1.05}{(A_v/A_m) + 0.05}\right]$$

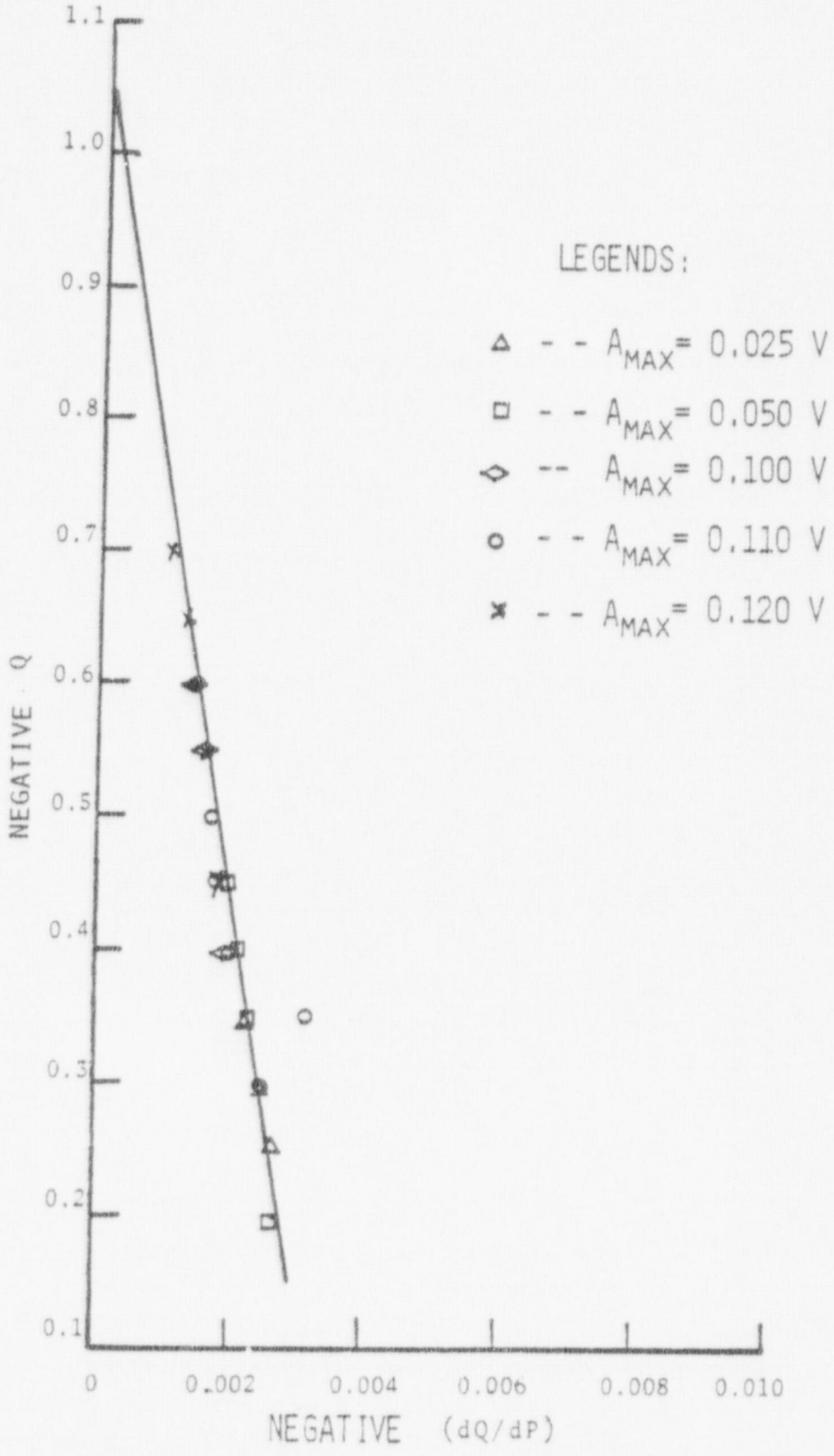

FIGURE 74. SIGNAL BURST WIDTH CORRECTION FACTOR

or $$\tau_b = \frac{\tau_v / 0.573}{\ln \left[\frac{1.05}{A_v / A_m} + 0.005 \right]}$$

Thus the time (τ_v) measured at a base level can be corrected to a time at the zero amplitude level.

Appendix-3

DETERMINATION OF CORRECTION FACTOR, K,

(ratio of actual number count to correct number count)

AND LIMITING PATH TIME FOR SOLID-PARTICLE-WATER SYSTEM.

The flow used for calibration had a known number density $(N_i)_o$, a uniform particle size, d_i, and all the particles had the same velocity (v_j). When the lower limit of the duration time discrimination, $\bar{\tau}$, was gradually raised the number count, n, started to decrease from a stable value, $(n)_o$, as discussed in Chapter III. In order to find the relationship between number count and the duration time, $\bar{\tau}$, during this gradual decrease the following analysis of the path length through an ellipsoid was done.

The equation of the ellopsoid is

$$\frac{x^2}{a^2} + \frac{y^2}{b^2} + \frac{z^2}{b^2} = 1$$

At $z=z_v$, (boundary of the projected base area of the central core)

$$\frac{x^2}{a^2} + \frac{y^2}{b^2} + \frac{z_v^2}{b^2} = 1$$

$$\frac{x^2}{a^2\left(1 - \frac{z_v^2}{b^2}\right)} + \frac{y^2}{b^2\left(1 - \frac{z_v^2}{b^2}\right)} = 1$$

$$\text{Area, } B_v, = \pi ab \left(1 - \frac{z_v^2}{b^2}\right)$$

Differentiating with respect to z_v^2

$$\frac{\partial(B_v)}{\partial(z_v^2)} = \pi ab \left(-\frac{1}{b^2}\right) = -\frac{\pi a}{b}$$

$$\therefore \quad \frac{\partial(B_v)}{\partial(\bar{\tau}_v^2)} = -\frac{\pi a}{4b}(v_j)_o \text{ as } z_v = \frac{\bar{\tau}_v}{2}(v_j)_o$$

Since $\dot{N} = B_v(v_j)_o(N_i)_o$

$$\frac{\partial \dot{N}}{\partial(\bar{\tau}_v^2)} = -\frac{\pi a}{4b}(N_i)_o(v_j)_o^3$$

Hence there is a linear relationship between the square of lower limit of the duration time discrimination and signal number count (Figure 75) and this was used to determine the limiting path time, $(\bar{\tau}_v)$, for the solid-particle system. (Chapter 3).

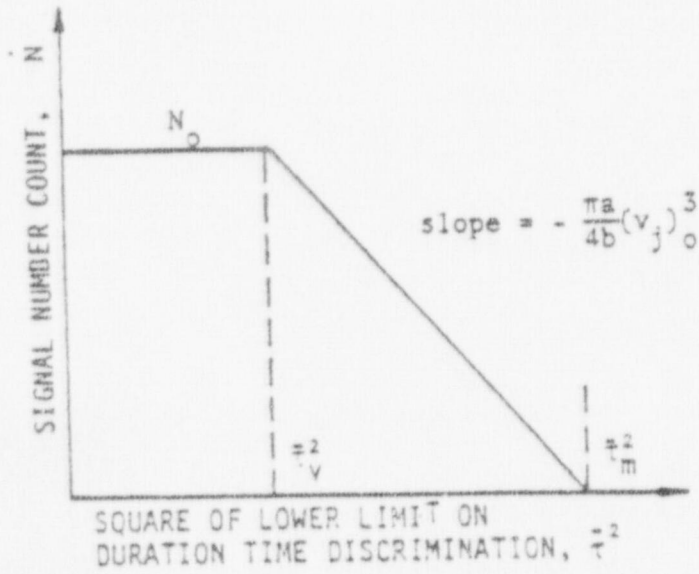

FIGURE 75. SIGNAL NUMBER COUNT VS. SQUARE OF LOWER-LIMIT ON DURATION TIME DISCRIMINATION.

CORRECTION FACTOR, K. (To convert the actual number count to the corrected number count)

For this calibration run the correction factor

$$K = \int_{o}^{\bar{B}_o} \left(\frac{\ell_v - \bar{\ell}_v}{\ell_m - \bar{\ell}_v}\right) \frac{dB_o}{B_o}$$

was further simplified as follows: The path length of any trajectory of the particle is given by the product of burst time duration, τ, and velocity, v.

Hence $\ell_v = (v_j)_o \bar{\tau}$

$$\bar{\ell}_v = (v_j)_o \bar{\tau}_v$$

$$\ell_m = (v_j)_o \bar{\tau}_m$$

$$\therefore \quad \frac{\ell_v - \bar{\ell}_v}{\ell_m - \bar{\ell}_v} = \left(\frac{\bar{\tau} - \bar{\tau}_v}{\bar{\tau}_m - \bar{\tau}_v}\right)$$

Hence $$K = \int_{o}^{B_o} \left(\frac{\ell_v - \bar{\ell}_v}{\ell_m - \bar{\ell}_v}\right) \frac{dB}{B_o}$$

But $B = B(\bar{\tau})$

Number count/sec, $\dot{n}_i = (\text{Base area})(v_j)_o(N_i)_o$

$$\dot{n}_i = B \times k$$

Since $(v_j)_o$ and $(N_i)_o$ were constants, thus

$$B = \frac{\dot{n}}{k}$$

Also, when the lower limit on time discrimination was gradually raised,

$$\frac{\dot{N}_o}{\bar{\tau}_m^2 - \bar{\tau}_v^2} = \frac{\dot{N}}{\bar{\tau}_m^2 - \bar{\tau}^2} \qquad \text{(See Figure 75)}$$

For a time, t, secs $N = \dot{n}t$ and $N_o = \dot{n}_o t$

$$\therefore \quad \frac{B}{B_o} = \frac{N}{N_o} = \frac{\bar{\tau}_m^2 - \bar{\tau}^2}{\bar{\tau}_m^2 - \bar{\tau}_v^2}$$

$$\frac{dB}{B_o} = - \frac{2\bar{\tau}d\bar{\tau}}{(\bar{\tau}_m^2 - \bar{\tau}_v^2)}$$

$$\therefore \quad K = \int_{\bar{\tau}_m}^{\bar{\tau}_v} \left(\frac{\bar{\tau} - \bar{\tau}_v}{\bar{\tau}_m - \bar{\tau}_v} \right) \left[- \frac{2\bar{\tau}d\bar{\tau}}{(\bar{\tau}_m^2 - \bar{\tau}_v^2)} \right] \qquad \begin{matrix} B \to o & \tau \to \bar{\tau}_m \\ B \to B_o & \tau \to \bar{\tau}_o \end{matrix}$$

$$= \frac{2}{(\bar{\tau}_m - \bar{\tau}_v)(\bar{\tau}_m^2 - \bar{\tau}_v^2)} \int_{\bar{\tau}_v}^{\bar{\tau}_m} (\tau^2 - \bar{\tau}_v . \bar{\tau}) d\bar{\tau}$$

$$= \frac{2}{(\bar{\tau}_m - \bar{\tau}_v)(\bar{\tau}_m^2 - \bar{\tau}_v^2)} \left\{ \left[\frac{1}{3}\bar{\tau}^3 - \frac{1}{2}\bar{\tau}_v \bar{\tau}^2 \right] \Bigg|_{\bar{\tau}_o}^{\bar{\tau}_m} \right\}$$

$$= \frac{1}{(\bar{\tau}_m - \bar{\tau}_v)(\bar{\tau}_m^2 - \bar{\tau}_v^2)} \left\{ \frac{2}{3}(\bar{\tau}_m^3 - \bar{\tau}_v^3) - \bar{\tau}_v(\bar{\tau}_m^2 - \bar{\tau}_v^2) \right\}$$

$$K = \frac{(2\tau_m^2 - \bar{\tau}_v\bar{\tau}_m - \tau_v^2)}{3(\bar{\tau}_m^2 - \tau_v^2)}$$

This correction factor was computed using the experimentally determined values of $\overline{\tau}_m$ and $\overline{\tau}_v$. Also, as expected, the correction factor was dependent only on the geometry of the measuring volume.

APPENDIX - 4

COMPUTER PROGRAM

```
C       THIS ROUTINE IS USED TO TRIGGER THE ANALOG TO DIGITAL

        CONVERSION ON FOUR CHANNELS AND STORE THE DATA

ADSF=701301
MPSK=701701
ADRB=701312
ADSC=701304
/
/
        .DEC
NDATA=1000
COUNT=4*NDATA-1
        .OCT
/
/
/
/
/
/
AUTO10=10                       /AUTO INCREMENT REGS
AUTO11=11
AUTO12=12
AUTO13=13
/
        .GLOBL  SAMPLE,HV1,VV1,TIME1,AMP1
/
/
        .DEFIN  GTDATA,CHAN,?L
        LAW     -CHAN   /LOAD TWO'S COMPL OF VISUAL CHAN#
                        /(=ACTUAL CHAN# + 1)
        ADSC            /START CONV
L       JMP     L       /WAIT FOR CONVERSION
AREG=CHAN-1/2+10
        DAC*    AREG
        .ENDM
/
/
/
        .DEFIN  INITA,AUTO,ADDR
        CLC             /INIT GIVEN AUTO INCREMENT
        TAD     ADDR    /REG WITH GIVEN ADDRESS
        DAC*    (AUTO
        .ENDM
/
/
        .DEFIN  NORML,ADDR      /USED FOR NORMALIZING DATA
        LAC*    ADDR    /AFTER ALL SAMPLING
        LRSS    3
        DAC*    ADDR
        ISZ     ADDR
        .ENDM
```

```
/
SAMPLE  0
        CAL     77      /.SETUP FOR PULSE INTERUPTS
        16
        MPSK            /AN UNLIKELY SKIP.(PULSE INT
                        /HARDWARE ONLY USES API
        ADINIT
/
/
/
        CAL     57      /.SETUP FOR A-D INTS
        16
        ADSF
        READY
/
/
/       INITIALIZATION
/
/
        INITA   AUTO10,HV1      /INIT AUTO REGS
        INITA   AUTO11,VV1
        INITA   AUTO12,TIME1
        INITA   AUTO13,AMP1
/
        LAC     (-NDATA
        DAC     CT
/
        LAC     APIFL
        ISA             /TURN ON API
/
/
/       WAIT FOR PULSE INTERUPTS
/
WAIT    JMP     WAIT
/
READY   0               /COME HERE ON A-D INTS
        ADRB            /READ A-D BUFFER
        DBR
        ISZ     READY   /RETURN TO THE ADDR AFTER THE WAIT LOOP
        JMP*    READY
/
/
ADINIT  0               /COME HERE ON PULSE INTS AND INITIATE
                        /CONVERSION ON THE 4 CHANNELS
        GTDATA  1
        GTDATA  3
        GTDATA  5
        GTDATA  7
        ISZ     CT
        JMP     NEWDAT  /GO GET MORE DATA
        DBK             /CLEAR LEVEL 3
        CLA             /FINISHED SAMPLING. TURN OFF API
        ISA
        700004
```

```
/
/       NOW NORMALIZE ALL THE DATA
/
NORM    LAC     (-NDATA)
        DAC     CT
        LAC     HVI
        DAC     ADDR1
        LAC     VVI
        DAC     ADDR2
        LAC     TIME1
        DAC     ADDR3
        LAC     AMP1
        DAC     ADDR4
/
LOOP=.
        NORML   ADDR1
        NORML   ADDR2
        NORML   ADDR3
        NORML   ADDR4
        ISZ     CT
        JMP     LOOP
/
/
DONE    JMP*    SAMPLE  /DONE! RETURN.
/
/
NEWDAT  DBK             /CLEAR PRIORITY LEVEL
        JMP*    (WAIT
/
/
CT      0
ADDR1   0
ADDR2   0
ADDR3   0
ADDR4   0
SIZE    0
APIFL   400000
        .END

DOSPIP VSA

>
```

```
C       THIS ROUTINE PROCESSES THE RAW DATA
C
C
C       HV,ETC., ARE DECLARED INTEGERS TO CONSERVE MEMORY SPACE
C
C
        SUBROUTINE PRDATA(HV,VV,TIME,AMP)
C
C
        INTEGER HV(2000),VV(2000),TIME(2000),AMP(2000)
        INTEGER COUNT(8000),HVC(30),VVC(30),AMPC(30)
        INTEGER HVMAX,VVMAX,AMPMAX,HVMIN,VVMIN,AMPMIN,HVSIZE,VVSIZE
        INTEGER AMSIZE
        INTEGER DIV1,DIV2,DIV3
        REAL VVSHFT,HVSHFT
        COMMON /COMCT/COUNT
        COMMON / /NDATA,DIV1,DIV2,DIV3,NGDATA,VVSHFT,HVSHFT,VVCON,TIMAN
        COMMON /GN/GAIN
215     FORMAT(8X,'MAX HORIZ VEL =',F6.3,' M/SEC',/
       1 8X,'MAX VERT VEL =',F6.3,' M/SEC',/)
220     FORMAT(8X,'MIN HORIZ VEL =',F6.3, 'M/SEC',/
       1 8X,'MIN VERT VEL =',F6.3,' M/SEC',/
       2 8X,'MIN AMPLITUDE=',I5,1X//)
221     FORMAT(9X,'MAX AMPLITUDE =',I5,/15X
       1 'CORRESPONDING TIME AND VELOCITIES: /20X,' HORIZ =',
       2 F6.3,' M/SEC'/20X,'VERTICAL =',F6.3,' M/SEC'/
       3 20X,'TIME = ',I5//)
225     FORMAT(8X,'HORIZ VEL CLASS SIZE=',F6.3,1X/,8X,'VERT VEL CLASS
       1 SIZE=', F6.3,1X/,8X,I5,' DATA REJECTED BY PATH LEN DISCR'//)
C
C       NUMBER OF 4-TUPLES OF DATA PER DATA SET
C
        NDATA=1000
C
C       DIV1 IS # OF AMPL CLASSES
C       DIV2 IS # VV CLASSES
C       DIV3 IS # HV CLASSES
C
        DIV1=30
        DIV2=10
        DIV3=10
C
C       INPUT # OF DATA SETS
C
        WRITE(4,11)
        READ(4,) NSETS
11      FORMAT(' INPUT # OF DATA SETS (<=100):')
C
```

```
C
      WRITE(4,13)
      READ(4,)ISKIP
13    FORMAT(' # TO BE SKP:')
      CALL SKP(ISKIP)
      VVSHFT=2.22
      HVSHFT=-2.22
C     INPUT CONVERSION TIME
C
      WRITE(4,12)
      READ(4,)CNTIME
12    FORMAT(' INPUT CONVERSION TIME:')
C
C     SCALE FACTORS AND GAIN
      WRITE(4,216)
216   FORMAT(' GAIN:')
      READ(4,) GAIN
217   FORMAT(' VVSCALE:')
218   FORMAT(' HVSCALE:')
      WRITE(4,217)
      READ(4,) VVSCAL
      WRITE(4,218)
      READ(4,)HVSCAL
C
C
      WRITE(4,212)
212   FORMAT(' FULL ANALYSIS?')
      READ(4,)IFULL
C
      WRITE(4,4001)
4001  FORMAT(' PLMIN,PLMAX:')
      READ(4,)PLMIN,PLMAX
      TIMAMP=32.
C
C
C
C     VELOCITY CONVERSION FACTORS
C
      VVCON=1/(369.*VVSCAL)
      HVCON=1/(369.*HVSCAL)
C
C
C
      DRCON=10000./(1.837*CNTIME)
      DRC100=DRCON/100.
C
C
C     ZERO OUT THE COUNT ARRAY
      DO 400 L=1,32
      DO 400 J=1,15
      DO 400 K=1,15
400   COUNT(IELT(L,J,K))=0
```

```
C
      LOOK AT ALL DAT SETS FOR MAX AND MIN
      DO 410 I=1,NSETS
      CALL DEVRD(I)
      CALL PLDISC(HV,VV,TIME,AMP,PLMIN,PLMAX)
      CALL ZMAX(HV,VV,AMP,HVMAX,VVMAX,AMPMAX,IAMAX)
      CALL ZMIN(HV,VV,AMP,HVMIN,VVMIN,AMPMIN)
410   CONTINUE
C
      ****
C
      WRITE(4,4002)
4002  FORMAT(' INPUT AMPMAX:')
      READ(4,) AMPMAX
C     AMPMAX OVERRIDDEN
C
      CALL DIVIDE(HVMAX,HVMIN,VVMAX,VVMIN,AMPMAX,AMPMIN,HVSIZE,
     1 VVSIZE,AMSIZE)
      NGDT=0
      REWIND 5
      CALL SKP(ISKIP)
      NBDT=0
C
      DO 420 I=1,NSETS
      CALL DEVRD(I)
      CALL PLDISC(HV,VV,TIME,AMP,PLMIN,PLMAX)
      CALL NRCNT(HV,VV,AMP,HVSIZE,VVSIZE,NBAD,HVC,VVC,AMPC,
     1HVMIN,VVMIN,AMPMIN,AMPMAX)
      NGDT=NGDT+NGDATA
      NBDT=NBDT+NBAD
420   CONTINUE
C
C
      WRITE OUT MAX AND MINS
C
      R1=HVMAX*HVCON
      R2=VVMAX*VVCON
      R3=HVMIN*HVCON
      R4=VVMIN*VVCON
      WRITE(6,215)R1,R2
      WRITE(6,220) R3,R4,AMPMIN
      R1=HV(IAMAX)*HVCON
      R2=VV(IAMAX)*VVCON
      WRITE(6,221) AMPMAX,R1,R2,TIME(IAMAX)
C
      II=NSETS*NDATA-NGDT
```

```
      WRITE(6,303) NBDT
303   FORMAT(4X ,I6,   DATA FALL BELOW THE MIN AMPLITUDE CLASS')
      R1=HVSIZE*HVCON
      R2=VVSIZE*VVCON
      WRITE(6,225) R1,R2,II
210   FORMAT(7X,I5,'-',I5,20X,I5,'-',I5,15X,I5,'-',I5,15X,I5)

C     CHECK IF A FULL ANALYSIS IS DESIRED
      IF (IFULL .EQ. 0)GOTO 3000


      WRITE(6,900)
      WRITE(6,901)

C     UNIT INFORMATION
901   FORMAT(////////60X,'DATA ANALYSIS'///////,
     1 45X,'DIAMETER IN MICRONS'//45X,'VELOCITY IN METERS'
     1,' PER SECOND'//45X,'DROPLET RATE IN NUMBER/SEC/SQ CM/(M/SEC
     2,'(M/SEC)/MICRON'//45X,'NUMBER DENSITY IN NUMBER/CC/MICRON')

      WRITE(6,900)
      LINECT=41
      WRITE(6,313)
      WRITE(6,301)
      WRITE(6,302)


C     PAGE THROW TO MAINTAIN MARGINS
900   FORMAT(1H1,////////)

313   FORMAT(45X,'DROPLET SIZE - VELOCITY DISTRIBUTION'///)
301   FORMAT(1H ,7X,' DIAMETER',21X,'AXIAL VEL.',18X,
     1 'LATERAL VEL.',13X,'NUMBER')
302   FORMAT(10X,'RANGE',25X,'RANGE',23X,'RANGE',19X,'COUNT',
     1 13X,'DROPLET RATE'////)
      DO 150 L=2,DIV1
      DO 150 J=2,DIV2
      DO 150 K=2,DIV3
      I1=L-1
      I2=J-1
      I3=K-1
      I = COUNT(IELT(I1,I2,I3))
      IF (I .EQ. 0)GOTO 150
```

```
C
C       CONVERT INTEGER DATA TO ACTUAL UNITS
C
        SIZE1=DIAM(AMPC(L-1))
        SIZE2=DIAM(AMPC(L))
        R3=VVC(J-1)*VVCON+VVSHFT
        R4=VVC(J)*VVCON+VVSHFT
        R5=HVC(K-1)*HVCON+HVSHFT
        R6=HVC(K)*HVCON+HVSHFT
        CTCON=DRCON/(HVSIZE*HVCON*VVSIZE*VVCON*(SIZE1-SIZE2))
        R7=I*CTCON
        WRITE(6,211) SIZE1,SIZE2,R3,R4,R5,R6,I,R7
211     FORMAT(7X,F5.2,':',F5.2,20X,F5.2,':',F5.2,15X,F5.2,':',F5.2,15
       1  I5,15X,E10.3)
        LINECT=LINECT-1
        IF (LINECT .GT.0) GOTO 150
        LINECT=52
        WRITE(6,900)
C       WRITE (6,210)AMPC(L-1),AMPC(L),VVC(J-1),VVC(J),HVC(K-1),HVC(K
C      1)
150     CONTINUE
        GOTO 3000
C
C
C       PRINT AVERAGE RESULTS
C
        WRITE(6,2111)
        DO 1500 L=2,DIV1
        DO 1500 J=2,DIV2
        DO 1500 K=2,DIV3
        I=COUNT(IELT(L-1,J-1,K-1))
        IF (I .EQ. 0) GOTO 1500
        SIZE1=DIAM(AMPC(L-1))
        SIZE2=DIAM(AMPC(L))
        SIZE=(SIZE1+SIZE2)/2
        R3=VVCON*(VVC(J-1)+VVC(J))/2 + VVSHFT
        R5=HVCON*(HVC(K-1)+HVC(K))/2 + HVSHFT
        CTCON=DRCON/(HVSIZE*HVCON*VVSIZE*VVCON*(SIZE1-SIZE2))
        R7=I*CTCON
        WRITE(6,2110) SIZE,R3,R5,R7
2110    FORMAT(7X,F5.2,15X,F5.2,15X,F5.2,15X,E10.3)
2111    FORMAT(1H1)
1500    CONTINUE
C
```

```
C
C       CALCULATE NUMBER DENSITIES
C
3000    WRITE(6,511)
        DO 510 L=2,DIV1
        DCOUNT=0.
        PMLV=0.
        PMLV2=0.
        PMAV=0.
        PMAV2=0.
        DO 520 J=2,DIV2
        ICUM=0
        ZVV=VVCON*(VVC(J)+VVC(J-1))/2 + VVSHFT
        DO 530 K=2,DIV3
        ZHV=HVCON*((HVC(K)+HVC(K-1))/2)+HVSHFT
        PMLV=PMLV+COUNT(IELT(L-1,J-1,K-1))*ZHV/ZVV
        PMLV2=PMLV2+COUNT(IELT(L-1,J-1,K-1))*ZHV*ZHV/ZVV
530     ICUM=ICUM+COUNT(IELT(L-1,J-1,K-1))
        DCOUNT=DCOUNT + ( ICUM/ZVV)
        PMAV2=PMAV2+ICUM
                    *ZVV
        PMAV=PMAV+ICUM
520     CONTINUE
        SIZE=(DIAM(AMPC(L-1))+DIAM(AMPC(L)))/2
        SIZERA=DIAM(AMPC(L-1))-DIAM(AMPC(L))
        ZNUMD=DCOUNT
                 *DRC100/SIZERA
        IF (ZNUMD .EQ. 0.)GOTO 510
        ZMLV=DRC100*PMLV/(SIZERA*ZNUMD)
        ZMLV2=DRC100*PMLV2/(SIZERA
                                *ZNUMD)
        ZMAV=PMAV*DRC100/(SIZERA
                              *ZNUMD)
        ZMAV2=DRC100*PMAV2/(SIZERA*ZNUMD)
        SDMAV=SQRT(ZMAV2-ZMAV*ZMAV)
        SDMLV=SQRT(ZMLV2-ZMLV*ZMLV)
        WRITE(6,513) SIZE,ZNUMD,ZMAV,SDMAV,ZMLV,SDMLV
513     FORMAT(15X,F5.2,32X,E10.3,8X,F5.2,10X,F5.2,10X,F5.2,10X,F5.2)
510     CONTINUE
C
        WRITE(6,900)
        ENDFILE 6
511     FORMAT(1H1,/////////50X,'DROPLET SIZE DISTRIBUTION'/////
        1  ,15X,'MEAN',10X,'NUMBER',11X,'MEAN',9X,'STD DEV',10X,
        2  'MEAN',9X,'STD DEV'/13X,'DIAMETER',7X,'DENSITY',8X,
        3  'AXIAL VEL',6X,'AXIAL VEL',6X,'LATERAL VEL',3X,'LATERAL VEL
        4 /13X,'(MICRONS)',4X,'(#/CC/MICRON)',5X,'(M/SEC)',8X,
        5  '(M/SEC)',9X,'(M/SEC)',7X,'(M/SEC)' ///)
512     FORMAT(22X,F5.2,'-',F5.2,12X,E10.3,40X,F5.2)
        END

DOSPIP V6A
```

```
C
C       THIS ROUTINE DISCRIMINATES ON THE BASIS OF PATH LENGTH
C
        SUBROUTINE PLDISC(HV,VV,TIME,AMP,PLMIN,PLMAX)
C
C
        INTEGER HV(2000),VV(2000),TIME(2000),AMP(2000)
        REAL RT1,RV1,PL,PLMIN
        INTEGER DIV1,DIV2,DIV3
        COMMON / /NDATA,DIV1,DIV2,DIV3,NGDATA,VVSHFT,HVSHFT,VVCON,TIM
C       RT1,RV1,ARE DUMMY VARIABLES TO EASE COMPUTATION-MULTIPLICATIO
C       OF  LARGE NUMBERS
C
C       THROW OUT BAD DATA BY FORCING A ZERO PATH LENGTH
C
        DO 20 I=1,NDATA
        IF (HV(I) .LT. 0) VV(I)=-1
        IF (VV(I) .LT. 0) VV(I)=-1
        IF (TIME(I) .LT. 0) VV(I)=-1
        IF (AMP(I) .LT. 0)  VV(I)=-1
20      CONTINUE
        J=1
        NLAR=0
        DO 10 I=1,NDATA
        IF (I .GT. 1000)STOP 5
        IF (VV(I) .LT. 0)GOTO 10
        IF (AMP(I) .LT. 1475)GOTO 7
        TIME(I)=16384-TIME(I)
        RV1=VV(I)*VVCON+VVSHFT
        RT1=TIME(I)/TIMAMP
        RT1=RT1/(SQRT(ALOG(1.05/(1475./AMP(I)+.05)))*1.146)
        PL=RV1*RT1
        IF (PL .LE. PLMAX) GOTO 6
        NLAR=NLAR+1
        VV(I)=-1
        GOTO 10
6       IF(PL.GT.PLMIN)GO TO 5
7       VV(I)=-1
        GO TO 10
5       J=J+1
10      CONTINUE
C
C       GIVE# OF DATA REJECTED FOR PL TOO LARGE
C
        WRITE(4,11) NLAR
11      FORMAT(1H ,I5,' DATA HAD PL TOO LARGE')
C
C       REMEMBER NUM OF GOOD DATA (MEETS PATH REQUIREMENT)
        NGDATA= J - 1
        END

DOSPIP  V6A

>
```

```
C       THIS ROUTINE DETERMINES THE MAXIMUM VALUES OF HV,VV,AND AMP
        SUBROUTINE ZMAX(HV,VV,AMP,HVMAX,VVMAX,AMPMAX,IAMAX)
        INTEGER HV(20),VV(20),AMP(20)
        INTEGER HVMAX,VVMAX,AMPMAX
        INTEGER DIV1,DIV2,DIV3
        COMMON / /NDATA,DIV1,DIV2,DIV3,NGDATA
C
        DO 10 I=1,NDATA
        IF (VV(I) .LT. 0)GOTO 10
        IF(HV(I).GT.HVMAX)HVMAX=HV(I)
        IF(VV(I).GT.VVMAX)VVMAX=VV(I)
        IF (AMP(I) .LE. AMPMAX)GOTO 10
        AMPMAX=AMP(I)
        IAMAX=I
10      CONTINUE
        END
```

```
DOSPIP V6A
```

```
C
C       THIS ROUTINE DETERMINES THE MINIMUM VALUES OF HV,VV,AMP
        SUBROUTINE ZMIN(HV,VV,AMP,HVMIN,VVMIN,AMPMIN)
        INTEGER HV(20),VV(20),AMP(20)
        INTEGER HVMIN,VVMIN,AMPMIN
        INTEGER HVMIN1,VVMIN1,AMMIN1
        INTEGER DIV1,DIV2,DIV3
        COMMON / /NDATA,DIV1,DIV2,DIV3,NGDATA
        DATA HVMIN1,VVMIN1,AMMIN1/100000,100000,100000/
        DO 10 I=1,NDATA
        IF (VV(I) .LT. 0)GOTO 10
        IF(HV(I).LT.HVMIN1)HVMIN1=HV(I)
        IF(VV(I).LT.VVMIN1)VVMIN1=VV(I)
        IF(AMP(I).LT.AMMIN1)AMMIN1=AMP(I)
10      CONTINUE
C
C       MAINTAIN LOCAL COPIES OF THE MINIMA
C
        HVMIN=HVMIN1
        VVMIN=VVMIN1
        AMPMIN=AMMIN1
        END
```

```
DOSPIP V6A
```

```
      THIS ROUTINE CLASSIFIES THE DATA

      SUBROUTINE NRCNT(HV,VV,AMP,HVSIZE,VVSIZE,NBAD,HVC,VVC,AMPC,
     1  HVMIN,VVMIN,AMPMIN,AMPMAX)


      INTEGER HVC(20),VVC(20),AMPC(20),HV(10),VV(10),AMP(10),
     ICOUNT(8000)
      INTEGER HVMIN,VVMIN,AMPMIN,HVSIZE,VVSIZE,AMSIZE,AMPMAX
      INTEGER DIV1,DIV2,DIV3
      COMMON /COMCT/COUNT
      COMMON / /NDATA,DIV1,DIV2,DIV3,NGDATA,VVSHFT,HVSHFT
C     HVC,ETC.,ARE THE LIMITS OF EACH INTERVAL OR CLASS
      HVC(1)=HVMIN
      VVC(1)=VVMIN
      AMPC(1)=AMPMAX
      DO 4 N=2,DIV1
C     THE UPPER LIMITS FOR EACH INTERVAL ARE GENERATED BY ADDING
C     SUITABLE NUMBER OF  'SIZES'
      HVC(N)=HVC(1)+(N-1)*HVSIZE
      VVC(N)=VVC(1)+(N-1)*VVSIZE
      AMPC(N)=0.95*AMPC(N-1)
4     CONTINUE
C     THE FOLLOWING DO LOOPS ASSIGN EACH SET OF VALUES IN
C     APPROPRIATE SIZE RANGE AND INCREMENT COUNT BY 1.

      NBAD=0

C     ONLY THE GOOD DATA (PATH TEST CRITERION) ARE CONSIDERED.

C     IF A DATA FALLS BELOW THE SMALLEST AMPLITUDE CLASS,
C     THEN NBAD IS INCREMENTED AND ITS CONTRIBUTION IS IGNORED
      IF (IFIR .NE. 0) GOTO 999

      DIV2=DIV2+2
      DIV3=DIV3+2
      IFIR=1
C     THE ABOVE NOW POINT TO THE LAST CLASS ELEMENTS
```

```
C
C
99      DO 99 I=1,NDATA
C       CHECK FOR REJECTED DATA
        IF (VV(I) .LT. 0) GOTO 99
        DO 51 N=2,DIV1
        IF(AMP(I).GE.AMPC(N)) GO TO 20
        IF (AMP(I) .GT. AMPMAX) GOTO 99
51      CONTINUE
C       FALLING THRU HERE MEANS DATA IS BAD
C
        NBAD = NBAD + 1
        GOTO 99
C
20      L=N-1
        DO 52 N=2,DIV2
        IF( VV(I).LE.VVC(N)) GO TO 21
52      CONTINUE
21      J=N-1
        DO 53 N=2,DIV3
        IF(HV(I).LE.HVC(N)) GO TO 22
53      CONTINUE
22      K=N-1
        COUNT(IELT(L,J,K))= COUNT(IELT(L,J,K)) + 1
99      CONTINUE
        END

DOSPIP  V6A

>
```

```
        FUNCTION DIAM(IAMP)
        COMMON /GN/GAIN
        DIAM=0.187*IAMP**.5N -26.0
        IF (DIAM .GE. 10.63)RETURN
        DIAM=0.1*IAMP/GAIN - 11.11
```

APPENDIX - 5

Results of the measurements in turbulent free stream air flow and adjacent to a solid surface.

DATA ANALYSIS

Free stream air flow

DIAMETER IN MICRONS

VELOCITY IN METERS PER SECOND

DROPLET RATE IN NUMBER/SEC/SQ CM/(M/SEC)/(M/SEC)/MICRON

NUMBER DENSITY IN NUMBER/ /CC/MICRON

DROPLET SIZE - VELOCITY DISTRIBUTION

DIAMETER RANGE	AXIAL VEL. RANGE	LATERAL VEL. RANGE	NUMBER COUNT	DROPLET RATE
87.70:82.01	0.93: 1.10	-0.09:-0.02	1	0.175E+04
87.70:82.01	1.26: 1.43	-0.09:-0.02	1	0.175E+04
87.70:82.01	1.26: 1.43	-0.02: 0.05	16	0.280E+05
87.70:82.01	1.26: 1.43	0.05: 0.13	1	0.175E+04
87.70:82.01	1.43: 1.60	-0.09:-0.02	6	0.105E+05
87.70:82.01	1.43: 1.60	-0.02: 0.05	22	0.385E+05
87.70:82.01	1.43: 1.60	0.05: 0.13	3	0.524E+04
87.70:82.01	1.43: 1.60	0.27: 0.34	1	0.175E+04
87.70:82.01	1.60: 1.77	-0.02: 0.05	4	0.699E+04
87.70:82.01	1.10: 1.26	-0.09:-0.02	1	0.184E+04
82.01:76.60	1.10: 1.26	-0.02: 0.05	1	0.184E+04
82.01:76.60	1.26: 1.43	-0.02: 0.05	2	0.367E+04
82.01:76.60	1.26: 1.43	0.05: 0.13	1	0.184E+04
82.01:76.60	1.43: 1.60	-0.09:-0.02	2	0.367E+04
82.01:76.60	1.43: 1.60	-0.02: 0.05	1	0.184E+04
82.01:76.60	1.43: 1.60	0.05: 0.13	1	0.184E+04
82.01:76.60	1.60: 1.77	-0.02: 0.05	2	0.367E+04
76.60:71.45	1.10: 1.26	-0.09:-0.02	2	0.380E+04
76.60:71.45	1.26: 1.43	-0.09:-0.02	1	0.193E+04
76.60:71.45	1.26: 1.43	-0.02: 0.05	1	0.193E+04
76.60:71.45	1.43: 1.60	-0.09:-0.02	1	0.193E+04
76.60:71.45	1.43: 1.60	-0.02: 0.05	5	0.960E+04
76.60:71.45	1.60: 1.77	-0.02: 0.05	3	0.579E+04
71.45:66.57	1.26: 1.43	-0.02: 0.05	1	0.204E+04
71.45:66.57	1.43: 1.60	-0.09:-0.02	1	0.204E+04
71.45:66.57	1.43: 1.60	-0.02: 0.05	1	0.204E+04
71.45:66.57	1.43: 1.60	0.05: 0.13	1	0.204E+04
66.57:61.93	1.26: 1.43	-0.02: 0.05	3	0.643E+04
66.57:61.93	1.26: 1.43	0.05: 0.13	1	0.214E+04
66.57:61.93	1.43: 1.60	-0.09:-0.02	2	0.429E+04
66.57:61.93	1.43: 1.60	-0.02: 0.05	4	0.857E+04
66.57:61.93	1.43: 1.60	0.05: 0.13	2	0.429E+04
66.57:61.93	1.60: 1.77	-0.02: 0.05	1	0.214E+04
66.57:61.93	1.60: 1.77	0.05: 0.13	1	0.214E+04
61.93:57.54	1.26: 1.43	-0.09:-0.02	1	0.220E+04
61.93:57.54	1.26: 1.43	-0.02: 0.05	3	0.673E+04
61.93:57.54	1.26: 1.43	0.05: 0.13	1	0.224E+04
61.93:57.54	1.43: 1.60	-0.02: 0.05	7	0.157E+05
61.93:57.54	1.43: 1.60	0.05: 0.13	1	0.224E+04
61.93:57.54	1.77: 1.93	-0.02: 0.05	1	0.224E+04
57.54:53.39	1.10: 1.26	0.27: 0.34	1	0.241E+04

57.54:53.35	1.26: 1.43	-0.02: 0.05	3	0.712E+04
57.54:53.35	1.43: 1.60	-0.09:-0.02	1	0.237E+04
57.54:53.35	1.43: 1.60	-0.02: 0.05	5	0.119E+05
57.54:53.35	1.43: 1.60	0.05: 0.13	1	0.237E+04
57.54:53.35	1.60: 1.77	-0.09:-0.02	1	0.237E+04
57.54:53.35	1.60: 1.77	-0.02: 0.05	1	0.237E+04
53.35:49.37	1.26: 1.43	-0.09:-0.02	3	0.749E+04
53.35:49.37	1.26: 1.43	0.13: 0.20	1	0.250E+04
53.35:49.37	1.43: 1.60	-0.09:-0.02	1	0.250E+04
53.35:49.37	1.43: 1.60	-0.02: 0.05	2	0.499E+04
53.35:49.37	1.43: 1.60	0.05: 0.13	2	0.499E+04
53.35:49.37	1.60: 1.77	-0.09:-0.02	2	0.499E+04
53.35:49.37	1.60: 1.77	-0.02: 0.05	2	0.499E+04
53.35:49.37	1.77: 1.93	-0.02: 0.05	1	0.250E+04
49.37:45.60	1.10: 1.26	-0.09:-0.02	1	0.264E+04
49.37:45.60	1.26: 1.43	-0.02: 0.05	1	0.264E+04
49.37:45.60	1.26: 1.43	0.05: 0.13	1	0.264E+04
49.37:45.60	1.43: 1.60	-0.09:-0.02	2	0.527E+04
49.37:45.60	1.43: 1.60	-0.02: 0.05	2	0.527E+04
49.37:45.60	1.43: 1.60	0.05: 0.13	2	0.527E+04
49.37:45.60	1.60: 1.77	-0.09:-0.02	2	0.527E+04
49.37:45.60	1.60: 1.77	-0.02: 0.05	2	0.527E+04
49.37:45.60	1.60: 1.77	0.05: 0.13	1	0.264E+04
45.60:42.01	1.10: 1.26	-0.02: 0.05	1	0.277E+04
45.60:42.01	1.26: 1.43	-0.09:-0.02	1	0.277E+04
45.60:42.01	1.26: 1.43	-0.02: 0.05	4	0.111E+05
45.60:42.01	1.26: 1.43	0.05: 0.13	1	0.277E+04
45.60:42.01	1.26: 1.43	0.13: 0.20	1	0.277E+04
45.60:42.01	1.43: 1.60	-0.09:-0.02	3	0.830E+04
45.60:42.01	1.43: 1.60	-0.02: 0.05	8	0.221E+05
45.60:42.01	1.43: 1.60	0.13: 0.20	1	0.277E+04
45.60:42.01	1.60: 1.77	0.05: 0.13	1	0.277E+04
42.01:38.60	1.10: 1.26	-0.09:-0.02	1	0.291E+04
42.01:38.60	1.10: 1.26	-0.02: 0.05	2	0.583E+04
42.01:38.60	1.10: 1.26	0.05: 0.13	1	0.291E+04
42.01:38.60	1.26: 1.43	-0.09:-0.02	3	0.874E+04
42.01:38.60	1.26: 1.43	-0.02: 0.05	6	0.175E+05
42.01:38.60	1.26: 1.43	0.05: 0.13	1	0.291E+04
42.01:38.60	1.43: 1.60	-0.16:-0.09	1	0.291E+04
42.01:38.60	1.43: 1.60	-0.09:-0.02	3	0.874E+04
42.01:38.60	1.43: 1.60	-0.02: 0.05	14	0.408E+05
42.01:38.60	1.43: 1.60	0.05: 0.13	3	0.874E+04
42.01:38.60	1.43: 1.60	0.34: 0.41	1	0.291E+04
42.01:38.60	1.60: 1.77	-0.02: 0.05	2	0.583E+04
42.01:38.60	1.60: 1.77	0.05: 0.13	1	0.291E+04
42.01:38.60	1.60: 1.77	0.13: 0.20	1	0.291E+04
42.01:38.60	1.77: 1.93	-0.02: 0.05	1	0.291E+04
38.60:35.37	1.10: 1.26	-0.0.: 0.05	2	0.6[illegible]E+04
38.60:35.37	1.26: 1.43	-0.09:-0.02	1	0.306E+04
38.60:35.37	1.26: 1.43	-0.02: 0.05	8	0.234E+05
38.60:35.37	1.43: 1.60	-0.09:-0.02	3	0.9[illegible]E+04
38.60:35.37	1.43: 1.60	-0.02: 0.05	10	0.294E+05

38.60:35.37	1.43: 1.60	0.05: 0.13	3	0.923E+04
38.60:35.37	1.43: 1.60	0.13: 0.20	1	0.308E+04
38.60:35.37	1.43: 1.60	0.20: 0.27	1	0.308E+04
38.60:35.37	1.60: 1.77	-0.09:-0.02	2	0.615E+04
38.60:35.37	1.60: 1.77	-0.02: 0.05	2	0.615E+04
38.60:35.37	1.60: 1.77	0.05: 0.13	1	0.308E+04
38.60:35.37	1.77: 1.93	0.05: 0.13	1	0.308E+04
38.60:35.37	1.77: 1.93	0.13: 0.20	1	0.308E+04
38.60:35.37	1.77: 1.93	0.20: 0.27	1	0.308E+04
35.37:32.28	0.93: 1.10	-0.02: 0.05	1	0.322E+04
35.37:32.28	1.10: 1.26	-0.09:-0.02	1	0.322E+04
35.37:32.28	1.10: 1.26	-0.02: 0.05	2	0.645E+04
35.37:32.28	1.10: 1.26	0.34: 0.41	1	0.322E+04
35.37:32.28	1.26: 1.43	-0.16:-0.09	1	0.322E+04
35.37:32.28	1.26: 1.43	-0.09:-0.02	3	0.967E+04
35.37:32.28	1.26: 1.43	-0.02: 0.05	6	0.193E+05
35.37:32.28	1.26: 1.43	0.13: 0.20	1	0.322E+04
35.37:32.28	1.43: 1.60	-0.09:-0.02	4	0.129E+05
35.37:32.28	1.43: 1.60	-0.02: 0.05	8	0.258E+05
35.37:32.28	1.43: 1.60	0.05: 0.13	2	0.645E+04
35.37:32.28	1.60: 1.77	-0.09:-0.02	1	0.322E+04
35.37:32.28	1.60: 1.77	-0.02: 0.05	8	0.258E+05
35.37:32.28	1.77: 1.93	0.13: 0.20	1	0.322E+04
32.28:29.35	1.10: 1.26	-0.16:-0.09	1	0.339E+04
32.28:29.35	1.10: 1.26	-0.09:-0.02	1	0.339E+04
32.28:29.35	1.10: 1.26	-0.02: 0.05	1	0.339E+04
32.28:29.35	1.26: 1.43	-0.16:-0.09	1	0.339E+04
32.28:29.35	1.26: 1.43	-0.09:-0.02	7	0.237E+05
32.28:29.35	1.26: 1.43	-0.02: 0.05	12	0.407E+05
32.28:29.35	1.26: 1.43	0.05: 0.13	3	0.102E+05
32.28:29.35	1.26: 1.43	0.13: 0.20	1	0.339E+04
32.28:29.35	1.43: 1.60	-0.16:-0.09	2	0.678E+04
32.28:29.35	1.43: 1.60	-0.09:-0.02	5	0.169E+05
32.28:29.35	1.43: 1.60	-0.02: 0.05	15	0.508E+05
32.28:29.35	1.43: 1.60	0.05: 0.13	4	0.136E+05
32.28:29.35	1.43: 1.60	0.13: 0.20	1	0.339E+04
32.28:29.35	1.60: 1.77	-0.16:-0.09	1	0.339E+04
32.28:29.35	1.60: 1.77	-0.09:-0.02	1	0.339E+04
32.28:29.35	1.60: 1.77	-0.02: 0.05	5	0.169E+05
32.28:29.35	1.60: 1.77	0.05: 0.13	1	0.339E+04
32.28:29.35	1.77: 1.93	-0.02: 0.05	3	0.102E+05
32.28:29.35	1.77: 1.93	0.05: 0.13	1	0.339E+04
29.35:26.52	1.10: 1.26	-0.02: 0.05	2	0.714E+04
29.35:26.52	1.10: 1.26	0.20: 0.27	1	0.357E+04
29.35:26.52	1.26: 1.43	-0.09:-0.02	3	0.107E+05
29.35:26.52	1.26: 1.43	-0.02: 0.05	6	0.214E+05
29.35:26.52	1.26: 1.43	0.05: 0.13	3	0.107E+05
29.35:26.52	1.26: 1.43	0.20: 0.27	1	0.357E+04
29.35:26.52	1.43: 1.60	-0.16:-0.09	1	0.357E+04
29.35:26.52	1.43: 1.60	-0.09:-0.02	4	0.143E+05
29.35:26.52	1.43: 1.60	-0.02: 0.05	13	0.464E+05
29.35:26.52	1.43: 1.60	0.05: 0.13	5	0.179E+05

29.35:26.57	1.43: 1.60	0.13: 0.20	1	0.357E+04
29.35:26.57	1.60: 1.77	-0.16:-0.09	1	0.357E+04
29.35:26.57	1.60: 1.77	-0.02: 0.05	8	0.286E+05
29.35:26.57	1.60: 1.77	0.05: 0.13	2	0.714E+04
29.35:26.57	1.77: 1.93	-0.02: 0.05	1	0.357E+04
26.57:23.94	0.93: 1.10	-0.16:-0.09	1	0.377E+04
26.57:23.94	1.10: 1.26	-0.09:-0.02	1	0.377E+04
26.57:23.94	1.10: 1.26	0.20: 0.27	1	0.377E+04
26.57:23.94	1.26: 1.43	-0.23:-0.16	1	0.377E+04
26.57:23.94	1.26: 1.43	-0.16:-0.09	3	0.113E+05
26.57:23.94	1.26: 1.43	-0.09:-0.02	4	0.151E+05
26.57:23.94	1.26: 1.43	-0.02: 0.05	12	0.453E+05
26.57:23.94	1.26: 1.43	0.05: 0.13	3	0.113E+05
26.57:23.94	1.26: 1.43	0.27: 0.34	1	0.377E+04
26.57:23.94	1.43: 1.60	-0.16:-0.09	1	0.377E+04
26.57:23.94	1.43: 1.60	-0.09:-0.02	15	0.566E+05
26.57:23.94	1.43: 1.60	-0.02: 0.05	21	0.793E+05
26.57:23.94	1.43: 1.60	0.05: 0.13	14	0.528E+05
26.57:23.94	1.43: 1.60	0.13: 0.20	3	0.113E+05
26.57:23.94	1.43: 1.60	0.20: 0.27	1	0.377E+04
26.57:23.94	1.60: 1.77	-0.23:-0.16	1	0.377E+04
26.57:23.94	1.60: 1.77	-0.09:-0.02	6	0.226E+05
26.57:23.94	1.60: 1.77	-0.02: 0.05	6	0.226E+05
26.57:23.94	1.60: 1.77	0.05: 0.13	4	0.151E+05
26.57:23.94	1.77: 1.93	-0.02: 0.05	2	0.755E+04
26.57:23.94	1.77: 1.93	0.05: 0.13	1	0.377E+04
23.94:21.42	1.10: 1.26	-0.09:-0.02	1	0.395E+04
23.94:21.42	1.10: 1.26	-0.02: 0.05	2	0.791E+04
23.94:21.42	1.26: 1.43	-0.16:-0.09	1	0.395E+04
23.94:21.42	1.26: 1.43	-0.09:-0.02	9	0.356E+05
23.94:21.42	1.26: 1.43	-0.02: 0.05	18	0.712E+05
23.94:21.42	1.26: 1.43	0.05: 0.13	2	0.791E+04
23.94:21.42	1.26: 1.43	0.27: 0.34	1	0.388E+04
23.94:21.42	1.26: 1.43	0.34: 0.41	1	0.395E+04
23.94:21.42	1.43: 1.60	-0.16:-0.09	1	0.395E+04
23.94:21.42	1.43: 1.60	-0.09:-0.02	9	0.356E+05
23.94:21.42	1.43: 1.60	-0.02: 0.05	26	0.10 E+06
23.94:21.42	1.43: 1.60	0.05: 0.13	9	0.35 E+05
23.94:21.42	1.43: 1.60	0.13: 0.20	1	0.3 E+04
23.94:21.42	1.43: 1.60	0.20: 0.27	1	0. E+04
23.94:21.42	1.60: 1.77	-0.09:-0.02	11	0. E+05
23.94:21.42	1.60: 1.77	-0.02: 0.05	12	0.4 E+05
23.94:21.42	1.60: 1.77	0.05: 0.13	5	0.1 E+05
23.94:21.42	1.77: 1.93	0.05: 0.13	1	0.3 E+04
23.94:21.42	1.93: 2.10	-0.02: 0.05	1	0.3 E+04
21.41:19.03	1.10: 1.26	-0.16:-0.09	1	0.4 E+04
21.41:19.03	1.10: 1.26	-0.09:-0.02	2	0.8 E+04
21.41:19.03	1.10: 1.26	-0.02: 0.05	5	0.2 E+05
21.41:19.03	1.10: 1.26	0.05: 0.13	2	0.8 E+04
21.41:19.03	1.26: 1.43	-0.09:-0.02	7	0.2 E+05
21.41:19.03	1.26: 1.43	-0.02: 0.05	16	0.6 E+05
21.41:19.03	1.26: 1.43	0.05: 0.13	4	0.1 E+05

21.42:19.03	1.26: 1.43	0.13: 0.20	3	0.125E+05
21.42:19.03	1.26: 1.43	0.20: 0.27	2	0.830E+04
21.42:19.03	1.26: 1.43	0.27: 0.34	1	0.415E+04
21.42:19.03	1.43: 1.60	-0.09:-0.02	14	0.581E+05
21.42:19.03	1.43: 1.60	-0.02: 0.05	36	0.149E+06
21.42:19.03	1.43: 1.60	0.05: 0.13	8	0.332E+05
21.42:19.03	1.43: 1.60	0.13: 0.20	3	0.125E+05
21.42:19.03	1.43: 1.60	0.20: 0.27	1	0.415E+04
21.42:19.03	1.43: 1.60	0.27: 0.34	1	0.415E+04
21.42:19.03	1.60: 1.77	-0.09:-0.02	11	0.457E+05
21.42:19.03	1.60: 1.77	-0.02: 0.05	21	0.872E+05
21.42:19.03	1.60: 1.77	0.05: 0.13	5	0.208E+05
21.42:19.03	1.60: 1.77	0.20: 0.27	1	0.415E+04
21.42:19.03	1.77: 1.93	-0.09:-0.02	2	0.830E+04
21.42:19.03	1.77: 1.93	-0.02: 0.05	3	0.125E+05
21.42:19.03	1.77: 1.93	0.05: 0.13	2	0.830E+04
19.03:16.76	1.10: 1.26	-0.09:-0.02	2	0.874E+04
19.03:16.76	1.10: 1.26	-0.02: 0.05	4	0.175E+05
19.03:16.76	1.10: 1.26	0.13: 0.20	1	0.457E+04
19.03:16.76	1.26: 1.43	-0.16:-0.09	2	0.874E+04
19.03:16.76	1.26: 1.43	-0.09:-0.02	10	0.437E+05
19.03:16.76	1.26: 1.43	-0.02: 0.05	27	0.118E+06
19.03:16.76	1.26: 1.43	0.05: 0.13	9	0.393E+05
19.03:16.76	1.26: 1.43	0.13: 0.20	2	0.874E+04
19.03:16.76	1.26: 1.43	0.20: 0.27	1	0.457E+04
19.03:16.76	1.26: 1.43	0.27: 0.34	2	0.874E+04
19.03:16.76	1.43: 1.60	-0.16:-0.09	2	0.874E+04
19.03:16.76	1.43: 1.60	-0.09:-0.02	17	0.743E+05
19.03:16.76	1.43: 1.60	-0.02: 0.05	41	0.179E+06
19.03:16.76	1.43: 1.60	0.05: 0.13	10	0.437E+05
19.03:16.76	1.43: 1.60	0.13: 0.20	5	0.219E+05
19.03:16.76	1.43: 1.60	0.34: 0.41	1	0.457E+04
19.03:16.76	1.60: 1.77	-0.16:-0.09	1	0.457E+04
19.03:16.76	1.60: 1.77	-0.09:-0.02	6	0.262E+05
19.03:16.76	1.60: 1.77	-0.02: 0.05	21	0.918E+05
19.03:16.76	1.60: 1.77	0.05: 0.13	4	0.175E+05
19.03:16.76	1.60: 1.77	0.13: 0.20	2	0.874E+04
19.03:16.76	1.60: 1.77	0.20: 0.27	2	0.874E+04
19.03:16.76	1.77: 1.93	-0.09:-0.02	4	0.175E+05
19.03:16.76	1.77: 1.93	-0.02: 0.05	4	0.175E+05
19.03:16.76	1.77: 1.93	0.05: 0.13	1	0.437E+04
19.03:16.76	1.93: 2.10	-0.09:-0.02	1	0.437E+04
16.76:14.60	0.93: 1.10	0.05: 0.13	1	0.461E+04
16.76:14.60	1.10: 1.26	-0.16:-0.09	1	0.461E+04
16.76:14.60	1.10: 1.26	-0.09:-0.02	4	0.185E+05
16.76:14.60	1.10: 1.26	-0.02: 0.05	4	0.185E+05
16.76:14.60	1.10: 1.26	0.05: 0.13	2	0.923E+04
16.76:14.60	1.26: 1.43	-0.23:-0.16	1	0.461E+04
16.76:14.60	1.26: 1.43	-0.16:-0.09	2	0.923E+04
16.76:14.60	1.26: 1.43	-0.09:-0.02	16	0.738E+05
16.76:14.60	1.26: 1.43	-0.02: 0.05	24	0.111E+06
16.76:14.60	1.26: 1.43	0.05: 0.13	9	0.415E+05

16.76:14.60	1.26: 1.43	0.13: 0.20	2	0.923E+04
16.76:14.60	1.26: 1.43	0.20: 0.27	1	0.461E+04
16.76:14.60	1.26: 1.43	0.41: 0.49	1	0.461E+04
16.76:14.60	1.43: 1.60	-0.16:-0.09	3	0.138E+05
16.76:14.60	1.43: 1.60	-0.09:-0.02	22	0.101E+06
16.76:14.60	1.43: 1.60	-0.02: 0.05	51	0.235E+06
16.76:14.60	1.43: 1.60	0.05: 0.13	19	0.877E+05
16.76:14.60	1.43: 1.60	0.13: 0.20	3	0.138E+05
16.76:14.60	1.60: 1.77	-0.16:-0.09	2	0.923E+04
16.76:14.60	1.60: 1.77	-0.09:-0.02	19	0.877E+05
16.76:14.60	1.60: 1.77	-0.02: 0.05	17	0.784E+05
16.76:14.60	1.60: 1.77	0.05: 0.13	10	0.461E+05
16.76:14.60	1.60: 1.77	0.13: 0.20	1	0.461E+04
16.76:14.60	1.60: 1.77	0.20: 0.27	3	0.138E+05
16.76:14.60	1.77: 1.93	-0.16:-0.09	1	0.461E+04
16.76:14.60	1.77: 1.93	-0.09:-0.02	2	0.923E+04
16.76:14.60	1.77: 1.93	-0.02: 0.05	5	0.231E+05
14.60:12.57	1.10: 1.26	-0.09:-0.02	1	0.461E+04
14.60:12.57	1.10: 1.26	-0.02: 0.05	9	0.415E+05
14.60:12.57	1.10: 1.26	0.05: 0.13	4	0.195E+05
14.60:12.57	1.10: 1.26	0.13: 0.20	1	0.461E+04
14.60:12.57	1.26: 1.43	-0.16:-0.09	2	0.923E+04
14.60:12.57	1.26: 1.43	-0.09:-0.02	15	0.692E+05
14.60:12.57	1.26: 1.43	-0.02: 0.05	38	0.175E+06
14.60:12.57	1.26: 1.43	0.05: 0.13	12	0.553E+05
14.60:12.57	1.26: 1.43	0.13: 0.20	4	0.195E+05
14.60:12.57	1.26: 1.43	0.41: 0.49	1	0.461E+04
14.60:12.57	1.43: 1.60	-0.16:-0.09	3	0.138E+05
14.60:12.57	1.43: 1.60	-0.09:-0.02	34	0.157E+06
14.60:12.57	1.43: 1.60	-0.02: 0.05	63	0.291E+06
14.60:12.57	1.43: 1.60	0.05: 0.13	23	0.106E+06
14.60:12.57	1.43: 1.60	0.13: 0.20	5	0.231E+05
14.60:12.57	1.43: 1.60	0.20: 0.27	1	0.461E+04
14.60:12.57	1.43: 1.60	0.27: 0.34	1	0.461E+04
14.60:12.57	1.43: 1.60	0.41: 0.49	1	0.461E+04
14.60:12.57	1.60: 1.77	-0.16:-0.09	4	0.195E+05
14.60:12.57	1.60: 1.77	-0.09:-0.02	15	0.692E+05
14.60:12.57	1.60: 1.77	-0.02: 0.05	36	0.166E+06
14.60:12.57	1.60: 1.77	0.05: 0.13	12	0.553E+05
14.60:12.57	1.60: 1.77	0.13: 0.20	2	0.923E+04
14.60:12.57	1.60: 1.77	0.20: 0.27	2	0.923E+04
14.60:12.57	1.77: 1.93	-0.09:-0.02	2	0.923E+04
14.60:12.57	1.77: 1.93	-0.02: 0.05	6	0.277E+05
14.60:12.57	1.77: 1.93	0.05: 0.13	3	0.138E+05
14.60:12.57	1.77: 1.93	0.34: 0.41	1	0.461E+04
14.60:12.57	1.93: 2.10	-0.02: 0.05	1	0.461E+04
14.60:12.57	2.10: 2.27	-0.09:-0.02	1	0.461E+04
12.56:10.62	1.10: 1.26	-0.09:-0.02	1	0.461E+04
12.56:10.62	1.10: 1.26	-0.02: 0.05	6	0.277E+05
12.56:10.62	1.10: 1.26	0.05: 0.13	2	0.923E+04
12.56:10.62	1.26: 1.43	-0.23:-0.16	1	0.461E+04
12.56:10.62	1.26: 1.43	-0.16: 0.09	4	0.184E+05

12.57:10.62	1.26: 1.43	-0.09:-0.02	25	0.128E+06
12.57:10.62	1.26: 1.43	-0.02: 0.05	41	0.210E+06
12.57:10.62	1.26: 1.43	0.05: 0.13	13	0.664E+05
12.57:10.62	1.26: 1.43	0.13: 0.20	8	0.409E+05
12.57:10.62	1.26: 1.43	0.20: 0.27	1	0.511E+04
12.57:10.62	1.26: 1.43	0.27: 0.34	1	0.511E+04
12.57:10.62	1.26: 1.43	0.34: 0.41	1	0.511E+04
12.57:10.62	1.43: 1.60	-0.23:-0.16	1	0.511E+04
12.57:10.62	1.43: 1.60	-0.16:-0.09	3	0.153E+05
12.57:10.62	1.43: 1.60	-0.09:-0.02	42	0.215E+06
12.57:10.62	1.43: 1.60	-0.02: 0.05	94	0.480E+06
12.57:10.62	1.43: 1.60	0.05: 0.13	36	0.184E+06
12.57:10.62	1.43: 1.60	0.13: 0.20	7	0.358E+05
12.57:10.62	1.43: 1.60	0.20: 0.27	5	0.256E+05
12.57:10.62	1.43: 1.60	0.27: 0.34	2	0.102E+05
12.57:10.62	1.43: 1.60	0.49: 0.56	1	0.511E+04
12.57:10.62	1.60: 1.77	-0.16:-0.09	4	0.204E+05
12.57:10.62	1.60: 1.77	-0.09:-0.02	29	0.148E+06
12.57:10.62	1.60: 1.77	-0.02: 0.05	47	0.240E+06
12.57:10.62	1.60: 1.77	0.05: 0.13	17	0.869E+05
12.57:10.62	1.60: 1.77	0.27: 0.34	2	0.102E+05
12.57:10.62	1.77: 1.93	-0.09:-0.02	5	0.256E+05
12.57:10.62	1.77: 1.93	-0.02: 0.05	5	0.256E+05
12.57:10.62	1.77: 1.93	0.05: 0.13	3	0.153E+05
12.57:10.62	1.77: 1.93	0.13: 0.20	1	0.511E+04
12.57:10.62	1.77: 1.93	0.20: 0.27	1	0.511E+04
12.57:10.62	1.93: 2.10	-0.09:-0.02	1	0.511E+04
12.57:10.62	1.93: 2.10	0.41: 0.49	1	0.511E+04

DROPLET SIZE DISTRIBUTION

DIAMETER RANGE	NUMBER DENSITY
87.70-82.01	0.115E+02
82.01-76.60	0.251E+01
76.60-71.45	0.301E+01
71.45-66.57	0.957E+00
66.57-61.93	0.348E+01
61.93-57.54	0.372E+01
57.54-53.35	0.366E+01
53.35-49.37	0.391E+01
49.37-45.60	0.419E+01
45.60-42.01	0.703E+01
42.01-38.60	0.144E+02
38.60-35.37	0.125E+02
35.37-32.28	0.157E+02
32.28-29.35	0.265E+02
29.35-26.67	0.221E+02
26.67-23.91	0.411E+02
23.91-21.42	0.516E+02
21.42-19.03	0.722E+02
19.03-16.76	0.920E+02
16.76-14.60	0.121E+03
14.60-12.57	0.170E+03
12.57-10.62	0.238E+03

DATA ANALYSIS

Adjacent to a solid surface

DIAMETER IN MICRONS

VELOCITY IN METERS PER SECOND

DROPLET RATE IN NUMBER/SEC/SQ CM/(M/SEC)/(M/SEC)/MICRON

NUMBER DENSITY IN NUMBER/ /CC/MICRON

DROPLET SIZE - VELOCITY DISTRIBUTION

DIAMETER RANGE	AXIAL VEL. RANGE	LATERAL VEL. RANGE	NUMBER COUNT	DROPLET RATE
87.70:82.01	0.67: 0.90	-0.09:-0.00	1	0.933E+03
87.70:82.01	0.67: 0.90	-0.00: 0.08	2	0.188E+04
87.70:82.01	0.90: 1.12	-0.17:-0.09	1	0.938E+03
87.70:82.01	0.90: 1.12	-0.09:-0.00	2	0.188E+04
87.70:82.01	0.90: 1.12	-0.00: 0.08	1	0.938E+03
87.70:82.01	1.12: 1.35	-0.09:-0.00	4	0.375E+04
87.70:82.01	1.12: 1.35	-0.00: 0.08	9	0.844E+04
87.70:82.01	1.35: 1.58	-0.00: 0.08	6	0.563E+04
82.01:76.60	0.67: 0.90	-0.00: 0.08	2	0.197E+04
82.01:76.60	0.90: 1.12	-0.09:-0.00	1	0.984E+03
82.01:76.60	0.90: 1.12	-0.00: 0.08	1	0.984E+03
82.01:76.60	1.12: 1.35	-0.00: 0.08	1	0.984E+03
76.60:71.45	0.90: 1.12	-0.00: 0.08	1	0.104E+04
76.60:71.45	1.12: 1.35	-0.09:-0.00	1	0.104E+04
76.60:71.45	1.12: 1.35	-0.00: 0.08	2	0.207E+04
71.45:66.57	0.67: 0.90	-0.00: 0.08	1	0.109E+04
71.45:66.57	0.90: 1.12	-0.00: 0.08	2	0.219E+04
71.45:66.57	1.12: 1.35	-0.09:-0.00	1	0.109E+04
71.45:66.57	1.12: 1.35	-0.00: 0.08	1	0.109E+04
71.45:66.57	1.35: 1.58	-0.09:-0.00	2	0.219E+04
66.57:61.93	0.67: 0.90	0.00: 0.16	1	0.115E+04
66.57:61.93	0.90: 1.12	-0.09:-0.00	1	0.115E+04
66.57:61.93	1.35: 1.58	-0.09:-0.00	1	0.115E+04
61.93:57.54	0.67: 0.90	-0.09:-0.00	2	0.242E+04
61.93:57.54	0.67: 0.90	-0.00: 0.08	1	0.121E+04
61.93:57.54	0.90: 1.12	-0.00: 0.08	2	0.242E+04
61.93:57.54	1.12: 1.35	-0.09:-0.00	2	0.242E+04
61.93:57.54	1.12: 1.35	-0.00: 0.08	1	0.121E+04
61.93:57.54	1.58: 1.80	-0.09:-0.00	1	0.121E+04
57.54:53.35	0.67: 0.90	-0.09:-0.00	2	0.255E+04
57.54:53.35	0.67: 0.90	-0.00: 0.08	1	0.127E+04
57.54:53.35	0.90: 1.12	-0.00: 0.08	4	0.509E+04
57.54:53.35	1.12: 1.35	-0.00: 0.08	3	0.382E+04
53.35:49.37	0.67: 0.90	-0.00: 0.08	1	0.134E+04
53.35:49.37	0.90: 1.12	-0.00: 0.08	3	0.402E+04
53.35:49.37	1.12: 1.35	-0.09:-0.00	6	0.804E+04
53.35:49.37	1.12: 1.35	-0.00: 0.08	5	0.670E+04
49.37:45.60	0.45: 0.67	-0.00: 0.08	1	0.134E+04
49.37:45.60	0.67: 0.90	-0.09:-0.00	1	0.134E+04
49.37:45.60	0.90: 1.12	-0.17:-0.09	1	0.134E+04
49.37:45.60	0.90: 1.12	-0.09: 0.00	2	0.268E+04

49.37:	45.60	1.12: 1.35	-0.00: 0.08	3	0.424E+04
49.37:	45.60	1.12: 1.35	0.08: 0.16	1	0.141E+04
49.37:	45.60	1.12: 1.35	0.41: 0.49	1	0.141E+04
49.37:	45.60	1.35: 1.58	-0.09:-0.00	1	0.141E+04
49.37:	45.60	1.35: 1.58	0.08: 0.16	1	0.141E+04
45.60:	42.01	0.67: 0.90	-0.00: 0.08	1	0.140E+04
45.60:	42.01	0.67: 0.90	0.08: 0.16	2	0.29?E+04
45.60:	42.01	0.90: 1.12	-0.09:-0.00	4	0.594E+04
45.60:	42.01	0.90: 1.12	-0.00: 0.08	5	0.742E+04
45.60:	42.01	0.90: 1.12	0.08: 0.16	3	0.445E+04
45.60:	42.01	1.12: 1.35	-0.09:-0.00	8	0.119E+05
45.60:	42.01	1.12: 1.35	-0.00: 0.08	9	0.134E+05
45.60:	42.01	1.12: 1.35	0.08: 0.16	1	0.148E+04
45.60:	42.01	1.35: 1.58	0.08: 0.16	1	0.148E+04
45.60:	42.01	0.45: 0.67	-0.09:-0.00	1	0.156E+04
42.01:	38.60	0.67: 0.90	-0.00: 0.08	4	0.625E+04
42.01:	38.60	0.90: 1.12	-0.09:-0.00	3	0.469E+04
42.01:	38.60	0.90: 1.12	-0.00: 0.08	5	0.781E+04
42.01:	38.60	0.90: 1.12	0.33: 0.41	1	0.156E+04
42.01:	38.60	1.12: 1.35	-0.09:-0.00	1	0.156E+04
42.01:	38.60	1.12: 1.35	-0.00: 0.08	5	0.781E+04
42.01:	38.60	1.12: 1.35	0.16: 0.24	1	0.156E+04
42.01:	38.60	1.12: 1.35	0.24: 0.33	1	0.156E+04
38.60:	35.37	0.67: 0.90	-0.09:-0.00	1	0.165E+04
38.60:	35.37	0.67: 0.90	-0.00: 0.08	2	0.330E+04
38.60:	35.37	0.67: 0.90	0.08: 0.16	3	0.495E+04
38.60:	35.37	0.67: 0.90	0.24: 0.33	1	0.165E+04
38.60:	35.37	0.90: 1.12	-0.17:-0.09	1	0.165E+04
38.60:	35.37	0.90: 1.12	-0.09:-0.00	1	0.165E+04
38.60:	35.37	0.90: 1.12	-0.00: 0.08	7	0.115E+05
38.60:	35.37	0.90: 1.12	0.08: 0.16	1	0.165E+04
38.60:	35.37	1.12: 1.35	-0.17:-0.09	1	0.165E+04
38.60:	35.37	1.12: 1.35	-0.09:-0.00	6	0.990E+04
38.60:	35.37	1.12: 1.35	-0.00: 0.08	6	0.990E+04
38.60:	35.37	1.12: 1.35	0.16: 0.24	1	0.165E+04
38.60:	35.37	1.12: 1.35	0.33: 0.41	1	0.165E+04
38.60:	35.37	1.35: 1.58	-0.09:-0.00	3	0.495E+04
38.60:	35.37	1.58: 1.80	-0.09:-0.00	1	0.165E+04
35.37:	32.28	0.45: 0.67	0.08: 0.16	2	0.343E+04
35.37:	32.28	0.45: 0.67	0.16: 0.24	1	0.173E+04
35.37:	32.28	0.67: 0.90	-0.09:-0.00	4	0.692E+04
35.37:	32.28	0.67: 0.90	-0.00: 0.08	5	0.865E+04
35.37:	32.28	0.90: 1.12	-0.17:-0.09	1	0.173E+04
35.37:	32.28	0.90: 1.12	-0.09:-0.00	8	0.138E+05
35.37:	32.28	0.90: 1.12	-0.00: 0.08	8	0.138E+05
35.37:	32.28	0.90: 1.12	0.08: 0.16	3	0.519E+04
35.37:	32.28	0.90: 1.12	0.24: 0.33	1	0.173E+04
35.37:	32.28	1.12: 1.35	-0.09:-0.00	7	0.121E+05
35.37:	32.28	1.12: 1.35	-0.00: 0.08	9	0.156E+05
35.37:	32.28	1.12: 1.35	0.08: 0.16	1	0.173E+04
35.37:	32.28	1.35: 1.58	-0.09:-0.00	2	0.346E+04
35.37:	32.28	1.35: 1.58	-0.00: 0.08	1	0.173E+04

32.28:29.35	0.45: 0.67	-0.09:-0.00	3	0.545E+04
32.28:29.35	0.67: 0.90	-0.09:-0.00	6	0.109E+05
32.28:29.35	0.67: 0.90	-0.00: 0.08	8	0.145E+05
32.28:29.35	0.67: 0.90	0.08: 0.16	1	0.182E+04
32.28:29.35	0.90: 1.12	-0.17:-0.09	1	0.182E+04
32.28:29.35	0.90: 1.12	-0.09:-0.00	15	0.273E+05
32.28:29.35	0.90: 1.12	-0.00: 0.08	10	0.182E+05
32.28:29.35	0.90: 1.12	0.16: 0.24	1	0.182E+04
32.28:29.35	1.12: 1.35	-0.17:-0.09	1	0.182E+04
32.28:29.35	1.12: 1.35	-0.09:-0.00	4	0.727E+04
32.28:29.35	1.12: 1.35	-0.00: 0.08	14	0.255E+05
32.28:29.35	1.12: 1.35	0.08: 0.16	4	0.727E+04
32.28:29.35	1.12: 1.35	0.16: 0.24	1	0.182E+04
32.28:29.35	1.35: 1.58	-0.09:-0.00	4	0.727E+04
32.28:29.35	1.35: 1.58	-0.00: 0.08	1	0.182E+04
29.35:26.57	0.67: 0.90	-0.09:-0.00	7	0.134E+05
29.35:26.57	0.67: 0.90	-0.00: 0.08	10	0.192E+05
29.35:26.57	0.67: 0.90	0.08: 0.16	1	0.192E+04
29.35:26.57	0.67: 0.90	0.16: 0.24	1	0.192E+04
29.35:26.57	0.67: 0.90	0.24: 0.33	2	0.383E+04
29.35:26.57	0.90: 1.12	-0.17:-0.09	1	0.192E+04
29.35:26.57	0.90: 1.12	-0.09:-0.00	7	0.134E+05
29.35:26.57	0.90: 1.12	-0.00: 0.08	16	0.307E+05
29.35:26.57	0.90: 1.12	0.08: 0.16	1	0.192E+04
29.35:26.57	0.90: 1.12	0.24: 0.33	2	0.383E+04
29.35:26.57	0.90: 1.12	0.33: 0.41	1	0.192E+04
29.35:26.57	1.12: 1.35	-0.17:-0.09	1	0.192E+04
29.35:26.57	1.12: 1.35	-0.09:-0.00	20	0.383E+05
29.35:26.57	1.12: 1.35	-0.00: 0.08	21	0.402E+05
29.35:26.57	1.12: 1.35	0.08: 0.16	4	0.766E+04
29.35:26.57	1.35: 1.58	-0.09:-0.00	3	0.575E+04
29.35:26.57	1.35: 1.58	-0.00: 0.08	4	0.766E+04
29.35:26.57	1.35: 1.58	0.24: 0.33	1	0.192E+04
29.35:26.57	1.58: 1.80	-0.09:-0.00	1	0.192E+04
26.57:23.94	0.45: 0.67	-0.17:-0.09	1	0.202E+04
26.57:23.94	0.45: 0.67	-0.00: 0.08	1	0.202E+04
26.57:23.94	0.45: 0.67	0.08: 0.16	1	0.202E+04
26.57:23.94	0.67: 0.90	-0.25:-0.17	1	0.202E+04
26.57:23.94	0.67: 0.90	-0.09:-0.00	4	0.810E+04
26.57:23.94	0.67: 0.90	-0.00: 0.08	18	0.364E+05
26.57:23.94	0.67: 0.90	0.08: 0.16	1	0.202E+04
26.57:23.94	0.67: 0.90	0.24: 0.33	1	0.202E+04
26.57:23.94	0.90: 1.12	-0.17:-0.09	2	0.405E+04
26.57:23.94	0.90: 1.12	-0.09:-0.00	11	0.223E+05
26.57:23.94	0.90: 1.12	-0.00: 0.08	21	0.425E+05
26.57:23.94	0.90: 1.12	0.08: 0.16	4	0.810E+04
26.57:23.94	0.90: 1.12	0.16: 0.24	2	0.405E+04
26.57:23.94	0.90: 1.12	0.33: 0.41	1	0.202E+04
26.57:23.94	1.12: 1.35	-0.17:-0.09	2	0.405E+04
26.57:23.94	1.12: 1.35	-0.09:-0.00	13	0.263E+05
26.57:23.94	1.12: 1.35	-0.00: 0.08	28	0.566E+05
26.57:23.94	1.12: 1.35	0.08: 0.16	5	0.101E+05

26.57:23.94	1.12: 1.35	0.16: 0.24	2	0.405E+04
26.57:23.94	1.35: 1.58	-0.17:-0.09	1	0.202E+04
26.57:23.94	1.35: 1.58	-0.09:-0.00	6	0.121E+05
26.57:23.94	1.35: 1.58	-0.00: 0.08	4	0.810E+04
26.57:23.94	1.35: 1.58	0.08: 0.16	2	0.405E+04
26.57:23.94	1.58: 1.80	-0.09:-0.00	2	0.405E+04
26.57:23.94	1.58: 1.80	-0.00: 0.08	1	0.202E+04
23.94:21.42	0.45: 0.67	-0.09:-0.00	1	0.212E+04
23.94:21.42	0.45: 0.67	-0.00: 0.08	4	0.848E+04
23.94:21.42	0.45: 0.67	0.16: 0.24	2	0.424E+04
23.94:21.42	0.67: 0.90	-0.09:-0.00	9	0.191E+05
23.94:21.42	0.67: 0.90	-0.00: 0.08	15	0.318E+05
23.94:21.42	0.67: 0.90	0.08: 0.16	1	0.212E+04
23.94:21.42	0.67: 0.90	0.16: 0.24	1	0.212E+04
23.94:21.42	0.90: 1.12	-0.17:-0.09	1	0.212E+04
23.94:21.42	0.90: 1.12	-0.09:-0.00	20	0.424E+05
23.94:21.42	0.90: 1.12	-0.00: 0.08	37	0.785E+05
23.94:21.42	0.90: 1.12	0.08: 0.16	3	0.636E+04
23.94:21.42	0.90: 1.12	0.16: 0.24	2	0.424E+04
23.94:21.42	0.90: 1.12	0.24: 0.33	2	0.424E+04
23.94:21.42	0.90: 1.12	0.33: 0.41	1	0.212E+04
23.94:21.42	1.12: 1.35	-0.17:-0.09	3	0.636E+04
23.94:21.42	1.12: 1.35	-0.09:-0.00	17	0.361E+05
23.94:21.42	1.12: 1.35	-0.00: 0.08	30	0.636E+05
23.94:21.42	1.12: 1.35	0.08: 0.16	5	0.106E+05
23.94:21.42	1.12: 1.35	0.16: 0.24	3	0.636E+04
23.94:21.42	1.12: 1.35	0.24: 0.33	6	0.127E+05
23.94:21.42	1.35: 1.58	-0.09:-0.00	9	0.191E+05
23.94:21.42	1.35: 1.58	-0.00: 0.08	2	0.424E+04
23.94:21.42	1.35: 1.58	0.16: 0.24	3	0.636E+04
23.94:21.42	1.58: 1.80	-0.09:-0.00	1	0.212E+04
23.94:21.42	1.58: 1.80	-0.00: 0.08	2	0.424E+04
21.42:19.03	0.45: 0.67	-0.09:-0.00	4	0.848E+04
21.42:19.03	0.45: 0.67	-0.00: 0.08	2	0.445E+04
21.42:19.03	0.45: 0.67	0.16: 0.24	1	0.223E+04
21.42:19.03	0.67: 0.90	-0.17:-0.09	1	0.223E+04
21.42:19.03	0.67: 0.90	-0.09:-0.00	14	0.312E+05
21.42:19.03	0.67: 0.90	-0.00: 0.08	17	0.379E+05
21.42:19.03	0.67: 0.90	0.08: 0.16	6	0.134E+05
21.42:19.03	0.67: 0.90	0.16: 0.24	5	0.111E+05
21.42:19.03	0.67: 0.90	0.33: 0.41	2	0.445E+04
21.42:19.03	0.90: 1.12	-0.17:-0.09	1	0.223E+04
21.42:19.03	0.90: 1.12	-0.09:-0.00	24	0.535E+05
21.42:19.03	0.90: 1.12	-0.00: 0.08	39	0.869E+05
21.42:19.03	0.90: 1.12	0.08: 0.16	5	0.111E+05
21.42:19.03	0.90: 1.12	0.16: 0.24	2	0.445E+04
21.42:19.03	0.90: 1.12	0.24: 0.33	2	0.445E+04
21.42:19.03	0.90: 1.12	0.33: 0.41	1	0.223E+04
21.42:19.03	1.12: 1.35	-0.17:-0.09	3	0.668E+04
21.42:19.03	1.12: 1.35	-0.09:-0.00	28	0.624E+05
21.42:19.03	1.12: 1.35	-0.00: 0.08	47	0.104E+06
21.42:19.03	1.12: 1.35	0.08: 0.16	0	0.000E+00

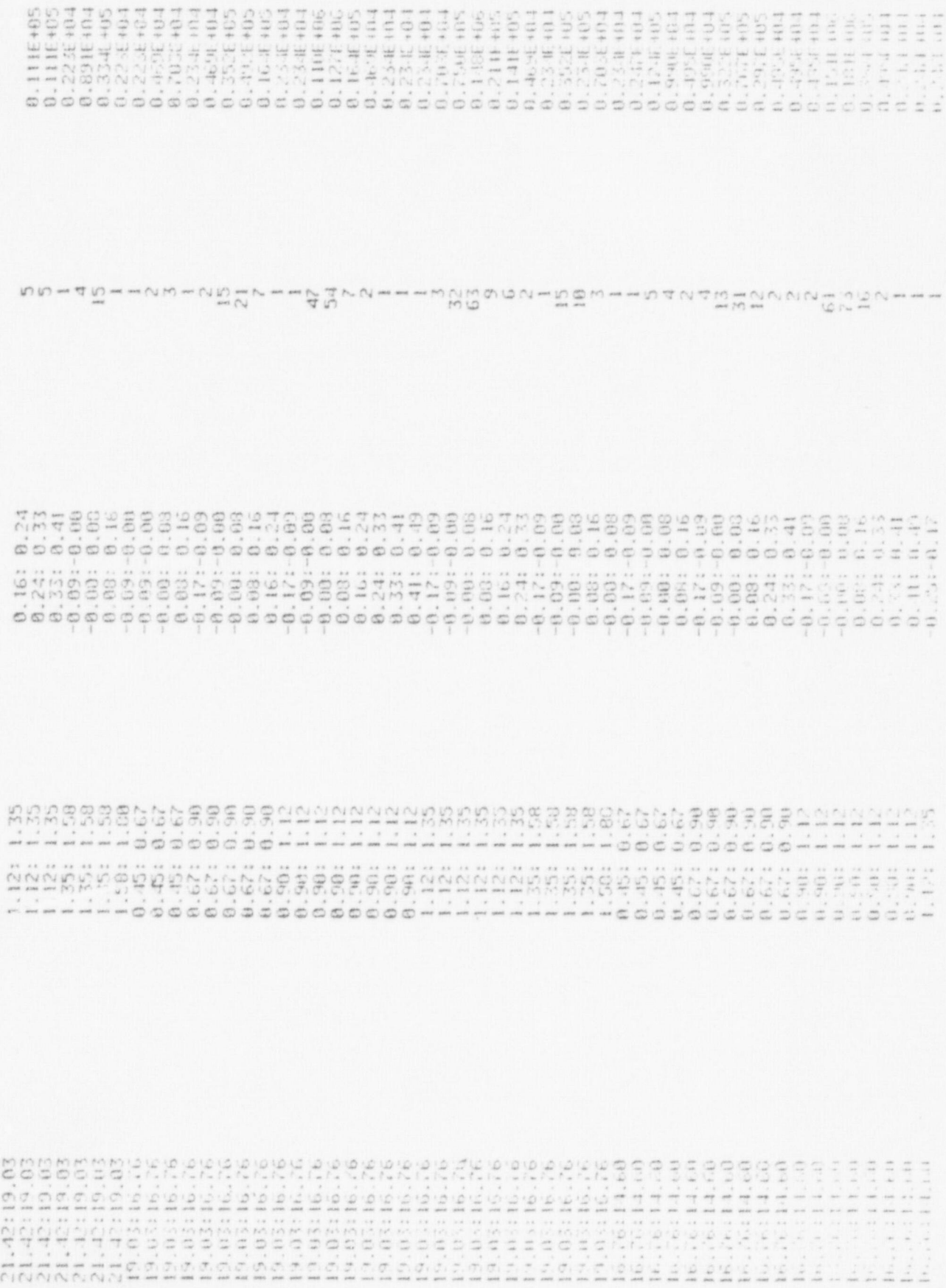

16.76: 14.60	1.12: 1.35	-0.17: -0.09	7	0.173E+05
16.76: 14.60	1.12: 1.35	-0.09: -0.00	56	0.139E+06
16.76: 14.60	1.12: 1.35	-0.00: 0.08	97	0.240E+06
16.76: 14.60	1.12: 1.35	0.08: 0.16	13	0.323E+05
16.76: 14.60	1.12: 1.35	0.16: 0.24	3	0.743E+04
16.76: 14.60	1.12: 1.35	0.33: 0.41	3	0.743E+04
16.76: 14.60	1.12: 1.35	0.41: 0.49	1	0.243E+04
16.76: 14.60	1.35: 1.58	-0.09: -0.00	12	0.297E+05
16.76: 14.60	1.35: 1.58	-0.00: 0.08	26	0.643E+05
16.76: 14.60	1.35: 1.58	0.08: 0.16	5	0.124E+05
16.76: 14.60	1.58: 1.80	-0.00: 0.08	1	0.247E+04
16.76: 14.60	1.80: 2.03	-0.09: -0.00	2	0.495E+04
11.60: 12.57	0.45: 0.67	-0.09: -0.00	4	0.165E+05
14.60: 12.57	0.45: 0.67	-0.00: 0.08	7	0.183E+05
11.60: 12.57	0.45: 0.67	0.08: 0.16	1	0.262E+04
14.60: 12.57	0.67: 0.90	-0.17: -0.09	7	0.183E+05
14.60: 12.57	0.67: 0.90	-0.09: -0.00	25	0.655E+05
11.60: 12.57	0.67: 0.90	-0.00: 0.08	38	0.996E+05
14.60: 12.57	0.67: 0.90	0.08: 0.16	12	0.314E+05
11.60: 12.57	0.67: 0.90	0.16: 0.24	2	0.524E+04
14.60: 12.57	0.67: 0.90	0.24: 0.33	2	0.524E+04
11.60: 12.57	0.90: 1.12	0.41: 0.49	1	0.262E+04
14.60: 12.57	0.90: 1.12	-0.17: -0.09	7	0.183E+05
11.60: 12.57	0.90: 1.12	-0.09: -0.00	57	0.149E+06
14.60: 12.57	0.90: 1.12	-0.00: 0.08	81	0.213E+06
11.60: 12.57	0.90: 1.12	0.08: 0.16	21	0.550E+05
14.60: 12.57	0.90: 1.12	0.16: 0.24	6	0.157E+05
11.60: 12.57	0.90: 1.12	0.24: 0.33	1	0.262E+04
14.60: 12.57	1.12: 1.35	0.41: 0.49	1	0.262E+04
11.60: 12.57	1.12: 1.35	-0.17: -0.09	4	0.105E+05
14.60: 12.57	1.12: 1.35	-0.09: -0.00	58	0.152E+06
11.60: 12.57	1.12: 1.35	-0.00: 0.08	81	0.212E+06
14.60: 12.57	1.12: 1.35	0.08: 0.16	6	0.157E+05
11.60: 12.57	1.12: 1.35	0.16: 0.24	7	0.183E+05
14.60: 12.57	1.12: 1.35	0.24: 0.33	1	0.262E+04
11.60: 12.57	1.12: 1.35	0.33: 0.41	3	0.786E+04
14.60: 12.57	1.12: 1.35	0.41: 0.49	1	0.262E+04
11.60: 12.57	1.35: 1.58	-0.17: -0.09	4	0.105E+05
14.60: 12.57	1.35: 1.58	-0.09: -0.00	16	0.419E+05
11.60: 12.57	1.35: 1.58	-0.00: 0.08	18	0.472E+05
14.60: 12.57	1.35: 1.58	0.08: 0.16	8	0.210E+05
11.60: 12.57	1.35: 1.58	0.16: 0.24	3	0.786E+04
14.60: 12.57	1.35: 1.58	0.24: 0.33	2	0.524E+04
11.60: 12.57	1.35: 1.58	0.33: 0.41	1	0.262E+04
14.60: 12.57	1.58: 1.80	-0.00: 0.08	2	0.524E+04
11.60: 12.57	0.45: 0.67	-0.09: -0.00	4	0.110E+05
14.60: 12.57	0.45: 0.67	-0.00: 0.08	7	0.183E+05
16.76: 10.63	0.45: 0.67	0.16: 0.24	2	0.524E+04
16.76: 10.63	0.67: 0.90	-0.17: -0.09	6	0.157E+05
16.76: 10.63	0.67: 0.90	-0.09: -0.00	35	0.917E+05
16.76: 10.63	0.67: 0.90	-0.00: 0.08	45	0.118E+06
16.76: 10.63	0.67: 0.90	0.08: 0.16	12	0.314E+05

12.57: 10.62	0.67: 0.90	0.16: 0.24	6	0.164E+05
12.57: 10.62	0.67: 0.90	0.24: 0.33	1	0.274E+04
12.57: 10.62	0.90: 1.12	-0.25:-0.17	1	0.274E+04
12.57: 10.62	0.90: 1.12	-0.17:-0.09	3	0.822E+04
12.57: 10.62	0.90: 1.12	-0.09:-0.00	80	0.219E+06
12.57: 10.62	0.90: 1.12	-0.00: 0.08	119	0.326E+06
12.57: 10.62	0.90: 1.12	0.08: 0.16	24	0.658E+05
12.57: 10.62	0.90: 1.12	0.16: 0.24	0	0.219E+05
12.57: 10.62	0.90: 1.12	0.24: 0.33	4	0.110E+05
12.57: 10.62	0.90: 1.12	0.33: 0.41	3	0.822E+04
12.57: 10.62	0.90: 1.12	0.41: 0.49	1	0.274E+04
12.57: 10.62	1.12: 1.35	-0.25:-0.17	1	0.274E+04
12.57: 10.62	1.12: 1.35	-0.17:-0.09	10	0.274E+05
12.57: 10.62	1.12: 1.35	-0.09:-0.00	85	0.233E+06
12.57: 10.62	1.12: 1.35	-0.00: 0.08	112	0.307E+06
12.57: 10.62	1.12: 1.35	0.08: 0.16	20	0.548E+05
12.57: 10.62	1.12: 1.35	0.16: 0.24	5	0.137E+05
12.57: 10.62	1.12: 1.35	0.24: 0.33	3	0.822E+04
12.57: 10.62	1.12: 1.35	0.33: 0.41	1	0.274E+04
12.57: 10.62	1.12: 1.35	0.41: 0.49	1	0.274E+04
12.57: 10.62	1.35: 1.58	-0.17:-0.09	2	0.548E+04
12.57: 10.62	1.35: 1.58	-0.09:-0.00	28	0.768E+05
12.57: 10.62	1.35: 1.58	-0.00: 0.08	39	0.107E+06
12.57: 10.62	1.35: 1.58	0.08: 0.16	7	0.192E+05
12.57: 10.62	1.35: 1.58	0.33: 0.41	1	0.274E+04
12.57: 10.62	1.58: 1.88	-0.00: 0.08	2	0.548E+04

DROPLET SIZE DISTRIBUTION

DIAMETER RANGE	NUMBER DENSITY
87.70-82.01	0.668E+01
82.01-76.60	0.196E+01
76.60-71.45	0.187E+01
71.45-66.57	0.223E+01
66.57-61.93	0.122E+01
61.93-57.54	0.383E+01
57.54-53.35	0.467E+01
53.35-49.37	0.553E+01
49.37-45.60	0.665E+01
45.60-42.01	0.149E+02
42.01-38.60	0.135E+02
38.60-35.37	0.187E+02
35.37-32.28	0.368E+02
32.28-29.35	0.519E+02
29.35-26.67	0.635E+02
26.67-23.94	0.945E+02
23.94-21.42	0.139E+03
21.42-19.03	0.194E+03
19.03-16.76	0.246E+03
16.76-14.68	0.388E+03
14.68-12.57	0.451E+03
12.57-10.62	0.628E+03

APPENDIX - 6

Results of the measurements in a rectangular channel with liquid film on wall.

DROPLET SIZE DISTRIBUTION

MEASURING LOCATION: 0.25mm FROM WALL

MEAN DIAMETER (MICRONS)	NUMBER DENSITY (#/CC/MICRON)	MEAN AXIAL VEL (M/SEC)	STD DEV AXIAL VEL (M/SEC)	MEAN LATERAL VEL (M/SEC)	STD DEV LATERAL VEL (M/SEC)
96.52	0.153E-01	4.65	0.00	0.14	0.00
73.77	0.195E-01	4.65	0.00	0.14	0.00
69.78	0.562E-01	5.10	0.00	0.46	0.09
64.84	0.190E+00	4.78	0.60	0.22	0.22
59.53	0.286E+00	4.81	0.51	0.25	0.24
55.24	0.396E+00	5.07	0.54	0.37	0.30
51.17	0.325E+00	5.00	0.73	0.15	0.28
47.30	0.615E+00	4.97	0.57	0.25	0.26
43.63	0.941E+00	4.98	0.51	0.26	0.26
40.15	0.968E+00	5.10	0.55	0.22	0.28
36.83	0.129E+01	4.93	0.50	0.19	0.34
33.68	0.136E+01	5.01	0.53	0.20	0.25
30.69	0.188E+01	4.92	0.49	0.27	0.28
27.85	0.205E+01	5.17	0.54	0.21	0.26
25.15	0.250E+01	5.02	0.58	0.24	0.27
22.58	0.450E+01	4.96	0.54	0.26	0.30
20.14	0.355E+01	5.17	0.46	0.26	0.23
17.83	0.314E+01	5.17	0.54	0.21	0.29
15.63	0.341E+01	5.18	0.51	0.27	0.27
13.54	0.396E+01	5.26	0.57	0.27	0.29
11.57	0.264E+01	5.26	0.47	0.25	0.23
10.06	0.361E+01	5.30	0.48	0.29	0.27
9.00	0.265E+01	5.28	0.53	0.25	0.28
7.99	0.313E+01	5.12	0.49	0.27	0.28
7.05	0.201E+01	5.22	0.79	0.30	0.31
6.12	0.187E+01	5.38	0.70	0.18	0.17

MEAN AXIAL AIR VELOCITY = 4.96

STANDARD DEVIATION OF AXIAL AIR VELOCITY = 1.31

MEAN LATERAL AIR VELOCITY = -0.11

STANDARD DEVIATION OF LATERAL AIR VELOCITY = 0.92

DROPLET SIZE DISTRIBUTION

Measuring location: 0.50mm from wall

MEAN DIAMETER (MICRONS)	NUMBER DENSITY (#/CC/MICRON)	MEAN AXIAL VEL (M/SEC)	STD DEV AXIAL VEL (M/SEC)	MEAN LATERAL VEL (M/SEC)	STD DEV LATERAL VEL (M/SEC)
73.03	0.207E-01	5.84	0.15	0.23	0.12
73.77	0.364E-01	5.25	0.31	0.20	0.11
68.78	0.679E-01	4.94	0.36	0.16	0.27
64.04	0.117E+00	4.83	0.52	0.11	0.17
59.53	0.193E+00	4.98	0.75	0.04	0.21
55.24	0.224E+00	4.87	0.60	0.04	0.16
51.17	0.256E+00	4.82	0.59	0.02	0.17
47.30	0.385E+00	4.94	0.52	0.18	0.19
43.63	0.497E+00	4.95	0.58	0.15	0.27
40.15	0.661E+00	4.93	0.62	0.22	0.23
36.83	0.704E+00	4.73	0.41	0.11	0.31
33.68	0.991E+00	4.93	0.57	0.11	0.21
30.69	0.916E+00	4.88	0.52	0.21	0.20
27.85	0.118E+01	4.98	0.54	0.13	0.24
25.15	0.140E+01	4.76	0.46	0.23	0.25
22.58	0.189E+01	4.89	0.55	0.18	0.24
20.14	0.129E+01	4.88	0.53	0.10	0.21
17.83	0.136E+01	5.11	0.59	0.17	0.27
15.63	0.145E+01	5.03	0.59	0.16	0.32
13.54	0.154E+01	5.08	0.45	0.17	0.27
11.57	0.193E+01	4.94	0.61	0.24	0.31
10.06	0.185E+01	5.01	0.56	0.12	0.21
9.08	0.211E+01	4.75	0.56	0.17	0.27
7.99	0.202E+01	4.91	0.77	0.24	0.37
7.03	0.287E+01	4.50	0.42	0.19	0.17
6.12	0.471E+01	4.44	0.33	0.21	0.28

MEAN AXIAL AIR VELOCITY = 4.79
STANDARD DEVIATION OF AXIAL AIR VELOCITY = 1.34
MEAN LATERAL AIR VELOCITY = -0.11
STANDARD DEVIATION OF LATERAL AIR VELOCITY = 0.91

DROPLET SIZE DISTRIBUTION

MEASURING LOCATION: 1.00mm FROM WALL

MEAN DIAMETER (MICRONS)	NUMBER DENSITY (#/CC-MICRON)	MEAN AXIAL VEL (M/SEC)	STD DEV AXIAL VEL (M/SEC)	MEAN LATERAL VEL (M/SEC)	STD DEV LATERAL VEL (M/SEC)
73.77	0.75EE-01	4.53	0.64	0.73	0.41
68.78	0.996E-01	4.89	0.43	0.91	0.49
64.04	0.111E+00	4.63	0.31	0.56	0.38
59.53	0.92?E-01	5.10	0.18	0.57	0.00
55.24	0.237E+00	4.78	0.51	0.39	0.31
51.17	0.355E+00	4.66	0.37	0.64	0.38
47.30	0.471E+00	4.67	0.33	0.56	0.34
43.63	0.593E+00	4.74	0.51	0.45	0.34
40.15	0.59?E+00	4.71	0.41	0.62	0.47
36.83	0.919E+00	4.59	0.39	0.53	0.42
33.68	0.98?E+00	4.70	0.37	0.53	0.37
30.69	0.101E+01	4.83	0.38	0.63	0.32
27.85	0.175E+01	4.85	0.40	0.43	0.37
25.15	0.261E+01	4.74	0.41	0.67	0.40
22.58	0.2?0E+01	4.84	0.41	0.64	0.43
20.14	0.337E+01	4.82	0.46	0.54	0.40
17.83	0.?1?E+01	4.69	0.42	0.57	0.41
15.63	0.4?5E+01	4.83	0.??	0.58	0.39
13.54	0.5?1E+01	4.??	0.41	0.57	0.38
11.??	0.?5?E+01	4.81	0.47	0.56	0.40
10.06	0.?9?E+??	4.??	0.40	0.65	0.39
9.00	0.??5E+??	4.81	0.41	0.66	0.36
7.99	0.?25E+??	4.??	0.39	0.58	0.39
7.03	0.?7?E+??	4.??	0.??	0.5??	0.42
6.12	0.?2?E+??	4.68	0.??	0.61	0.42

MEAN AXIAL AIR VELOCITY = 4.69
STANDARD DEVIATION OF AXIAL AIR VELOCITY = 0.51
MEAN LATERAL AIR VELOCITY = 0.55
STANDARD DEVIATION OF LATERAL AIR VELOCITY = 0.44

DROPLET SIZE DISTRIBUTION

MEASURING LOCATION; 2,00mm FROM WALL

MEAN DIAMETER (MICRONS)	NUMBER DENSITY (#/CC/MICRON)	MEAN AXIAL VEL (M/SEC)	STD DEV AXIAL VEL (M/SEC)	MEAN LATERAL VEL (M/SEC)	STD DEV LATERAL VEL (M/SEC)
96.52	0.665E-01	4.60	0.16	0.09	0.26
79.03	0.104E+00	4.56	0.30	0.37	0.35
73.77	0.189E+00	4.64	0.50	0.41	0.27
68.79	0.102E+00	5.17	0.35	0.39	0.50
64.04	0.251E+00	4.97	0.41	0.37	0.37
59.53	0.250E+00	4.66	0.18	0.25	0.30
55.24	0.201E+00	4.59	0.27	0.41	0.25
51.17	0.211E+00	4.60	0.16	0.36	0.50
47.30	0.860E+00	4.75	0.41	0.44	0.38
43.63	0.845E+00	4.67	0.36	0.36	0.47
40.15	0.111E+01	4.76	0.38	0.31	0.33
36.83	0.969E+00	4.71	0.43	0.43	0.38
33.68	0.112E+01	4.85	0.47	0.26	0.30
30.69	0.133E+01	4.60	0.36	0.34	0.30
27.85	0.136E+01	4.75	0.43	0.39	0.41
25.15	0.170E+01	4.86	0.56	0.42	0.33
22.58	0.214E+01	4.80	0.52	0.38	0.49
20.14	0.210E+01	4.87	0.49	0.32	0.33
17.83	0.175E+01	4.87	0.45	0.33	0.46
15.63	0.153E+01	4.89	0.57	0.41	0.31
13.54	0.186E+01	5.08	0.59	0.46	0.37
11.57	0.222E+01	4.84	0.38	0.32	0.40
10.06	0.342E+01	4.63	0.36	0.42	0.39
9.00	0.424E+01	4.80	0.49	0.44	0.40
7.99	0.353E+01	4.79	0.41	0.46	0.40
7.02	0.441E+01	4.68	0.48	0.46	0.40
6.12	0.646E+01	4.47	0.22	0.40	0.39

MEAN AXIAL AIR VELOCITY = 4.38
STANDARD DEVIATION OF AXIAL AIR VELOCITY = 0.27
MEAN LATERAL AIR VELOCITY = 0.28
STANDARD DEVIATION OF LATERAL AIR VELOCITY = 0.35

DROPLET SIZE DISTRIBUTION

MEASURING LOCATION: 3.00mm FROM WALL

MEAN DIAMETER (MICRONS)	NUMBER DENSITY (#/CC/MICRON)	MEAN AXIAL VEL (M/SEC)	STD DEV AXIAL VEL (M/SEC)	MEAN LATERAL VEL (M/SEC)	STD DEV LATERAL VEL (M/SEC)
84.57	0.160E-01	5.22	0.00	0.25	0.00
79.03	0.387E-01	4.53	0.60	0.12	0.11
73.77	0.165E-01	5.62	0.00	0.25	0.00
68.78	0.101E+00	4.83	0.55	0.22	0.18
64.04	0.824E-01	4.97	0.45	0.39	0.39
59.53	0.209E+00	5.15	0.33	0.16	0.11
55.24	0.314E+00	5.41	0.32	0.20	0.20
51.17	0.349E+00	4.79	0.52	0.09	0.19
47.30	0.539E+00	5.13	0.50	0.31	0.34
43.63	0.712E+00	5.02	0.47	0.21	0.24
40.15	0.667E+00	5.01	0.42	0.20	0.26
36.83	0.925E+00	5.07	0.32	0.16	0.24
33.68	0.123E+01	5.17	0.46	0.26	0.34
30.69	0.160E+01	5.07	0.48	0.24	0.38
27.85	0.109E+01	5.36	0.57	0.24	0.24
25.15	0.146E+01	4.94	0.51	0.24	0.31
22.58	0.216E+01	5.27	0.39	0.17	0.24
20.14	0.176E+01	5.22	0.52	0.20	0.33
17.83	0.156E+01	5.23	0.43	0.17	0.26
15.63	0.182E+01	5.34	0.68	0.19	0.22
13.54	0.134E+01	5.21	0.47	0.20	0.28
11.57	0.161E+01	5.37	0.45	0.24	0.30
10.06	0.250E+01	5.38	0.46	0.22	0.20
9.00	0.104E+01	5.71	0.73	0.20	0.16
7.99	0.871E+00	5.51	0.60	0.10	0.18
7.03	0.264E+00	5.77	1.20	0.23	0.29
6.12	0.522E+00	5.11	0.39	0.17	0.23

MEAN AXIAL AIR VELOCITY = 4.75

STANDARD DEVIATION OF AXIAL AIR VELOCITY = 0.61

MEAN LATERAL AIR VELOCITY = -0.28

STANDARD DEVIATION OF LATERAL AIR VELOCITY = 0.98

DROPLET SIZE DISTRIBUTION

MEASURING LOCATION: 4.00mm FROM WALL

MEAN DIAMETER (MICRONS)	NUMBER DENSITY (#/CC/MICRON)	MEAN AXIAL VEL (M/SEC)	STD DEV AXIAL VEL (M/SEC)	MEAN LATERAL VEL (M/SEC)	STD DEV LATERAL VEL (M/SEC)
64.04					
59.53	0.382E-01	4.97	0.00	-0.43	0.00
55.24	0.429E-01	4.65	0.00	0.81	0.00
51.17	0.794E-01	5.30	0.00	0.19	0.12
47.30	0.133E+00	5.01	0.58	0.42	0.48
43.63	0.265E+00	5.26	0.42	0.42	0.45
40.15	0.297E+00	4.97	0.19	0.44	0.40
36.83	0.506E+00	4.60	0.28	0.50	0.42
33.63	0.642E+00	5.08	0.40	0.26	0.41
30.69	0.759E+00	4.90	0.59	0.29	0.32
27.85	0.667E+00	4.96	0.58	0.39	0.38
25.15	0.111E+01	5.17	0.47	0.45	0.51
22.58	0.144E+01	5.34	0.56	0.22	0.30
20.14	0.152E+01	5.32	0.42	0.35	0.36
17.83	0.112E+01	5.26	0.46	0.26	0.33
15.63	0.947E+00	4.93	0.47	0.34	0.34
13.54	0.112E+01	5.49	0.52	0.29	0.33
11.57	0.792E+00	5.45	0.48	0.21	0.38
10.06	0.139E+01	5.60	0.57	0.20	0.29
9.00	0.131E+01	5.52	0.75	0.36	0.30
7.03	0.448E+00	5.65	0.65	0.24	0.32
6.12	0.542E+00	5.21	0.67	0.37	0.54
	0.344E+00	5.74	0.48	0.20	0.12

MEAN AXIAL AIR VELOCITY = 5.00
STANDARD DEVIATION OF AXIAL AIR VELOCITY = 0.69
MEAN LATERAL AIR VELOCITY = 0.14
STANDARD DEVIATION OF LATERAL AIR VELOCITY = 0.73

DROPLET SIZE DISTRIBUTION

MEASURING LOCATION: 5.00mm FROM WALL

MEAN DIAMETER (MICRONS)	NUMBER DENSITY (#/CC/MICRON)	MEAN AXIAL VEL (M/SEC)	STD DEV AXIAL VEL (M/SEC)	MEAN LATERAL VEL (M/SEC)	STD DEV LATERAL VEL (M/SEC)
96.52	0.365E-01	5.32	0.00	0.12	0.27
90.30	0.374E-01	5.46	0.22	-0.03	0.10
84.57	0.454E-01	4.72	0.76	-0.04	0.11
79.03	0.148E+00	5.09	0.44	0.25	0.16
73.77	0.725E-01	5.48	0.39	0.02	0.32
68.78	0.235E+00	5.33	0.67	0.22	0.23
64.04	0.208E+00	5.49	0.48	0.05	0.19
59.53	0.317E+00	5.54	0.62	0.11	0.18
55.23	0.518E+00	5.26	0.63	0.16	0.16
51.17	0.463E+00	5.46	0.47	0.15	0.27
47.30	0.917E+00	5.29	0.52	0.17	0.20
43.63	0.922E+00	5.42	0.58	0.18	0.24
40.15	0.105E+01	5.46	0.54	0.12	0.21
36.83	0.142E+01	5.48	0.51	0.17	0.32
33.68	0.181E+01	5.43	0.53	0.08	0.17
30.69	0.152E+01	5.48	0.57	0.07	0.17
27.85	0.211E+01	5.48	0.57	0.13	0.20
25.15	0.209E+01	5.47	0.51	0.14	0.30
22.58	0.390E+01	5.59	0.51	0.14	0.22
20.11	0.232E+01	5.60	0.51	0.14	0.21
17.83	0.237E+01	5.61	0.50	0.12	0.19
15.63	0.232E+01	5.73	0.49	0.16	0.20
13.54	0.243E+01	5.83	0.54	0.14	0.20
11.57	0.208E+01	5.83	0.43	0.18	0.22
10.06	0.284E+01	5.76	0.00	0.11	0.22
9.00	0.211E+01	5.93	0.54	0.10	0.17
7.39	0.138E+01	5.97	0.58	0.14	0.23
7.03	0.979E+00	6.23	0.76	0.13	0.22
6.12	0.613E+00	5.65	0.31	0.29	0.30

MEAN AXIAL AIR VELOCITY = 5.77
STANDARD DEVIATION OF AXIAL AIR VELOCITY = 0.64
MEAN LATERAL AIR VELOCITY = 0.10
STANDARD DEVIATION OF LATERAL AIR VELOCITY = 0.28

APPENDIX - 7

Results of the measurements in a rectangular channel without liquid film on wall.

DROPLET SIZE DISTRIBUTION

MEASURING LOCATION: 0.25mm FROM WALL

MEAN DIAMETER (MICRONS)	NUMBER DENSITY (#/CC/MICRON)	MEAN AXIAL VEL (M/SEC)	STD DEV AXIAL VEL (M/SEC)	MEAN LATERAL VEL (M/SEC)	STD DEV LATERAL VEL (M/SEC)
96.76	0.568E-02	3.42	0.00	-0.06	0.00
79.24	0.273E-02	8.29	0.00	0.46	0.00
73.96	0.576E-02	8.29	0.00	0.07	0.00
59.69	0.372E-02	7.47	0.00	-0.06	0.00
55.48	0.104E-01	5.60	1.92	-0.06	0.00
51.32	0.111E-01	8.29	0.00	0.03	0.06
47.45	0.117E-01	8.29	0.00	-0.10	0.06
43.77	0.124E-01	8.29	0.00	-0.15	0.06
40.28	0.178E-01	8.07	0.36	-0.06	0.09
36.96	0.595E-01	8.25	0.55	-0.07	0.08
33.80	0.366E-01	8.67	0.41	-0.04	0.19
30.79	0.399E-01	7.35	2.62	-0.08	0.13
27.95	0.784E-01	7.86	1.55	-0.02	0.14
25.24	0.104E+00	7.58	1.69	-0.06	0.10
22.66	0.136E+00	8.62	0.79	-0.13	0.10
20.22	0.172E+00	7.77	2.07	-0.07	0.09
17.89	0.218E+00	7.94	1.93	-0.04	0.23
15.68	0.206E+00	6.88	2.42	-0.07	0.10
13.59	0.240E+00	7.53	2.21	-0.08	0.12
11.60	0.179E+00	7.05	2.47	-0.01	0.11
10.09	0.813E+00	6.22	2.57	-0.03	0.09
9.03	0.581E+00	5.28	2.58	-0.06	0.12
8.02	0.913E+00	5.59	2.67	-0.01	0.12
7.06	0.691E+00	6.02	2.66	0.01	0.08
6.14	0.172E+01	7.83	2.43	-0.00	0.11

MEAN AXIAL AIR VELOCITY = 8.72
STANDARD DEVIATION OF AXIAL AIR VELOCITY = 0.59
MEAN LATERAL AIR VELOCITY = 0.03
STANDARD DEVIATION OF LATERAL AIR VELOCITY = 0.17

DROPLET SIZE DISTRIBUTION

MEASURING LOCATION: 0.50mm FROM WALL

MEAN DIAMETER (MICRONS)	NUMBER DENSITY (#/CC/MICRON)	MEAN AXIAL VEL (M/SEC)	STD DEV AXIAL VEL (M/SEC)	MEAN LATERAL VEL (M/SEC)	STD DEV LATERAL VEL (M/SEC)
96.76	0.842E-02	8.09	0.65	-0.22	0.18
90.62	0.365E-02	6.56	0.00	-0.01	0.00
84.78	0.686E-02	7.35	0.00	-0.12	0.11
79.24	0.360E-02	7.35	0.00	-0.23	0.00
73.96	0.343E-02	8.15	0.00	-0.01	0.00
55.40	0.173E-01	7.90	0.64	-0.18	0.09
51.32	0.142E-01	7.60	0.37	-0.08	0.10
47.45	0.147E-01	7.75	1.01	-0.01	0.17
43.77	0.313E-01	7.67	0.76	-0.04	0.15
40.28	0.415E-01	8.11	0.56	-0.03	0.28
36.96	0.327E-01	8.09	0.65	0.02	0.15
33.80	0.579E-01	7.23	2.18	-0.08	0.17
30.79	0.757E-01	8.43	0.48	-0.03	0.13
27.95	0.108E+00	8.21	0.56	-0.05	0.11
25.24	0.121E+00	8.52	0.64	-0.07	0.12
22.66	0.141E+00	8.49	0.54	-0.05	0.12
20.22	0.221E+00	8.42	0.70	-0.06	0.08
17.83	0.201E+00	8.83	0.49	-0.07	0.17
15.68	0.247E+00	8.62	0.65	-0.05	0.14
13.59	0.356E+00	7.13	2.48	0.03	0.25
11.60	0.291E+00	7.86	1.97	0.00	0.21
10.09	0.587E+00	7.65	1.94	0.01	0.21
9.03	0.337E+00	7.38	2.31	-0.03	0.12
8.02	0.122E+01	7.29	2.22	0.03	0.18
7.06	0.190E+01	7.13	2.29	0.11	0.30
6.14	0.318E+01	7.87	1.79	0.05	0.22

MEAN AXIAL AIR VELOCITY = 8.82
STANDARD DEVIATION OF AXIAL AIR VELOCITY = 0.59
MEAN LATERAL AIR VELOCITY = -0.05
STANDARD DEVIATION OF LATERAL AIR VELOCITY = 0.10

DROPLET SIZE DISTRIBUTION

MEASURING LOCATION: 0.75mm FROM WALL

MEAN DIAMETER (MICRONS)	NUMBER DENSITY (#/CC/MICRON)	MEAN AXIAL VEL (M/SEC)	STD DEV AXIAL VEL (M/SEC)	MEAN LATERAL VEL (M/SEC)	STD DEV LATERAL VEL (M/SEC)
96.76	0.367E-02	5.31	0.00	0.04	0.00
84.78	0.407E-02	5.31	0.00	-0.11	0.00
79.24	0.427E-02	5.31	0.00	-0.11	0.00
68.96	0.568E-02	4.43	0.00	0.04	0.00
51.32	0.871E-02	3.54	0.00	0.04	0.00
47.45	0.777E-02	8.37	0.44	-0.11	0.00
43.77	0.819E-02	8.37	0.44	-0.04	0.07
40.28	0.223E-01	6.46	1.58	0.01	0.06
36.96	0.396E-01	8.60	0.55	-0.08	0.23
33.80	0.524E-01	6.84	2.36	-0.07	0.12
30.79	0.213E-01	7.90	0.62	-0.04	0.07
27.95	0.336E-01	6.58	2.36	0.05	0.12
25.24	0.955E-01	6.82	2.45	0.02	0.12
22.66	0.138E+00	7.80	1.91	0.02	0.11
20.22	0.166E+00	7.72	1.99	0.01	0.16
17.89	0.275E+00	8.29	1.76	-0.03	0.12
15.68	0.405E+00	8.00	2.01	0.00	0.19
13.59	0.688E+00	8.52	1.65	-0.01	0.15
11.60	0.680E+00	8.46	1.66	-0.01	0.16
10.09	0.107E+01	8.73	1.51	0.01	0.16
9.03	0.102E+01	8.78	1.69	-0.02	0.15
8.02	0.174E+01	8.19	2.23	0.00	0.15
7.06	0.206E+01	8.50	2.03	0.01	0.14
6.14	0.334E+01	9.02	1.53	0.01	0.14

MEAN AXIAL AIR VELOCITY = 9.16
STANDARD DEVIATION OF AXIAL AIR VELOCITY = 0.48
MEAN LATERAL AIR VELOCITY = 0.01
STANDARD DEVIATION OF LATERAL AIR VELOCITY = 0.17

DROPLET SIZE DISTRIBUTION

MEASURING LOCATION: 1.00mm FROM WALL

MEAN DIAMETER (MICRONS)	NUMBER DENSITY (#/CC/MICRON)	MEAN AXIAL VEL (M/SEC)	STD DEV AXIAL VEL (M/SEC)	MEAN LATERAL VEL (M/SEC)	STD DEV LATERAL VEL (M/SEC)
96.76	0.149E-01	7.48	0.83	-0.04	0.12
90.62	0.268E-02	8.70	0.00	-0.28	0.00
79.24	0.653E-02	7.90	0.00	0.02	0.00
73.96	0.135E-01	8.08	0.34	-0.06	0.13
68.96	0.146E-01	7.86	0.57	-0.04	0.26
64.21	0.177E-01	8.53	0.33	-0.10	0.15
59.69	0.242E-01	7.87	0.46	-0.02	0.11
55.40	0.278E-01	8.39	0.83	0.11	0.21
51.32	0.382E-01	8.29	0.67	-0.15	0.15
47.45	0.739E-01	8.00	1.07	-0.03	0.11
43.77	0.101E+00	8.53	0.70	-0.04	0.16
40.28	0.845E-01	8.25	0.77	-0.10	0.15
36.96	0.134E+00	8.03	1.12	-0.05	0.13
33.80	0.194E+00	8.64	0.58	-0.03	0.14
30.79	0.263E+00	8.55	0.73	-0.04	0.16
27.95	0.317E+00	8.71	0.62	-0.03	0.14
25.24	0.289E+00	8.78	0.55	-0.07	0.15
22.66	0.458E+00	8.61	1.01	-0.02	0.14
20.22	0.549E+00	8.63	0.61	0.00	0.30
17.89	0.736E+00	8.80	0.59	-0.02	0.12
15.68	0.934E+00	8.94	0.55	-0.01	0.14
13.59	0.113E+01	8.79	0.81	0.00	0.11
11.60	0.888E+00	8.99	0.78	0.00	0.22
10.09	0.192E+01	8.74	1.19	-0.01	0.14
9.03	0.147E+01	8.71	1.41	-0.02	0.16
8.02	0.180E+01	8.75	1.15	0.01	0.13
7.06	0.226E+01	8.46	1.42	0.01	0.13
6.14	0.506E+01	8.45	1.51	0.01	0.18

MEAN AXIAL AIR VELOCITY = 9.00
STANDARD DEVIATION OF AXIAL AIR VELOCITY = 0.59
MEAN LATERAL AIR VELOCITY = 0.01
STANDARD DEVIATION OF LATERAL AIR VELOCITY = 0.16

DROPLET SIZE DISTRIBUTION

MEASURING LOCATION: 1.50mm FROM WALL

MEAN DIAMETER (MICRONS)	NUMBER DENSITY (#/CC/MICRON)	MEAN AXIAL VEL (M/SEC)	STD DEV AXIAL VEL (M/SEC)	MEAN LATERAL VEL (M/SEC)	STD DEV LATERAL VEL (M/SEC)
96.76	0.333E-01	5.77	1.36	0.02	0.17
90.62	0.387E-02	8.72	0.00	-0.13	0.09
84.78	0.475E-02	7.49	0.40	-0.04	0.00
73.96	0.226E-02	8.72	0.00	-0.22	0.00
68.96	0.291E-02	7.10	0.00	0.14	0.00
64.21	0.827E-02	7.91	0.00	-0.10	0.23
55.40	0.345E-01	8.40	0.69	-0.09	0.11
51.32	0.158E-01	8.06	0.31	0.07	0.19
47.45	0.320E-01	8.36	0.56	-0.06	0.23
43.77	0.537E-01	8.41	0.70	-0.10	0.08
40.28	0.836E-01	7.81	1.40	-0.09	0.15
36.96	0.129E+00	8.48	0.69	-0.02	0.23
33.80	0.182E+00	8.64	0.63	-0.01	0.18
30.79	0.262E+00	8.59	0.72	-0.05	0.16
27.95	0.382E+00	8.78	0.58	-0.03	0.15
25.24	0.463E+00	8.76	0.61	-0.01	0.18
22.66	0.600E+00	8.65	0.63	-0.02	0.18
20.22	0.774E+00	8.75	0.62	-0.01	0.21
17.89	0.855E+00	8.82	0.76	0.00	0.19
15.68	0.103E+01	8.93	0.63	0.00	0.18
13.59	0.136E+01	9.02	0.71	0.01	0.18
11.60	0.140E+01	9.08	0.60	0.01	0.19
10.09	0.203E+01	9.15	0.68	0.01	0.20
9.03	0.170E+01	9.21	0.76	0.04	0.17
8.02	0.128E+01	9.40	0.87	0.07	0.18
7.06	0.122E+01	9.07	1.43	0.02	0.17
6.14	0.333E+01	9.08	1.12	0.04	0.18

MEAN AXIAL AIR VELOCITY = 9.08

STANDARD DEVIATION OF AXIAL AIR VELOCITY = 0.62

MEAN LATERAL AIR VELOCITY = 0.06

STANDARD DEVIATION OF LATERAL AIR VELOCITY = 0.23

DROPLET SIZE DISTRIBUTION

MEASURING LOCATION: 2.00mm FROM WALL

MEAN DIAMETER (MICRONS)	NUMBER DENSITY (#/CC/MICRON)	MEAN AXIAL VEL (M/SEC)	STD DEV AXIAL VEL (M/SEC)	MEAN LATERAL VEL (M/SEC)	STD DEV LATERAL VEL (M/SEC)
96.76	0.995E-02	7.71	0.40	0.01	0.28
90.62	0.309E-02	6.53	0.00	-0.15	0.00
84.78	0.139E-01	7.69	1.85	-0.07	0.30
79.24	0.305E-02	7.33	0.00	0.07	0.00
73.96	0.844E-02	8.38	0.37	0.00	0.10
68.96	0.116E-01	8.51	0.40	-0.09	0.10
64.21	0.614E-02	8.51	0.40	0.07	0.00
59.69	0.194E-01	8.51	0.40	-0.18	0.19
55.40	0.241E-01	7.19	1.98	0.10	0.18
51.32	0.298E-01	8.18	0.63	-0.03	0.16
47.45	0.284E-01	9.02	0.26	-0.12	0.13
43.77	0.563E-01	8.41	0.76	-0.07	0.16
40.28	0.990E-01	8.62	0.61	-0.06	0.25
36.96	0.170E+00	8.58	0.75	-0.02	0.22
33.80	0.201E+00	8.79	0.69	-0.04	0.15
30.79	0.316E+00	8.79	0.62	-0.08	0.17
27.95	0.355E+00	8.70	0.64	-0.03	0.21
25.24	0.464E+00	8.91	0.59	-0.05	0.15
22.66	0.508E+00	9.02	0.55	-0.06	0.21
20.22	0.686E+00	9.02	0.61	-0.03	0.21
17.89	0.791E+00	8.99	0.59	0.02	0.21
15.68	0.839E+00	9.16	0.66	-0.03	0.22
13.59	0.112E+01	9.17	0.57	0.03	0.25
11.60	0.113E+01	9.16	0.69	0.06	0.27
10.09	0.156E+01	9.29	0.62	0.05	0.27
9.03	0.112E+01	9.42	0.69	0.07	0.25
8.02	0.723E+00	9.37	0.75	0.14	0.30
7.06	0.649E+00	9.51	0.92	0.18	0.36
6.14	0.202E+01	9.53	0.75	0.11	0.32

MEAN AXIAL AIR VELOCITY = 8.89
STANDARD DEVIATION OF AXIAL AIR VELOCITY = 0.61
MEAN LATERAL AIR VELOCITY = 0.32
STANDARD DEVIATION OF LATERAL AIR VELOCITY = 0.37

FOR MEASURING LOCATION AT 3.00MM FROM WALL SEE PAGE- 73

DROPLET SIZE DISTRIBUTION

MEASYRING LOCATION: 4.00mm FROM WALL

MEAN DIAMETER (MICRONS)	NUMBER DENSITY (#/CC/MICRON)	MEAN AXIAL VEL (M/SEC)	STD DEV AXIAL VEL (M/SEC)	MEAN LATERAL VEL (M/SEC)	STD DEV LATERAL VEL (M/SEC)
96.76	0.107E-01	8.52	0.49	-0.01	0.25
90.62	0.388E-02	7.10	1.14	0.06	0.09
84.78	0.189E-02	7.67	0.00	0.70	0.00
79.24	0.511E-02	8.94	0.37	-0.01	0.14
73.96	0.371E-02	8.68	1.15	-0.09	0.09
68.96	0.220E-02	7.67	0.00	0.16	0.00
64.21	0.146E-01	8.52	0.49	0.22	0.25
59.69	0.255E-01	8.83	0.74	0.17	0.29
55.40	0.417E-01	8.98	0.58	0.19	0.41
51.32	0.310E-01	8.72	0.37	0.23	0.28
47.45	0.745E-01	8.79	0.71	0.18	0.36
43.77	0.865E-01	9.05	0.90	0.07	0.33
40.28	0.111E+00	9.21	3.59	0.09	0.26
36.96	0.172E+00	9.33	0.83	0.07	0.31
33.80	0.173E+00	9.27	0.67	0.10	0.28
30.79	0.246E+00	9.30	0.65	0.11	0.32
27.95	0.305E+00	9.44	0.50	0.06	0.27
25.24	0.351E+00	9.46	0.61	0.08	0.32
22.66	0.391E+00	9.32	0.52	0.13	0.27
20.22	0.479E+00	9.46	0.68	0.09	0.30
17.89	0.554E+00	9.48	0.44	0.10	0.28
15.68	0.422E+00	9.70	0.57	0.17	0.30
13.59	0.247E+00	9.85	0.64	0.17	0.29
11.60	0.128E+00	10.25	0.72	0.06	0.23
10.09	0.123E+00	10.43	0.92	0.11	0.42
9.03	0.892E-01	10.7[illegible]	0.63	0.16	0.27
8.02	0.418E-01	10.03	1.04	0.20	0.17
7.06	0.199E-01	8.[illegible]1	0.38	0.26	0.09
6.14	0.635E-01	10.23	0.90	-0.09	0.13

MEAN AXIAL AIR VELOCITY = 9.87

STANDARD DEVIATION OF AXIAL AIR VELOCITY = 0.52

MEAN LATERAL AIR VELOCITY = 0.21

STANDARD DEVIATION OF LATERAL AIR VELOCITY = 0.31

DROPLET SIZE DISTRIBUTION

MEASURING LOCATION: 5.00mm FROM WALL

MEAN DIAMETER (MICRONS)	NUMBER DENSITY (#/CC/MICRON)	MEAN AXIAL VEL (M/SEC)	STD DEV AXIAL VEL (M/SEC)	MEAN LATERAL VEL (M/SEC)	STD DEV LATERAL VEL (M/SEC)
.40	0.200E-02	10.33	0.00	-0.13	0.00
33.46	0.320E-02	11.66	0.00	-0.38	0.00
30.79	0.115E-01	10.77	0.00	0.03	0.11
27.95	0.134E-01	9.73	0.21	-0.05	0.11
25.24	0.425E-01	10.80	0.42	-0.08	0.21
22.66	0.134E+00	11.16	0.35	0.03	0.30
20.22	0.267E+00	11.20	0.52	0.02	0.19
17.89	0.401E+00	11.18	0.48	-0.03	0.21
15.68	0.826E+00	11.20	0.59	0.08	0.27
13.59	0.113E+01	11.24	0.53	0.06	0.28
11.60	0.175E+01	11.29	0.53	0.10	0.32
10.09	0.367E+01	11.29	0.56	0.11	0.30
9.03	0.372E+01	11.31	0.56	0.12	0.31
8.02	0.436E+01	11.27	0.59	0.18	0.35
7.06	0.451E+01	11.12	0.67	0.24	0.36
6.14	0.816E+01	11.20	0.63	0.20	0.36

MEAN AXIAL AIR VELOCITY = 11.36
STANDARD DEVIATION OF AXIAL AIR VELOCITY = 0.64
MEAN LATERAL AIR VELOCITY = 0.36
STANDARD DEVIATION OF LATERAL AIR VELOCITY = 0.39

NRC FORM 335 (7-77)

U.S. NUCLEAR REGULATORY COMMISSION

BIBLIOGRAPHIC DATA SHEET

1. REPORT NUMBER (Assigned by DDC)
NUREG/CR-0457

4. TITLE AND SUBTITLE (Add Volume No., if appropriate)
Development of a Laser Doppler Anemometer Technique for the Measurement of Two Phase Dispersed Flow

2. (Leave blank)

3. RECIPIENT'S ACCESSION NO.

7. AUTHOR(S)
J. Srinivasan

5. DATE REPORT COMPLETED
MONTH: May YEAR: 1978

9. PERFORMING ORGANIZATION NAME AND MAILING ADDRESS (Include Zip Code)
SUNY at Stony Brook
Stony Brook, New York 11794

DATE REPORT ISSUED
MONTH YEAR

6. (Leave blank)

8. (Leave blank)

12. SPONSORING ORGANIZATION NAME AND MAILING ADDRESS (Include Zip Code)
Reactor Safety Research Division
U.S. Nuclear Regulatory Commission
Washington D. C. 20555

10. PROJECT/TASK/WORK UNIT NO.

11. CONTRACT NO.
FIN B6211

13. TYPE OF REPORT
Thesis

PERIOD COVERED (Inclusive dates)

15. SUPPLEMENTARY NOTES

14. (Leave blank)

16. ABSTRACT (200 words or less)

A new optical technique using Laser Doppler Anemometry is presented for the measurement of the local number densities and two dimensional velocity probability densities of particles in a dilute dispersed flow. The measurement involves discrimination on the signal amplitude, resident time, and frequency of Doppler signals caused by the scattered light from individual particles in the probing volume. A predominant direction of flow is assumed and the flow may be turbulent with a wide distribution of particle sizes.

17. KEY WORDS AND DOCUMENT ANALYSIS

17a. DESCRIPTORS

17b. IDENTIFIERS/OPEN-ENDED TERMS

18. AVAILABILITY STATEMENT
UNRESTRICTED

19. SECURITY CLASS (This report)

21. NO. OF PAGES

20. SECURITY CLASS (This page)

22. PRICE
$

120555028651 1 R2R4AN
US NRC
ADM TIDC DSB
MIKE ATSALINOS
016
WASHINGTON DC 20555